Long term NOAA-AVHRR GIMMS-NDVI - rainfall relationships and trends 1981 to 2003 for entire DeSurvey area of interest

Töttrup, Christian; Helldén, Ulf

2007

A Surveillance System for Assessing and Monitoring Desertification
www.desurvey.net

European Commission
6th Framework Programme:
Global Change & Ecosystems.
Integrated Project Contract N°. 003950

Project No.: 003950
DeSurvey
A Surveillance System for Assessing and Monitoring Desertification

Instrument: IP
Thematic Priority: Global Change and Ecosystems

Deliverable 1.5.1.17:

Long term NOAA-AVHRR (MEDOKADS/Pathfinder/GIMMS) NDVI-rainfall relationships and trends 1989 to current for entire DeSurvey area of interest

Lead contractor for D1.5.1.17: EC-JRC-IES (Partner 19)

Sub-deliverable 1.5.1.17 (1):

Long term NOAA-AVHRR GIMMS-NDVI rainfall relationships and trends 1981 to 2003 for entire DeSurvey area of interest

Report authors: Christian Töttrup & Ulf Helldén, Lund University (Partner 7)

Due date of deliverable: month 30
Actual submission date: month 33

Start date of project: March 12, 2005 Duration: 60 months

Dissemination level: Public **Revision:** Version 1

Content **Page**

Long term NOAA-AVHRR GIMMS-NDVI - rainfall relationships and trends 1981 to 2003 for entire DeSurvey area of interest

Christian Töttrup & Ulf Helldén, Partner 7 (Lund University)

Abstract

The paper presents results of a study on the use of the NOAA AVHRR data for desertification monitoring on a regional-global level. It is based on processing of the GIMMS 8 km global NDVI data set. Time series of annual integrated NDVI and standardized annual NDVI anomalies from the 1981-2003 periodic means were compared with a corresponding rainfall data set (i.e. 1981-2003) as well as a historical rainfall set (1901-2002). Both sets were derived from 2.5 degrees and 0.5 degrees global gridded climate data respectively.

The areas studied include the Mediterranean basin (Southern Europe and Northern Africa), the Sahel from the Atlantic to the Red Sea, major parts of the drylands of Southern Africa, China and the drylands of South America, i.e. important parts of the desertification prone areas of the world (Cf. fig. 1)

It is concluded that the suggested methodology is a robust and reliable way to assess and monitor desertification on a global, national and regional scale. The results of the applied methodology indicate a strong general relationship between NDVI and rainfall over time. The results of performed trend analysis cannot be used to verify any systematic generic land degradation/desertification trend at the regional-global level in any of the regions studied. On the contrary, a "greening-up" seems to be evident over the past 20 years in several of the regions when interpreting the NDVI as a proxy for biomass cover and seasonal vegetation growth.

This is most obvious in the African Sahel region south of the Sahara.

0. INTRODUCTION

This report is a part of and a sub-deliverable to the DeSurvey ,WP 1.5.1 Deliverable 1.5.1.17: "Long term NOAA-AVHRR (MEDOKADS/Pathfinder/GIMMS) NDVI-rainfall relationships and trends 1989 to current for entire DeSurvey area of interest" under the leadership of partner 19 (EC JRC-IES). It covers the use of the GIMMS NDVI.

1. DESERTIFICATION

Desertification is land degradation in arid, semi-arid and dry sub-humid areas resulting from various factors, including climatic variations and human activities. Degradation implies the reduction of the resource potential of the landscape through different processes (UNCED 1992).

Embedded in the term desertification is much controversy on the actual magnitude of the problem with published figures suggesting that anything between 17 to more than 70 per cent of the worlds drylands may be 'desertified' (Reynolds et al. 2003). Another crucial issue relates to the actual causes of desertification with much of the debate focusing on the extent to which it is mainly driven by climate or by human influences.

In March 2006 we carried out a survey among the scientists of Desurvey (about 90 persons) to find out about their desertification/land degradation concepts. We offered everyone an opportunity to provide an anonymous opinion about what key indicator/ variable they would prefer as a proxy and most important "stock" for desertification if they were to

assess or simulate desertification through system dynamic modeling. Sixty five of them responded. A vast majority of the votes fell on the following two alternatives (Fig. 1):

D) Green & woody biomass (natural & crops productivity)
E) Vegetation fractional cover (canopy and field cover)

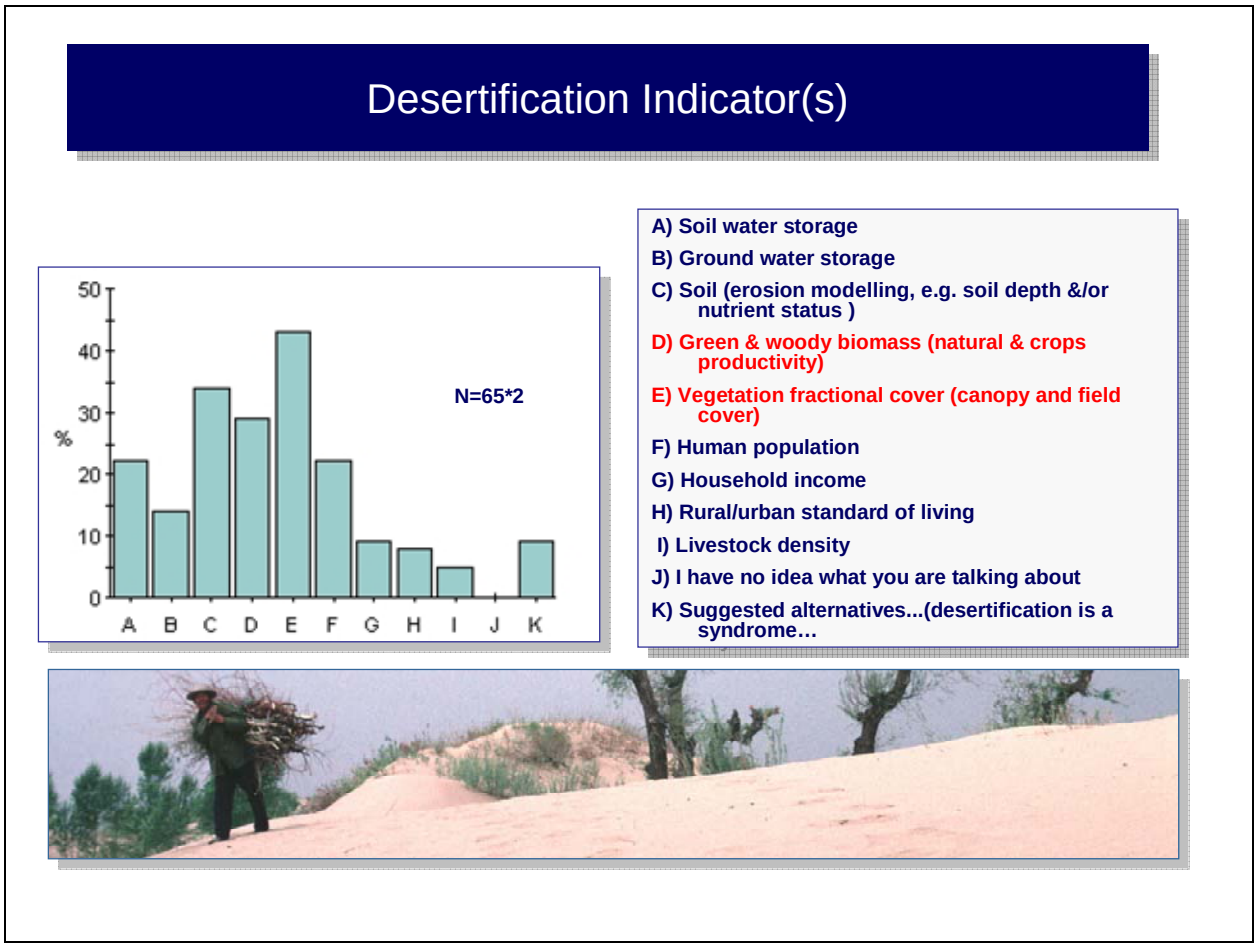

Fig. 1. The result of a survey of DeSurvey desertification concepts in March 2006. Each scientist supplied two votes. 65 out of 90 answered. A vast majority of the DeSurvey scientists preferred vegetation related indicators as proxies for desertification in a theoretical system dynamic modeling attempt. (Photo: U.Helldén, 1994, Korquin Sandy Lands, I. Mongolia, China)

Desertification may express itself in many ways. Serious desertification ultimately results in long lasting and observable loss of vegetation cover and biomass productivity over time and in space.

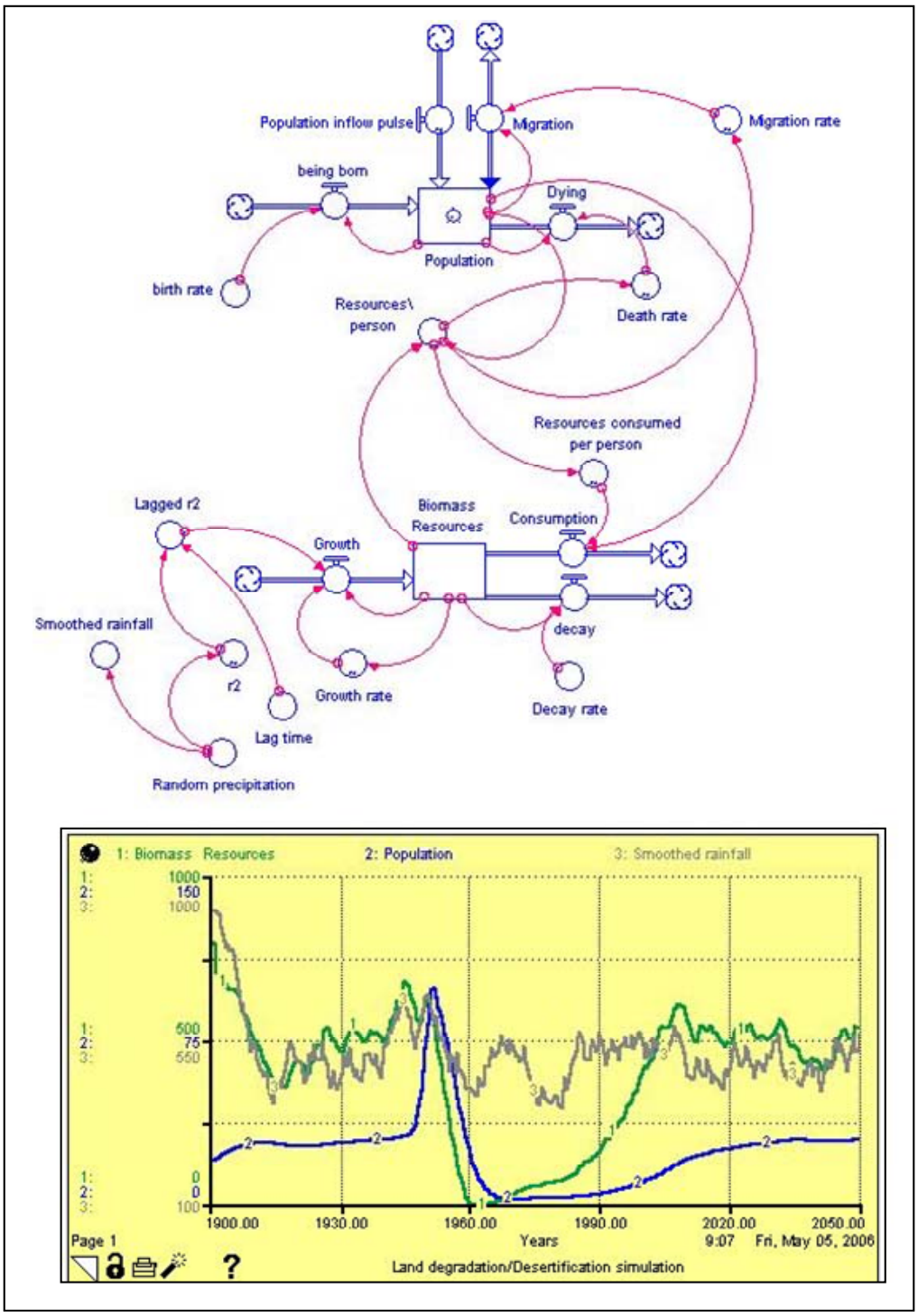

Fig. 2. The LU system dynamic conceptual model simulating desertification 1900-2050 over a 1 km^2 Sahelian arid environment. The graph illustrates the development of 1: Biomass resources (tons), 2: Population 3: Smoothed random rainfall (100-1000 mm), assuming a population perturbation (new settlements, 80 people 1946-1950). Over consumption leads to a collapse of the resources mainly caused by a decreasing regrowth rate modelled as a function of the remaining biomass stock. The growth rate starts decreasing when the biomass stock goes below the 30% threshold (soil water decrease & erosion) and above the 60% level (competition for space and water) (from Thornes and Helldén 2006).

We assume the two main limiting and driving factors of vegetation growth and coverage in the drylands of the world are water availability on the one hand and the production/ management and removal/consumption of biomass through human induced activities (food, fodder and fuelwood/energy production and consumption) on the other hand as indicated by the LU-Conceptual Model of Desertification (Fig. 2). Rural population pressure and dynamics, expressed as population density variation, may be a proxy that can be related to the human impact on vegetation growth and removal (Cf. Fig. 5.1.21 & 5.2.22).

Please refer to Desurvey deliverable 1.3.3.1 by Thornes and Helldén (2006) for a comprehensive summary of prevailing concepts of desertification and a discussion of its syndromes.

2. OBJECTIVES

Long-term trends and variability of vegetation conditions were studied using NDVI data from 1981 to 2003. The overall objective was to develop a simple, yet robust, standardized method for the identification of areas where vegetative production or cover is consistently declining possibly indicating desertification. Further analysis were undertaken to determine whether long-term trends in vegetation dynamics are mainly a function of existing rainfall variability or whether a possible anthropogenic factor exist. The approach was used to identify desertification 'hot-spots' i.e. areas with long-term strong negative (or positive) trends in vegetation productivity that cannot be explained by rainfall variability alone thus pointing towards another, possibly human, causative factor.

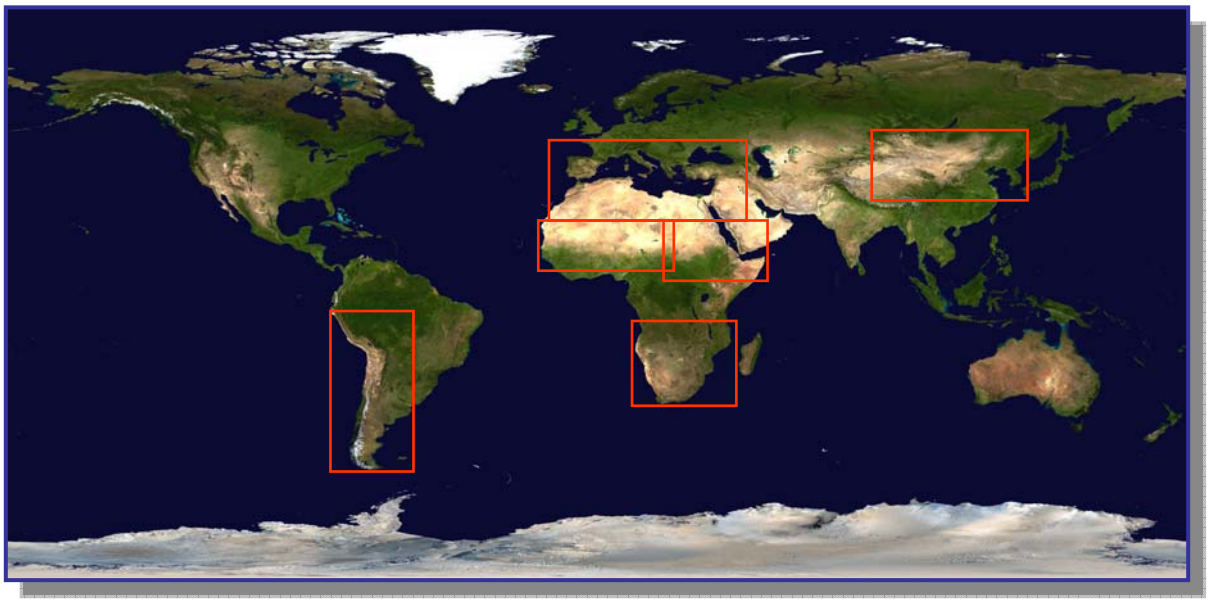

Fig 3. This paper presents results of a study on the use of NOAA AVHRR data for desertification monitoring on a regional-global level. It is based on processing of the GIMMS 8 km global NDVI data set. Time series of annual integrated NDVI and standardized annual NDVI anomalies from the averages of the 1981-2003 period were compared with a corresponding rainfall data set (i.e. 1981-2003) as well as a historical rainfall set (1901-2002).

The areas studied include the Mediterranean basin (Southern Europe and Northern Africa), the Sahel from the Atlantic to the Red Sea, major parts of the drylands of Southern Africa, China and the drylands of South America, i.e. important parts of the desertification prone areas of the world (Cf. fig. 3). However, it is only the Mediterranean basin, Inner Mongolia in China, Senegal in west Sahel and Chile that are of immediate interest for DeSurvey and listed as study objects in the official Description of Work of the consortium.

3. DATA DESCRIPTION

3.1. NDVI data

Time series of the normalized difference vegetation index (NDVI) data were used to investigate long-term trends and variability in vegetation condition. The NDVI is computed as the difference between near infrared (NIR) and red (RED) reflectance divided by their sum:

$$NDVI = (NIR - RED) / (NIR + RED)$$

The NDVI can be understood as a measure of photosynthetic activity, since chlorophyll will absorb red light and leaves will reflect near infrared light and it has been shown that NDVI is sensitive to the presence, density and condition of vegetation. When measured over time the annually integrated NDVI can be used as a proxy for the distribution of annual biom.ass NPP and fractional vegetation cover. The NDVI and its relation to green biomass was first suggested and demonstrated by Rouse et al. (1973) and Tucker (1979).

Landsat satellite based NDVI was early applied in the Sudan for drought impact monitoring and analysis of precipitation-biomass variations and relationships using time integrated NDVI as a proxy for biomass growth (Helldén 1984). NOAA AVHRR based NDVI was early used for assessing interannual vegetation dynamics in relation to precipitation variability in desertification related studies in the Sahel in Africa e.g. by Hielkema et al (1987), Dregne and Tucker (1988), Helldén and Eklundh (1988) and later on by e.g. Helldén (1991), Tucker et al (1991), Tappan et al (1992), Nicholson and Tucker (1998) and Eklundh (1996, 1998). A recent study based on 1 km NOAA AVHRR NDVI data (MEDOKADS) covering Spain was presented by Udelhoven et al. (2007).

NOAA GIMMS NDVI data from July 1981 to December 2003 were downloaded from the Global Land Cover Facility (GLCC) Distributed Active Archive Center at the Goddard Flight Center, Greenbelt USA (http://glcf.umiacs.umd.edu/index.shtml). The NOAA GIMMS NDVI data were generated from the original 1.1 km^2 NOAA AVHRR data as bi-weekly maximum value composites aggregated to an 8 ×8 km pixel resolution. For a full description of the data please refer to Pinzon et al. (2004), Pinzon (2002), Tucker et al. (2005).

The quality and consistency of the GIMMS data were assured by the correction for [a] sensor degradation; [b] sensor inter-calibration differences; [c] solar zenith and viewing angles; [d] volcanic aerosols; [e] atmospheric water vapor and [f] cloud cover (Tucker et

al. 2005). The actual consistency of this correction procedure was tested by looking at the temporal variation in NDVI over presumably invariant desert targets. Figure 4 shows the NDVI time series from the two targets and though the slopes are very close to zero it is worth noting that while the Taklimakan Desert target (40N; 85E) is statistical insignificant the downwards slope for the Arabian Desert (25N; 40E) target is actually statistical significant ($p<0.1$). Still, these indeed small residual trends are assumed to be insignificant relative to NDVI changes caused by human and/or biophysical factors.

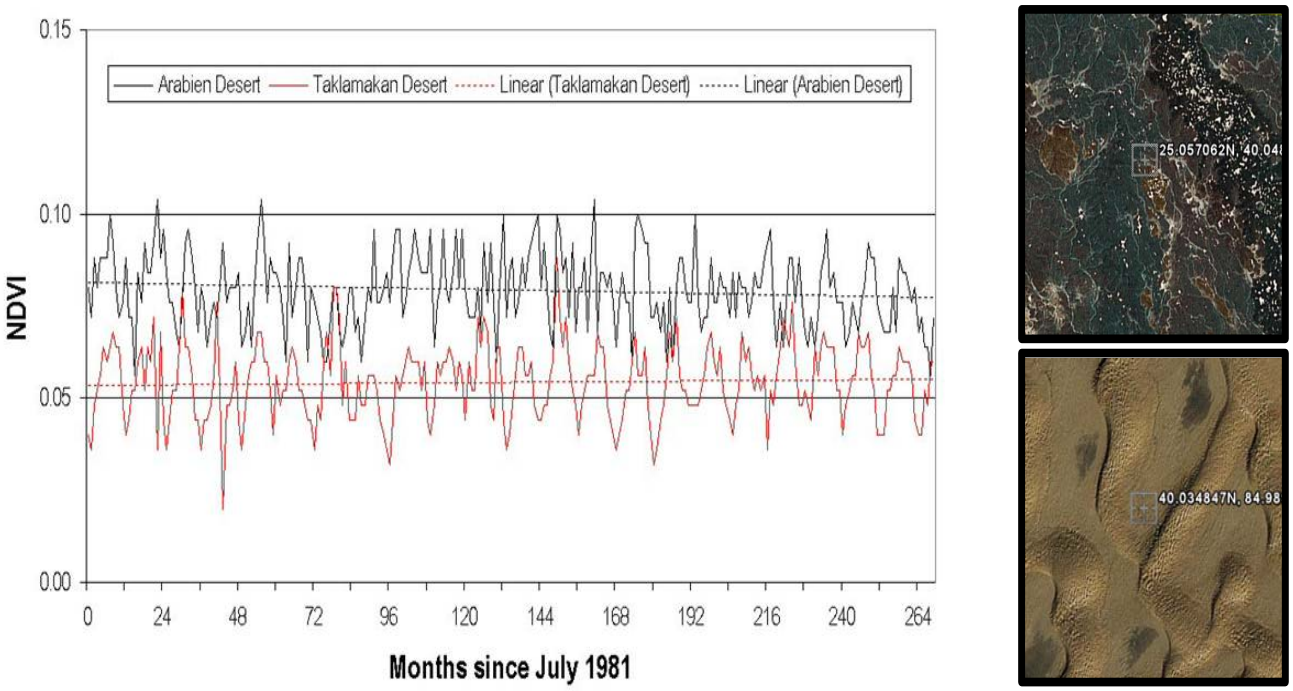

Fig. 4. NDVI temporal development curves over two desert targets. Note: attempted replication of an evaluation documented by Tucker et al. (2005).

In order to reduce the data material and to obtain an improved cloud screening the bi-weekly GIMMS NDVI data were further decomposed into monthly values using a maximum value compositing routine as described by Holben (1986). For additional discussions of the GIMMS data correction please refer to UTRIER (2007).

3.2 Precipitation data

Three types of rainfall data were initially considered in the study.

- [i] long-term historical rainfall station measurements from the Global Historical Climatology Network (GHCN) (1697-2004).
- [ii] gridded 2.5^{0} rainfall data from the Global Precipitation and Climatology Project (GPCP) derived by merging information from low-orbit-satellite microwave data, geosynchronous-orbit satellite infrared data, and rain gauge observations (1979-2005).
- [iii] high resolution gridded 0.5^{0} precipitation data from the Climate Research Unit (CRU), University of East Anglia, constructed from meteorological stations (1901-2002).

All data sets have their strengths and weaknesses.

3.2.1 GHCN climate data

The Global Historical Climatology Network (GHCN) is a comprehensive global climate data set comprised of surface station observations of precipitation and temperature on a monthly basis. GHCN is produced jointly by the National Climatic Data Center, Arizona State University, and Carbon Dioxide Information Analysis Center at Oak Ridge National Laboratory.

The current "GHCN version 2" data set was released in the late 1990s and continues to be updated. For this study the GHCN version 2 data set had station data from as early as 1697 and up until 2004. Version 2 has significant improvements over the previous version 1 data set including more data (e.g., the precipitation data set has data from over 20,000 stations), better Quality Control, homogeneity adjustments, and a wider selection of metadata. Quality control included visual inspection of graphs of all station time series, tests for precipitation digitized 6 months out of phase, tests for different stations having identical data, and other tests.

Despite the improvements though, the GHCN version 2 data set suffer from several problems and shortcomings in relation to the present study. First of all, it is all too evident that the station data are not continuous i.e. whole years as well as monthly values are missing for most stations. Actually out of approximately 1000 stations located in the Mediterranean only 5 stations had a complete precipitation record over the cause of the GIMMS data period (i.e. from July 1981 to December 2003), 49 stations had five or less missing months while 70 stations had 10 months or less without any data.

3.2.2 Global Precipitation Climatology Project (GPCP, 2.5^0 spatial resolution)

In light of the obvious problems with the GHCN data alternative indications of precipitation were required. To this end the usefulness of data from the Global Precipitation Climatology Project (GPCP) was investigated. GPCP is an element of the Global Energy and Water Cycle Experiment (GEWEX) established by the World Climate Research Program (WCRP) in 1986 with the initial goal of providing monthly mean precipitation data on a 2.5°× 2.5° latitude-longitude grid. Monthly mean precipitation estimates are being produced beginning in 1979 and going through 2005. The GPCP has accomplished this by merging infrared and microwave satellite estimates of precipitation with rain gauge data from more than 6,000 stations. Infrared precipitation estimates are obtained from GOES (United States), GMS (Japan) and Meteosat (European Community) geostationary satellites and National Oceanic and Atmospheric Administration (NOAA) operational polar orbiting satellites. Microwave estimates are obtained from the U.S. Defense Meteorological Satellite Program (DMSP) satellites using the Special Sensor Microwave Imager (SSM/I).

The benefits of GPCP are their spatial nature and full correspondence to the GIMMS data time series but there are certainly also problems and shortcomings with this data source in relation to the present study. First, data are distributed in a 2.5°× 2.5° grid. This corresponds to approximately 275 km, which is a very coarse scale in relation to the 8 km grid provided by the GIMMS data. Moreover, local precipitation differences cannot be discerned in the GPCP data due to the coarse resolution. Irrespectively of these problems,

the GPCP data has found their usefulness in global climatic studies as well as in studies of regional vegetation dynamics (Herrmann et al. 2005).

3.2.3 GHCN vs. GPCP

Figure 5 illustrates the comparison of GHCN and GPCP data at four selected stations. The co-variation between the two data sets is quite good although there is a clear tendency of GPCP to over-estimate at lower amounts of rainfall. So despite the fact station data are naturally believed to be the most accurate source of rainfall data the similarities found between the two data sets here suggests that GPCP will provide a sufficient proxy for recent spatio-temporal trends in rainfall. We decided not to use the GHCN station data in the following climate-NDVI study but to stick to the gridded precipitation data to simplify the spatial analysis.

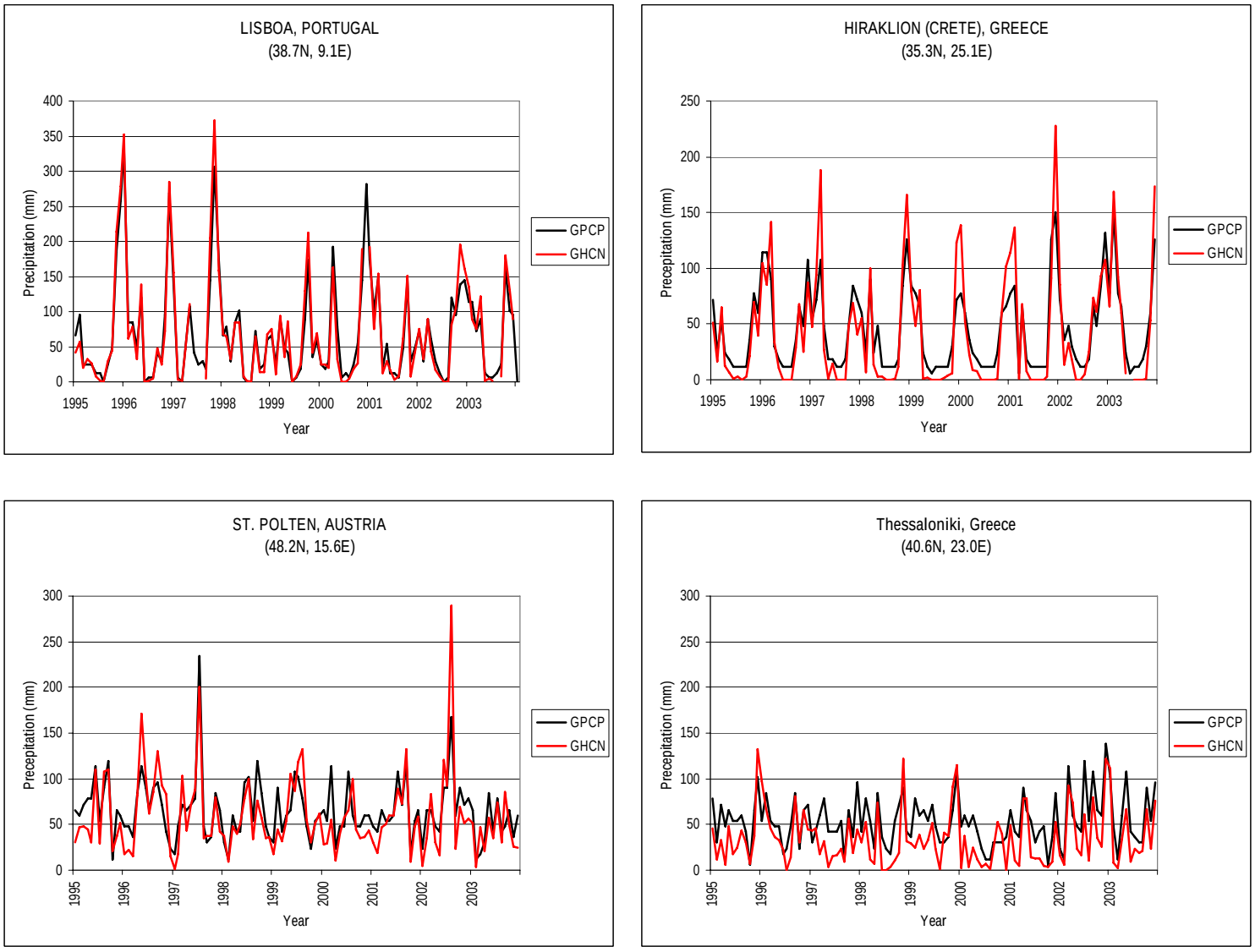

Fig 5. The relationship between GHCN and GPCP for selected stations. The Pearson correlation coefficients (r) for the entire time-series from 1979 to 2003 are as follows Lisboa (r=.95), Crete (r=.88), St. Polten (r=.77) and Thessaloniki (r=.72).

3.2.4 CRU gridded climate data [0.5^{o} spatial resolution] .

A high resolution gridded dataset from the Climate Research Unit (CRU), University of East Anglia, represented the third climate dataset considered for this study. CRU-TS 2.1 is a database of monthly climate observations constructed from meteorological stations. The database includes nine climate variables (daily mean, minimum and maximum temperature, diurnal temperature range, precipitation, wet day frequency, frost day frequency, vapor pressure and cloud cover) and extends over the global land surface. The database is checked for inhomogeneities in the station records using an automated method that refines previous methods by using incomplete and partially overlapping records and by detecting inhomogeneities with opposite signs in different seasons. The method includes the development of reference series using neighboring stations. Information from different sources about a single station may be combined, even without an overlapping period, using a reference series. Thus, a longer station record may be obtained and fragmentation of records reduced. The reference series also enables 1961–90 normals to be calculated for a larger proportion of stations. The climate variables and station anomalies are interpolated onto a 0.5° grid covering the global land surface (excluding Antarctica) for the period 1901–2002.

CRU-TS 2.1 and time-series analysis

For this study both the precipitation and the surface temperature data was requested and obtained from CRU (http://www.cru.uea.ac.uk/). These data are referred to as CRUP (Climate Research Unit Precipitation) and CRUT (Climate Research Unit Temperature). There are two critical points as to the usefulness of CRU-TS data for time series analysis:

1. The grids are based on raw station data. If in July 1907 there is a grid-point in central Africa that is greater than 1200 km from the nearest station with temperature measurements for July 1907, that grid-point for July 1907 will be given an imposed value. The imposed value will be the average of all July temperatures at that grid-point from 1961-90. This feature is called 'relaxation to the climatology', and the feature applies mostly early in the 20th century, outside the 'developed world', and for less-well-reported variables; for these cases less raw station data are available. 'Relaxation to the climatology' was included to ensure that the data-set is complete in both space and time. The feature is based on the assumption that if there is no time-specific information available, the best estimate for that moment in time is a long-term average. The term 'best estimate' is important: CRU TS 2.1 is the best estimate of the spatial pattern of climate at each moment in time. Although this is a valuable feature, it may be problematic when examining changes at a grid-box, or for a region. The effects of this feature can be found by inspecting the time-series at the level of the grid-box to see whether there are periods when each January (or each February, or ...) has the same value. Obviously, if a grid-box includes this feature, then calculating the least-squares regression line for 1901-2002 is meaningless and misleading!

2. Each monthly grid is an interpolation based on the set of stations available at that moment in time. From one month to the next, the network of available stations will change. This is because the availability of data from a particular station tends to fluctuate over time. Again, this interpolation method was adopted to give a best estimate of the spatial pattern of climate at each moment in time. However, it does mean that the changes over time at an individual grid-box will not be due solely to genuine changes in climate, but also to fluctuations in the network of stations. The effect of such fluctuations is minimized by interpolating station anomalies rather than station absolute values, but cannot be entirely

removed. Where the station network is dense, the effect of any individual station entering or leaving the network will be minimal. However, where the station network is sparse, the presence or absence of a single station may have a significant effect on the time-series at a nearby grid-box. The effect on a time-series analysis might be thought of in terms of the proportion of the variability and trend at a grid-box that is contributed by this feature. This effect can be reduced by increasing the scale of aggregation (i.e. the number of grid-boxes that are being averaged into a region). The reduction is achieved because the station network is being made denser relative to the number of regions. However, even increasing the scale of aggregation cannot entirely eliminate this effect.

So the bottom line is that the CRU-TS 2.1 data is correct as it stands, in that it is the result of accurately carrying out the method adopted, and that it accurately reflects the real-world experience, as far as the methods and data can tell. A full documentation of the CRU-TS data was given by Mitchell and Jones (2005).

3.2.5. CRUP vs. GPCP

Figure 6 illustrates the comparisons between CRUP and GPCP. The comparison is based on mean monthly rainfall in the dryland zone ($0.1 < NDVI < 0.5$) as estimated by CRUP and GPCP respectively.

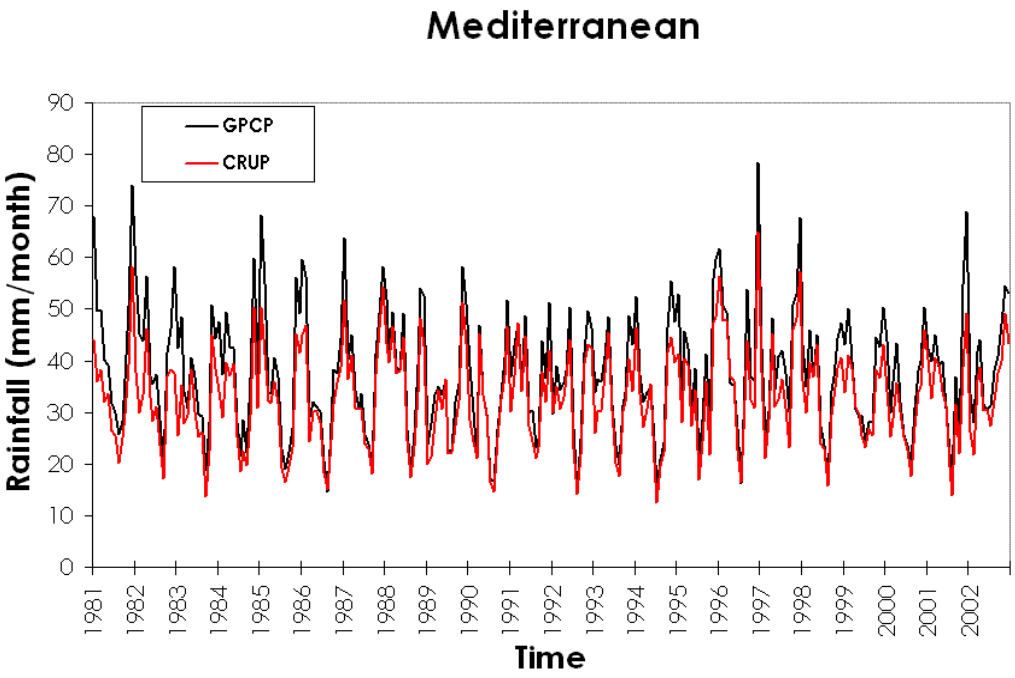

West Africa

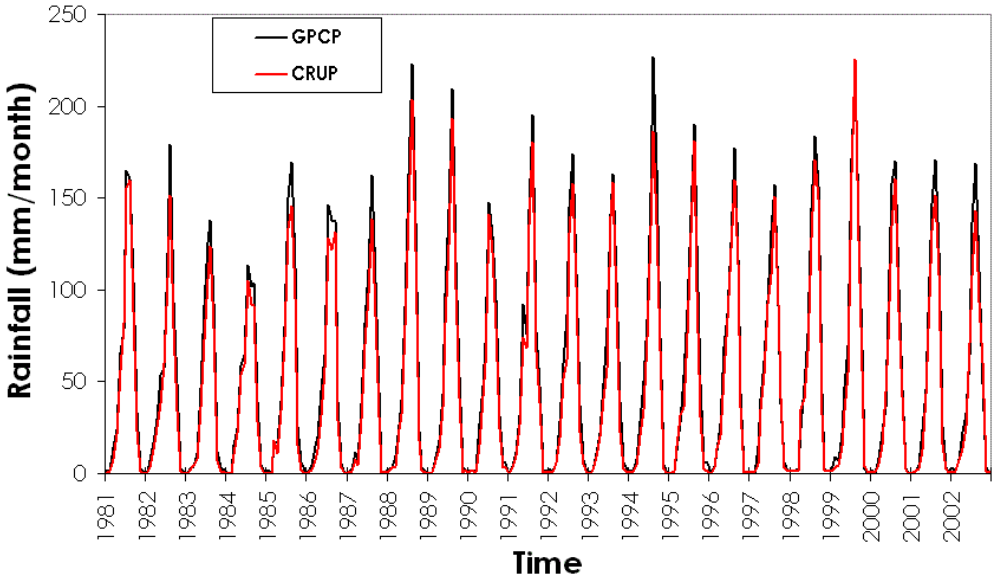

East Africa

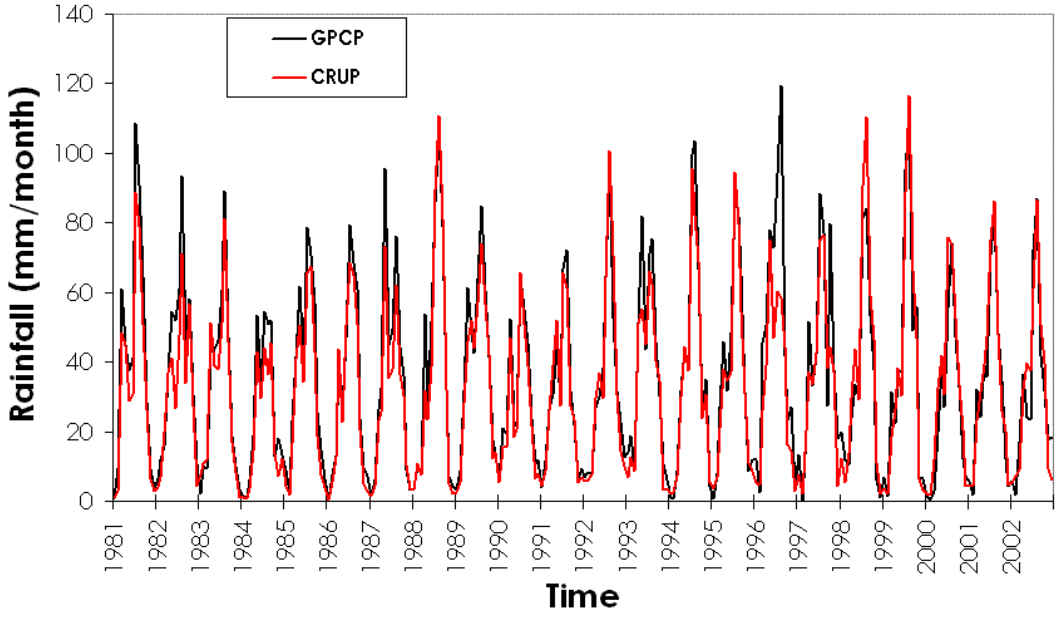

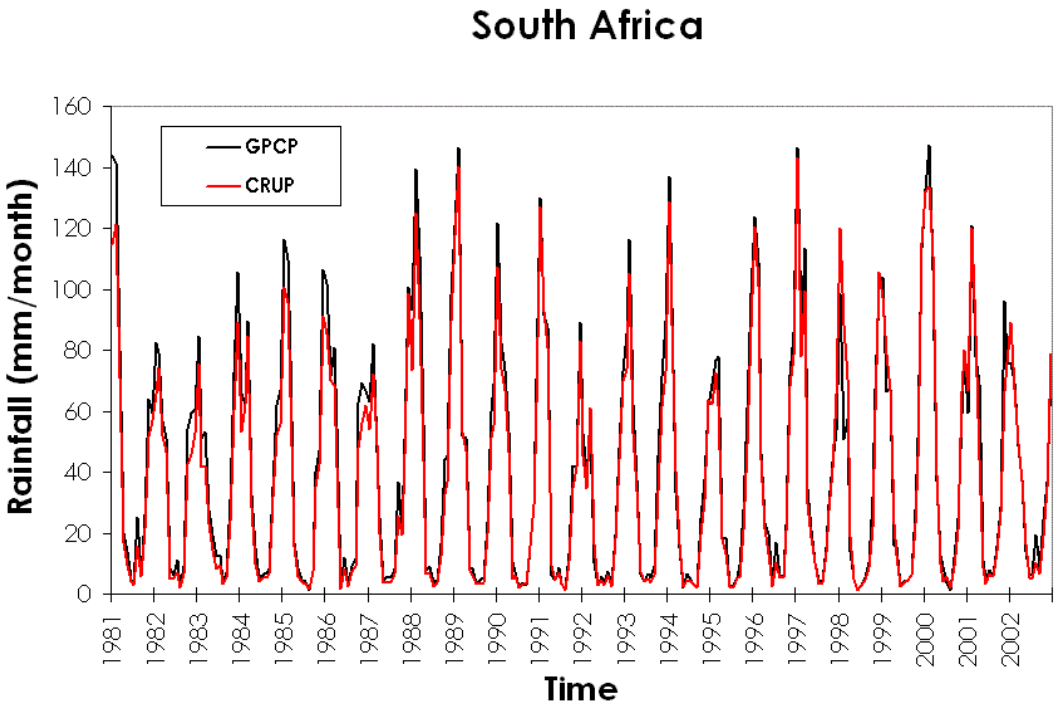
South Africa
GPCP
CRUP
Rainfall (mm/month)
Time
0
20
40
60
80
100
120
140
160
1981
1982
1983
1984
1985
1986
1987
1988
1989
1990
1991
1992
1993
1994
1995
1996
1997
1998
1999
2000
2001
2002

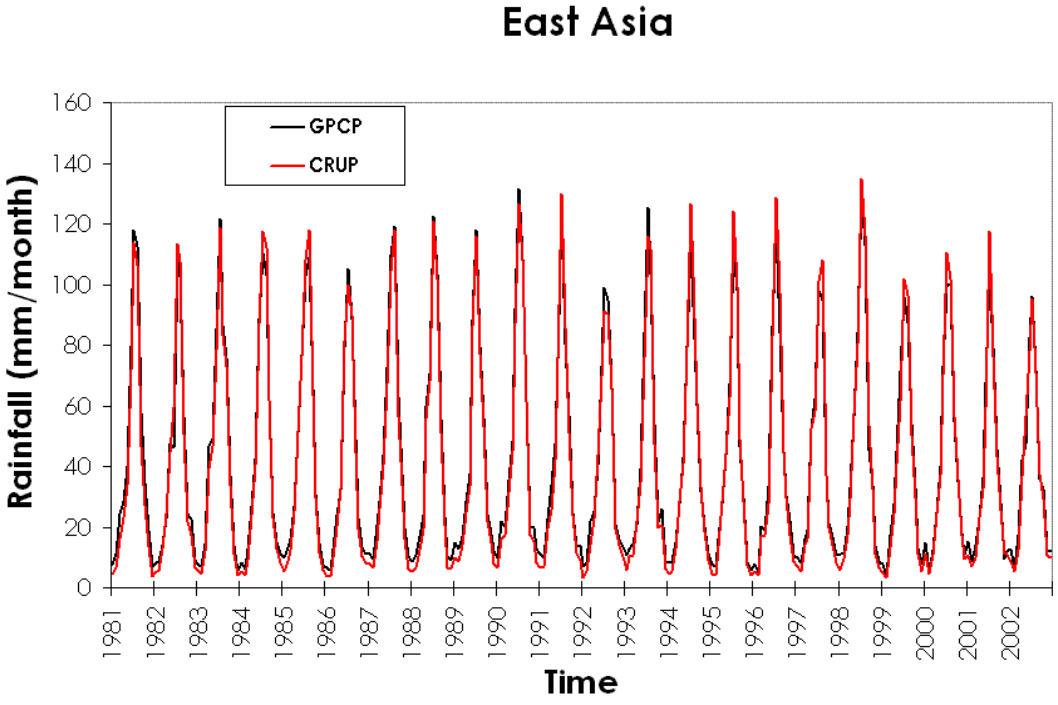
East Asia
GPCP
CRUP
Rainfall (mm/month)
Time
0
20
40
60
80
100
120
140
160
1981
1982
1983
1984
1985
1986
1987
1988
1989
1990
1991
1992
1993
1994
1995
1996
1997
1998
1999
2000
2001
2002

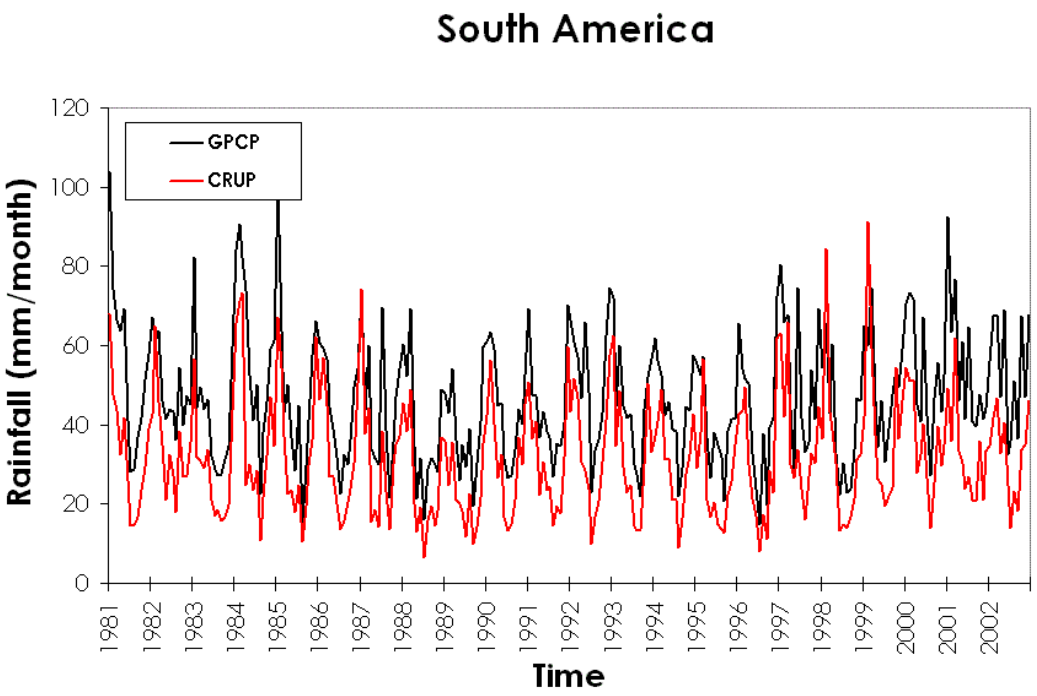

Fig. 6. The relationship between CRUP and GPCP (mean monthly values for the area defined by 0.1<NDVI<0.5).

The comparison between CRU-TS and GPCP do indeed demonstrate good correspondence on the regional level and as such they could be used in a complimentary way. For example, for the period 1981 to 2002 the parallel usage of the two datasets may be used to indicate areas where either [i] CRU-TS are problematic, [ii] GPCP are problematic or [iii] both datasets are problematic. For historical analysis drawing on the full length of the CRU-TS data set visually inspections of any grid boxes of particular interest (e.g. a Hot Spot region) is recommended in order to detect periods of prolonged 'relaxation'.

4. METHODOLOGICAL REVIEW

4.1 Data integration

In order to reduce the amount of data to be processed long-term NDVI and rainfall climatologies were created by integrating monthly NDVI and rainfall values over time. Rather than using the calendar year as the integration period both NDVI and rainfall was integrated over their respective seasons as determined from monthly time series plots (Fig. 7-8).

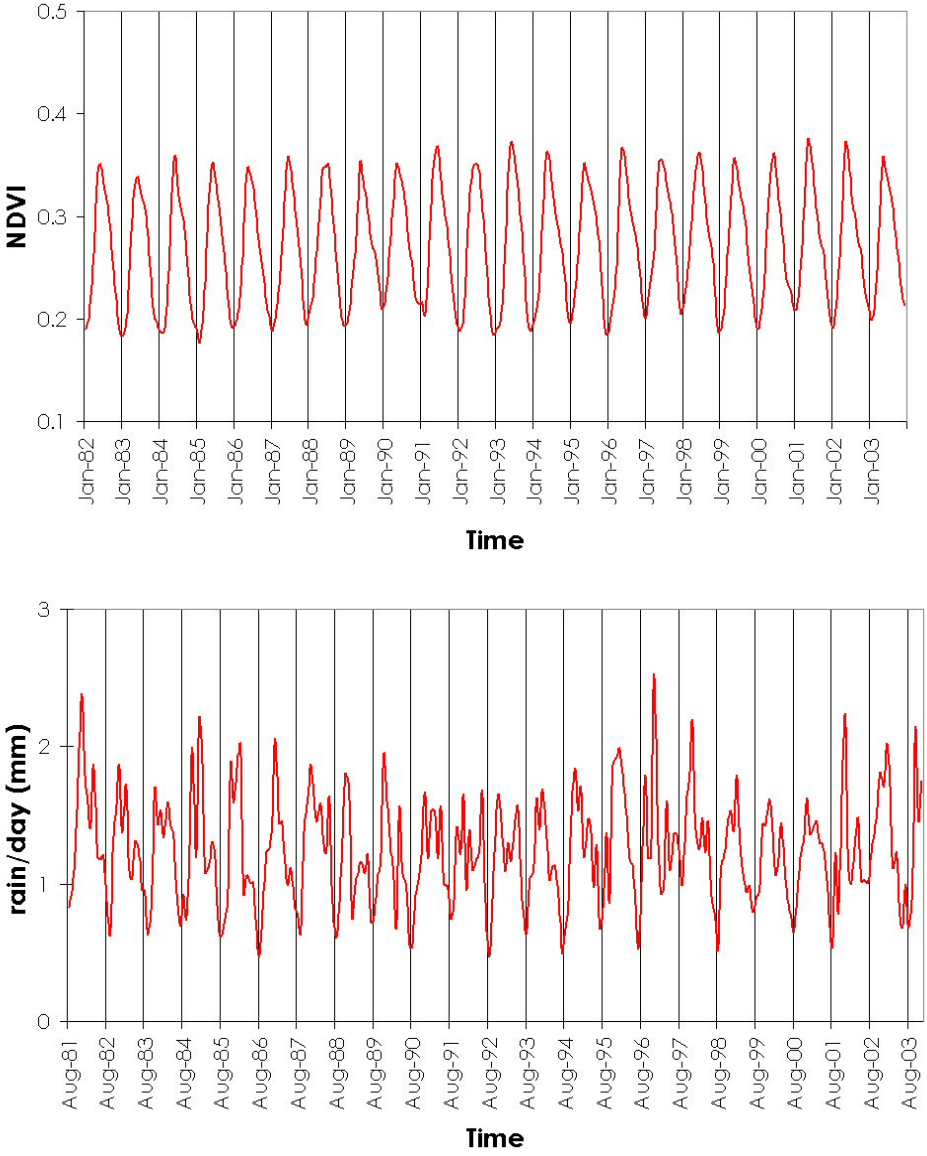

Figure 7. Example of monthly development curves of NDVI and rainfall (Mediterranean basin).

The time series plots (cf. figure 7) represent the temporal development curves of monthly NDVI and rainfall as averaged within the desertification prone areas being defined as those parts of the study regions that had a long-term (1981-2003) mean monthly NDVI value between 0.1 and 0.5.

The seasons or integration periods were based on a full year of data (i.e. 12 months) and defined as the time period between the approximate locations of two local minimum values. It is worth having in mind that the integration periods for NDVI and rainfall may not necessarily be the same but depends on the time-lag between the response of vegetation to rainfall which vary by region as a function of both bio-physical and human factors.

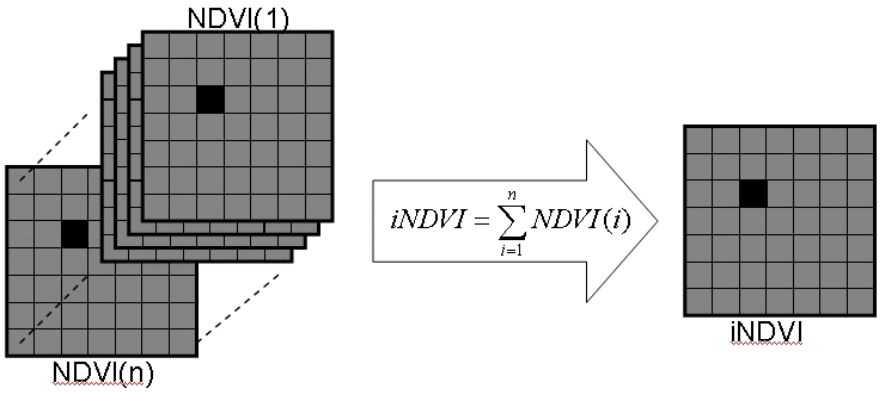

Figure 8. Illustration of the per-pixel integration routine applied in this study.

4.2 Vegetation trend analyses

One of the advantages of NDVI is that it allows for reliable monitoring of variations in phenological and biophysical vegetation parameters. Several studies have focused on using the NDVI to monitor the biomass production of a given area. It is commonly agreed that the net primary production (NPP) of a given area, or pixel, can be estimated by using the annual temporally integrated vegetation index - iNDVI (e.g. Hielkema et al., 1987; Diallo, 1991; Rasmussen, 1998a, 1998b; Ricotta et al., 1999; Maselli, 2000). It has not been the purpose of this study to attempt to calibrate the observed iNDVI measures into NPP, but rather to detect temporal trends and deviations (anomalies) in the evolution of vegetation productivity. As such, iNDVI expressed as the temporal integrated vegetation index is used as a proxy for vegetation productivity. A simple and efficient way to analyze change in temporal sequences of satellite data is using a per pixel linear least square regression techniques (Fuller 1998; Runnström 2000; Rigina and Rasmussen 2003). The linear trend curve of each pixel over time can be interpreted as a measure of declining or increasing vegetation productivity for that pixel.

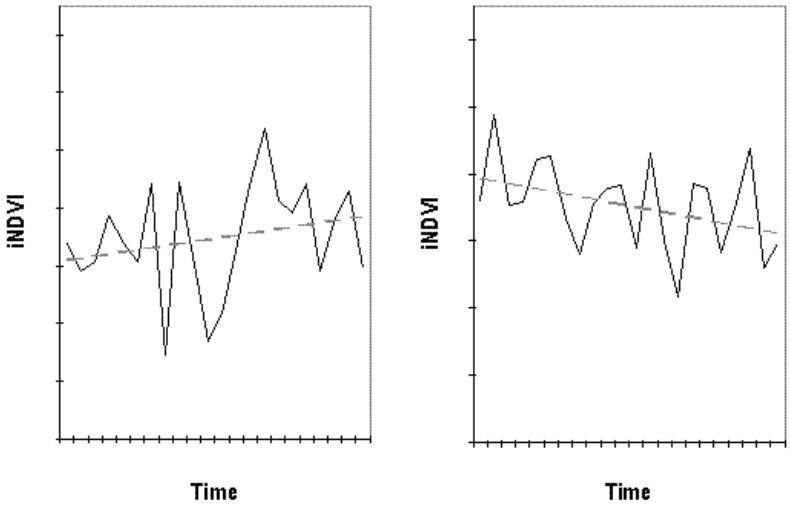

Fig. 9. Illustration of temporal trends in iNDVI. Pixel with negative trend in vegetation productivity (left) and pixel with positive trend in vegetation productivity.

Annual measures of vegetation productivity were computed by integrating NDVI over the phenological year for each year of available GIMMS data. Linear least square regression was used to compute the 22-year trend line for each single pixel.

The simple linear regression given by:

$$Y = a + \beta * X$$

Where Y is the dependent variable (i.e. NDVI), X is the independent variable (i.e. time), a is the intercept i.e. it represent the value of Y when X = 0, the value of β represents the slope of the line that provides the best linear estimate of Y from X change or the change in Y associated with one unit increase in X. β is also referred to as the regression coefficient. The significance of β, i.e. the chance that the estimated β is actually different from 0, can be estimated using a t-test:

$$t = \beta - 0 / std.\ \beta$$

The problem with this test, however, is that the t-value will get high if the standard error (std.) is low. Therefore the t-test will over-reject the null hypothesis in cases where the time-series is characterized by high standard deviations such as when abrupt changes occur during the time series. Similar you will come to put too strong emphasis on time-series where the slope is very small, yet significant due to only minor variations around the mean.

Analogous to this is the coefficient of determination (r^2), which provides a measure of the explanatory power of the linear model. Still, the r^2 value is of little importance when looking at temporal trends because the mission is not to be able to predict a certain NDVI value on the basis of a given time period. In fact no one will expect a simple temporal linear function to be able to predict highly erratic inter-annual NDVI values.

Others have suggested using non-parametric tests to determine whether a time-series is characterized by drastic disruption leading to higher standard deviations and lower r^2 values. Such tests can be justified by the wish to look for certain 'chock' events (e.g. fires). Yet, this type of tests will tend to overlook events characterized by more gradual changes (e.g. soil nutrients) and as such they do not conform to a more generic framework for assessing vegetation trends in desertification prone areas.

Actually these considerations suggest an approach where the magnitude of the slope (i.e. the inclination of the slope expressed in either absolute or relative terms) rather than the significance of the slope (or the r^2) is used as the preferred measure for the vegetation trends through the investigated time period. The problem with this approach is its sensitivity to outliers or extreme values, which can significantly alter the inclination of a slope line. However, the improved processing used to prepare the GIMMS data (Tucker et al. 2005) as well as the relatively long-time series (+20 years) is significantly going to depress those influences and one can expect that any larger area showing a considerable change in absolute magnitude is likely to reflect a real surface vegetation trend. The initial value, however will always exhibit strong control over the magnitude of β (and so may the end value) so any steep slopes should be carefully inspected with respect to start (and end) values.

Autocorrelation is a common problem in time-series analysis. Auto-correlation refers to the fact that observations in a time series are rarely independent. While this is very much the case for monthly values which have a strong seasonal cycle the problem is less apparent in an annually merged data set.

4.3 Vegetation versus Rainfall analysis

Since rainfall in drylands represents an important limiting factor for vegetation growth, analyses were undertaken in order to investigate to what extent rainfall variability can explain NDVI variability.

The coefficient of determination (r^2) and its associated Pearson correlation coefficient (r) are the single most important measures of the ability to predict NDVI as a function of rainfall. If rainfall lets you predict NDVI with a high degree of confidence we may argue that the human factor are of minor importance though it is recognized that both factors may interact in a complex feedback system. Nevertheless, we need to control trends in vegetation dynamics for the influence of rainfall before we can elucidate on the possible human influence.

4.4 NDVI and Rainfall anomalies

Measurements from different distributions, describing different variables and populations, can be standardized (normalized) in order to provide a way of comparing them that includes consideration of their respective distributions. This is carried out by transforming the original observations into z-scores which are expressed as standardized deviations from their mean. The z-core distributions always have a mean of 0 and a standard deviation equal to 1 (Abdi 2007).

The **z-score,** also called the **standard score**, the **normal score**, the **standard normal variate**, the **standard normal deviate** or the **standardized score** is a dimensionless quantity. It is derived by subtracting the population mean from an individual raw score and then dividing the difference by the population standard deviation (Snedecore and Cochran 1980, Hammond & McCullagh 1982).

The z-score indicates how many standard deviations an observation is above or below the mean. In other words, it represents the distance between the raw score and the population mean in units of the standard deviation. *Z* is negative when the raw score is below the mean, positive when above.

The standard score is: $$z = \frac{x - \mu}{\sigma}$$

where:
x is a raw score to be standardized
σ is the standard deviation of the population
μ is the mean of the population.

The annual variability of NDVI and rainfall as well as their spatio-temporal relationship was investigated by calculating yearly NDVI and rainfall anomalies to allow for comparative analysis expressing both variables in terms of data converted to z-scores.

The z-scores were calculated on a per pixel basis to assess each pixel´s annual deviation from its long term 1982-2003 period pixel mean.

The z-score of a given observation also provides insight on how "typical" this observation is to the population. For example, by empirical rule, if data follow a bell-shaped curve (i.e. a normal distribution), then approximately 95% of the data should have the z-score between -2 and 2. Hayes (2000) has proposed a typology for interpreting rainfall z -scores (see Table 1)

Table 1. A nominal classification scheme of rainfall anomalies.

Above 2.0	Extremely wet
Above 1.5	Very wet
Above 1.0	Moderately wet
Between –1.0 and 1.0	Near normal
Less than –1.0	Moderately dry
Less than –1.5	Severely dry
Less than –2.0	Extremely dry

The anomalies (z-scores) have certain advantages over absolute values such as annual integrated NDVI and total annual rainfall. First of all and due to the standardization procedure the z-scores represent an efficient way to visually compare the spatial relationship between NDVI and rainfall. Further standard analysis of the relationship between NDVI and rainfall tend to be influenced by the presence of spatial auto-correlation (i.e. the phenomenon where locational similarity is matched by value similarity), which in essence means that they are merely expressing an underlying geographical relationship rather than a true relationship of dependence. The z-scores methodological approach provides a very robust and valid estimate of temporal (rather than spatial & geographical transect driven) NDVI and rainfall variability.

The method was successfully demonstrated and proposed by Helldén and Eklundh (1988) in a desertification and drought impact study on Ethiopian precipitation and NDVI time series relationships.

4.5 Residual analysis

The resulting regression equation represents the statistical association between the dependent variable (i.e. iNDVI) and the independent variable (i.e. annual Rainfall) and allow for the prediction of iNDVI as would be expected given the observed values for annual rainfall. The model residuals, (i.e. the difference between observed and expected iNDVI) was computed for each pixel and subsequently inspected for any systematic trends that could invalidate the initial model specification. Of particular concern when analyzing temporal data is the presence of any temporal trend in the residuals. If the residuals exhibit a significant temporal trend it indicates the presence of an unidentified and unmeasured temporal determinant. Alternatively if the residuals are free from any temporal trend it is likely that there are no other factors responsible for the residual trend, indicating that rainfall remain the major explanatory factor with respect to trends in vegetation dynamics.

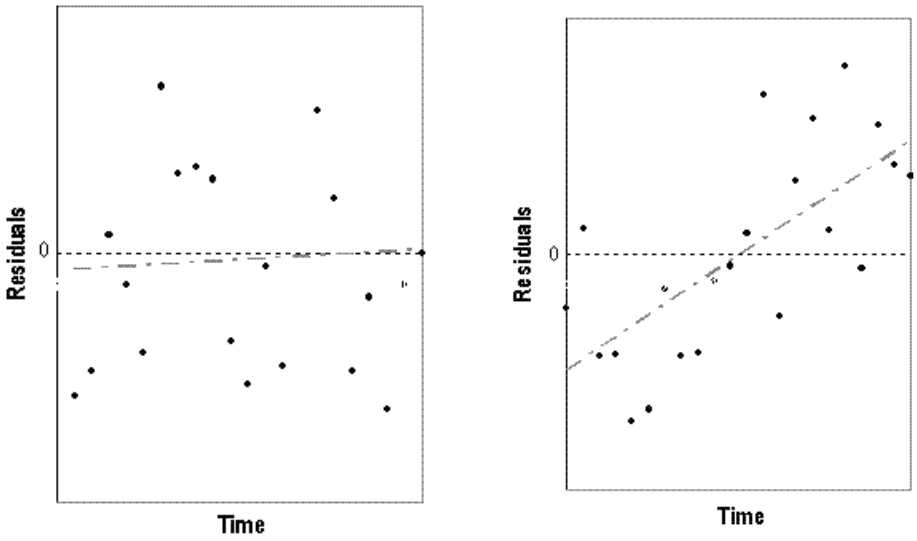

Fig. 10. Illustration of residual plots. Pixels where residuals distribute evenly above and below zero (left) and pixels with a clear systematic pattern in the residuals suggesting that an additional important explanatory variable is missing (right).

4.5.1. Hot Spot analysis. Desertification hot spots were identified by manually identifying and delineating areas with the largest negative (and positive) residual trends. We extracted the area mean iNDVI and anomalies from these areas for each year in the times series (1981-2003) and compared them to a historical climatology (1902 - 2002) in order to evaluate whether the deviating trend in vegetation productivity could have been inherited from the past climate or whether more recent and possible human factors could be the cause.

The procedure can be carried out automatically by allowing the user of the system to define the NDVI residual threshold values of interest, followed by a threshold/density slicing based classification leading to the machine plotting of the anomaly areas to be further investigated. The corresponding rainfall anomalies can be identified in the data base and plotted together with the NDVI anomalies for further analysis and considerations on an annual basis for the period of interest.

Fig. 11. A “Hot Spot” in the Sudan. (Photo: U. Helldén, 1976).

5. RESULTS

5.1. THE MEDITERRANEAN BASIN

5.1.1. Mediterranean basin overview

Maps of national borders, mean monthly NDVI and mean annual rainfall are illustrated below. From the maps it can be seen that the drylands (0.1 < NDVI < 0.5) within this region are mainly confined to the Iberian peninsular, the Middle East including Turkey and the Maghrebian countries[1].

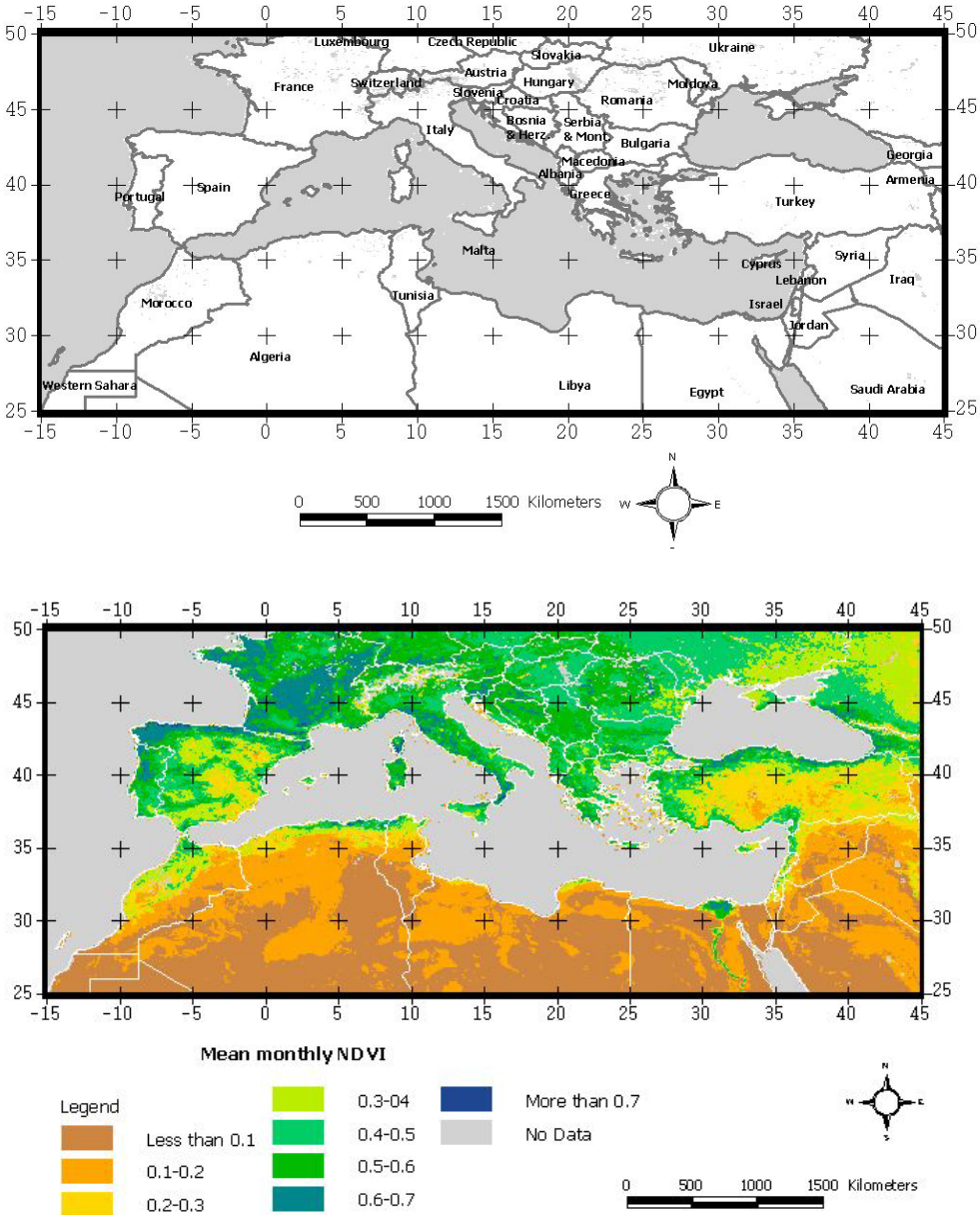

Figure 5.1.1 Country overview (top) and the mean monthly NDVI based on data from 1982 to 2003 (bottom).

[1] The Maghrebian countries include Morocco, Algeria, Tunisia, Libya

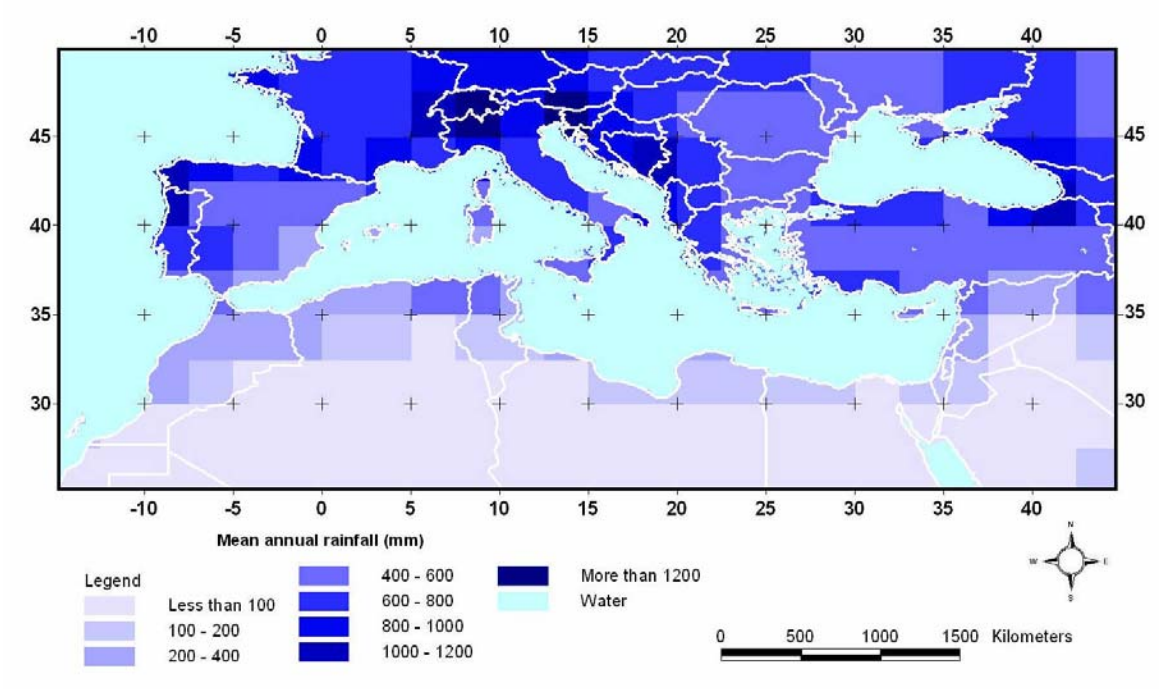

Figure 5.1.2. Mean annual rainfall based on 2.5 degree (~ 275 km) gridded rainfall data from 1982 to 2003.

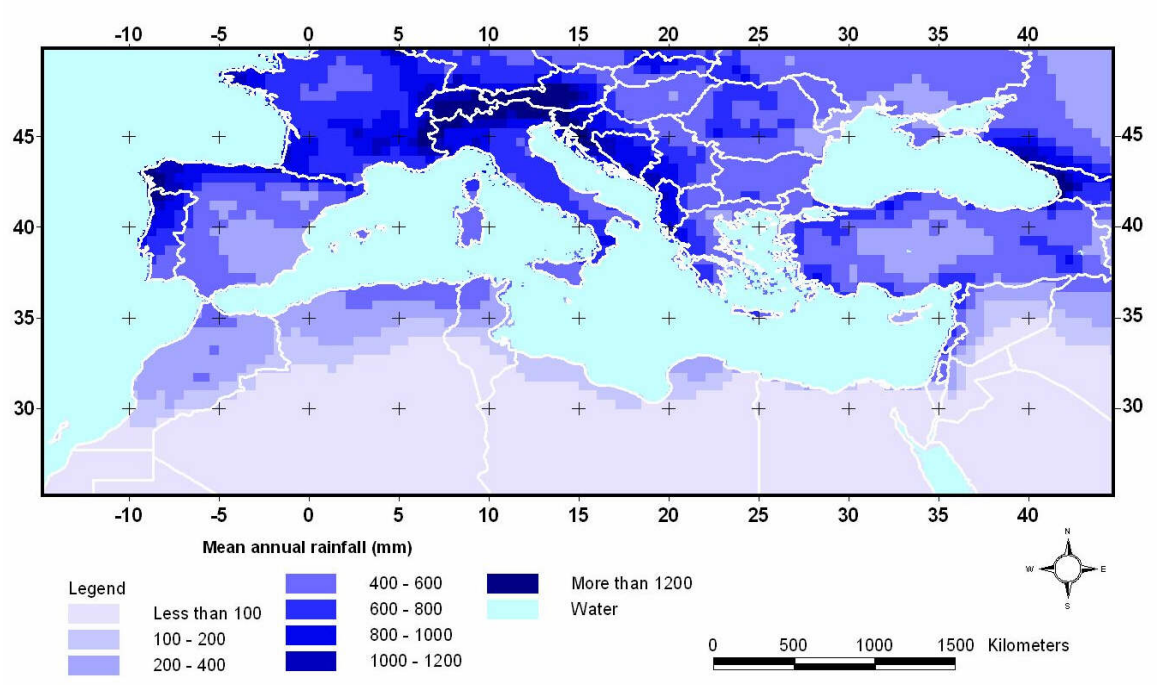

Fig. 5.1.3. Mean annual rainfall based on 0.5 degree (~55 km) gridded rainfall data from 1982 to 2002.

Inspection of time-series plots of both rainfall and NDVI revealed that the appropriate seasons for the drylands (i.e. the area delineated by a minimum of 0.1 and a maximum of

0.5 NDVI based on the long-term monthly average) of the Mediterranean Sea was “August to July” and “January to December” for rainfall and NDVI respectively (Figure 5.1.4).

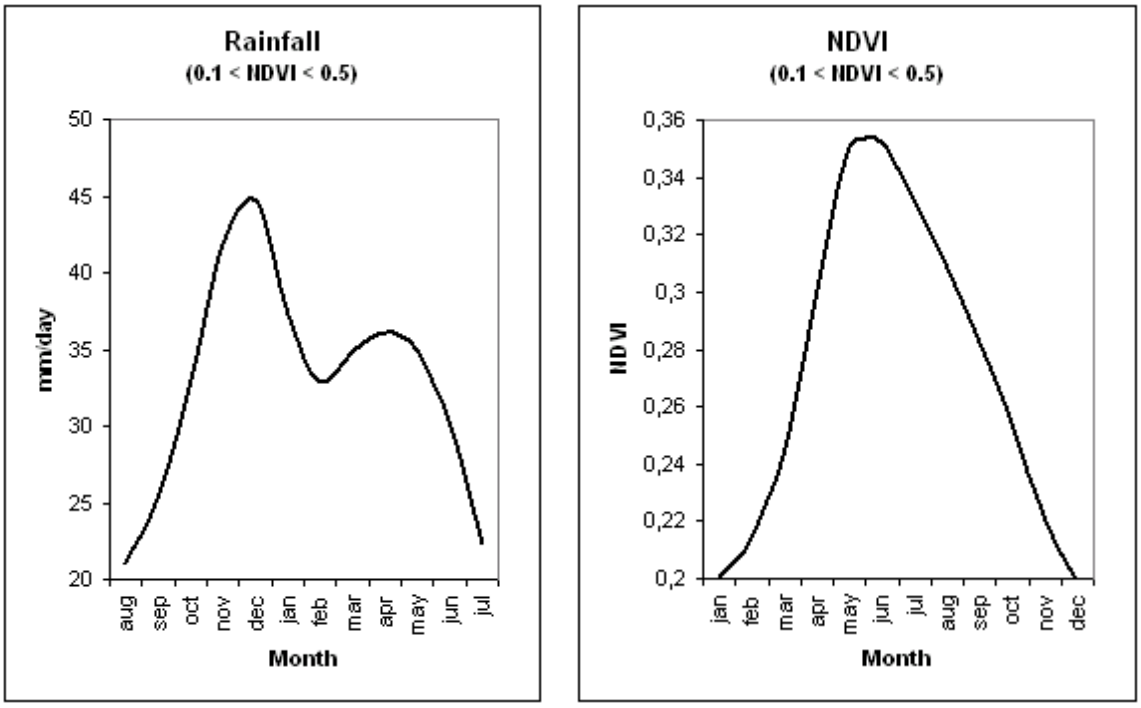

Figure 5.1.4. Monthly time-series plots of rainfall (left) and NDVI (right). The displayed values are mean values as calculated from the area defined by $0.1 \leq NDVI \leq 0.5$. From the time-series plots it appears that rainfall tend to have a local minimum in August while NDVI has its minimum in January.

Consequently total annual rainfall was calculated by summarizing rainfall received within the months from August and until July the following year. Similar the annual vegetation productivity was estimated by integrating NDVI over the months from January to December as indicated in the chapter on methodology and data integration (Cf. Fig 7).

5.1.2. Vegetation trend analysis

The following figures summarize the results of the trend analysis approaches previously described under methods.

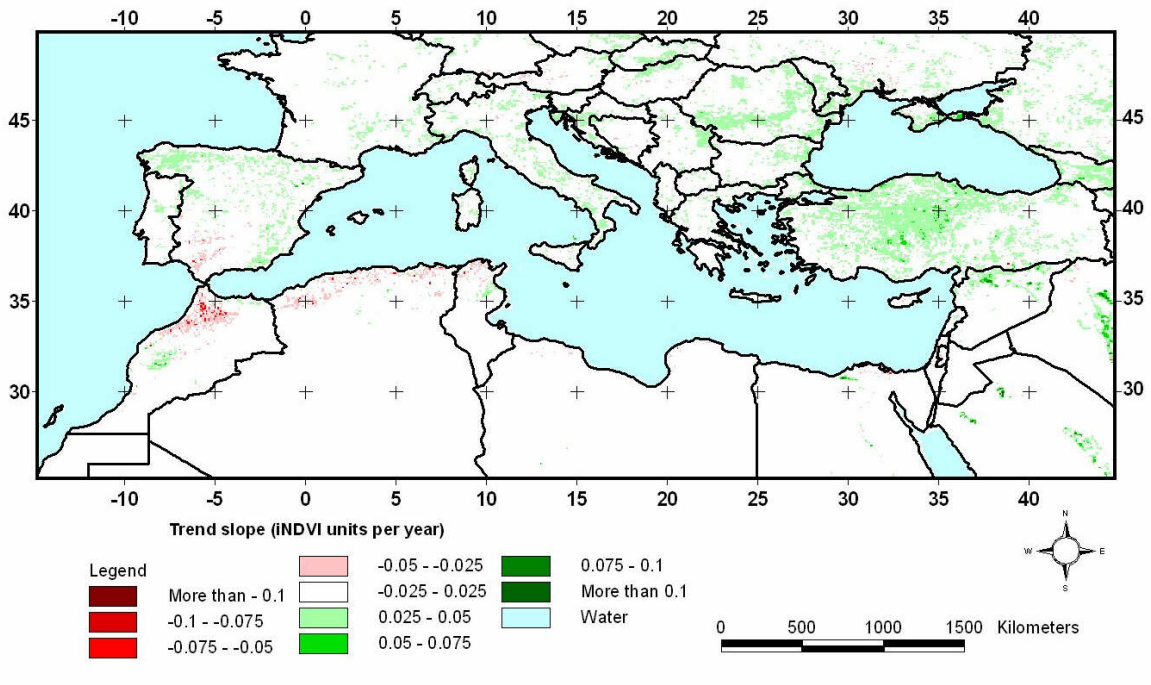

Figure 5.1.5. Linear trends in vegetation productivity based on linear least square regression (1982-2002) based on annual integrated NDVI values. The trend is expressed as iNDVI-units per year.

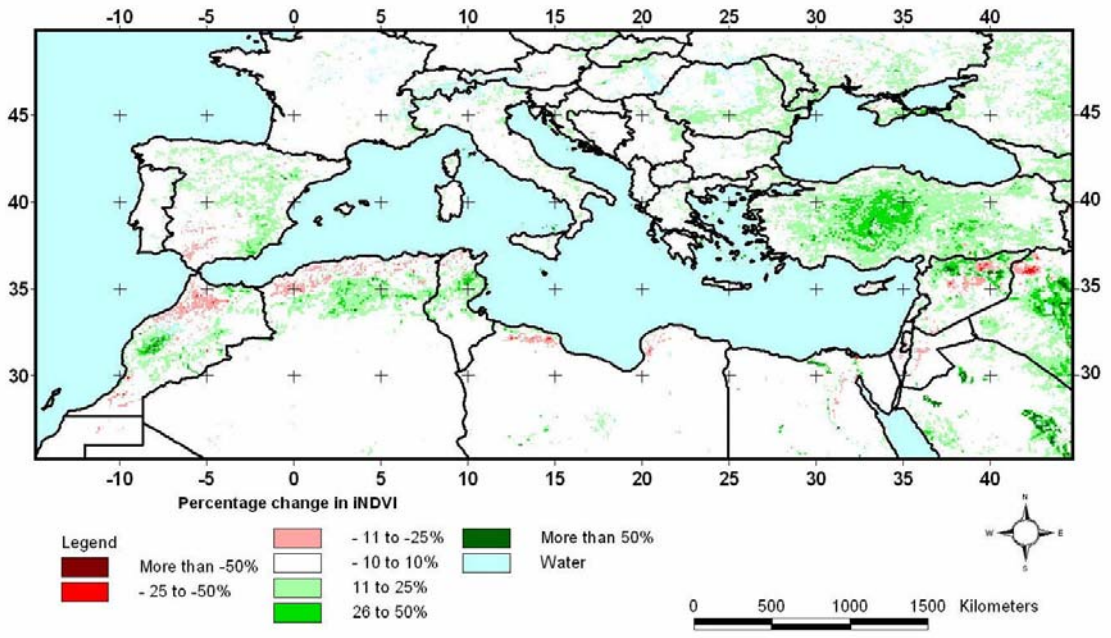

Figure 5.1.6. Linear trends in vegetation productivity for the period 1982 to 2002 based on annual integrated NDVI values. The trend is expressed as percentages i.e. the relative difference between the start and the end value of the linear trend.

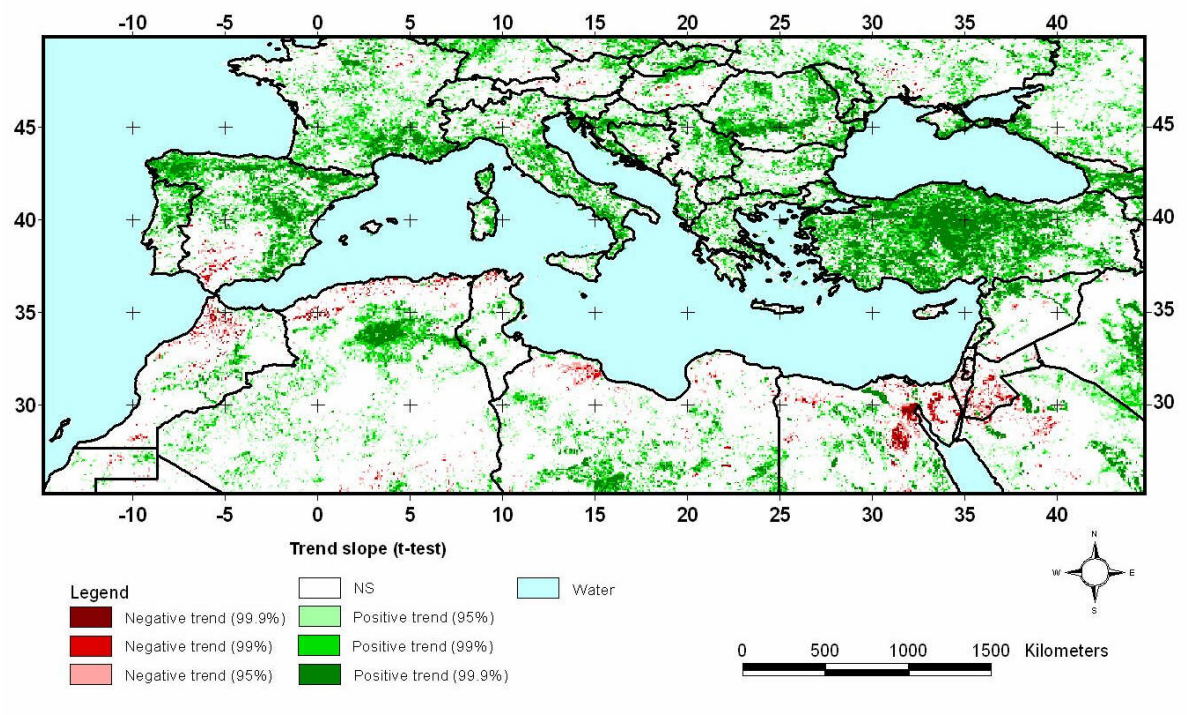

Fig. 5.1.7. Trend slope in NDVI based on linear least square regression (1982-2002).iNDVI trend slope (t-test).

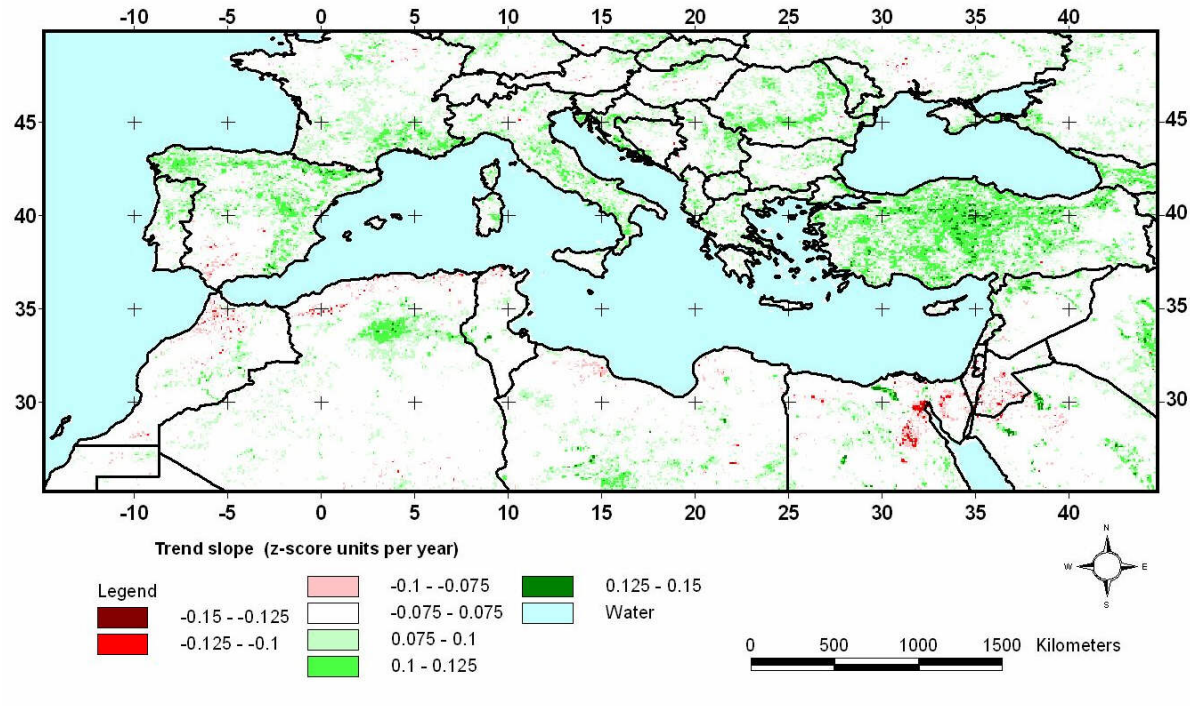

Figure 5.1.8. Standardized trend slope in NDVI based on linear least square regression and expressed as z-score units per year (1982-2002).

Figures 5.1.5-5.1.8 confirms the points raised in the method section regarding the relative merits of the different characteristics (inclination, relative change or statistical significance) of the trend line. Especially it is clear that the statistical test is putting too much emphasis on areas with rather small slope inclinations. There is equally a tendency for the relative change to put emphasis on areas where the intercept value i.e. the starting point is low. In that case a relative low absolute slope value may actually come out as a quite significant relative change.

5.1.3. Vegetation versus rainfall analysis

The next step was to investigate how rainfall variability has influenced the observed variability and trend in iNDVI. Figure 5.1.9 (left) indicates the relationship between mean NDVI and mean annual rainfall for the 1982-2003 period. The strong positive relationship (r^2=0.8) confirms the fact that higher rainfalls normally yields higher vegetation productivity.

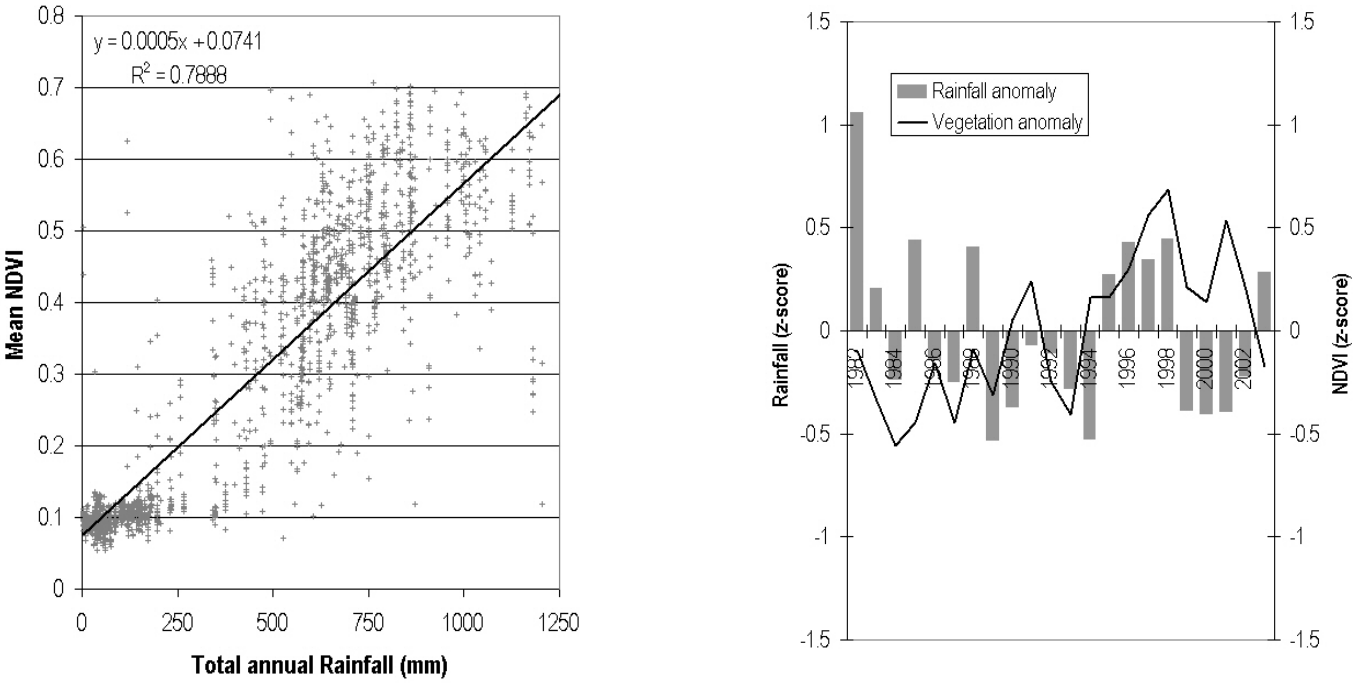

Fig. 5.1.9. (LEFT) Mean NDVI plotted against total mean annual rainfall. The displayed values are mean values for the period 1982-2003. (RIGHT) Average area z-scores of NDVI and rainfall for west Sahel for each year 1982-2003. On display are mean z-scores as calculated from the area defined by 0.1 < NDVI < 0.5 where NDVI refers to the mean monthly NDVI for the period .

Yet, the relationship illustrated in Figure 5.1.9 (left) is biased due to the presence of spatial auto-correlation i.e. the phenomenon where locational (geographic position) similarity is matched by value similarity. Consequently Fig. 5.1.9 (left) demonstrates the geographic relationship between long-term means of total annual rainfall and monthly NDVI. In order to avoid this bias the anomaly analysis was introduced (figure 5.1.9 [right], figure 5.1.10, 5.1.11-5.1.15).

The results from the anomaly analysis illustrate a significant and valid relationship between rainfall variability and NDVI variability for large parts of the Mediterranean drylands. Figure 5.1.9 underlines the importance that NDVI trends should be controlled for rainfall variability before elucidating on the possible anthropogenic causes.

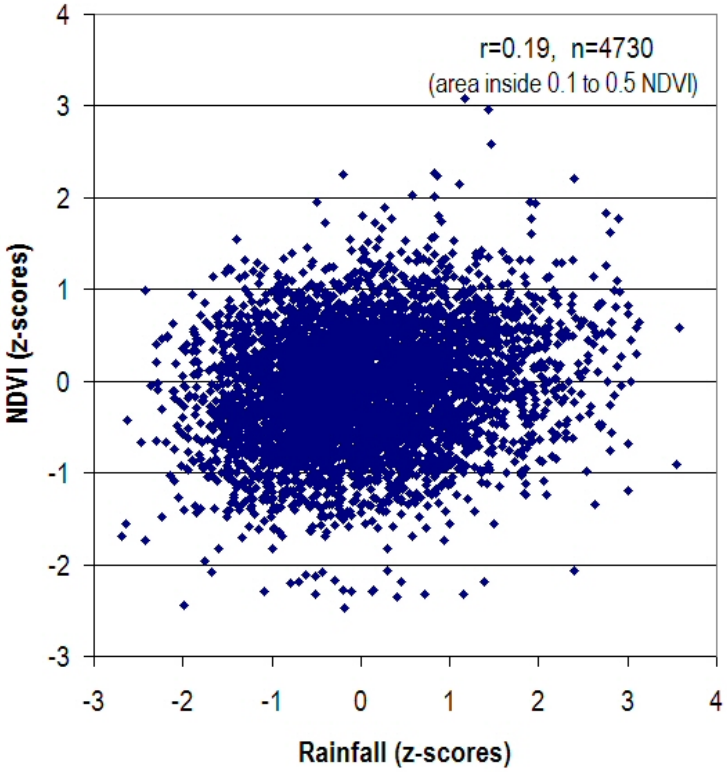

Fig. 5.1.10. Annual NDVI anomalies plotted against annual rainfall anomalies. Every pixel in the 2.5 degree rainfall data was selected and plotted against the average NDVI value for the corresponding NDVI 8 km pixels under each 2.5^0 cell. Only pixels inside the area defined by 0.1<NDVI<0.5 where NDVI denotes mean monthly NDVI for the 1982-2003 period. All data for the 1982-2003 period were merged into one data set.

However, it should be noted that it is only a fraction (4%) of the interannual NDVI anomaly variation that can be explained by corresponding interannual (seasonal) rainfall anomalies under the given circumstances (Fig 5.1.10). It implies there are large areas (many pixels) where the strong NDVI-rainfall anomaly relationship is not valid. This is also illustrated in the figures below.

The following maps summarize the results from the per pixel analysis of the temporal relationship between rainfall and NDVI.

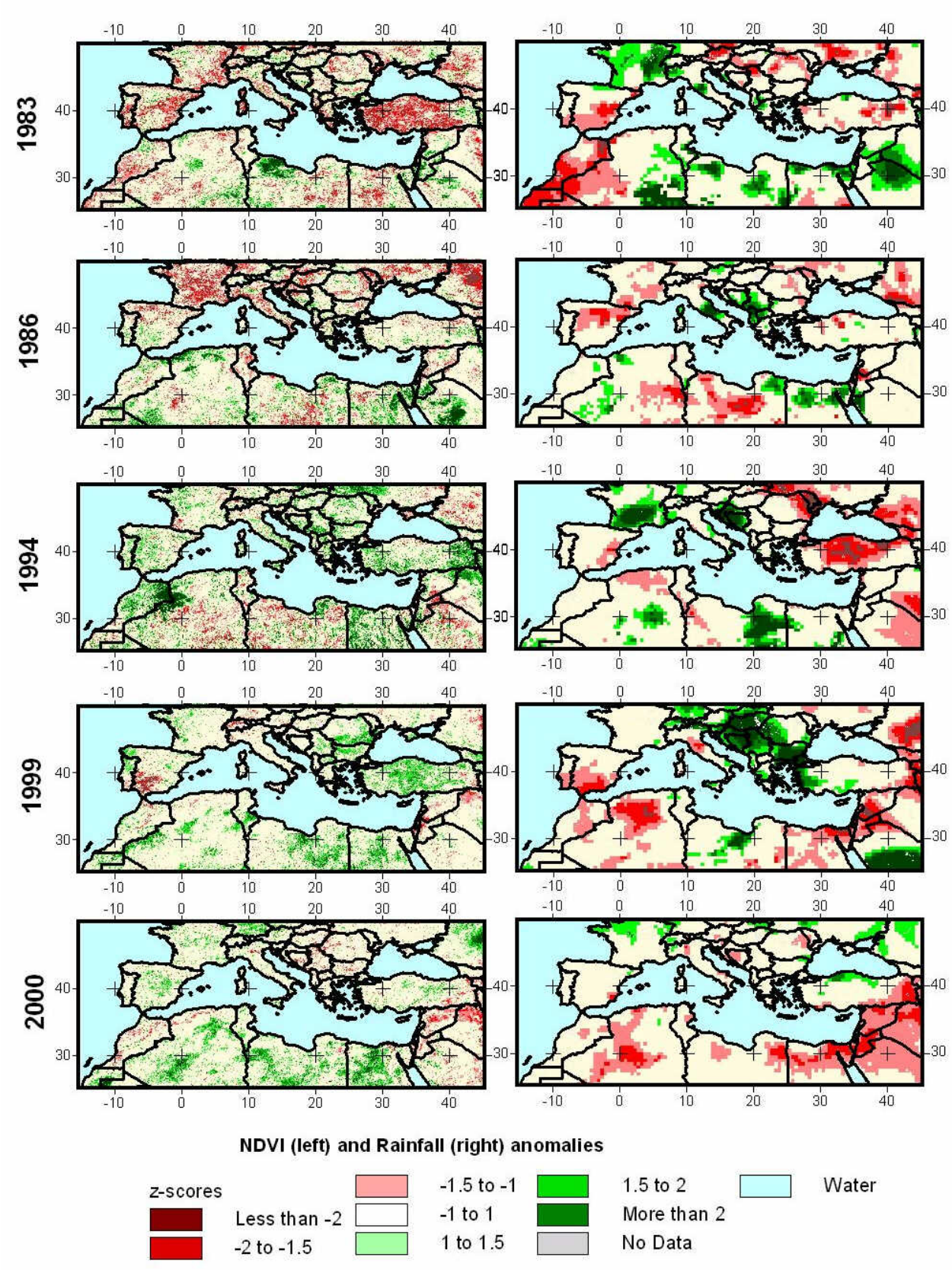

Figure 5.1.11. NDVI (8 km) and rainfall (0.5 degree grid) anomalies for 5 random "non-calendar" years during the 1982 to 2003 period.

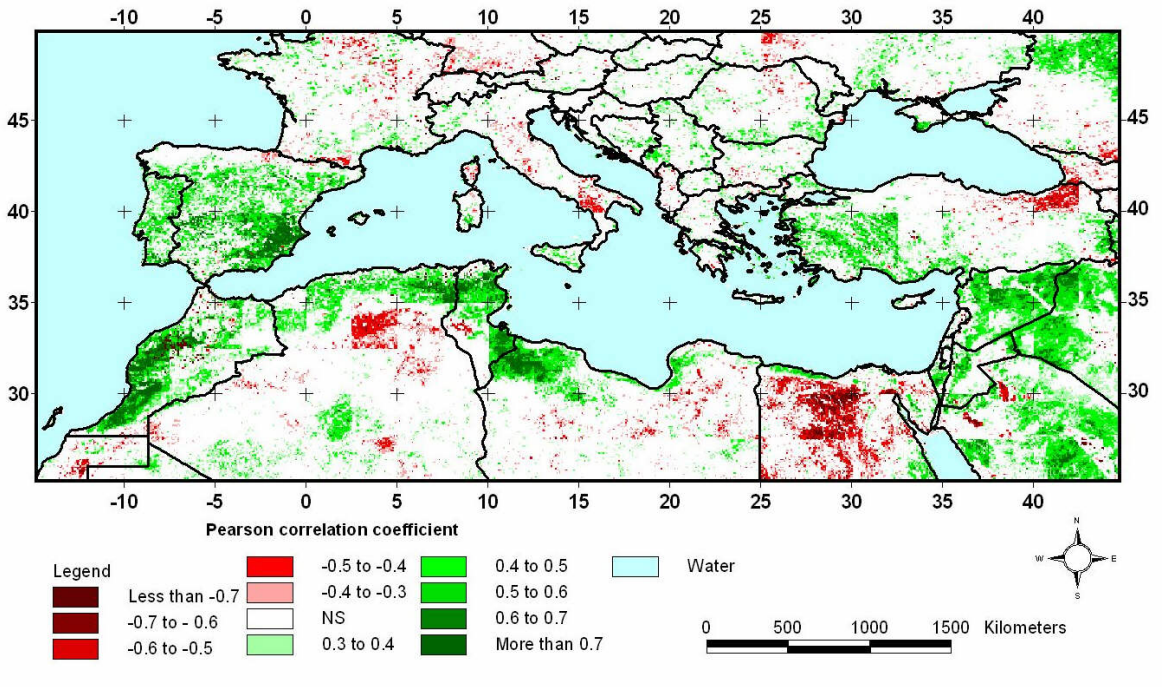

Fig. 5.1.12. Total annual rainfall (2.5 degree) vs. annual integrated NDVI (1982-2003).

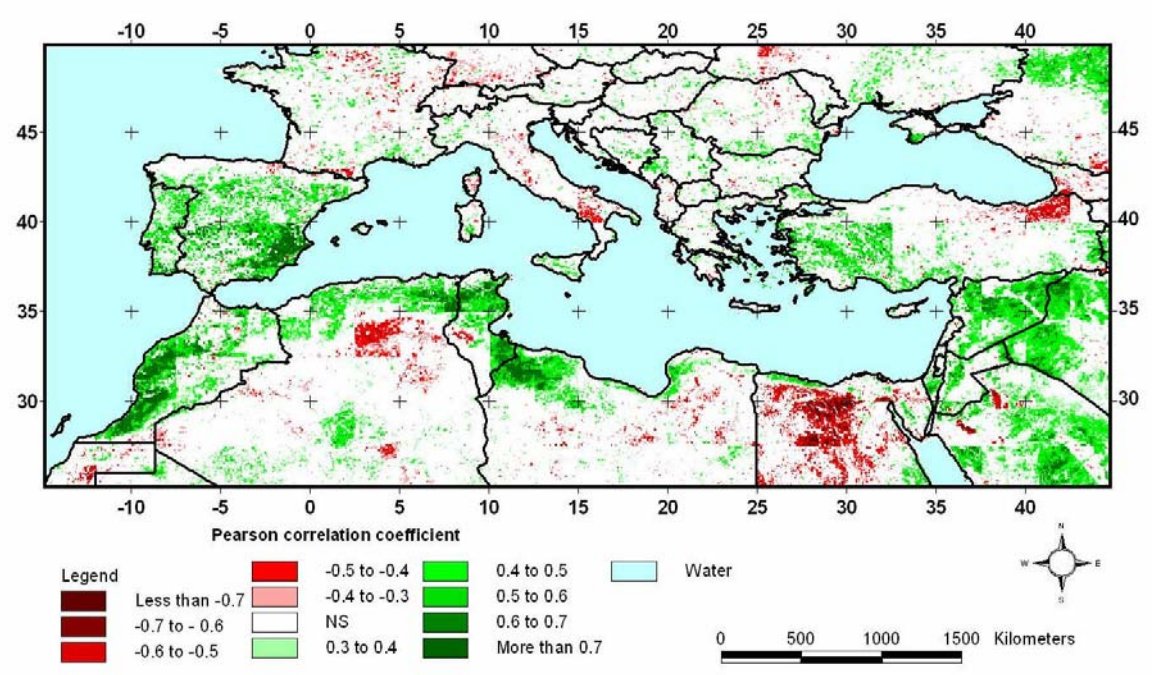

Fig. 5.1.13. Rainfall anomaly (2.5 degree) vs. NDVI anomaly (1982-2003).

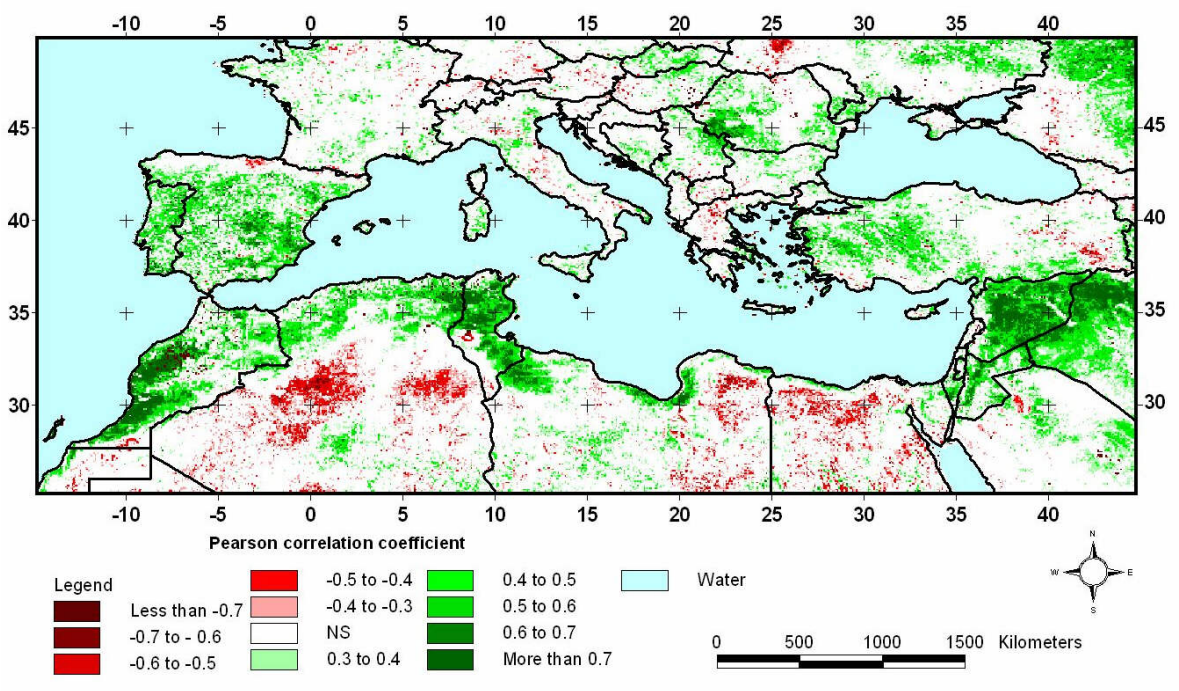

Fig. 5.1.14 Total annual rainfall (0.5 degree) vs. annual integrated NDVI (1982-2002)

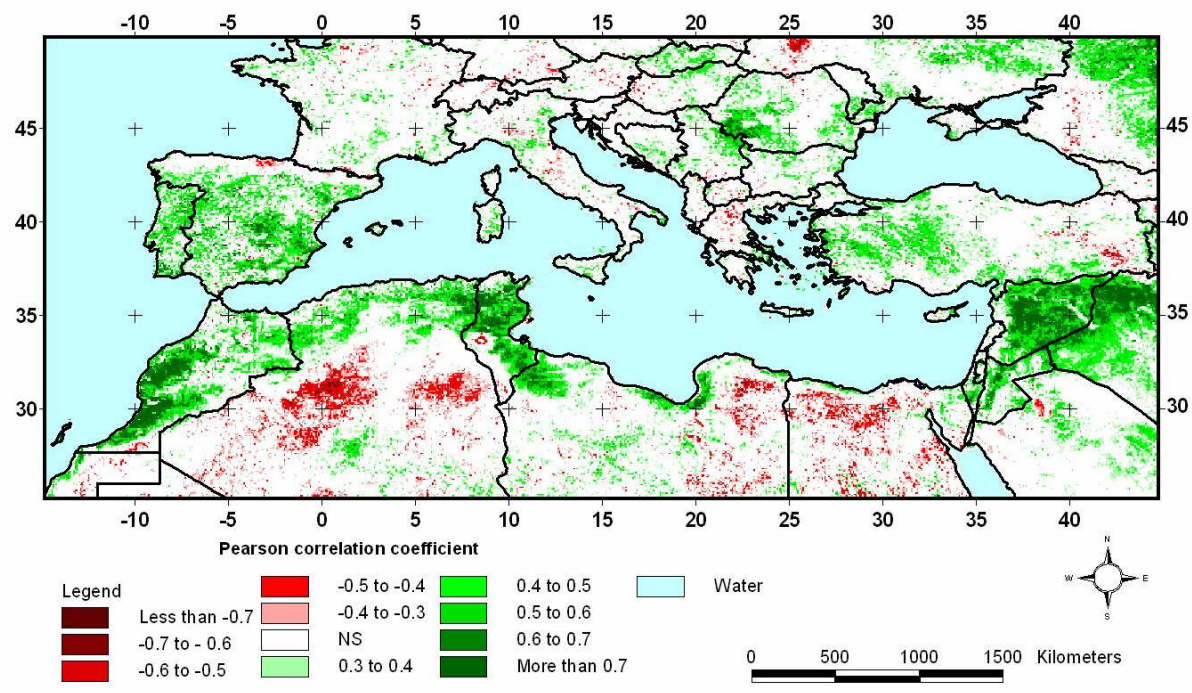

Fig. 5.1.15. Rainfall anomaly (0.5 degree) vs. NDVI anomaly (1982-2002).

As expected one can see a relatively good correlation between rainfall and NDVI for most of the dryland region. Areas of negative correlation are also found but they are to a large extent located in the very dry parts (mean NDVI < 0.1 and annual rainfall < 100 mm) where the validity of both rainfall data and NDVI can be questioned (e.g. fewer climate stations and soil background influence). It is interesting to note the strong agreement between the top maps (based on 2.5 degree gridded data) and the bottom maps (based on 0.5 on degree gridded data) as well as the almost identical patterns observed between the use of integrated data and standardized (z-scores) data.

5.1.4. Residual analysis

The model residuals (i.e. the difference between observed and expected iNDVI) was computed for each pixel and subsequently inspected for any systematic trends that could invalidate the initial model specification.

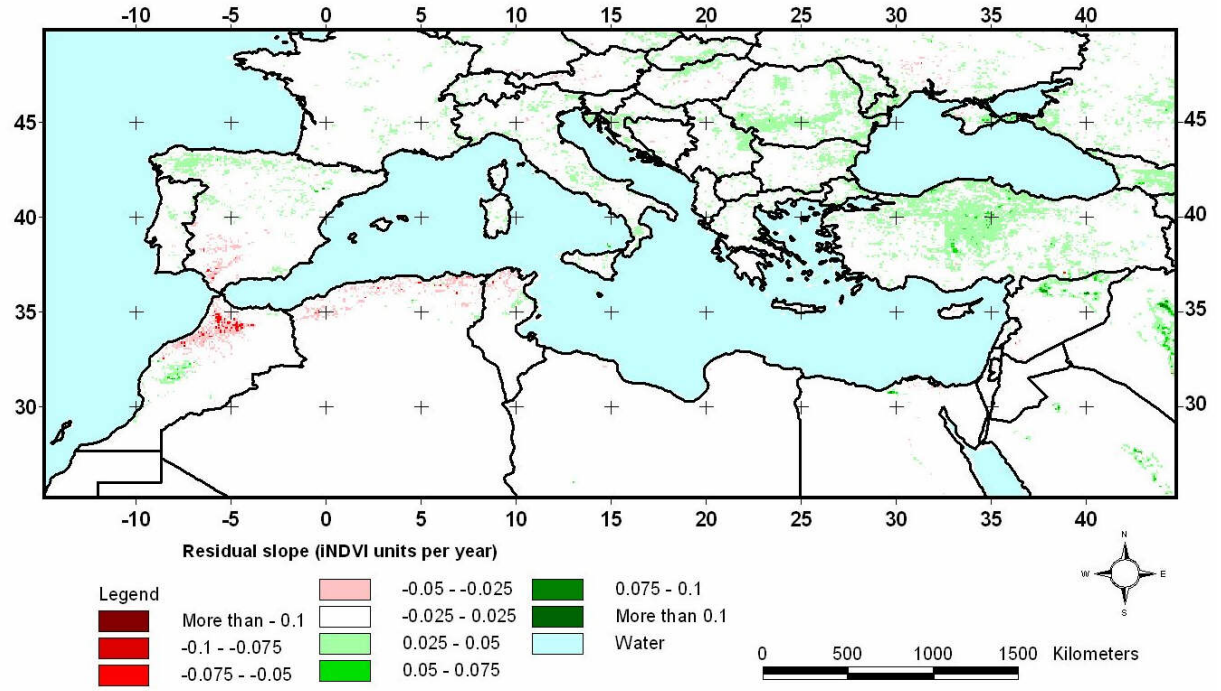

Fig. 5.1.16. Linear trends in residual slope of iNDVI when controlled for annual rainfall (2.5 degree) for the period 1982 to 2003. The trend is expressed in absolute values i.e. change in iNDVI units per year.

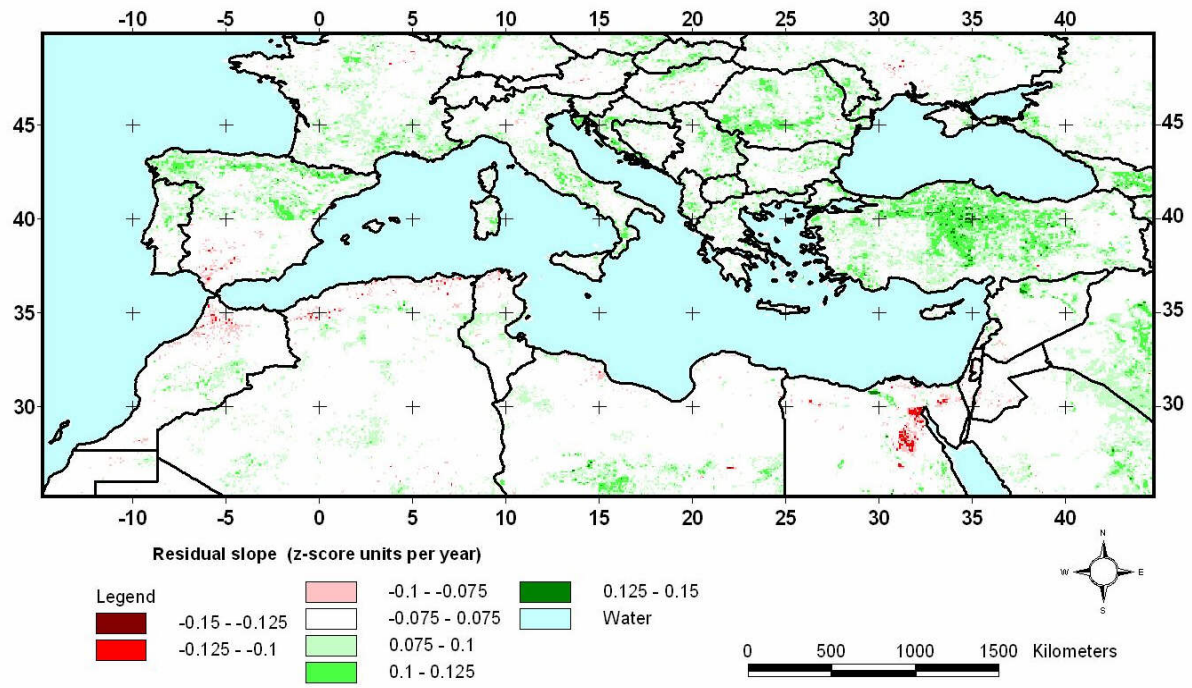

Fig. 5.1.17. Linear trends in residual slope of iNDVI z-scores when controlled for annual rainfall (2.5 degree) for the period 1982 to 2003. The trend is expressed in absolute values i.e. change in z-score units per year.

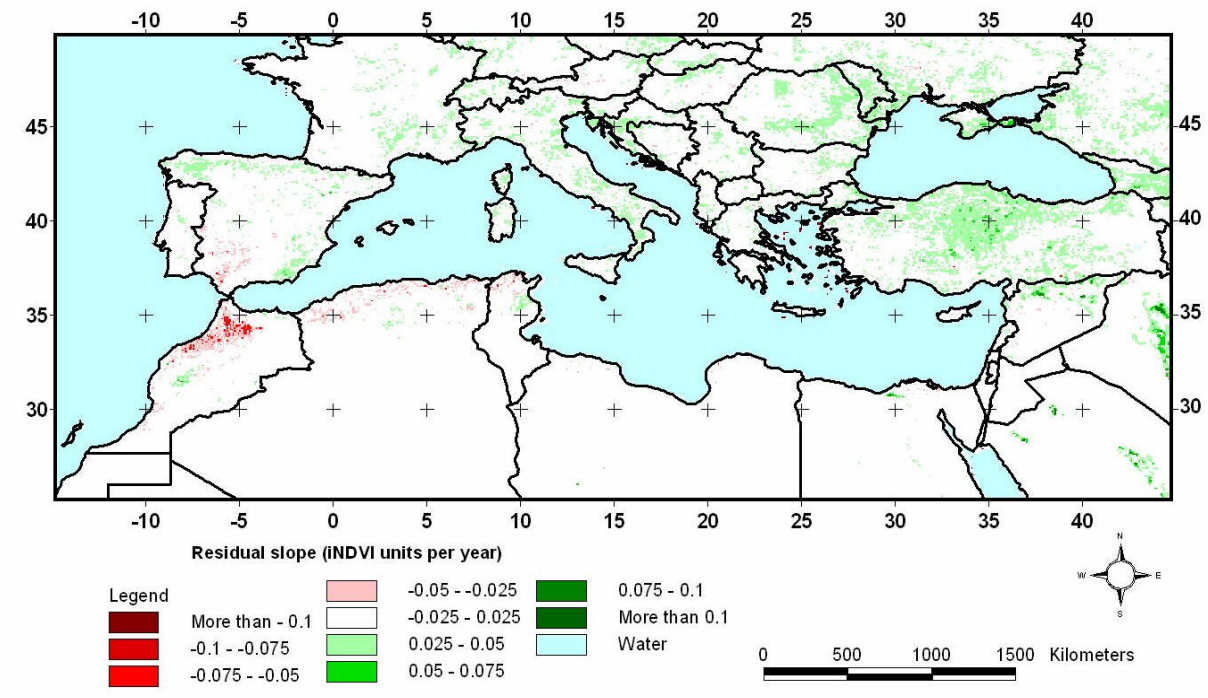

Fig. 5.1.18. Linear trends in residual slope of iNDVI when controlled for annual rainfall (0.5 degree) for the period 1982 to 2002. The trend is expressed in absolute values i.e. change in iNDVI units per year

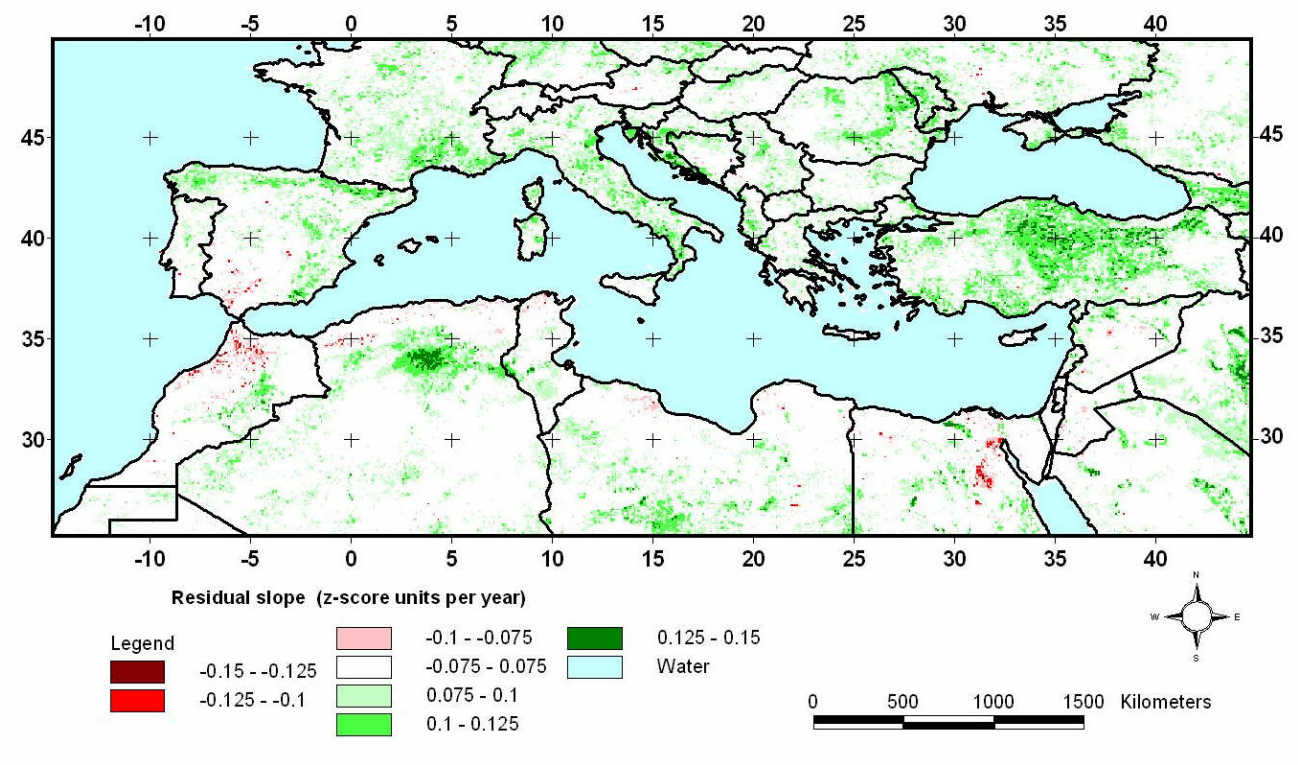

Fig. 5.1.19. Linear trends in residual slope of iNDVI z-scores when controlled for annual rainfall (0.5 degree) for the period 1982 to 2002. The trend is expressed in absolute values i.e. change in z-score units per year.

5.1.5. Hot Spot analysis

Example areas with significant residual trends (negative as well as positive) were identified and the trends in vegetation productivity relative to the long-term precipitation anomaly trends in the area were studied. A population density map is also presented for comparison (Fig 5.1.20-5.1.26).

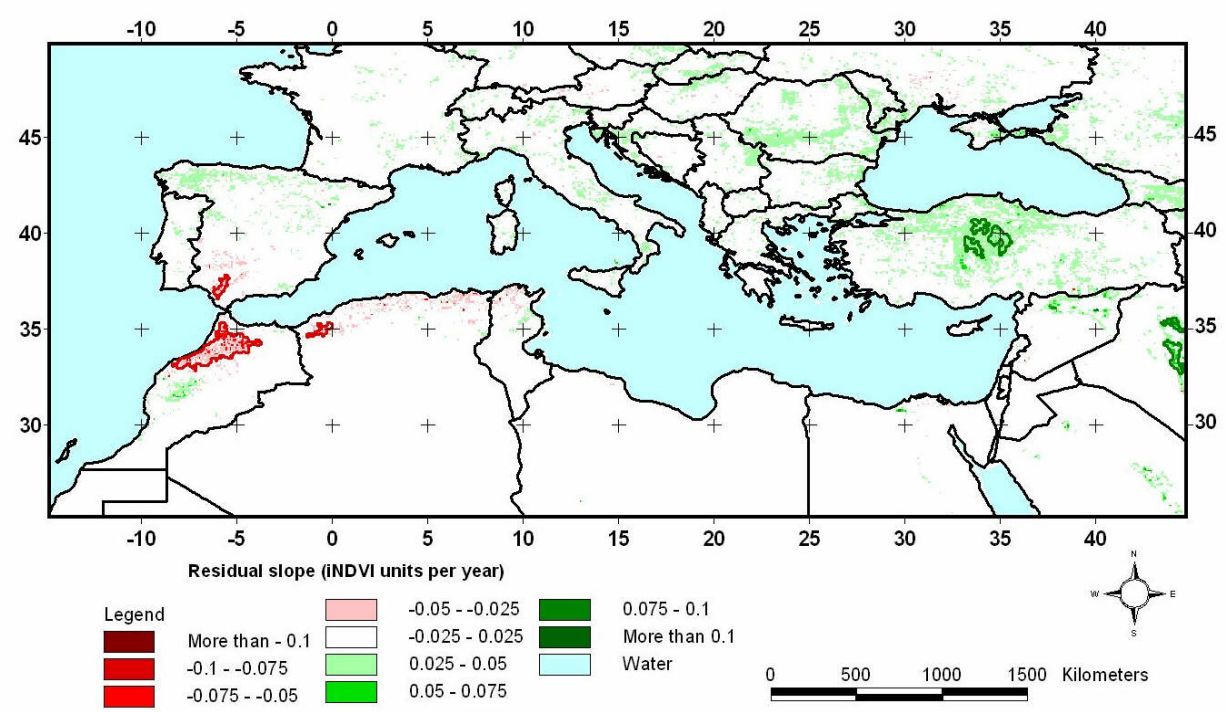

Fig. 5.1.20. Mediterranean basin negative (red) and positive (green) hot spots.

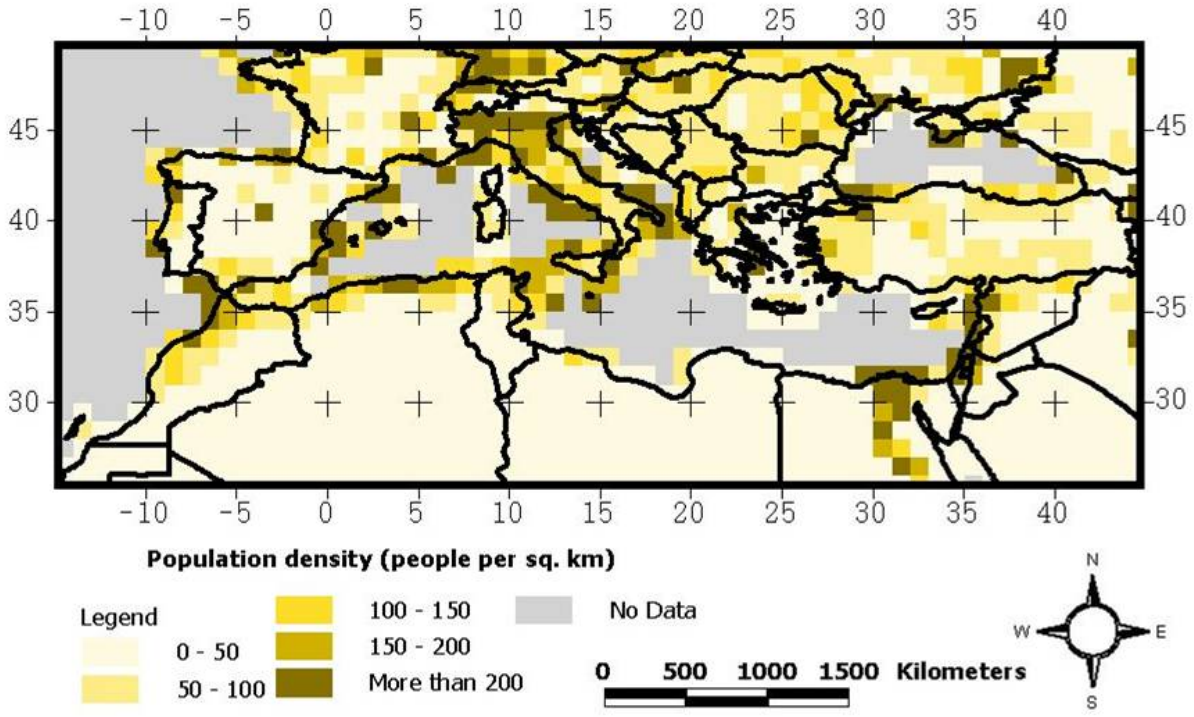

Figure 5.1.21. A Population density map of the countries bordering the Mediterranean Sea. Data are from 2000 and produced by CIESIN (2005).

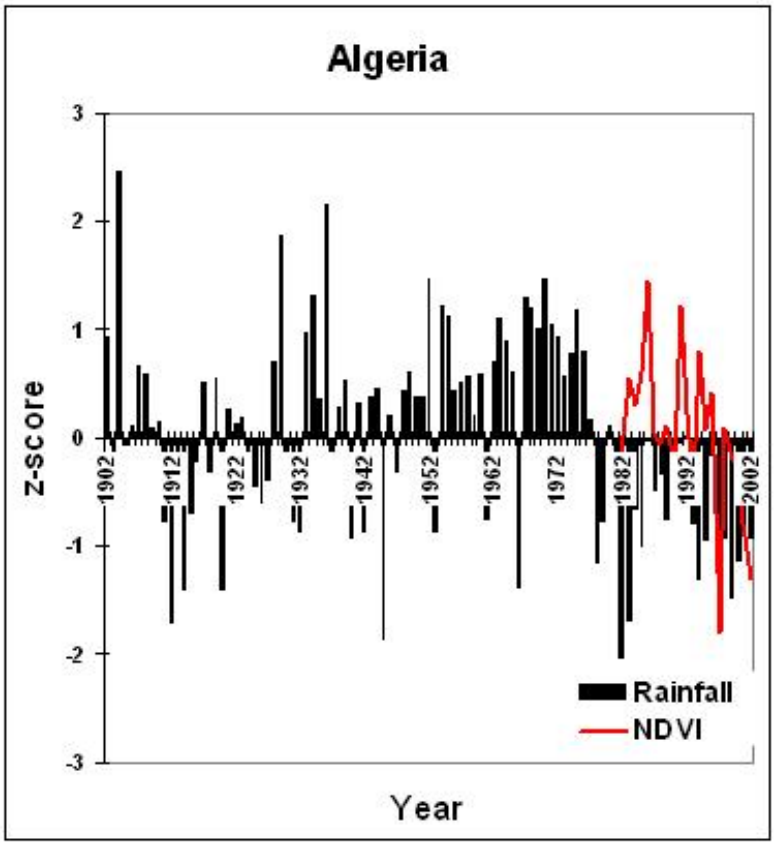

Fig 5.1.22. Algerian negative hot spot rainfall and NDVI anomalies.

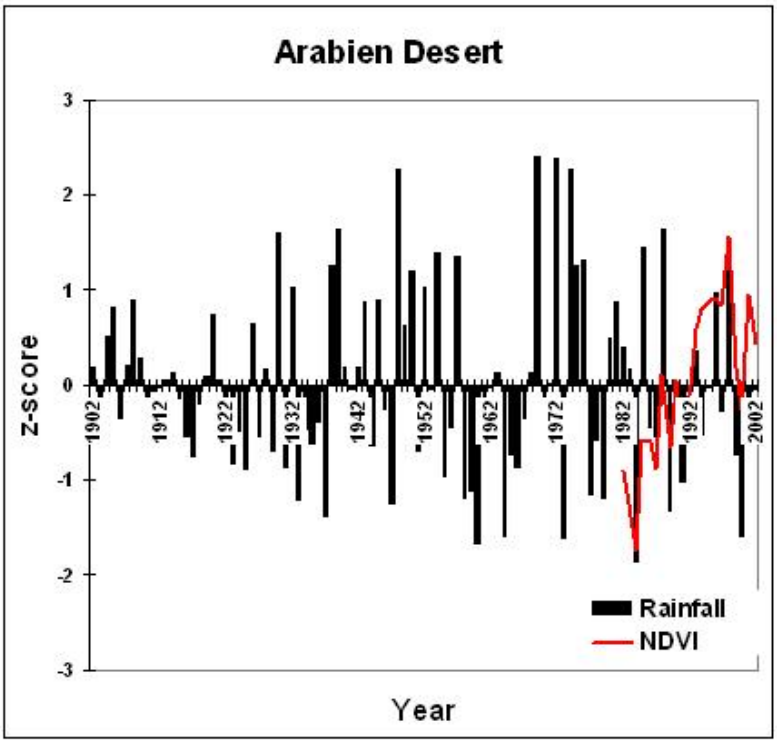

Fig. 5.1.23. Arabian Desert positive hot spot rainfall and NDVI anomalies

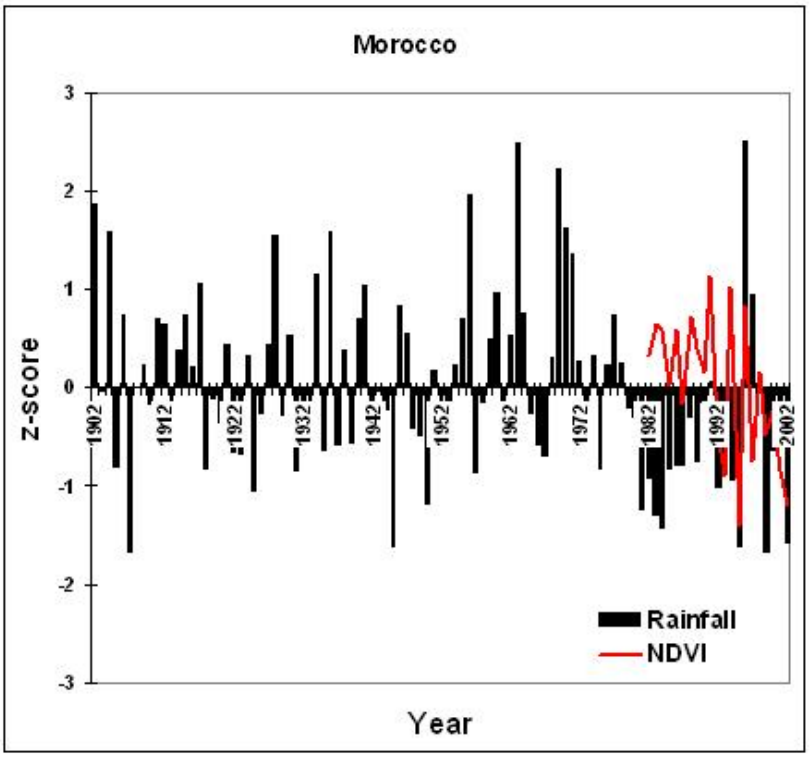

Fig. 5.1.24. Morocco negative hot spot rainfall and NDVI anomalies

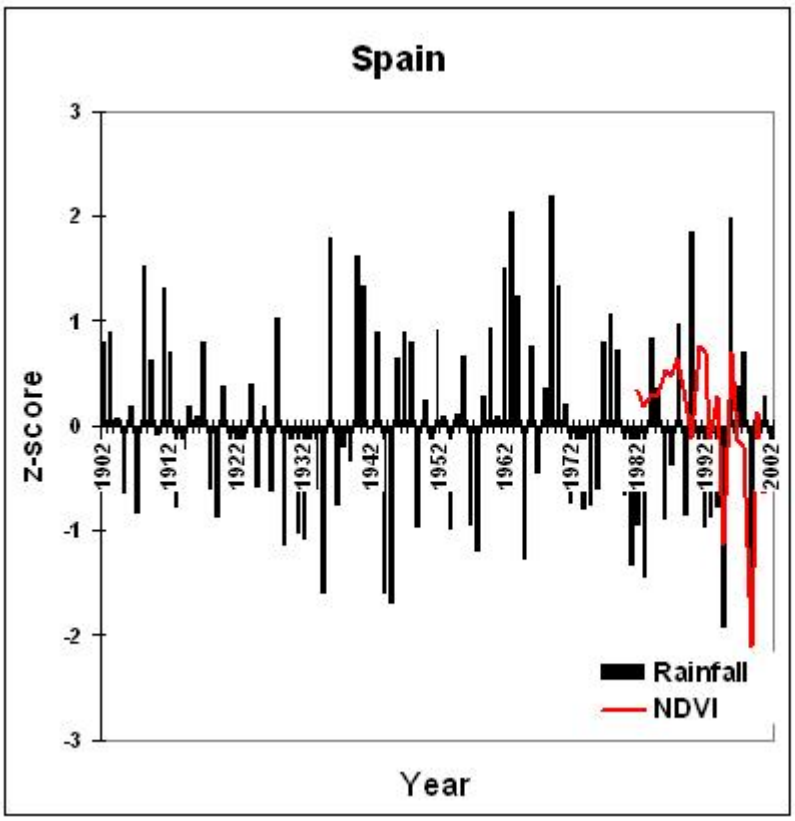

Fig. 5.1.25. Spain negative hot spot rainfall and NDVI anomalies

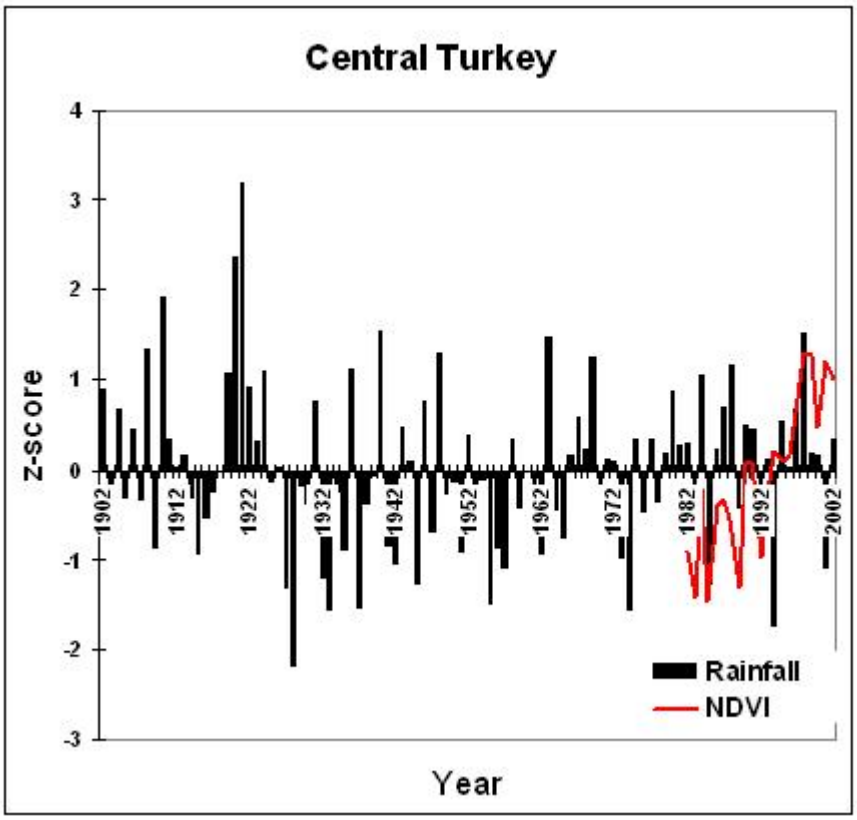

Fig. 5.1.26. Central Turkey positive hot spot rainfall and NDVI anomalies

5.1.6. Desertification comments

- Signs of desertification, as reflected by significant downward trends in the vegetation productivity, after it was controlled for rainfall variability, are found in the Southern Iberian Peninsular as well as in the northern parts of Morocco, Algeria and Tunisia. The fact that these areas are closely associated with the most densely populated areas of the Maghrebian countries further supports the hypothesis that these downwards trends may be caused by humans (Cf. fig. 5.1.21)

- The trend maps reveal areas of strong positive trends in vegetation productivity including scattered areas in the Arabian and Mesopotamia[2] drylands, central Turkey as well as the central parts of Morocco. The positive trends in the Arabian and Mesopotamia drylands can be explained by the development of large irrigations schemes (Weiss et al. 2001) whereas no immediate explanation, at present, is available for the positive trends in remaining Turkey and Morocco.

[2] Mesopotamia refers to the region now occupied by modern Iraq, eastern Syria, southeastern Turkey, and Southwest Iran.

- The overall generic trend in the Mediterranean basin seems to be a general "greening up" over the 1982-2003 period rather than a systemic growth of land degradation/ desertification, expressed in terms of decreasing vegetation cover conditions, over large areas. This may, to some extent, be due to the "Green House" effects including increased CO_2 concentrations in the atmosphere and increased temperatures possibly increasing the length of the growing season and causing its earlier start as indicated in a NOAA AVHRR study on global terrestrial NPP by Nemani et al. (2003). The result of growing pollution of the atmosphere by active nitrogen from industry, raining down as a fertilizer on the global terrestrial bio-production systems, may add to the increasing "greenness" over time.

- An increasing abandonment of agriculture and marginal lands by farmers looking for an improved standard of living in the urban centers is also likely to result in re-vegetated farm-land and increased greenness in the Mediterranean drylands as suggested by Grove and Rackham (2003) and illustrated by Fig. 5.1.27. This is of course more true for the European part of the Mediterranean basin than for the non-European part, simply because Europe is in the forefront of the urbanization process so far.

Fig 5.1.27. Deserted farm and agricultural land, Alentejo, Portugal (left) & growing demands for crop land and fuelwood, downstrem Oued oum Zessari, Tunisia (right). (Photos: U.Helldén, 2007).

5.2. WEST AFRICA

5.2.1. West Africa overview

The region extends from Senegal in the west to Niger in the east and between 7^{o} to 17^{o} Northern latitude. The northern limit of this region follows the southern border of the Saharan desert while the southern limit is demarcated by the sub-humid forest belt.

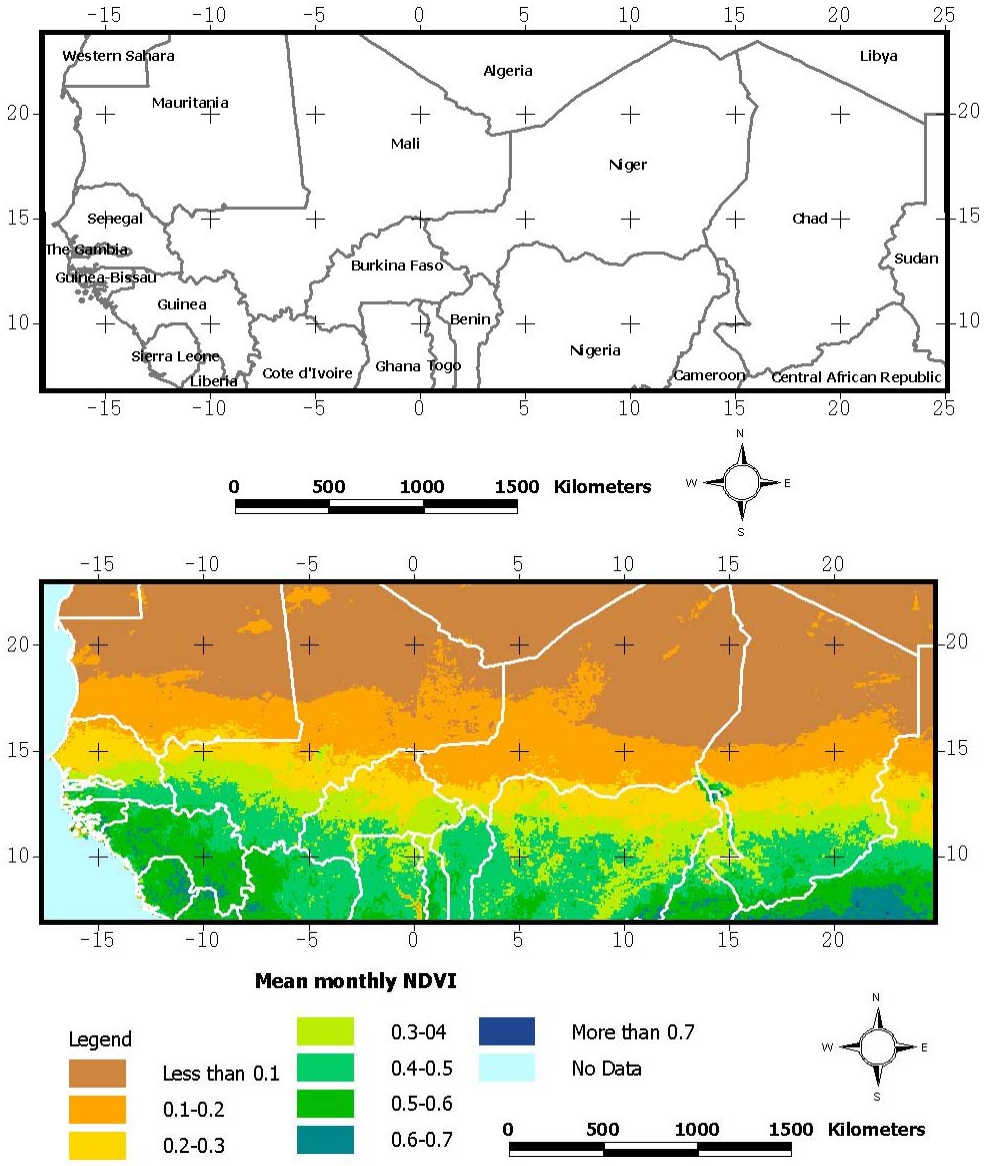

Figure 5.2.1. Country overview (top) and the mean monthly NDVI based on data from 1982 to 2003 (bottom).

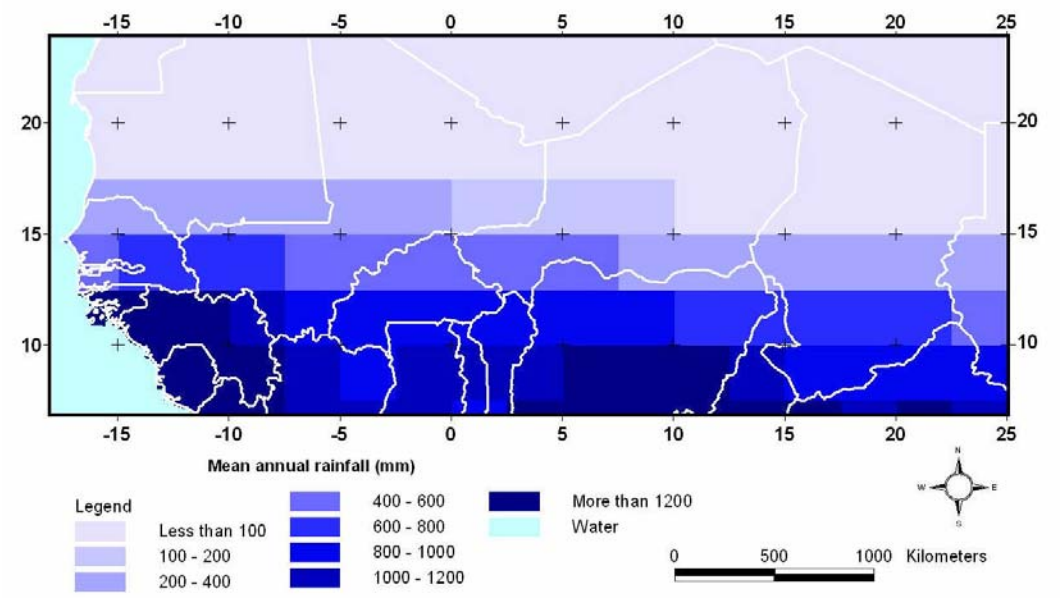

Figure 5.2.2. Mean annual rainfall based on 2.5 degree (~ 275 km) gridded rainfall data from 1982 to 2003.

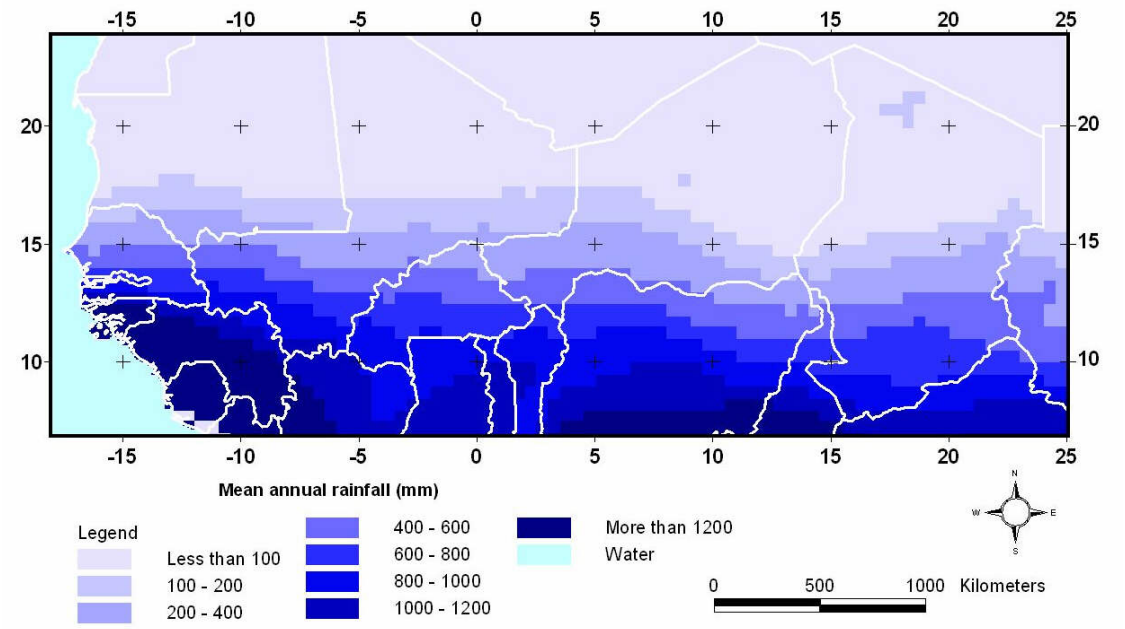

Fig. 5.2.3. Mean annual rainfall based on 0.5 degree (~55 km) gridded rainfall data from 1982 to 2002.

Inspection of time-series plots of both rainfall and NDVI revealed that the appropriate seasons for the Sahel (i.e. here defined as the area delineated by a minimum of 0.1 and a maximum of 0.5 NDVI based on the long-term monthly average) was “March to February” and “January to December” for NDVI and rainfall respectively (figure 6.4).

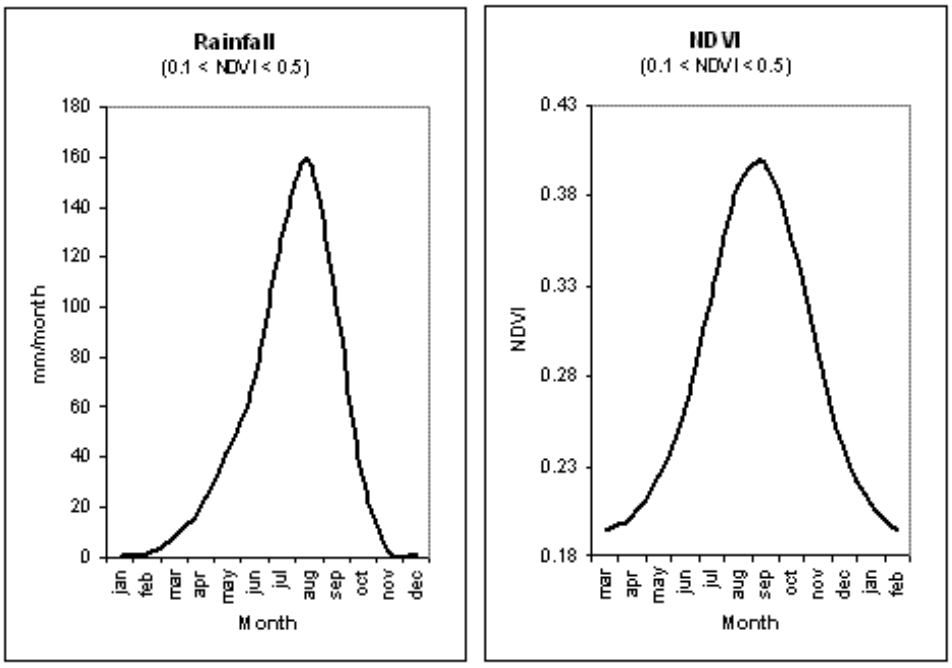

Figure 5.2.4. Monthly time-series plots of rainfall (left) and NDVI (right). The displayed values are mean values as calculated from the area defined by $0.1 \leq NDVI \leq 0.5$. From the time-series plots it appears that rainfall tend to have a local minimum in January while NDVI has its minimum in March.

Consequently total annual rainfall was calculated by summarizing rainfall received within the months from January to December. Similar the annual vegetation productivity was estimated by integrating NDVI over the months from March and until February the following year

5.2.2. Vegetation trend analysis

The following figures summarize the results of the trend analysis approaches described under methods.

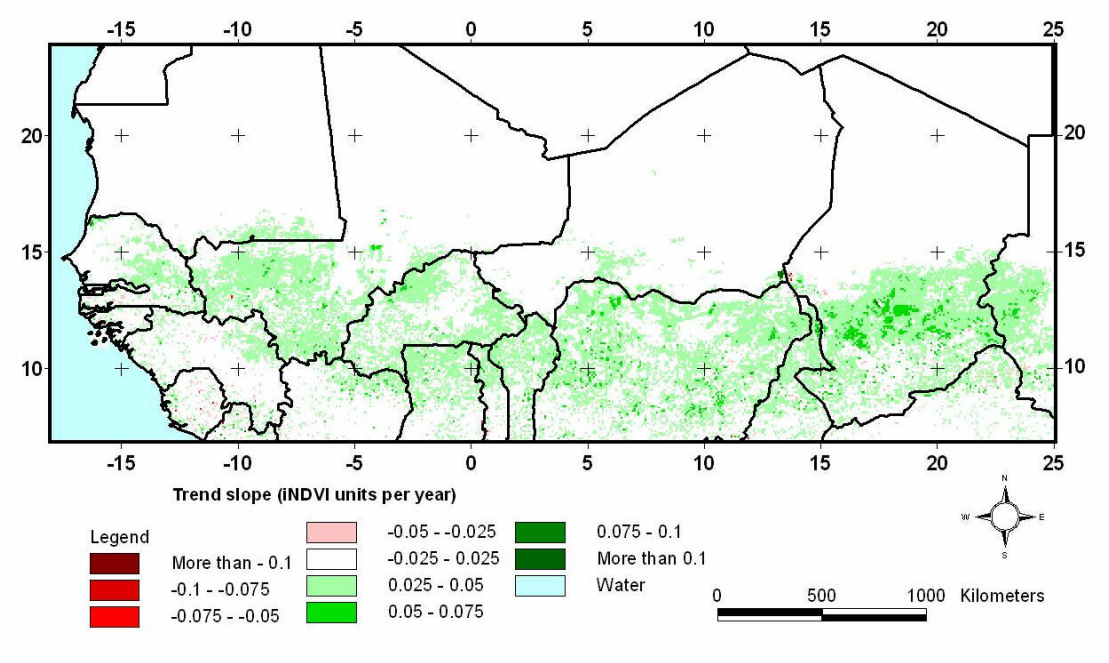

Figure 5.2.5. Linear trends in vegetation productivity for the period 1982 to 2002 based on annual integrated NDVI values. The trend is expressed in absolute values i.e. change in iNDVI units per year.

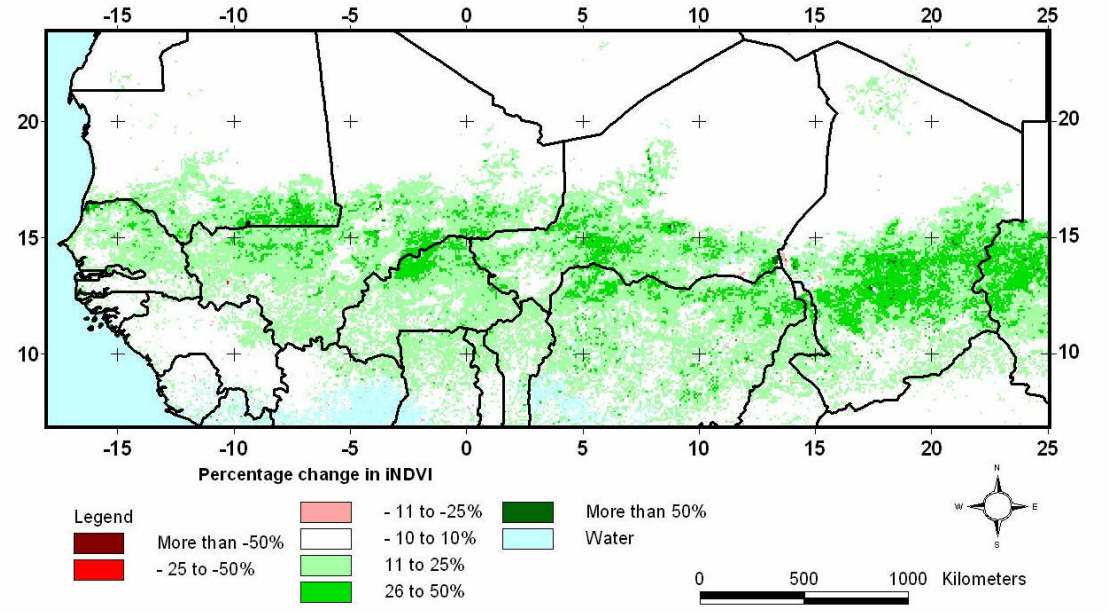

Fig 5.2.6. Linear trends in vegetation productivity for the period 1982 to 2002 based on annual integrated NDVI values. The trend is expressed as percentages i.e. the relative difference between the start and the end value of the linear trend

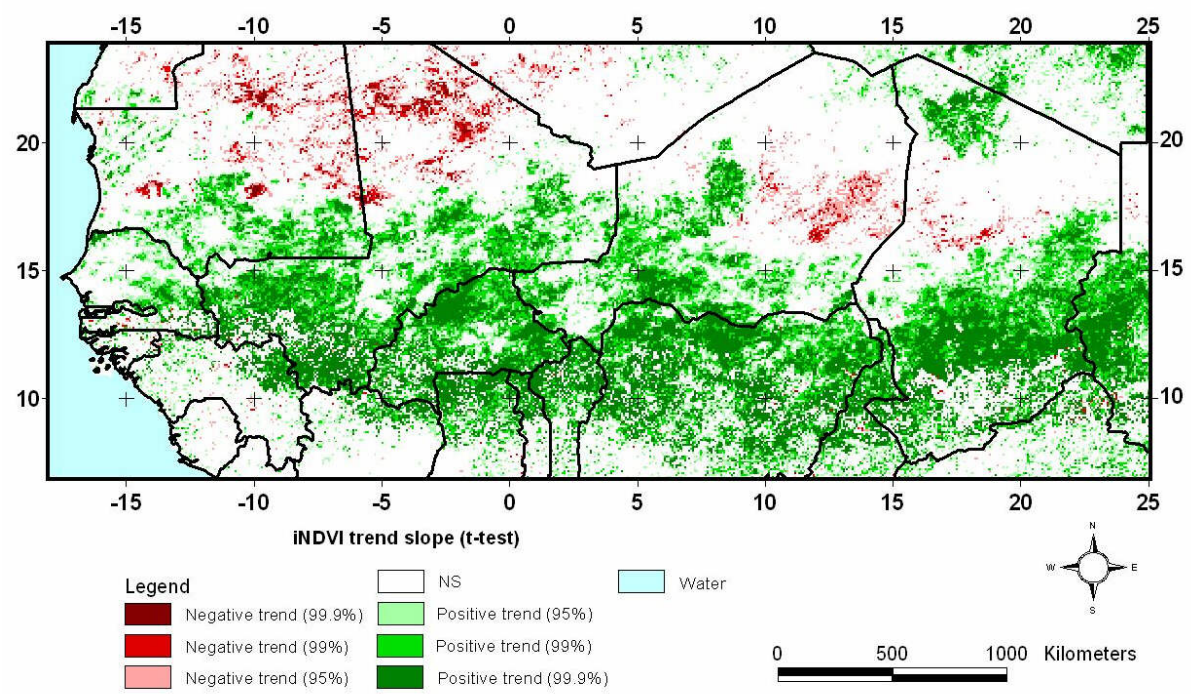

Fig. 5.2.7. Trend slope in NDVI based on linear least square regression (1982-2002). iNDVI trend slope (t-test).

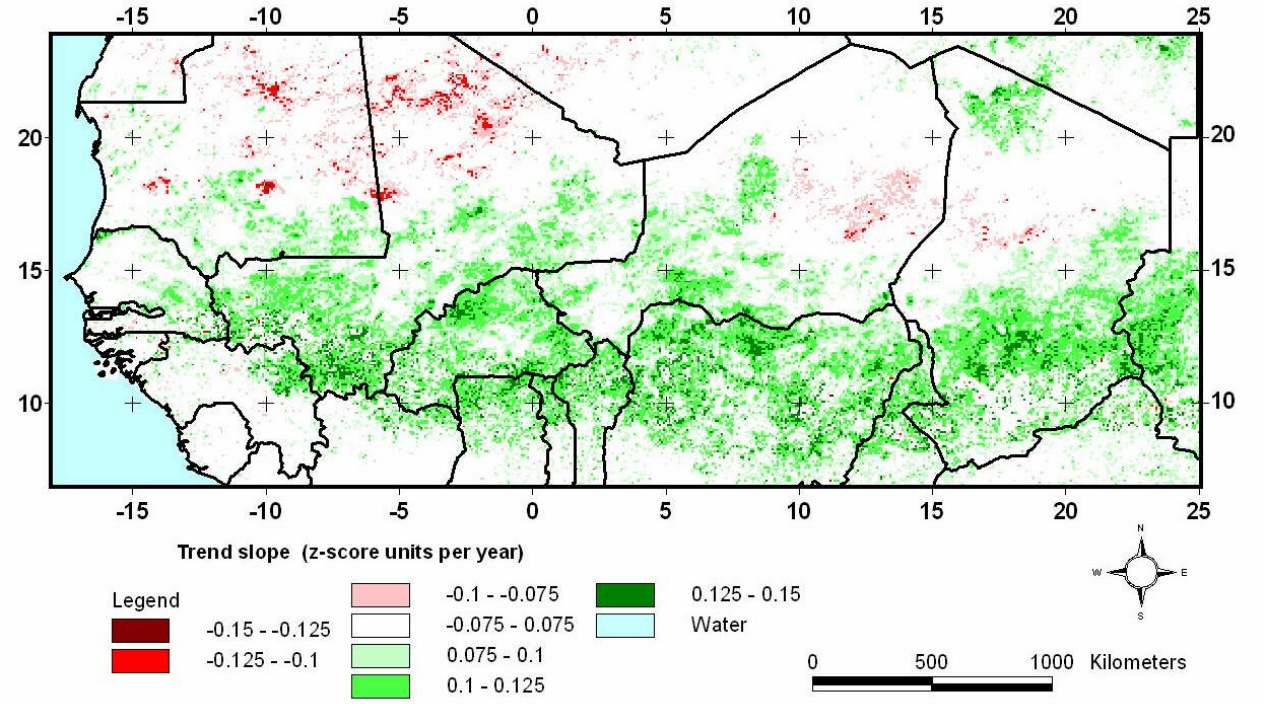

Figure 5.2.8. Standardized trend slope in NDVI based on linear least square regression and expressed as z-score units per year (1982-2002).

The figures 5.2.5-5.2.8 confirm the points raised in the method sections regarding the relative merits of the different characteristics (inclination, relative change or statistical significance) of the trend line. Especially it is clear that the statistical test is placing too

much emphasis on areas with rather small slope inclinations. There is equally a tendency for the relative change to put emphasis on areas where the intercept value i.e. the starting point is low. In that case a relative low absolute slope value may actually come out as a quite significant relative change.

5.2.3. Vegetation versus rainfall analysis

Figure 5.2.9 (left) indicates the relationship between mean NDVI and mean annual rainfall. The strong positive relationship (r^2=0.9) confirms the fact that higher rainfalls normally yields higher vegetation productivity.

Yet, the relationship illustrated in Figure 5.2.9 (left) is biased due to the presence of spatial auto-correlation i.e. the phenomenon where locational (geographic position) similarity is matched by value similarity. Consequently Fig. 5.2.9 (left) demonstrates the geographic relationship between long-term means of total annual rainfall and monthly NDVI .In order to avoid this bias the anomaly analysis was introduced (figure 5.2.9 [right], figure 5.2.10, 5.2.11-5.2.15).

The results from the anomaly analysis illustrate a significant and valid relationship between rainfall variability and NDVI variability for large parts of the West Sahelian drylands. Despite the generalization level of these figures it remains clear that rainfall and NDVI are indeed closely associated. Figure 5.2.9 thereby supports the idea that NDVI trends should be controlled for rainfall variability before elucidating on the possible anthropogenic causes.

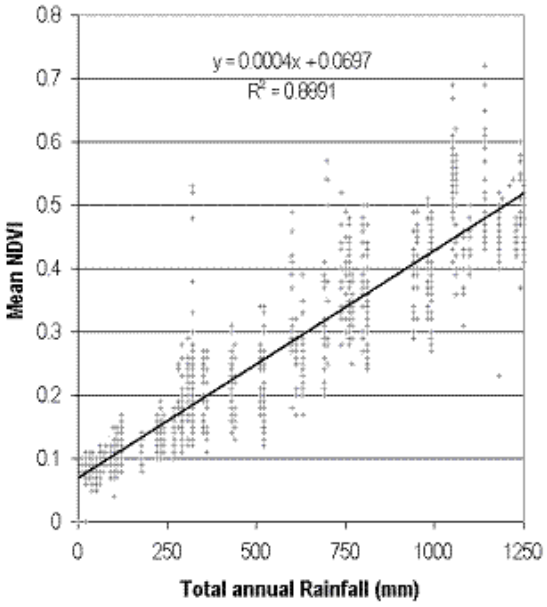

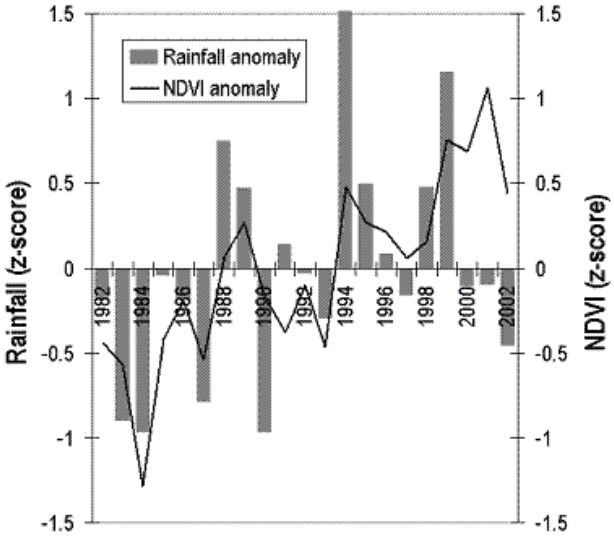

Fig. 5.2.9. (LEFT) Mean NDVI plotted against total mean annual rainfall. The displayed values are mean values for the period 1982-2003. (RIGHT) Average area z-scores of NDVI and rainfall for west Sahel for each year 1982-2003. On display are mean z-scores as calculated from the area defined by 0.1 < NDVI < 0.5 where NDVI refers to the mean monthly NDVI for the period.

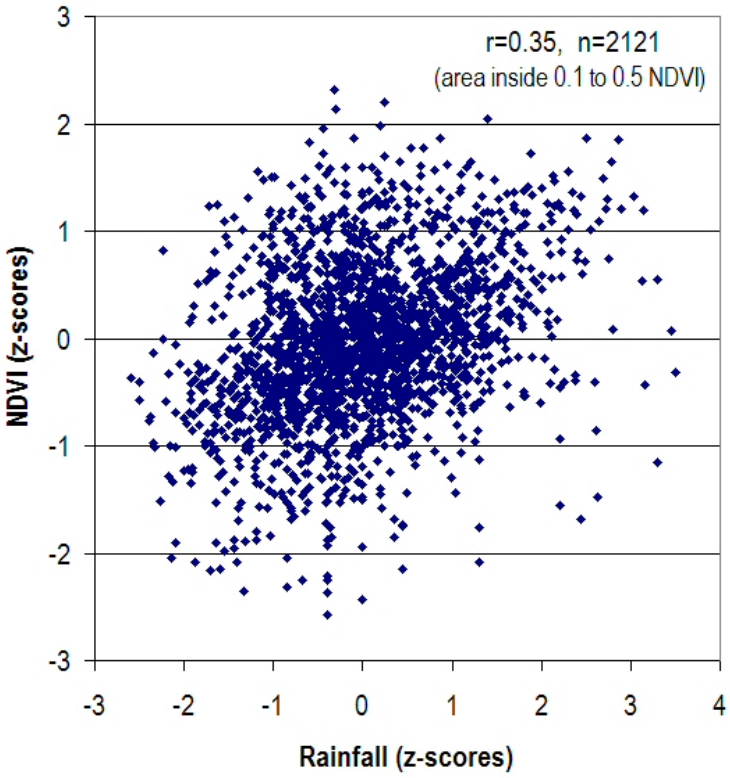

Fig. 5.2.10. Annual NDVI anomalies plotted against annual rainfall anomalies. Every pixel in the 2.5 degree rainfall data was selected and plotted against the average NDVI value for the corresponding NDVI 8 km pixels under each 2.5^0 cell. Only pixels inside the area defined by 0.1<NDVI<0.5 where NDVI denotes mean monthly NDVI for the 1982-2003 period. All data for the 1982-2003 period were merged into one data set.

However, it should be noted that it is only a fraction (16%) of the interannual NDVI anomaly variation that can be explained by corresponding interannual (seasonal) rainfall anomalies under the given circumstances (Fig 5.2.10.). It implies there are large areas (many pixels) where the strong NDVI-rainfall anomaly relationship is not valid. This is also illustrated in the figures below.

The following maps summarize the results from the per pixel analysis of the temporal relationship between rainfall and NDVI.

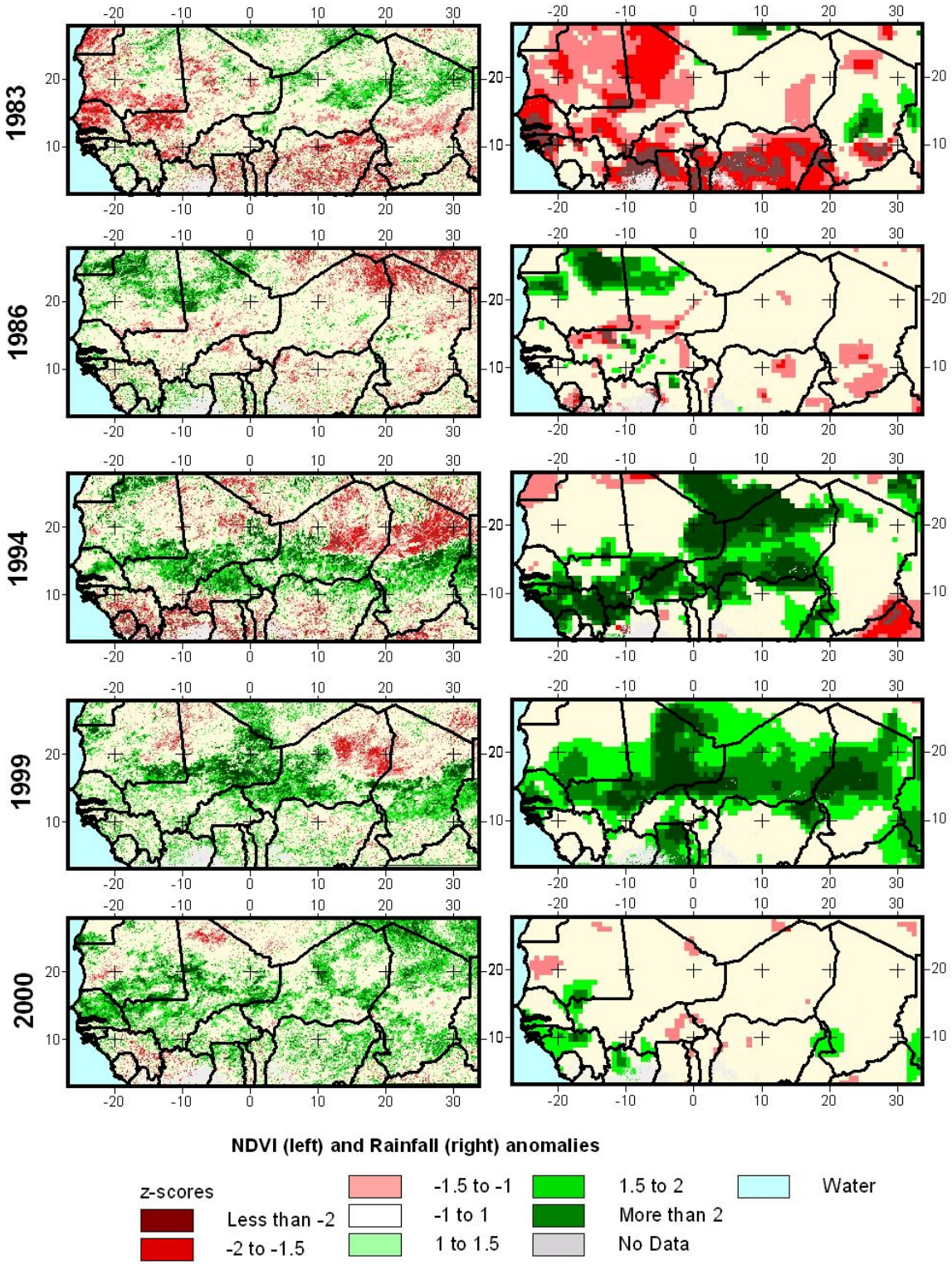

Figure 5.2.11. NDVI (8 km) and rainfall (0.5 degree grid) anomalies for 5 random "non-calendar" years during the 1982 to 2003 period.

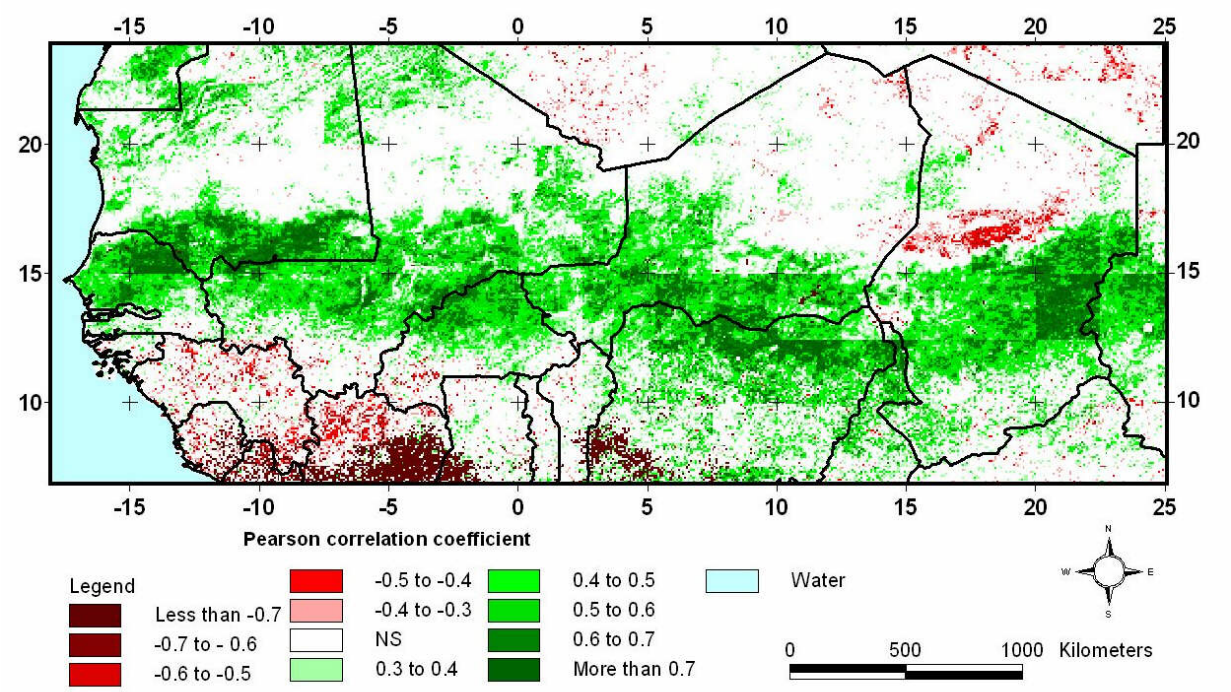

Fig. 4.2.12. Total annual rainfall (2.5 degree) vs. annual integrated NDVI (1982-2003)

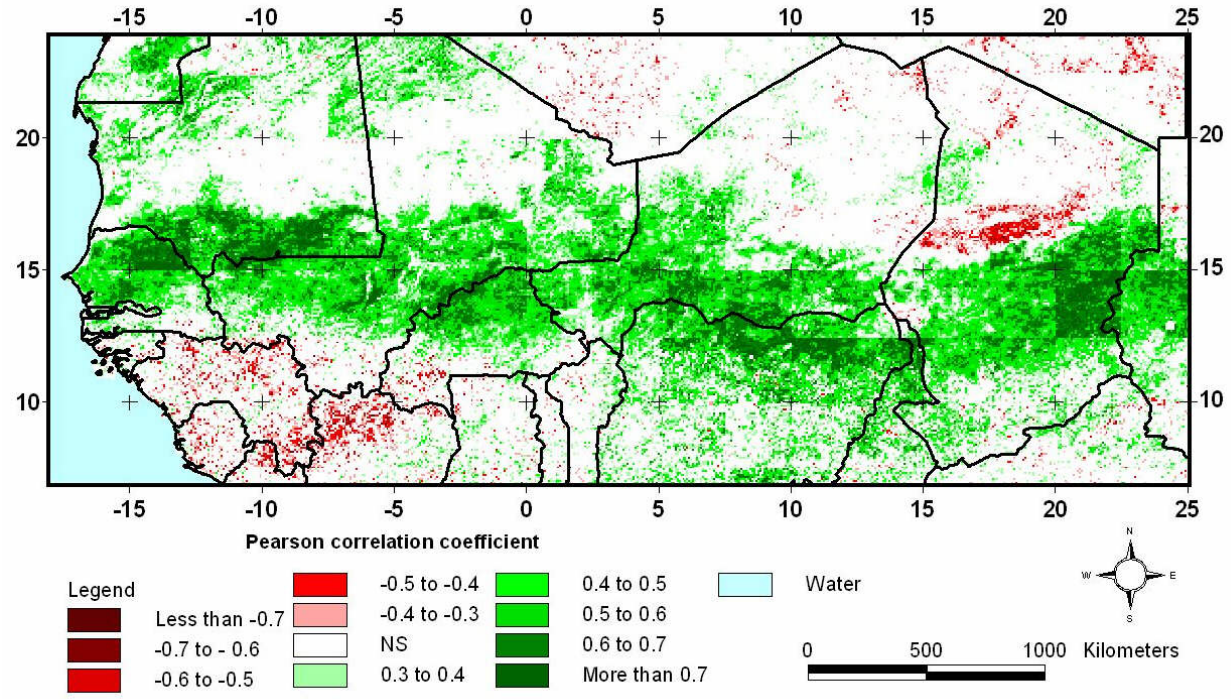

Fig. 5.2.13. Rainfall anomaly (2.5 degree) vs. NDVI anomaly (1982-2003).

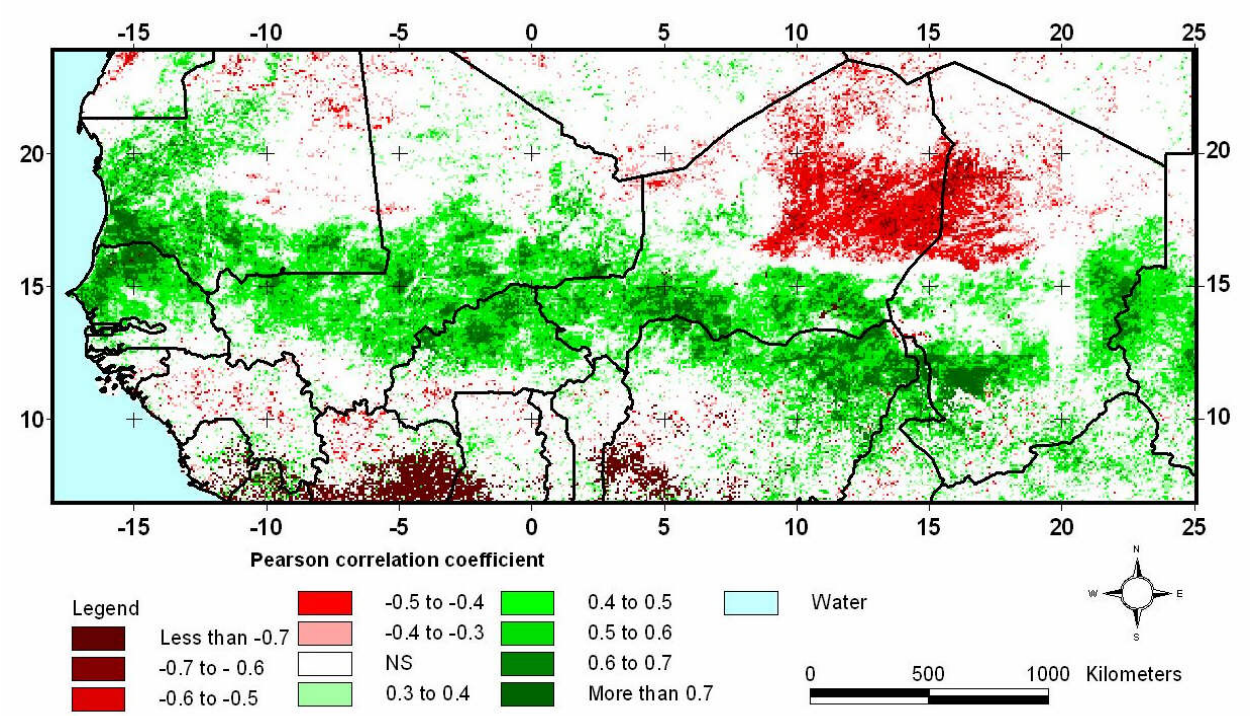

Fig. 5.2.14 Total annual rainfall (0.5 degree) vs. annual integrated NDVI (1982-2002)

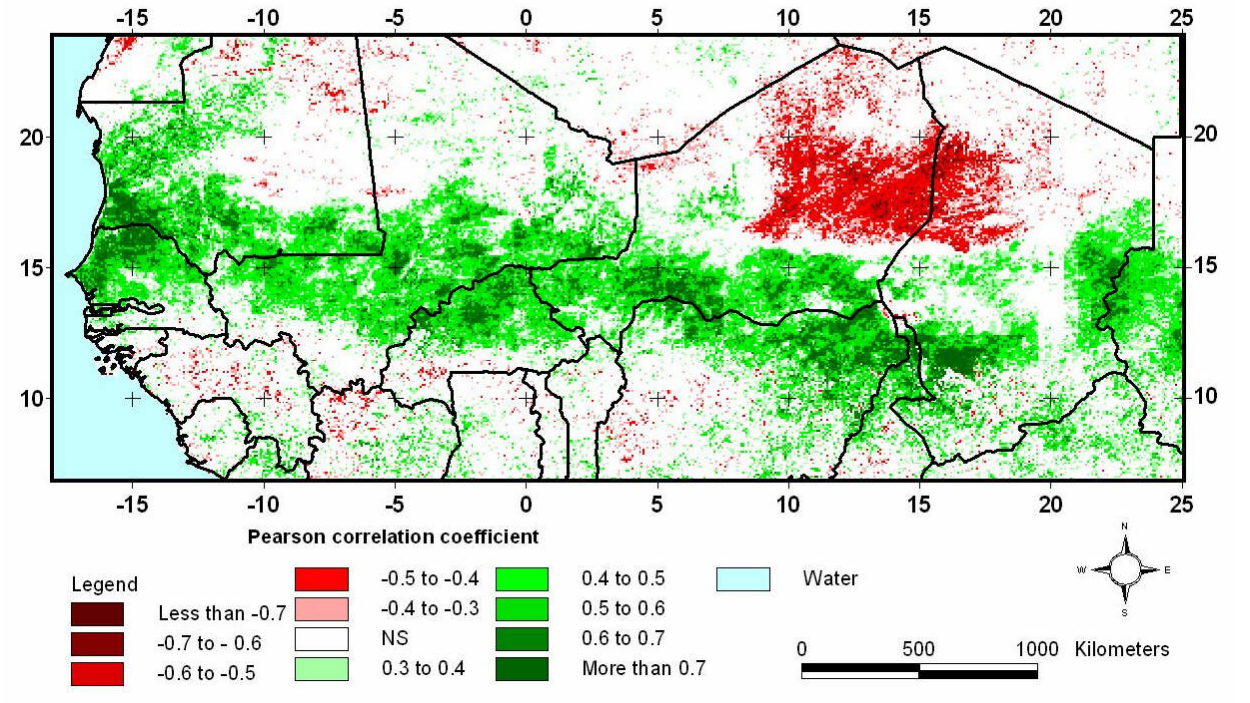

Fig. 5.2.15. Rainfall anomaly (0.5 degree) vs. NDVI anomaly (1982-2002)

5.2.4. Residual analysis

The model residuals (i.e. the difference between observed and expected iNDVI) were computed for each pixel and subsequently inspected for any systematic trends that could invalidate the initial model specification.

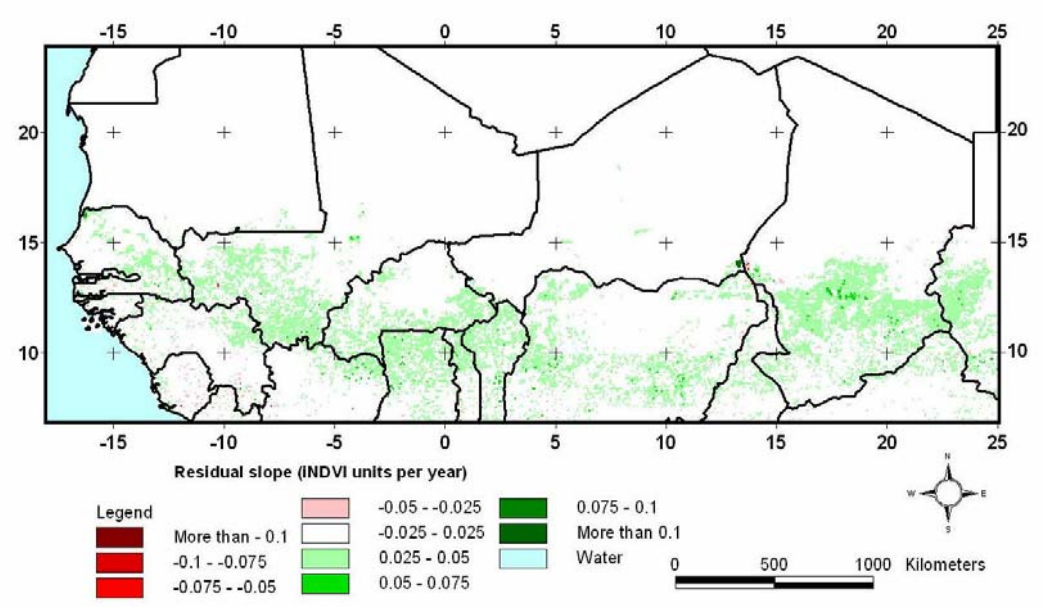

Fig. 5.2.16. Linear trends in residual slope of iNDVI when controlled for annual rainfall **(2.5 degree)** for the period 1982 to 2003. The trend is expressed in absolute values i.e. change in iNDVI units per year.

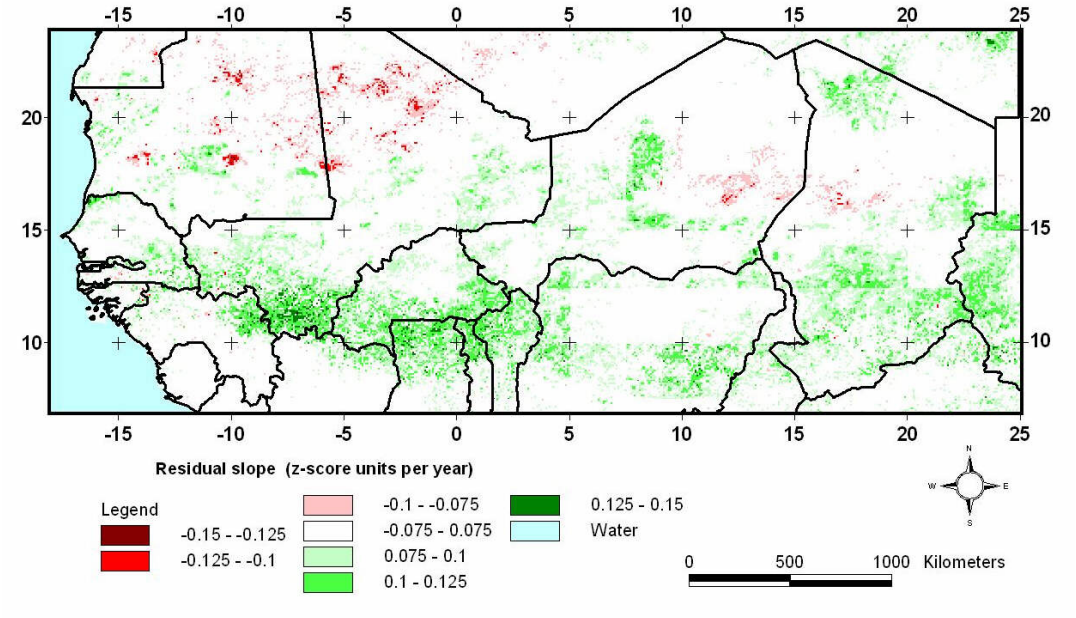

Fig. 5.2.17. Linear trends in residual slope of iNDVI z-scores when controlled for annual rainfall **(2.5 degree)** for the period 1982 to 2003. The trend is expressed in absolute values i.e. change in z-score units per year.

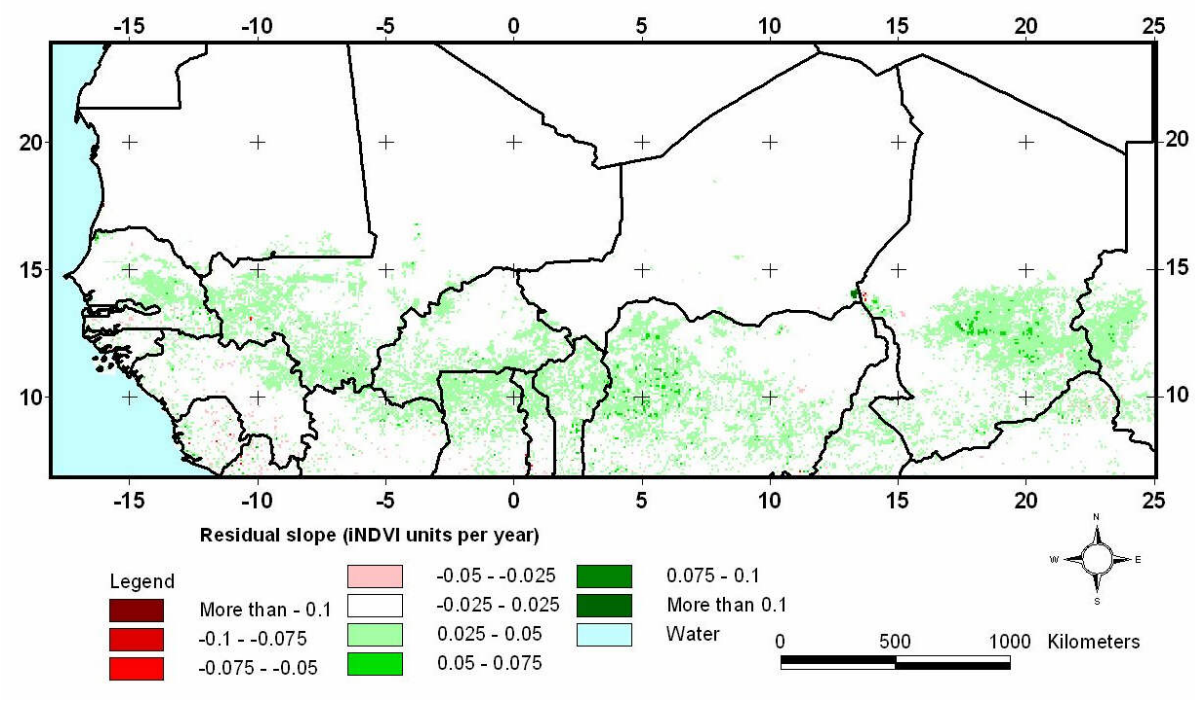

Fig. 5.2.18. Linear trends in residual slope of iNDVI when controlled for annual rainfall **(0.5 degree)** for the period 1982 to 2002. The trend is expressed in absolute values i.e. change in iNDVI units per year.

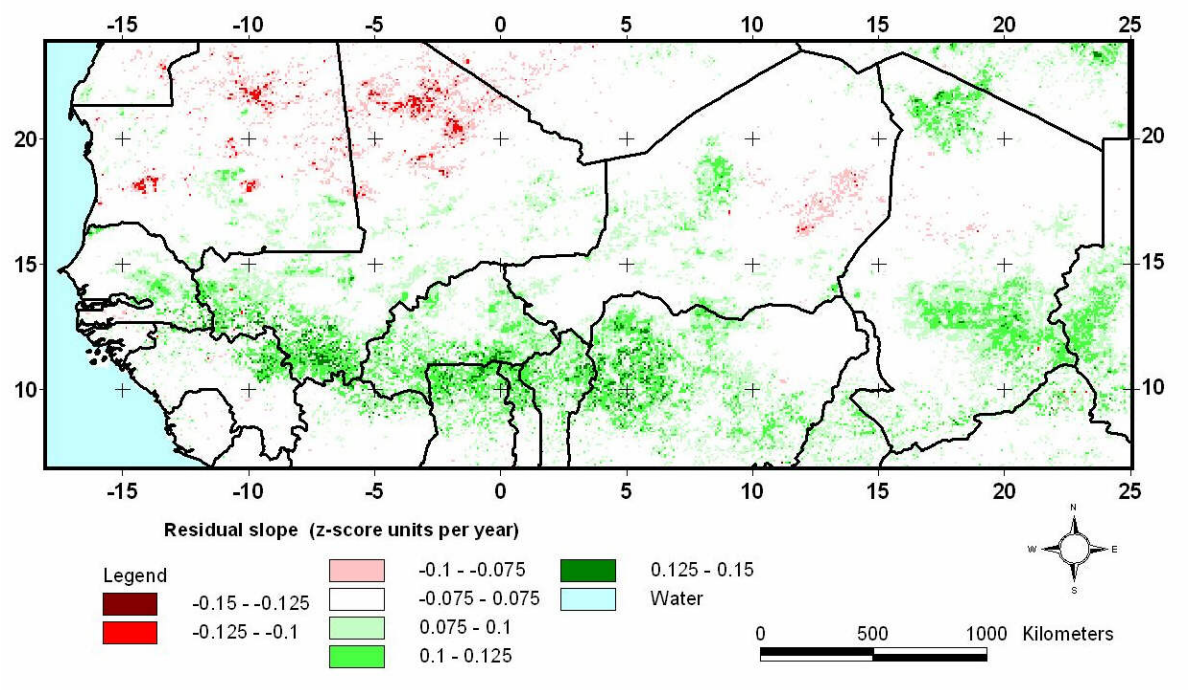

Fig. 5.2.19. Linear trends in residual slope of iNDVI z-scores when controlled for annual rainfall **(0.5 degree)** for the period 1982 to 2002. The trend is expressed in absolute values i.e. change in z-score units per year.

5.2.5. Hot Spot analysis

Example areas with significant residual trends (negative as well as positive) were identified and the trends in vegetation productivity relative to the long-term precipitation anomaly trends in the area were studied. A population density map is also presented for comparison (Fig 5.2.20-5.2.26).

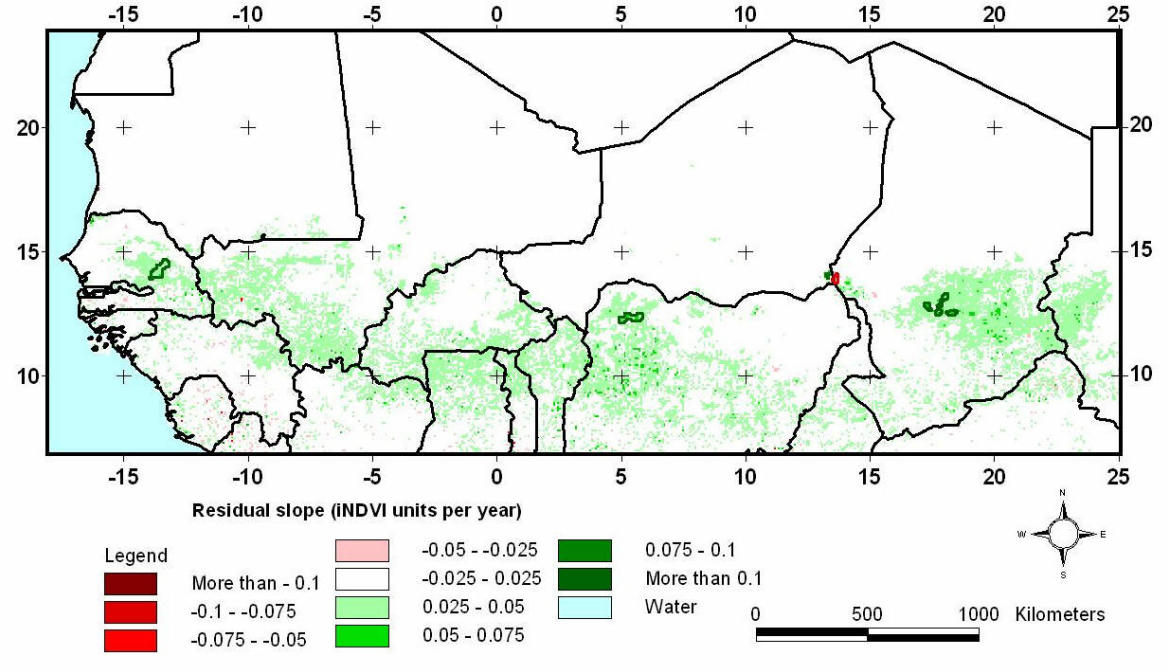

Fig. 5.2.20 West African negative (red vectors) and positive (green vectors) hot spots.

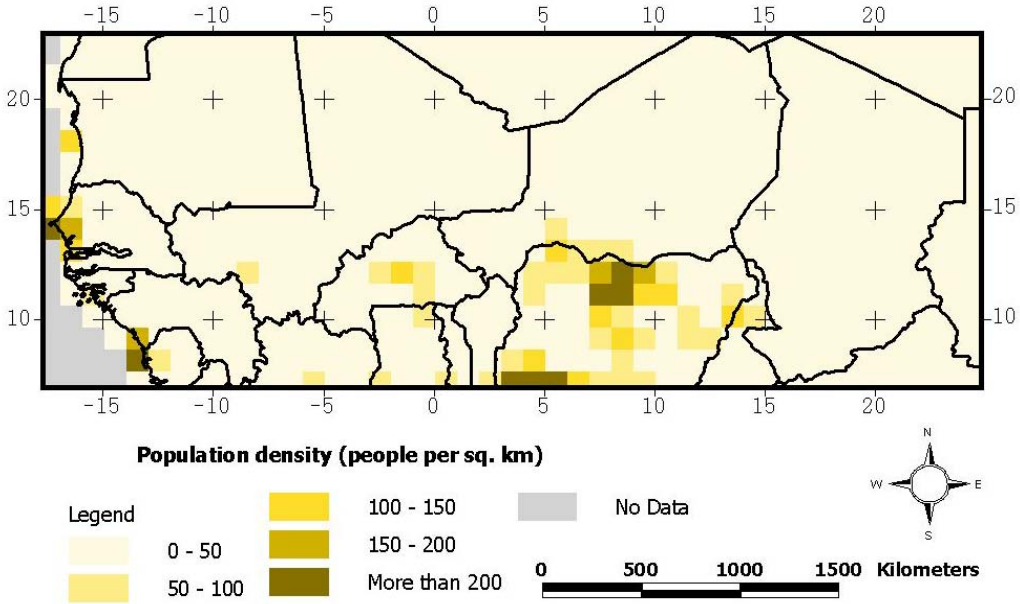

Figure 5.2.22. A population density map of the West African countries. Data are from 2000 and produced by CIESIN (2005).

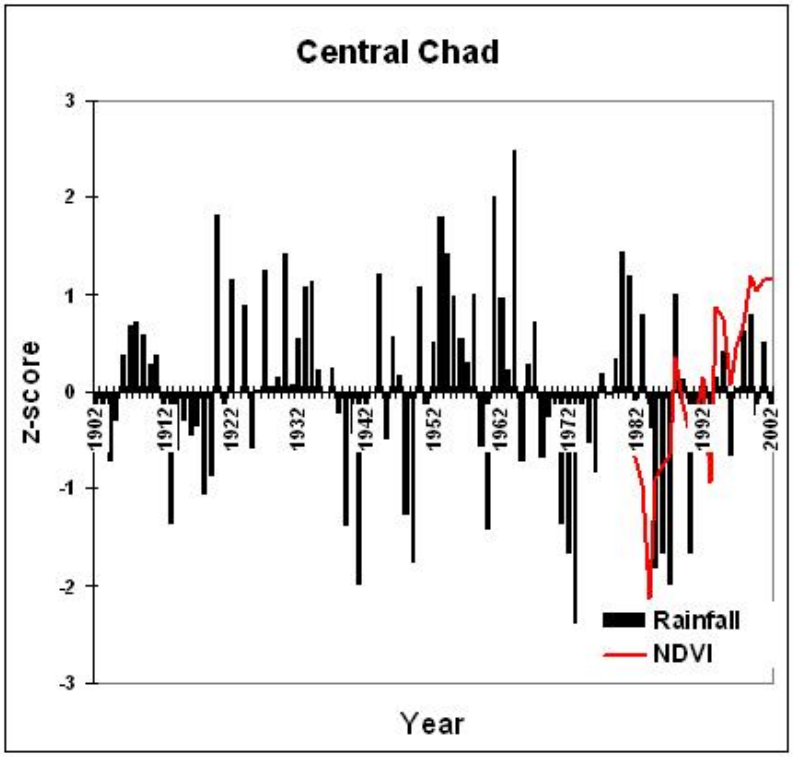

Fig. 5.2.20. Central Chad positive (green) Hot Spot with rainfall and NDVI anomalies.

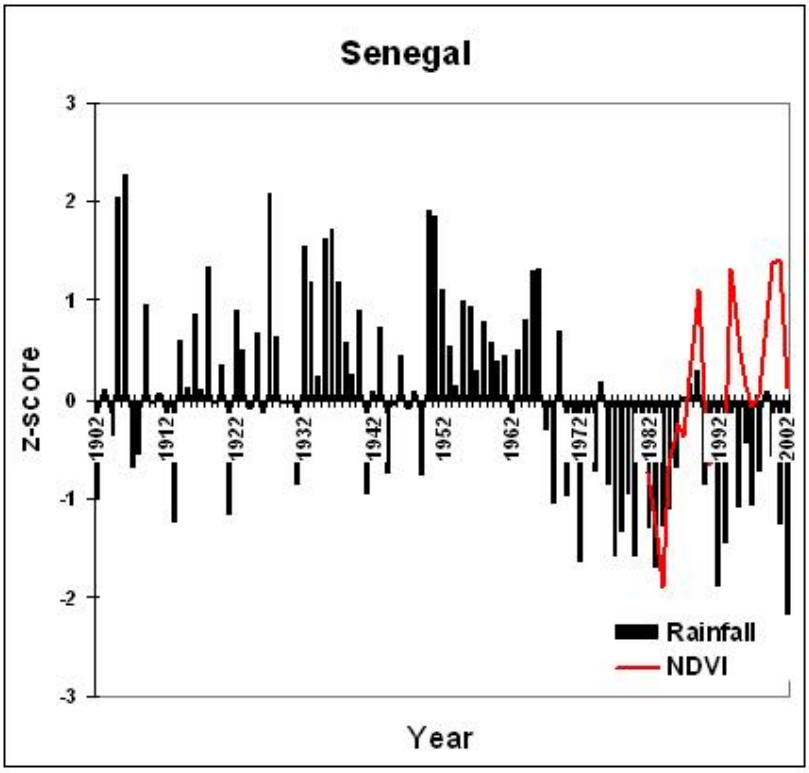

Fig. 5.2.21. Senegal positive (green) Hot Spot with rainfall and NDVI anomalies

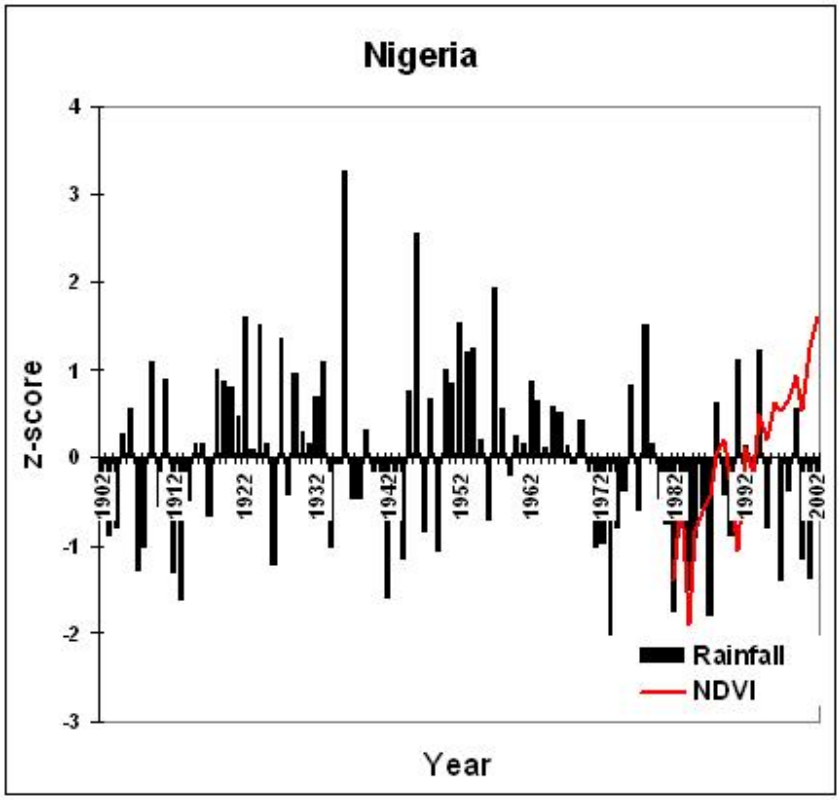

Fig. 5.2.22 Nigeria positive (green) Hot Spot with rainfall and NDVI anomalies

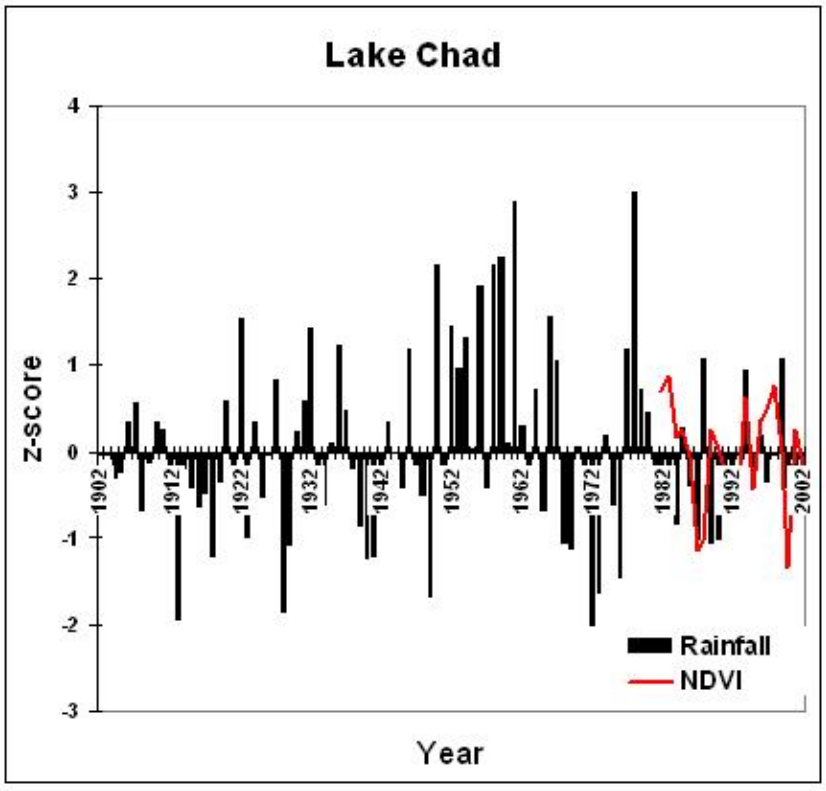

Fig. 5.2.23 Lake Chad negative (red) Hot Spot with rainfall and NDVI anomalies.

5.2.6. Desertification comments

- Signs of desertification, as reflected by significant downward trends in the vegetation productivity, after it was controlled for rainfall variability, are hardly found anywhere except in the surroundings of Lake Chad and in extreme desert conditions inside the Sahara, of no interest for this study.

- The trend maps reveal very large areas of strong positive trends in vegetation productivity, very much as a result of increasing precipitation since around 1982, the driest peak of the Sahelian drought (1964-2002). Similar results were presented by Eklundh and Olsson (2003) based on the analysis of 1982-1999 AVHRR NDVI Pathfinder data.

- However, there is also an obvious positive trend in the integrated NDVI and its anomalies that cannot be explained by increased precipitation only. This may, to some extent, be due to the "Green House" effects including increased CO_2 concentrations in the atmosphere and increased temperatures possibly increasing the length of the growing season and causing its earlier start as indicated in a NOAA AVHRR study on global terrestrial NPP by Nemani et al. (2003). Hickler et al. (2005) demonstrated that a process-based ecosystem model driven by climatic and atmospheric CO_2 data alone closely reproduced the satellite observed greening trend of the Sahel vegetation and its interannual variation 1982-1998. The satellite data used was the GIMMS NOAA-AVHRR NDVI data set covering the period 1982-1998. Changes in precipitation were identified as the primary driver of the aggregated simulated vegetation changes with CO2 having a minor positive effect.

Fig. 5.2.24. (LEFT) **Mar 1983**--a very dry year in the Sahel (Senegal) in the dry season. (RIGHT) **Dec 1994**--a wet year in the Sahel (Senegal) at the end of the rainy season (Photo: G.Tappan, USGS).

5.3. EAST AFRICA

5.3.1. East Africa overview

This study region extends from Sudan in the west to Somalia in the east and between 5° to 23° Northern latitude.

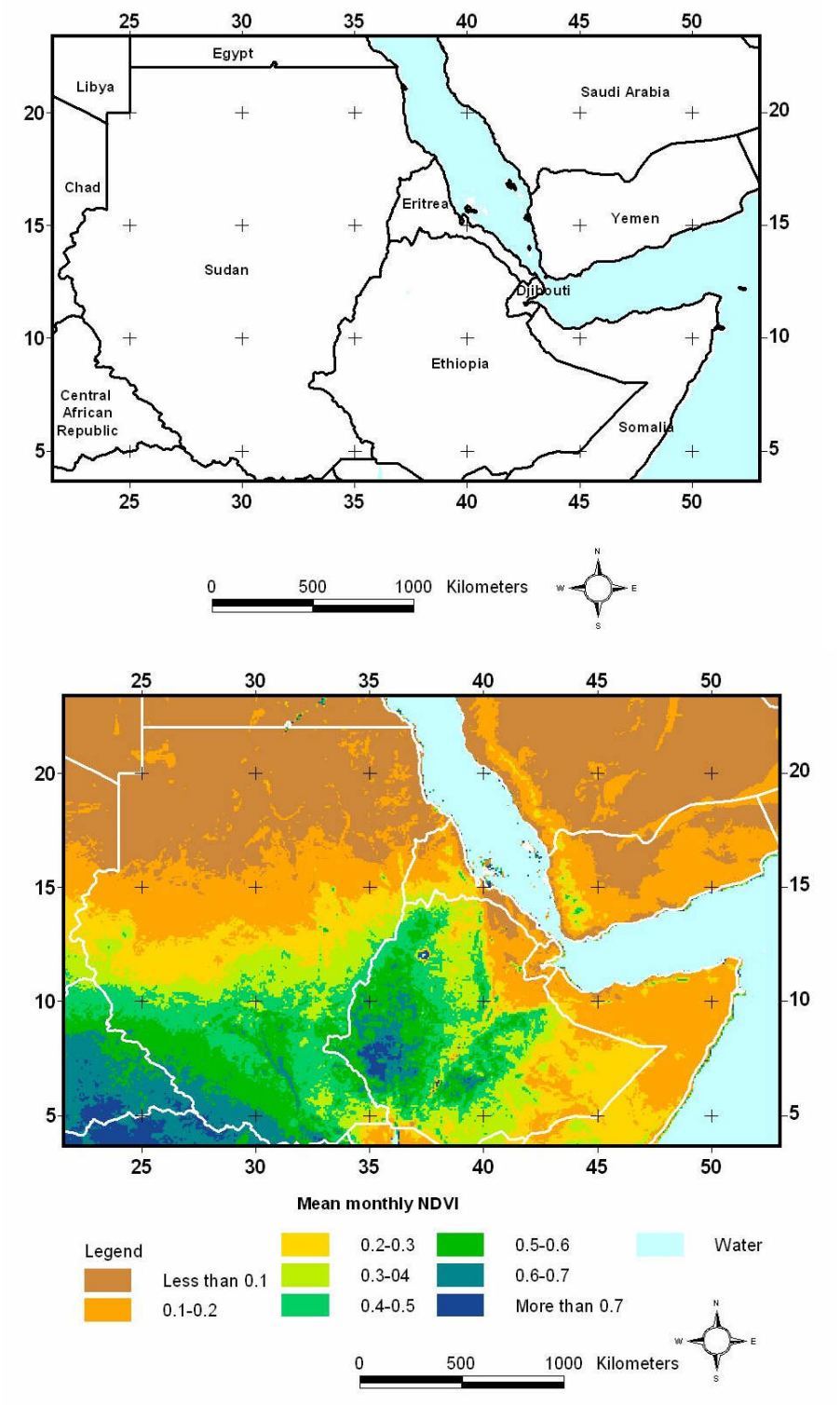

Figure 5.3.1. Country overview (top) and the mean monthly NDVI based on data from 1982 to 2003 (bottom).

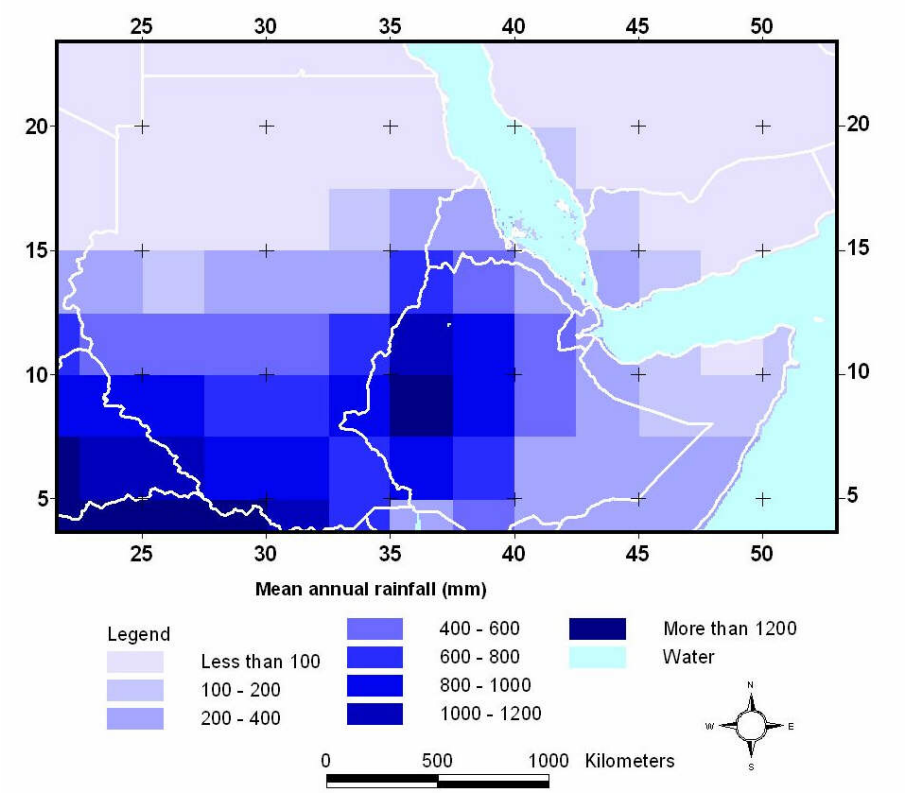

Figure 5.3.2. Mean annual rainfall based on 2.5 degree (~ 275 km) gridded rainfall data from 1982 to 2003.

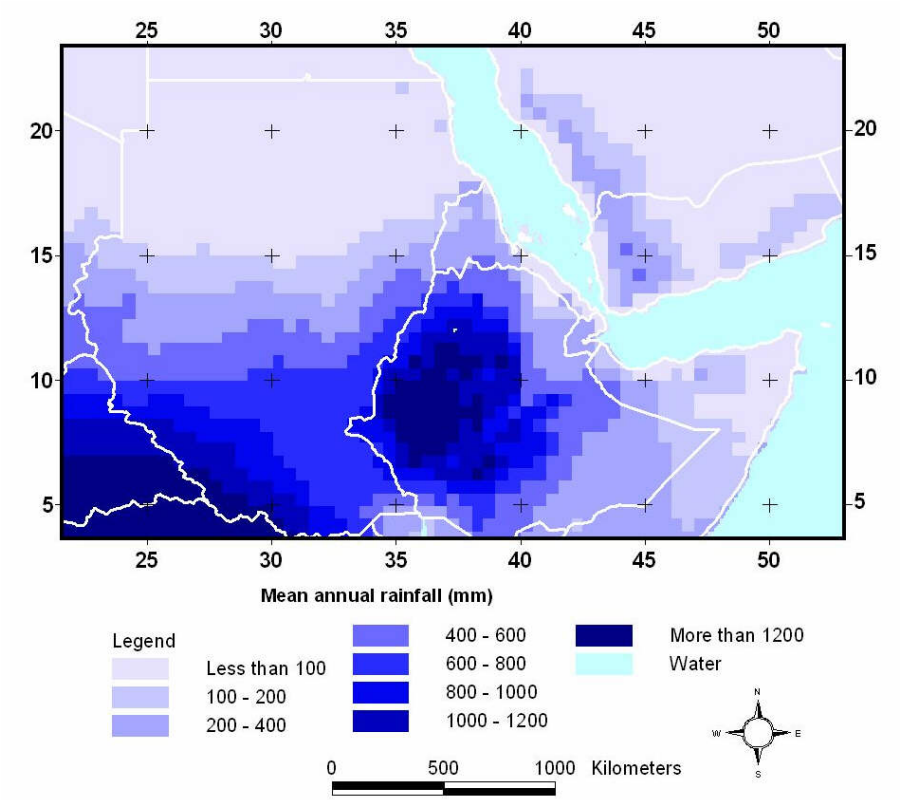

Fig. 5.3.3. Mean annual rainfall based on 0.5 degree (~55 km) gridded rainfall data from 1982 to 2002.

Inspection of time-series plots of both rainfall and NDVI revealed that the appropriate seasons for the drylands (i.e. the area delineated by a minimum of 0.1 and a maximum of 0.5 NDVI based on the long-term monthly average) of the East African region was "January to December" and "March to February" for rainfall and NDVI respectively (figure 5.3.4).

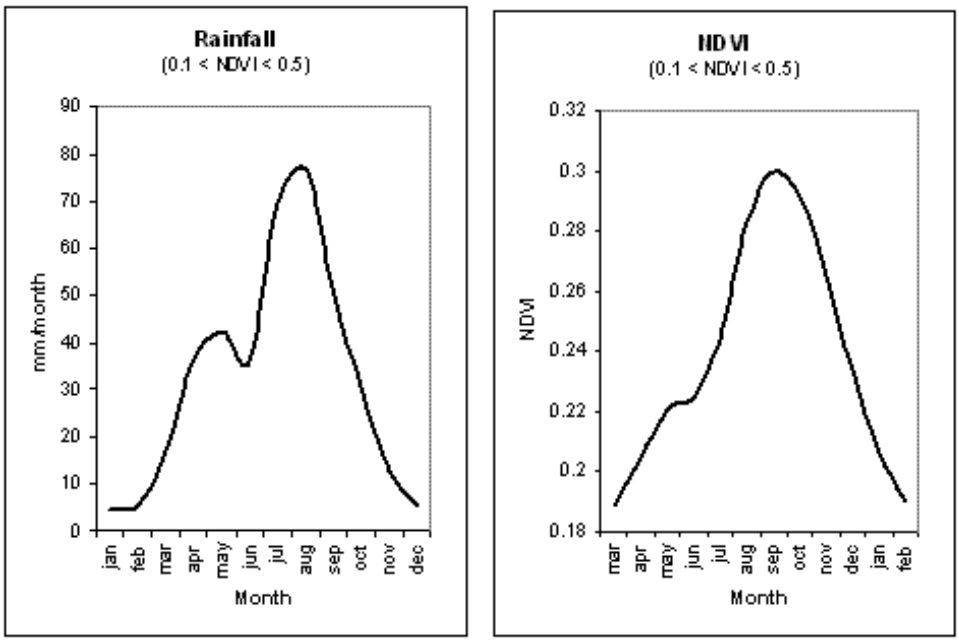

Figure 5.3.4. Monthly time-series plots of rainfall (left) and NDVI (right). The displayed values are mean values as calculated from the area defined by $0.1 \leq NDVI \leq 0.5$.

Consequently total annual rainfall was calculated by summarizing rainfall received within the months from January to December. Similar the annual vegetation productivity was estimated by integrating NDVI over the months from March and until February the following year.

5.3.2. Vegetation trend analysis

The following figures summarize the results of the trend analysis approaches described under methods.

Figure 5.3.5-5.3.8 confirm the points raised in the method sections regarding the relative merits of the different characteristics (inclination, relative change or statistical significance) of the trend line. Especially it is clear that the statistical test is placing too much emphasis on areas with rather small slope inclinations. There is equally a tendency for the relative change to put emphasis on areas where the intercept value i.e. the starting point is low. In that case a relative low absolute slope value may actually come out as a quite significant relative change.

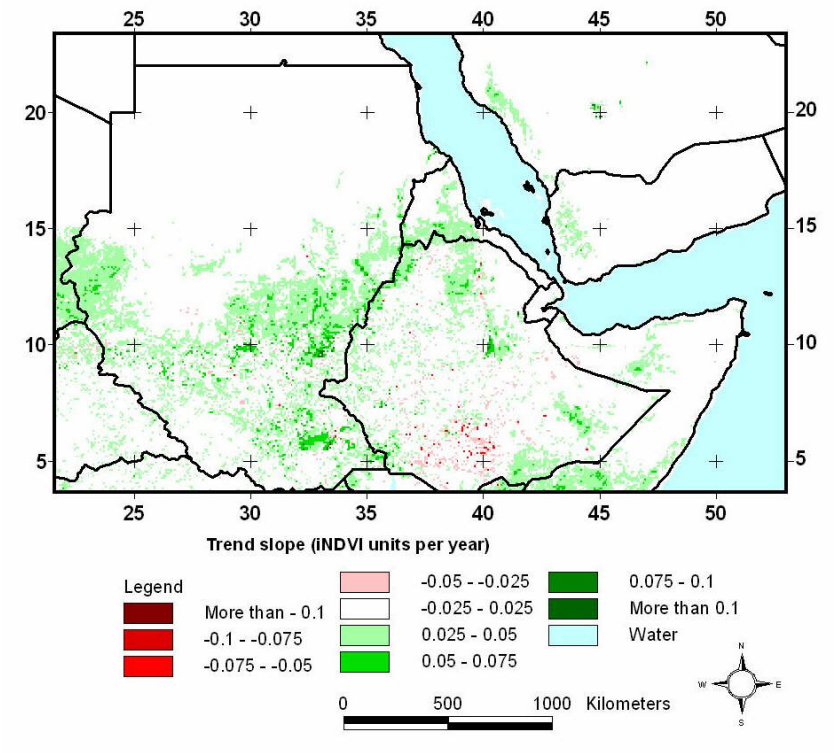

Figure 5.3.5. Linear trends in vegetation productivity for the period 1982 to 2002 based on annual integrated NDVI values. The trend is expressed in absolute values i.e. change in iNDVI units per year.

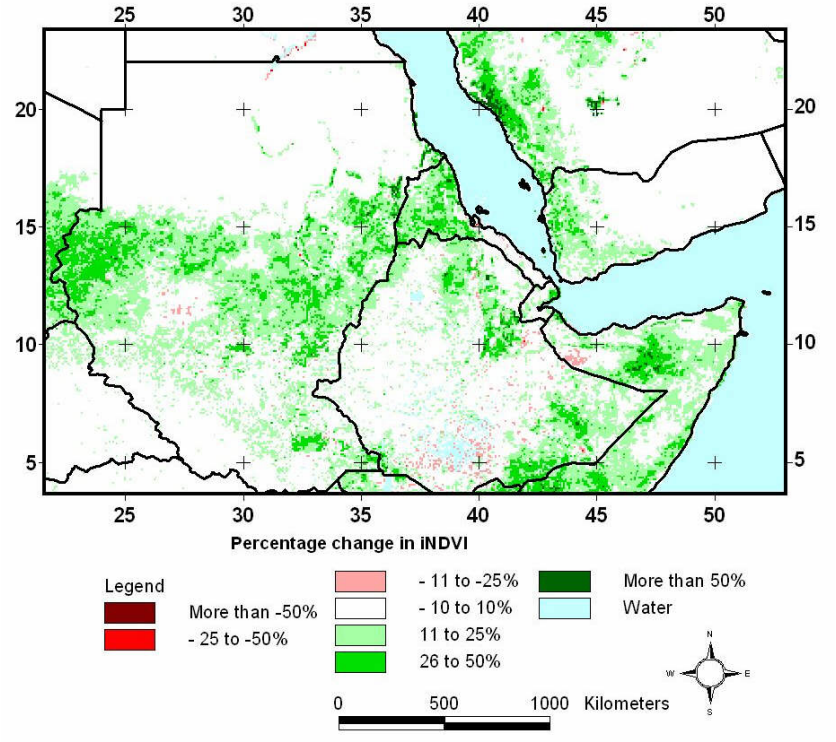

Fig 5.3.6. Linear trends in vegetation productivity for the period 1982 to 2002 based on annual integrated NDVI values. The trend is expressed as percentages i.e. the relative difference between the start and the end value of the linear trend

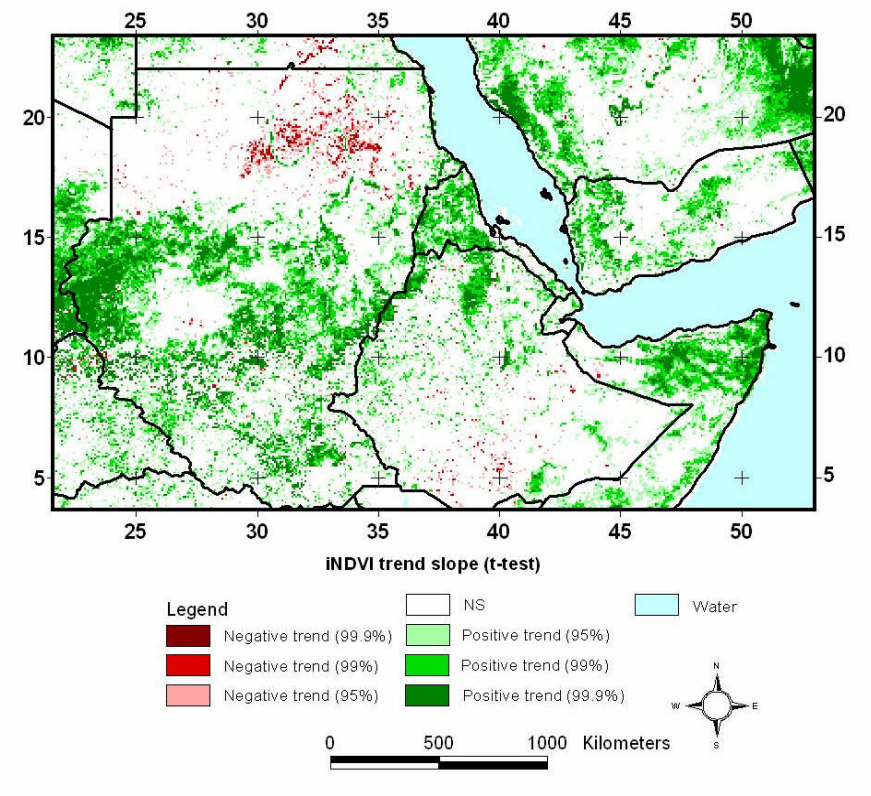

Fig. 5.3.7. Trend slope in NDVI based on linear least square regression (1982-2002). iNDVI trend slope (t-test)

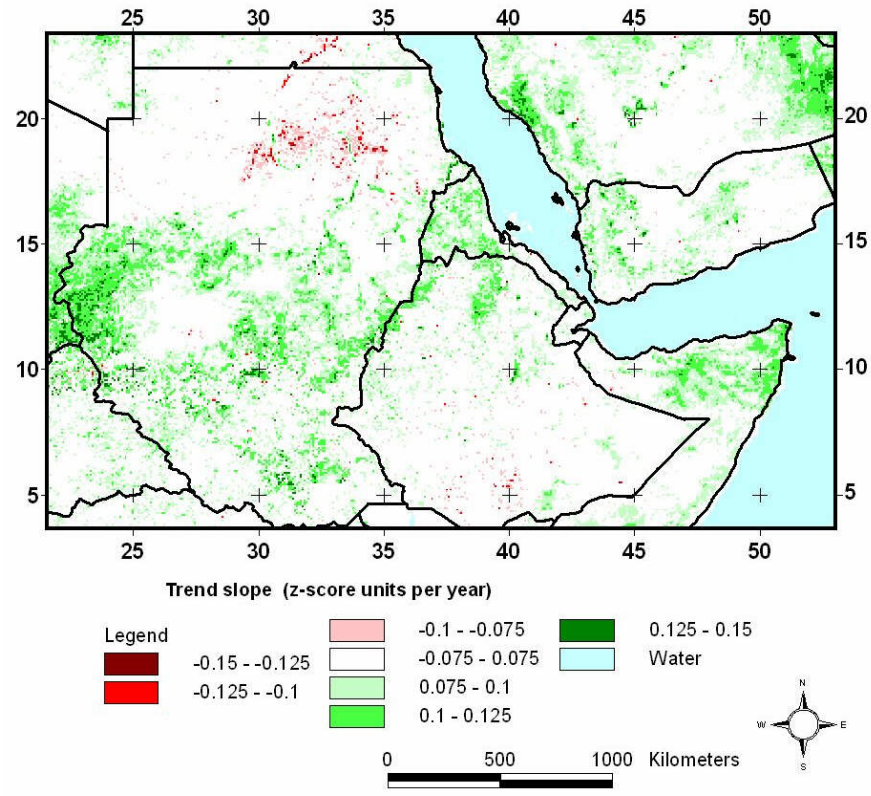

Figure 5.3.8. Standardized trend slope in NDVI based on linear least square regression and expressed as z-score units per year (1982-2002).

5.3.3. Vegetation versus rainfall analysis

Figure 5.3.9 (left) indicates the relationship between mean NDVI and mean annual rainfall. The strong positive relationship (r^2=0.9) confirms the fact that higher rainfalls normally yields higher vegetation productivity.

Yet, the relationship illustrated in Figure 5.3.9 (left) is biased due to the presence of spatial auto-correlation i.e. the phenomenon where locational (geographic position) similarity is matched by value similarity. Consequently Fig. 5.3.9 (left) demonstrates the geographic relationship between long-term means of total annual rainfall and monthly NDVI .In order to avoid this bias the anomaly analysis was introduced (figure 5.3.9 [right], figure 5.3.10, 5.3.11-5.3.15).

The results from the anomaly analysis illustrate a significant and valid relationship between rainfall variability and NDVI variability for large parts of the East African drylands. Despite the generalization level of these figures it remains clear that rainfall and NDVI are indeed closely associated. Figure 5.3.9 thereby supports the idea that NDVI trends should be controlled for rainfall variability before elucidating on the possible anthropogenic causes.

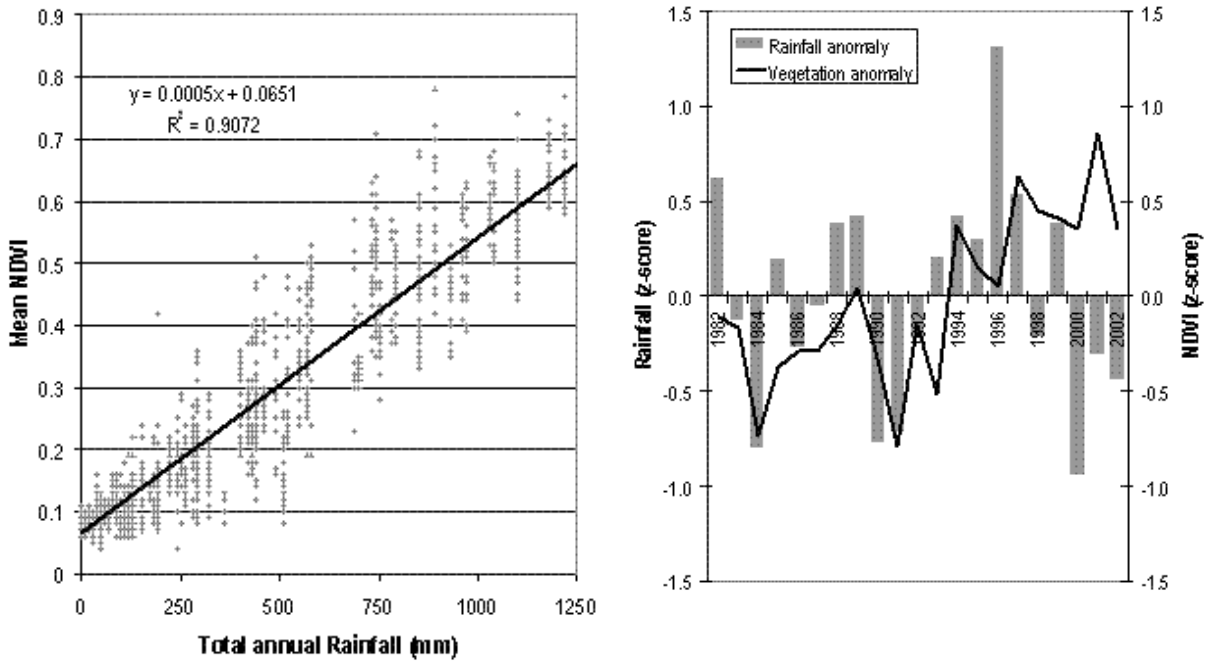

Fig. 5.3.9. (LEFT) Mean NDVI plotted against total mean annual rainfall. The displayed values are mean values for the period 1982-2003. (RIGHT) Average area z-scores of NDVI and rainfall for East Sahel for each year 1982-2003. On display are mean z-scores as calculated from the area defined by 0.1 < NDVI < 0.5 where NDVI refers to the mean monthly NDVI for the period.

Despite the generalization level of these figures it remains clear that rainfall and NDVI are indeed closely associated in East African Sahel. Figure 5.3.9 thereby supports the idea that NDVI trends should be controlled for rainfall variability before elucidating on the possible anthropogenic causes.

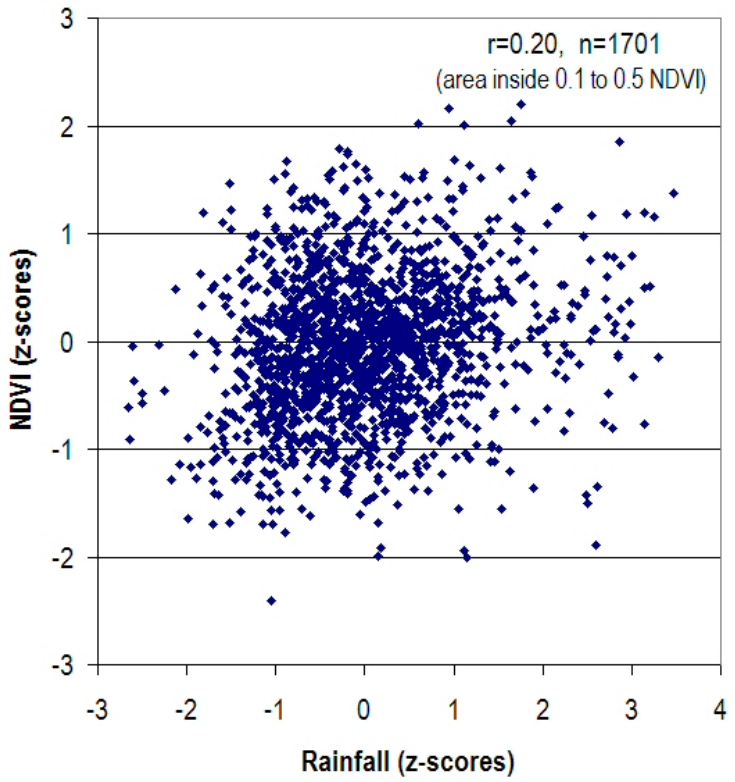

Fig. 5.3.10. Annual NDVI anomalies plotted against annual rainfall anomalies. Every pixel in the 2.5 degree rainfall data was selected and plotted against the average NDVI value for the corresponding NDVI 8 km pixels under each 2.5^0 cell. Only pixels inside the area defined by 0.1<NDVI<0.5 where NDVI denotes mean monthly NDVI for the 1982-2003 period. All data for the 1982-2003 period were merged into one data set.

It should be noted that it is only a fraction (4%) of the interannual NDVI anomaly variation that can be explained by the corresponding interannual (seasonal) rainfall anomalies under the given circumstances (Fig 5.3.10.). It implies there are large areas (many pixels) where the strong NDVI-rainfall anomaly relationship is not valid. This is also illustrated in the figures below.

The following maps summarizes the results from the per pixel analysis of the temporal relationship between rainfall and NDVI.

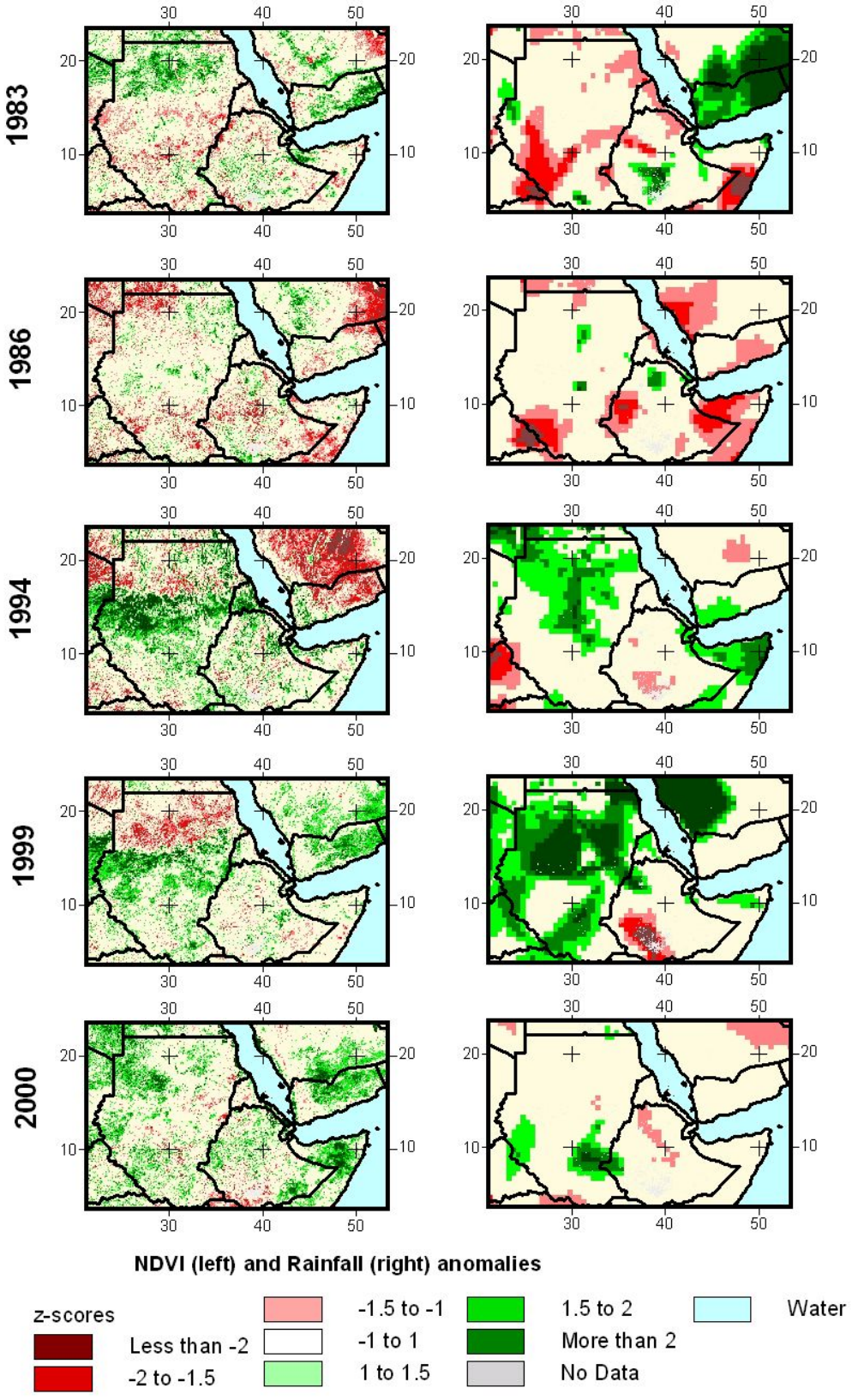

Figure 5.3.11. NDVI (8 km) and rainfall (0.5 degree grid) anomalies for 5 random “non-calendar” years during the 1982 to 2003 period.

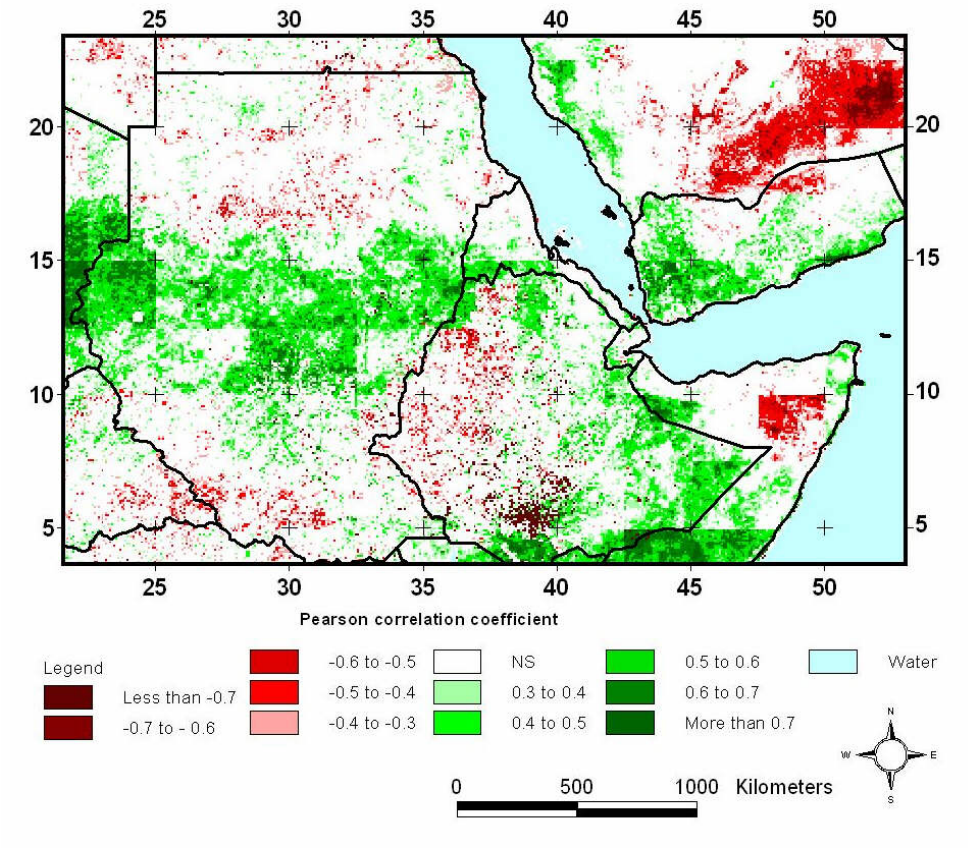

Fig. 5.3.12. Total annual rainfall (2.5 degree) vs. annual integrated NDVI (1982-2003)

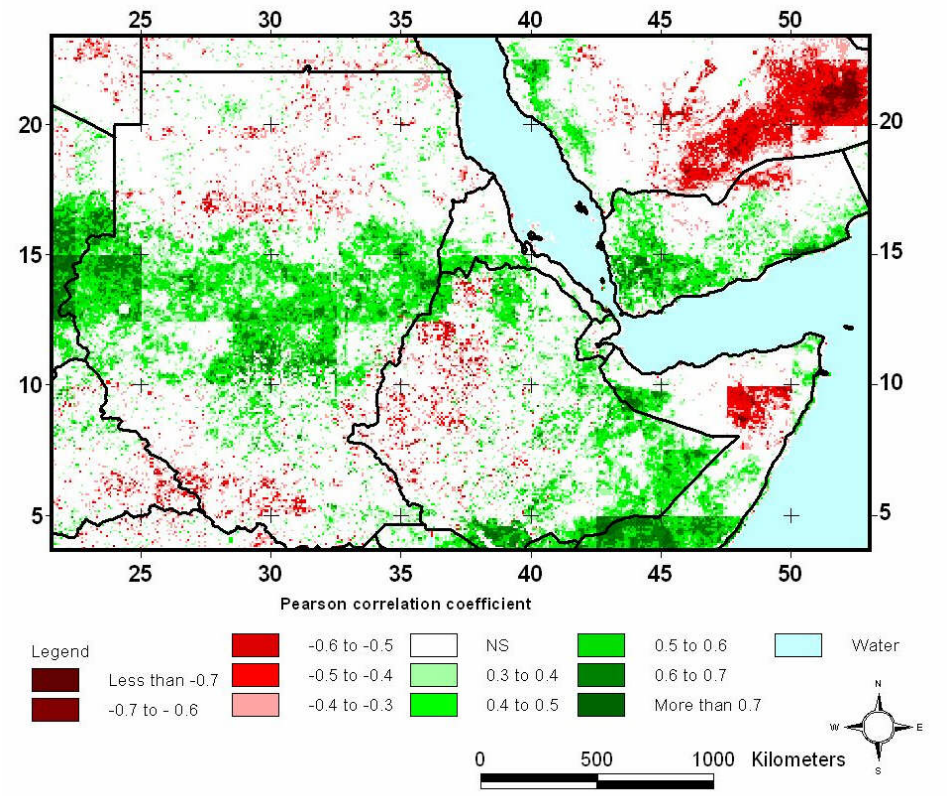

Fig. 5.3.13. Rainfall anomaly (2.5 degree) vs. NDVI anomaly (1982-2003).

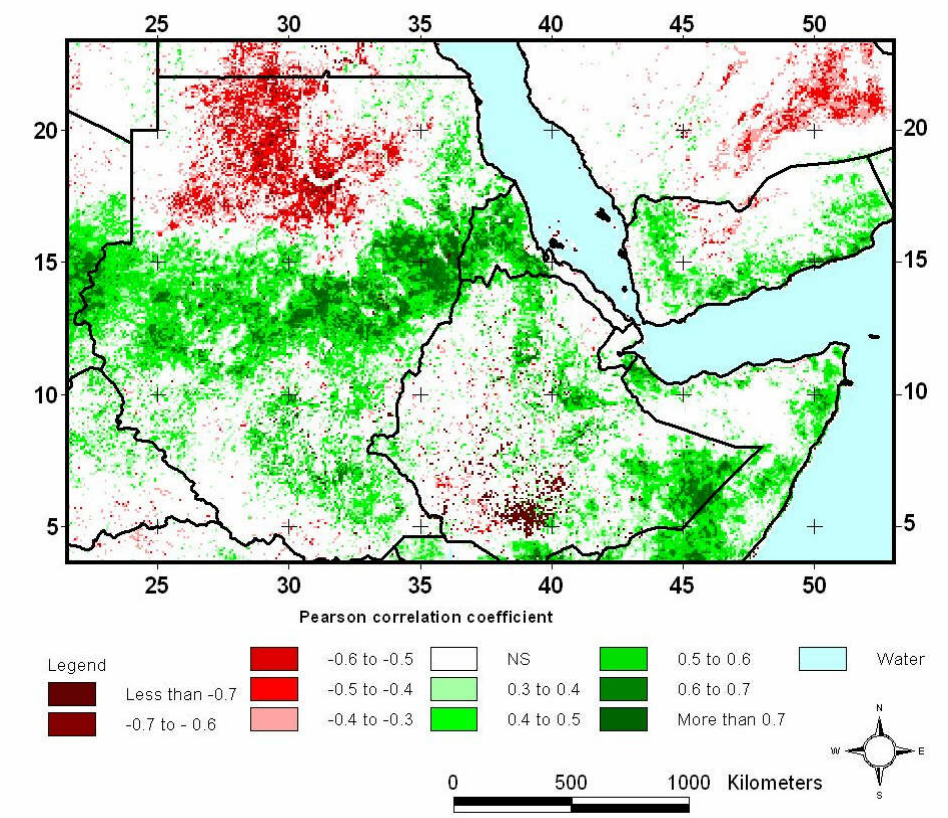

Fig. 5.3.14. Total annual rainfall (0.5 degree) vs. annual integrated NDVI (1982-2002**)**

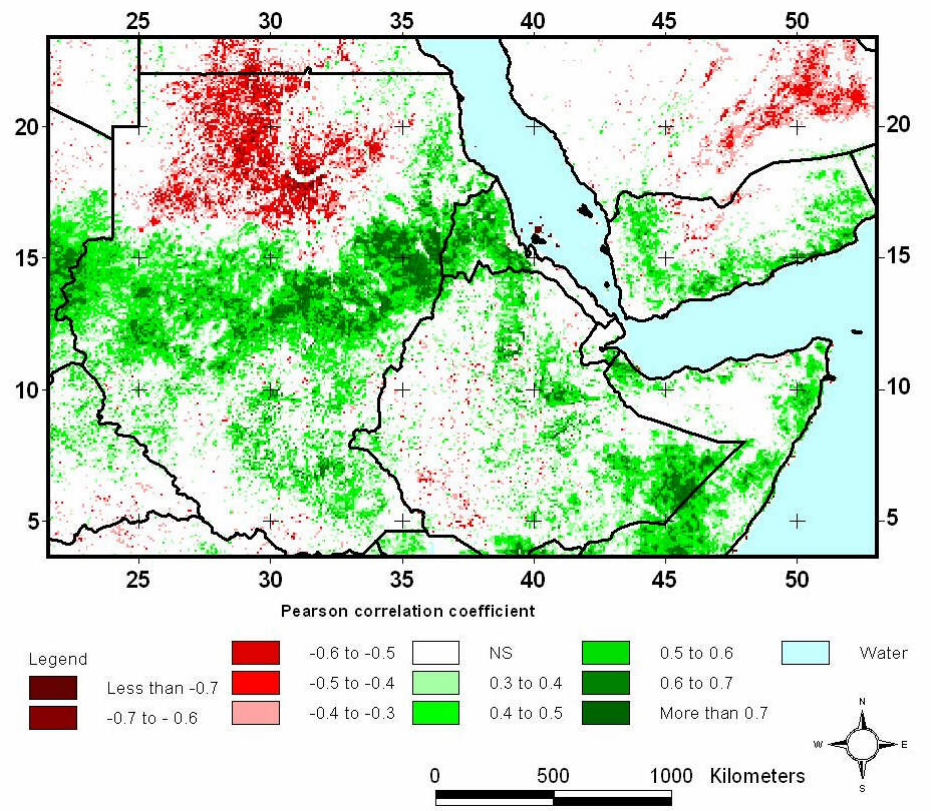

Fig. 5.3.15. Rainfall anomaly (0.5 degree) vs. NDVI anomaly (1982-2002).

5.3.4. Residual analysis

The model residuals (i.e. the difference between observed and expected iNDVI) were computed for each pixel and subsequently inspected for any systematic trends that could invalidate the initial model specification.

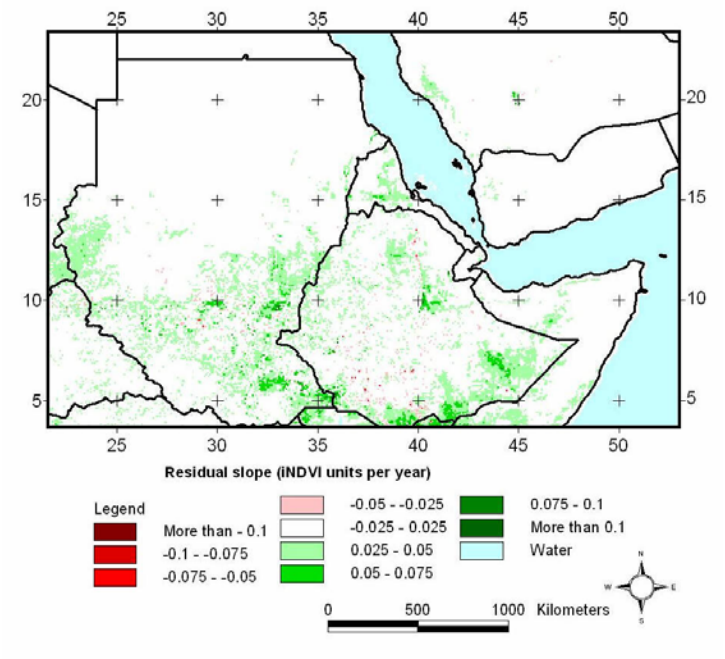

Fig. 5.3.16. Linear trends in residual slope of iNDVI when controlled for annual rainfall **(2.5 degree)** for the period 1982 to 2003. The trend is expressed in absolute values i.e. change in iNDVI units per year.

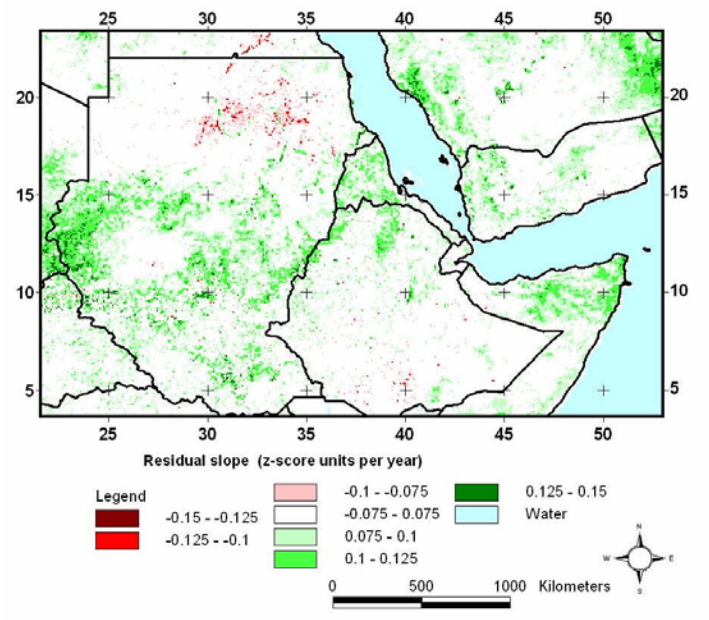

Fig. 5.3.17. Linear trends in residual slope of iNDVI z-scores when controlled for annual rainfall **(2.5 degree)** for the period 1982 to 2003. The trend is expressed in absolute values i.e. change in z-score units per year.

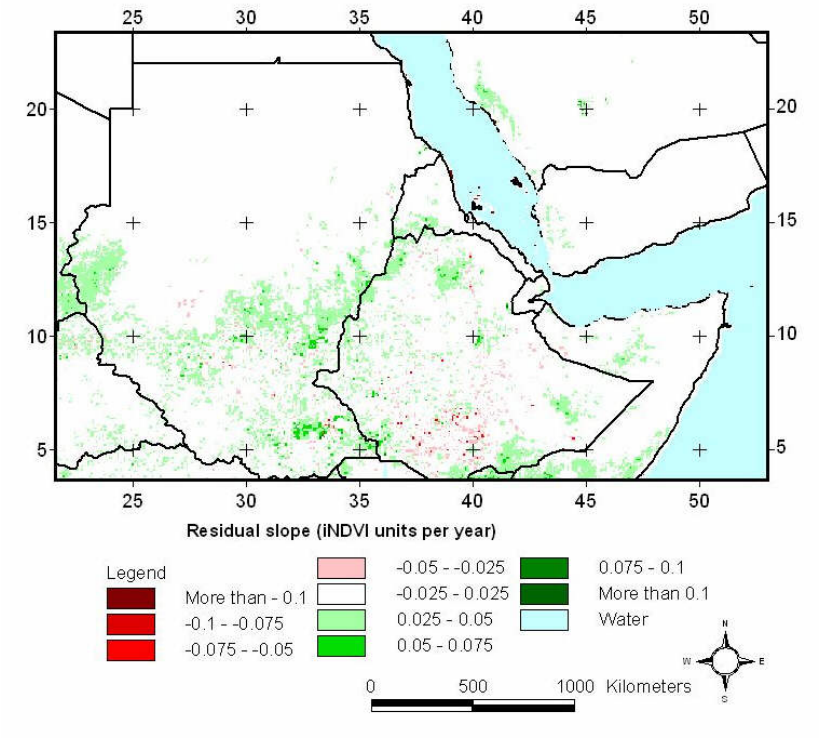

Fig. 5.3.18. Linear trends in residual slope of iNDVI when controlled for annual rainfall **(0.5 degree)** for the period 1982 to 2002. The trend is expressed in absolute values i.e. change in iNDVI units per year

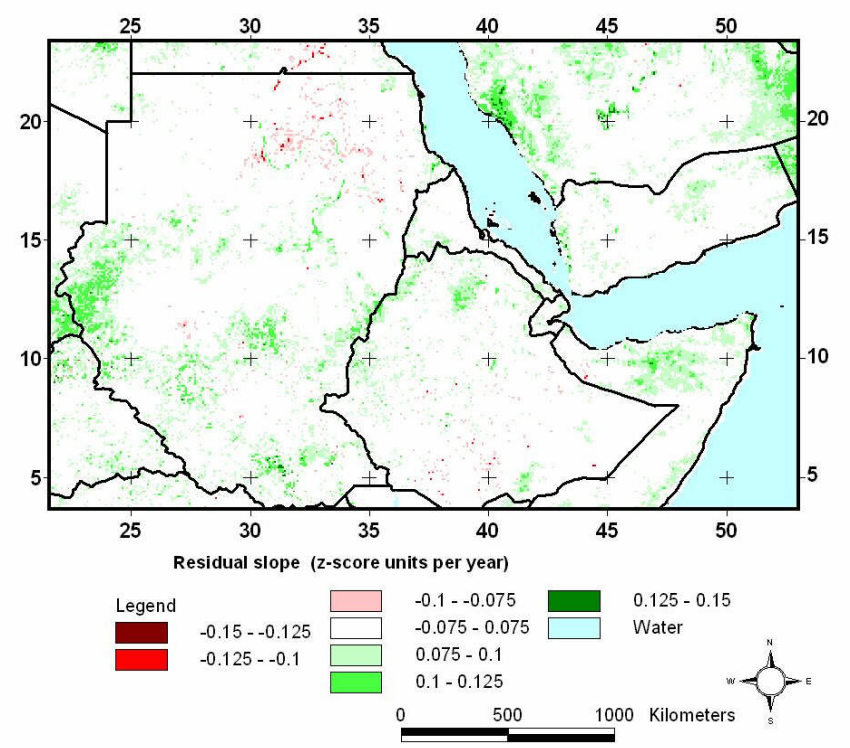

Fig. 5.3.19. Linear trends in residual slope of iNDVI z-scores when controlled for annual rainfall **(0.5 degree)** for the period 1982 to 2002. The trend is expressed in absolute values i.e. change in z-score units per year.

5.3.5. Hot Spot analysis

Example areas with significant residual trends (negative as well as positive) were identified and the trend in vegetation productivity relative to the long-term precipitation anomaly trends in the area were studied (Fig 5.3.20-5.3.23).

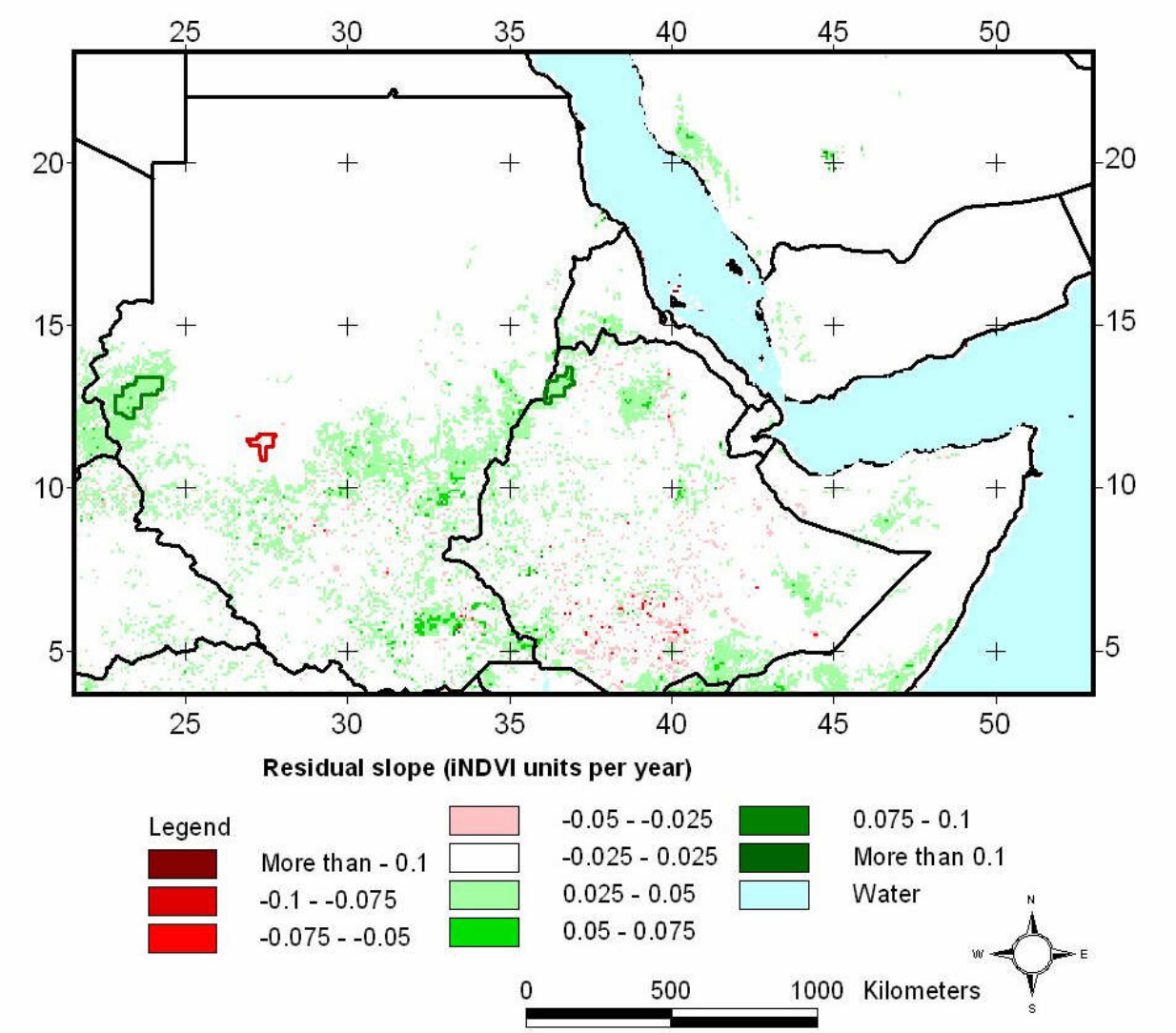

Fig. 5.3.20. East African negative (red vectors) and positive (green vectors) hot spots.

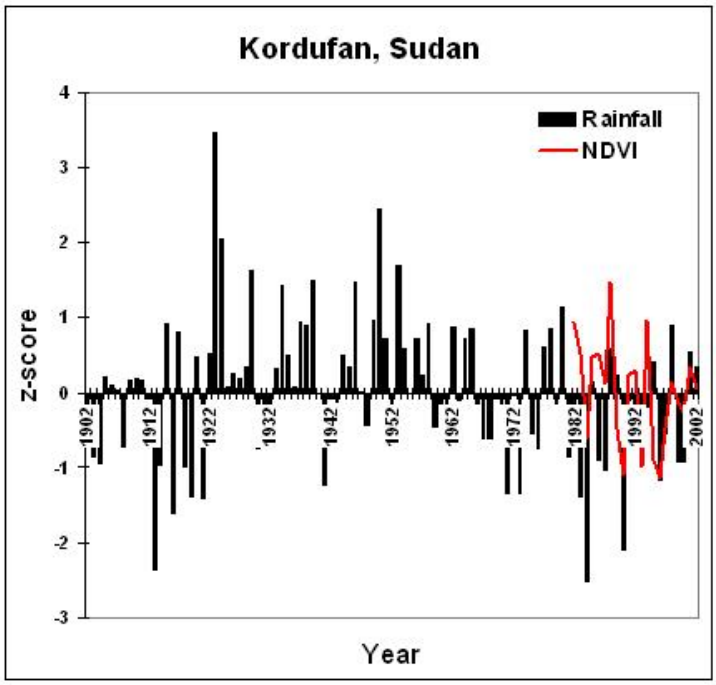

Fig. 5.3.21 Kordofan negative (red) Hot Spot with rainfall and NDVI anomalies

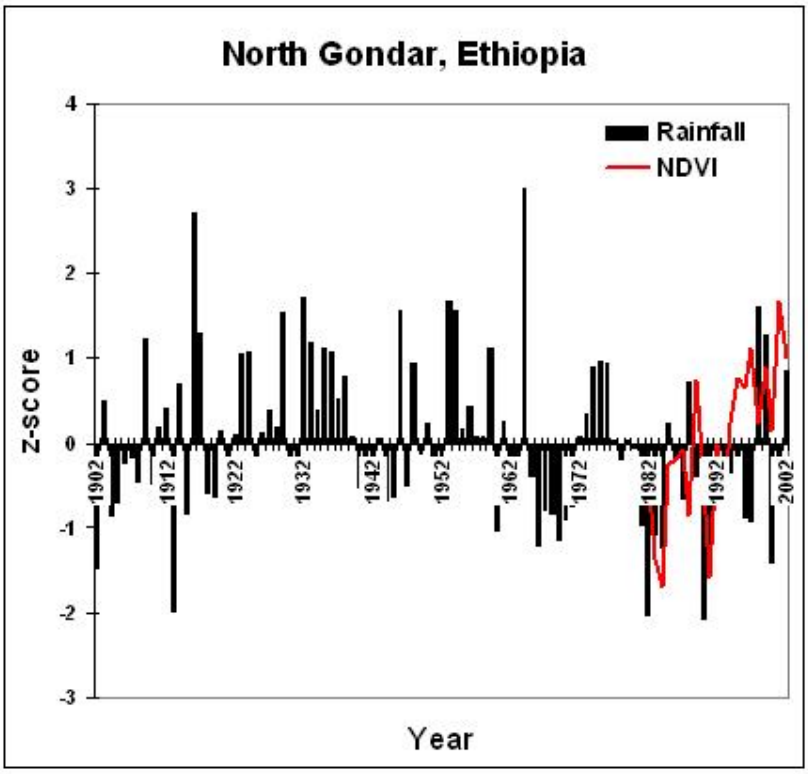

Fig. 5.3.22 North Gondar positive (green) Hot Spot with rainfall and NDVI anomalies

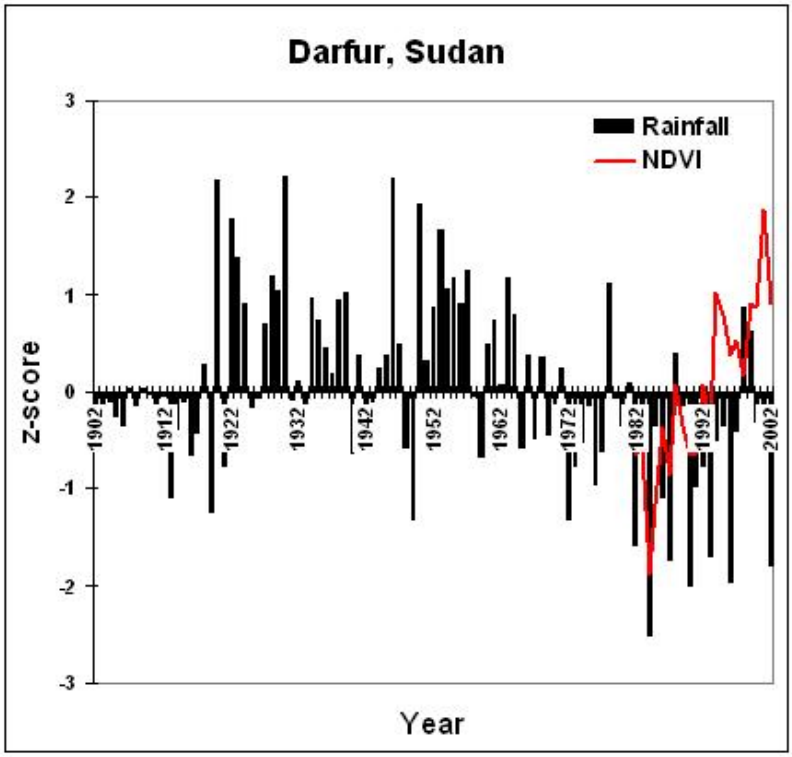

Fig. 5.3.23. Darfur positive (green) Hot Spot with rainfall and NDVI anomalies

5.3.6. Desertification comments.

The development pattern and history is very similar to what has been said about west Sahel. It is repeated below for the sake of easy access:

- Signs of desertification, as reflected by significant downward trends in the vegetation productivity, after it was controlled for rainfall variability, are hardly found anywhere except for scattered areas in south Ethiopia and a more significant area in Darfur, the Sudan.

- The trend maps reveal very large areas of strong positive trends in vegetation productivity, very much as a result of increasing precipitation since around 1982, the driest peak of the Sahelian drought (1964-2002). Similar results were presented by Eklundh and Olsson (2003) based on the analysis of 1982-1999 AVHRR NDVI Pathfinder data.

- However, there is also an obvious positive trend in the integrated NDVI and its anomalies that cannot be explained by increased precipitation alone. This may, to some extent, be due to the "Green House" effects including increased CO_2 concentrations in

the atmosphere and increased temperatures possibly increasing the length of the growing season and causing its earlier start as indicated in a NOAA AVHRR study on global terrestrial NPP by Nemani et al. (2003). Hickler et al. (2005) demonstrated that a process-based ecosystem model driven by climatic and atmospheric CO_2 data alone closely reproduced the satellite observed greening trend of the Sahel vegetation and its interannual variation 1982-1998. The satellite data used was the GIMMS NOAA-AVHRR NDVI data set covering the period 1982-1998. Changes in precipitation were identified as the primary driver of the aggregated simulated vegetation changes with CO2 having a minor positive effect.

Fig. 5.3.24. Rain fed millet cultivation in North Kordofan, the Sudan, grasslands just north of Kagmar a “normal” year (annual precipitation~200 mm) (Photo: U. Helldén, 1989)

Fig. 5.3.25. Rain fed millet cultivation in North Kordofan, the Sudan, grasslands in the extreme drought and Sahelian famine year 1983 (Photo: E. Ahlcrona).

5.4. SOUTH AFRICA

5.4.1. South Africa overview

This study region lies within the 10th^{o} and 45th^{o} eastern longitude and from Malawi in the North to Cape Agulhas in the South

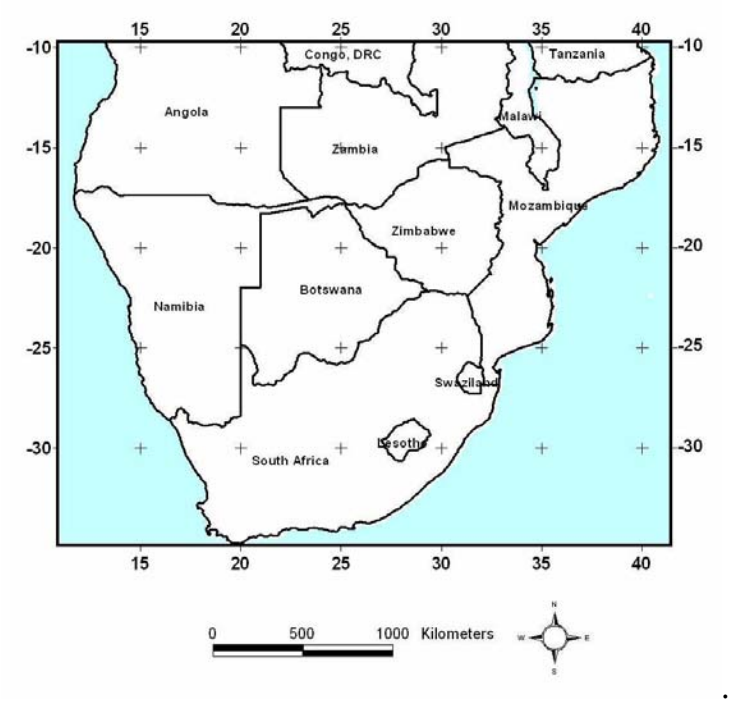

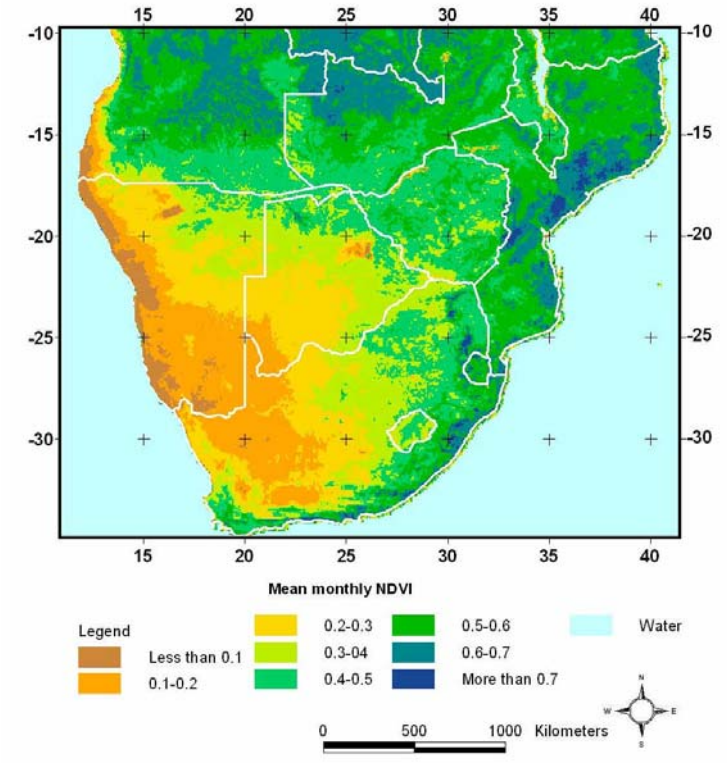

Figure 5.4.1. Country overview (top) and the mean monthly NDVI based on data from 1982 to 2003 (bottom).

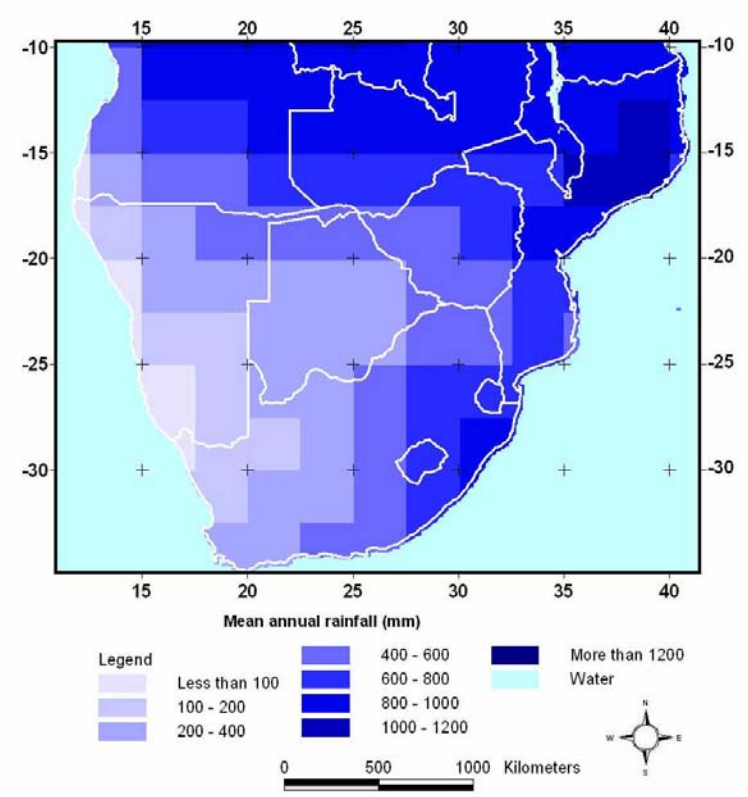

Figure 5.4.2. Mean annual rainfall based on 2.5 degree (~ 275 km) gridded rainfall data from 1982 to 2003.

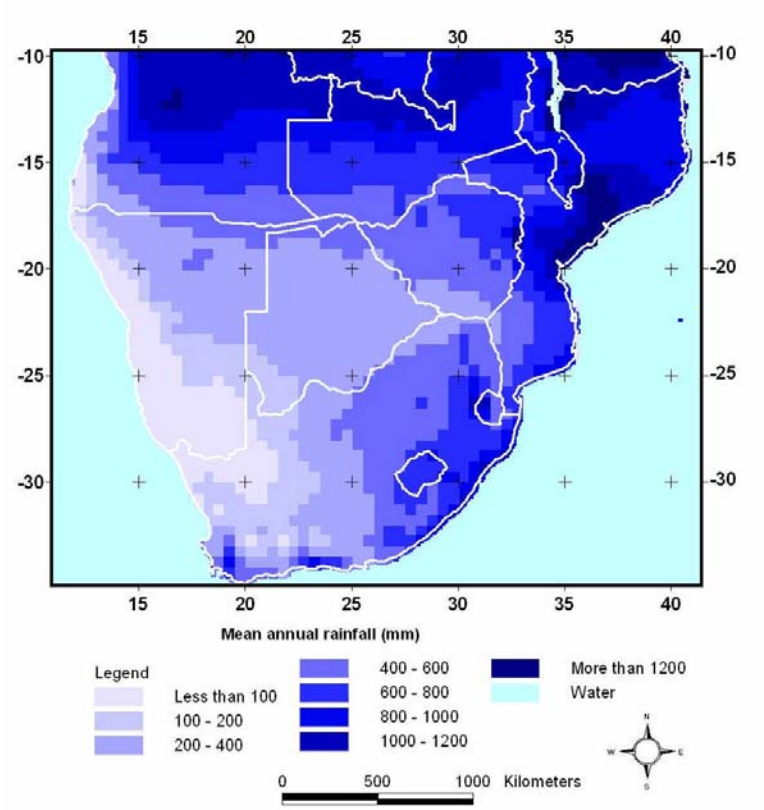

Fig. 5.4.3. Mean annual rainfall based on 0.5 degree (~55 km) gridded rainfall data from 1982 to 2002.

Inspection of time-series plots of both rainfall and NDVI revealed that the appropriate seasons for the drylands (i.e. the area delineated by a minimum of 0.1 and a maximum of 0.5 NDVI based on the long-term monthly average) of the South African region was “July to June” and “September to August” for rainfall and NDVI respectively (figure 5.4.4).

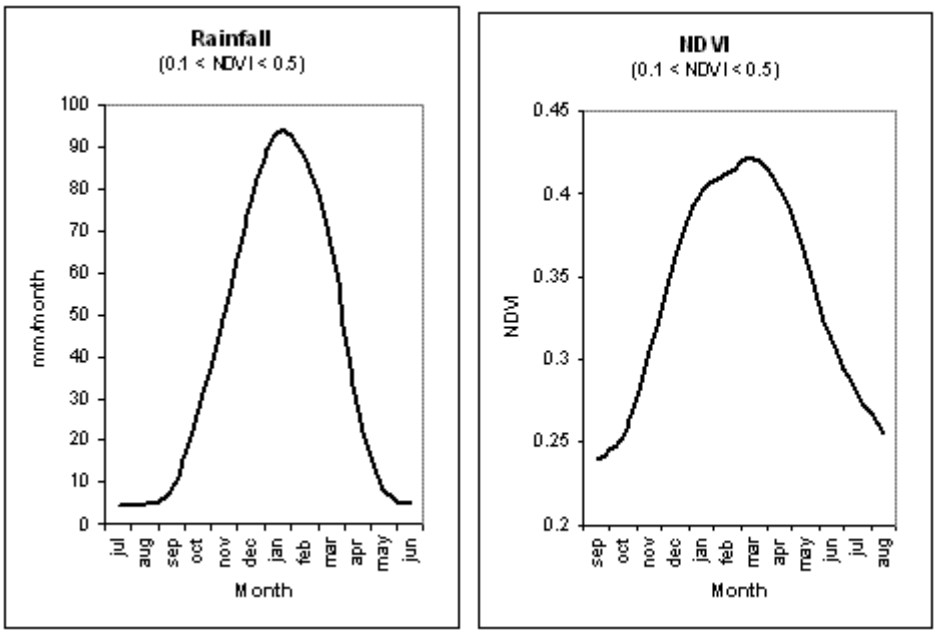

Figure 5.4.4. Monthly time-series plots of rainfall (left) and NDVI (right). The displayed values are mean values as calculated from the area defined by $0.1 \leq NDVI \leq 0.5$.

Consequently total annual rainfall was calculated by summarizing rainfall received within the months from July to June. Similar the annual vegetation productivity was estimated by integrating NDVI over the months from September and until August the following year.

5.4.2. Vegetation trend analysis

The following figures summarize the results of the trend analysis approaches described under methods.

Figure 5.4.5-5.4.8 confirm the points raised in the method sections regarding the relative merits of the different characteristics (inclination, relative change or statistical significance) of the trend line. Especially it is clear that the statistical test is placing too much emphasis on areas with rather small slope inclinations. There is equally a tendency for the relative change to put emphasis on areas where the intercept value i.e. the starting point is low. In that case a relative low absolute slope value may actually come out as a quite significant relative change.

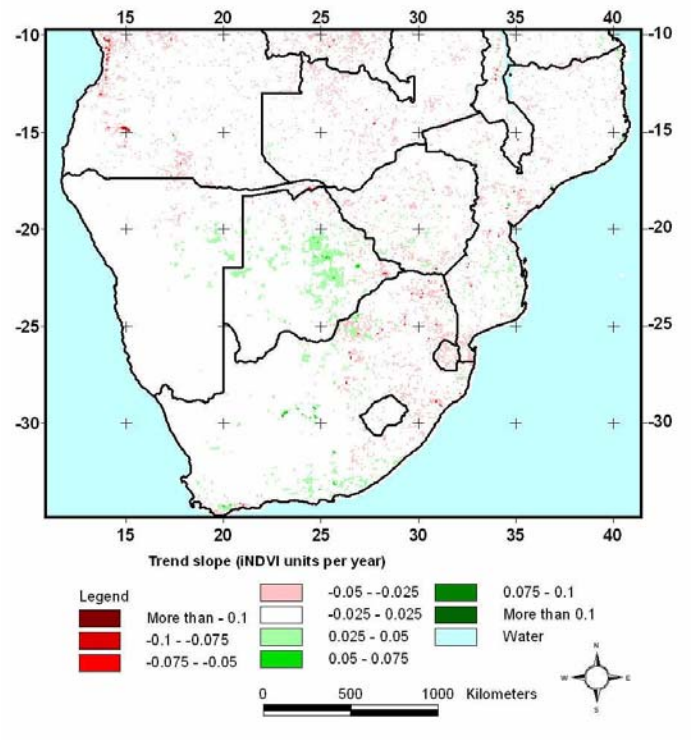

Figure 5.4.5. Linear trends in vegetation productivity for the period 1982 to 2002 based on annual integrated NDVI values. The trend is expressed in absolute values i.e. change in iNDVI units per year.

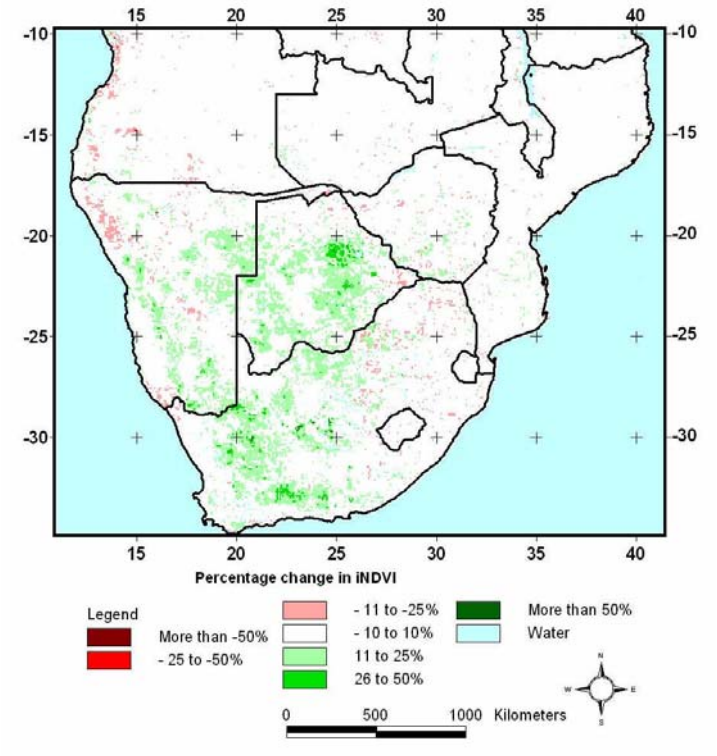

Fig 5.4.6. Linear trends in vegetation productivity for the period 1982 to 2002 based on annual integrated NDVI values. The trend is expressed as percentages i.e. the relative difference between the start and the end value of the linear trend

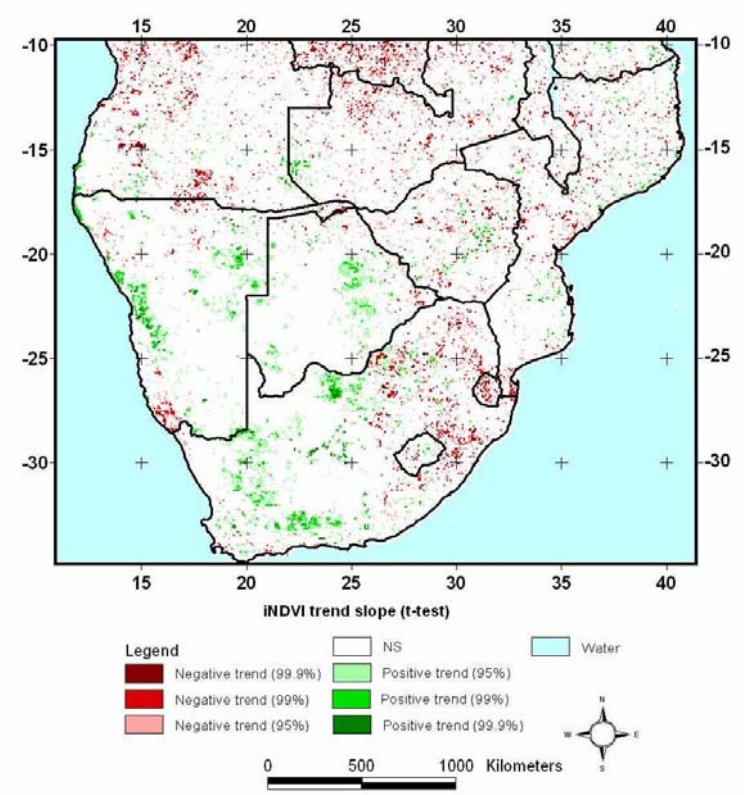

Fig. 5.4.7. Trend slope in NDVI based on linear least square regression (1982-2002). iNDVI trend slope (t-test).

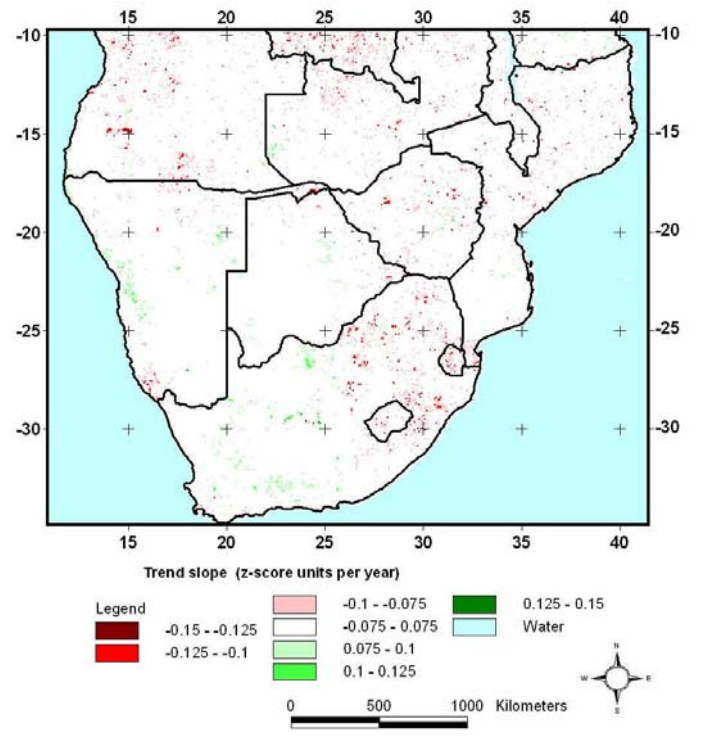

Figure 5.4.8. Standardized trend slope in NDVI based on linear least square regression and expressed as z-score units per year (1982-2002).

5.4.3. Vegetation versus rainfall analysis

Figure 5.4.9 (left) indicates the relationship between mean NDVI and mean annual rainfall. The strong positive relationship (r^2=0.9) confirms the fact that higher rainfalls normally yields higher vegetation productivity.

Yet, the relationship illustrated in Figure 5.4.9 (left) is biased due to the presence of spatial auto-correlation i.e. the phenomenon where locational (geographic position) similarity is matched by value similarity. Consequently Fig. 5.4.9 (left) demonstrates the geographic relationship between long-term means of total annual rainfall and monthly NDVI .In order to avoid this bias the anomaly analysis was introduced (figure 5.4.9 [right], figure 5.4.10, 5.4.11-5.4.15).

The results from the anomaly analysis illustrate a significant and valid relationship between rainfall variability and NDVI variability for large parts of the South African drylands. Despite the generalization level of these figures it remains clear that rainfall and NDVI are indeed closely associated in the South African region. Figure 5.4.9 thereby supports the idea that NDVI trends should be controlled for rainfall variability before elucidating on the possible anthropogenic causes.

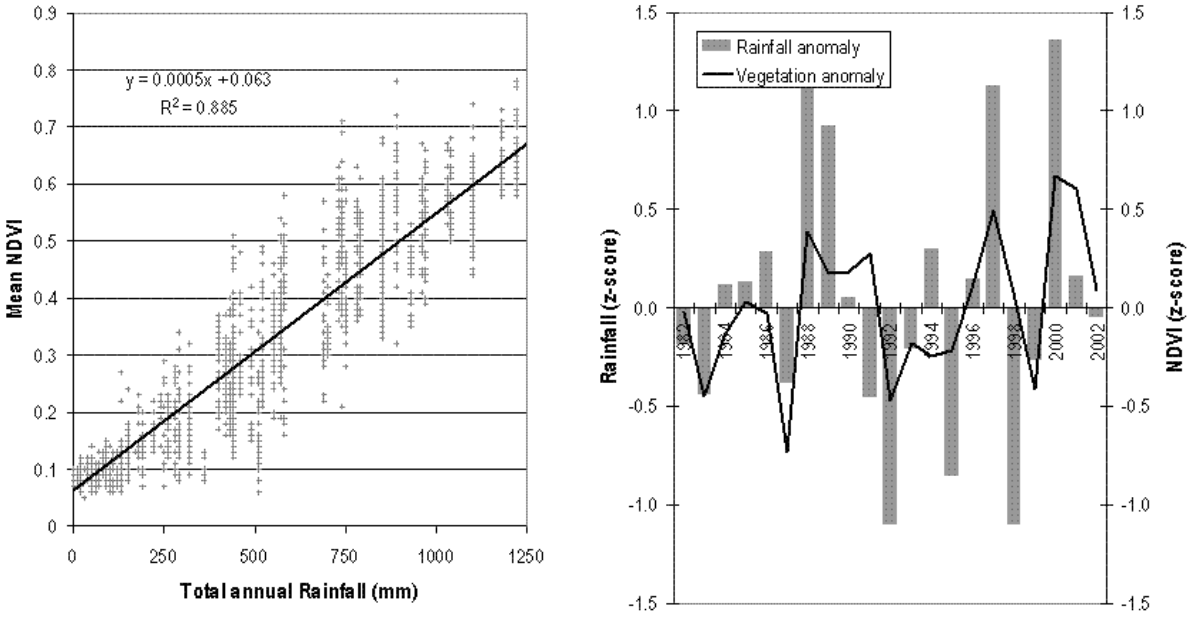

Fig. 5.4.9. (LEFT)Annual rainfall plotted against mean NDVI. The displayed values are mean values for the period 1982 to 2003. (RIGHT) Average z-scores of NDVI and rainfall for West Sahel. On display are mean z-scores as calculated from the area defined by 0.1 < NDVI < 0.5.

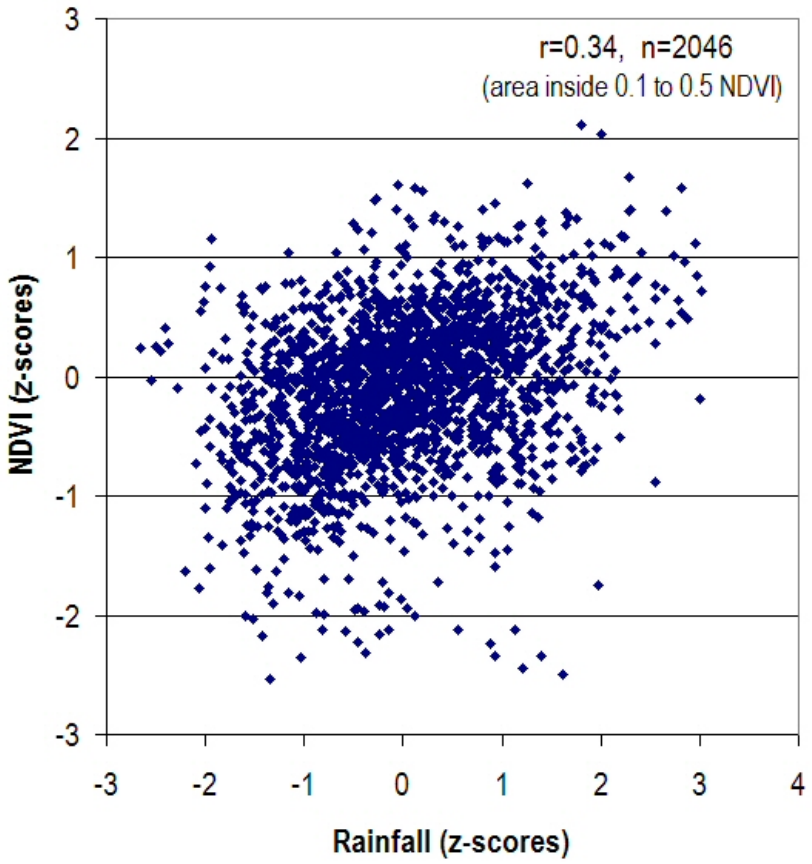

Fig. 5.4.10. Annual NDVI anomalies plotted against annual rainfall anomalies. Every pixel in the 2.5 degree rainfall data was selected and plotted against the average NDVI value for the corresponding NDVI 8 km pixels under each 2.5^0 cell. Only pixels inside the area defined by 0.1<NDVI<0.5 where NDVI denotes mean monthly NDVI for the 1982-2003 period. All data for the 1982-2003 period were merged into one data set.

It should be noted that it is only a fraction (~12 %) of the interannual NDVI anomaly variation that can be explained by corresponding interannual (seasonal) rainfall anomalies under the given circumstances (Fig 5.4.10.). It implies there are large areas (many pixels) where the strong NDVI-rainfall anomaly relationship is not valid. This is also illustrated in the figures below.

The following maps summarizes the results from the per pixel analysis of the temporal relationship between rainfall and NDVI.

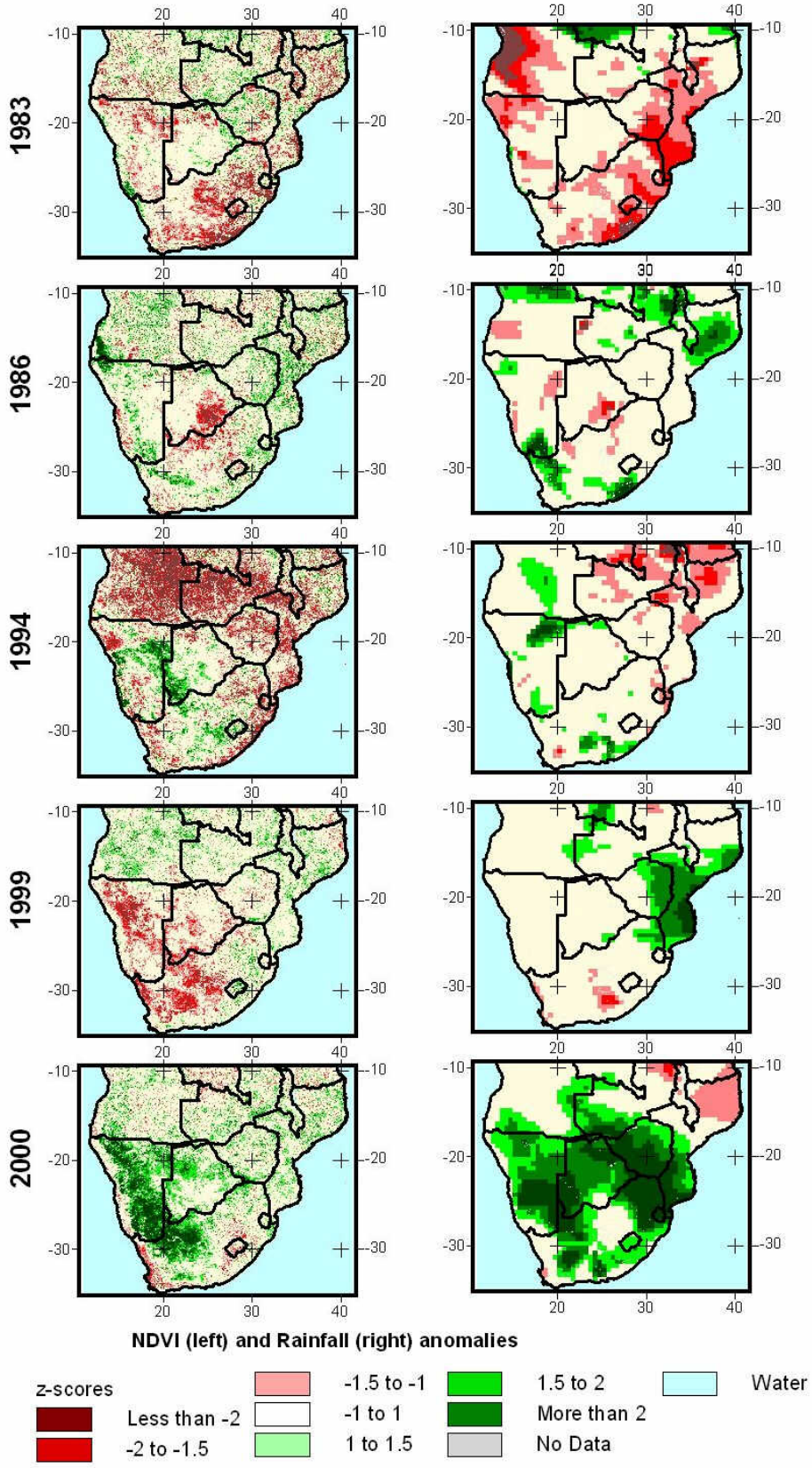

Figure 5.4.11. NDVI (8 km) and rainfall (0.5 degree grid) anomalies for 5 random "non-calendar" years during the 1982 to 2003 period.

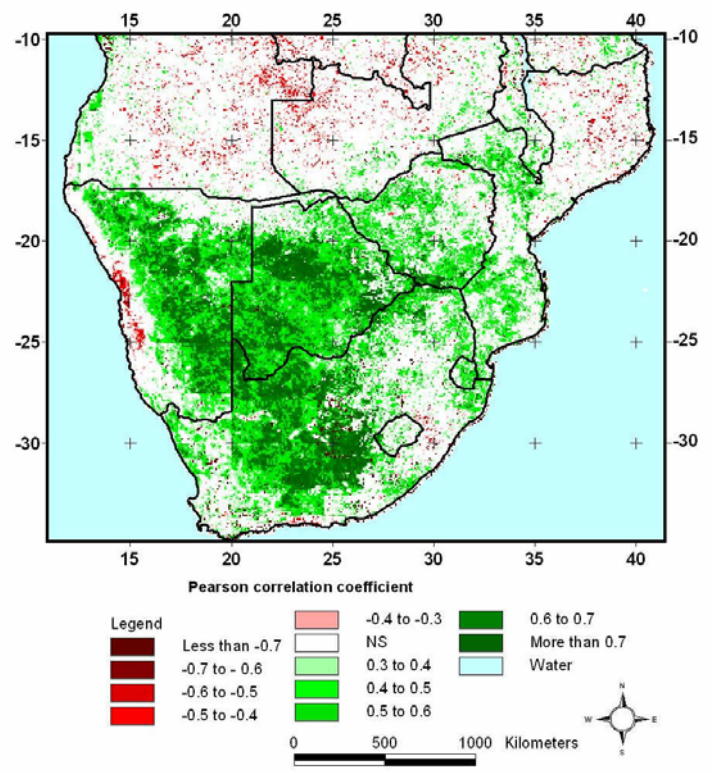

Fig. 5.4.12. Total annual rainfall (2.5 degree) vs. annual integrated NDVI (1982-2003)

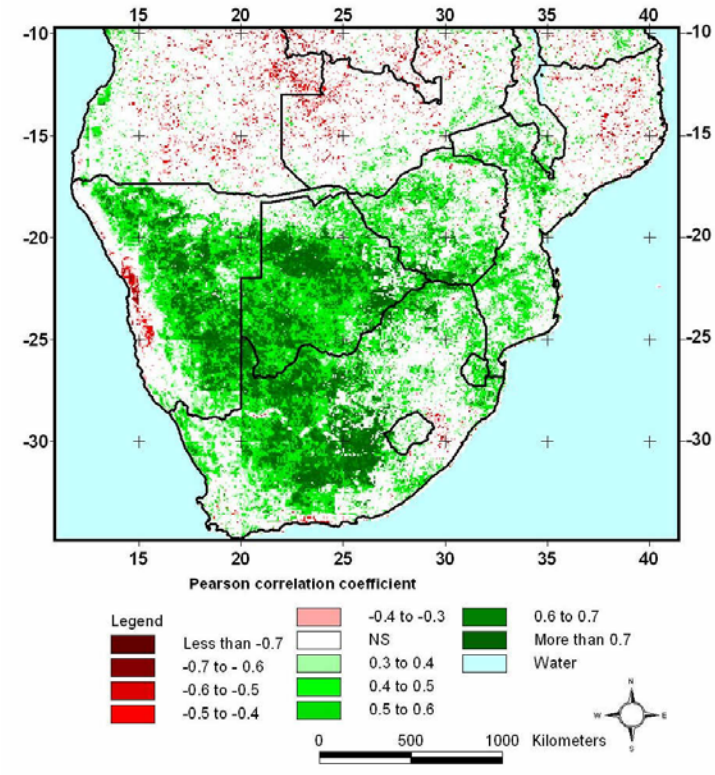

Fig. 5.4.13. Rainfall anomaly (2.5 degree) vs. NDVI anomaly (1982-2003).

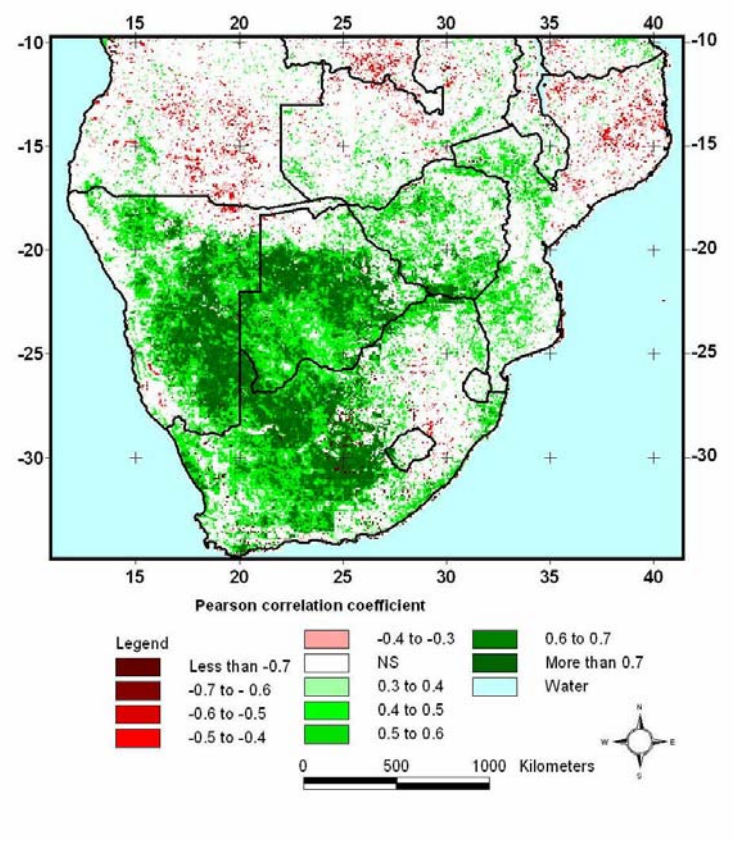

Fig. 5.4.14. Total annual rainfall (0.5 degree) vs. annual integrated NDVI (1982-2002**)**

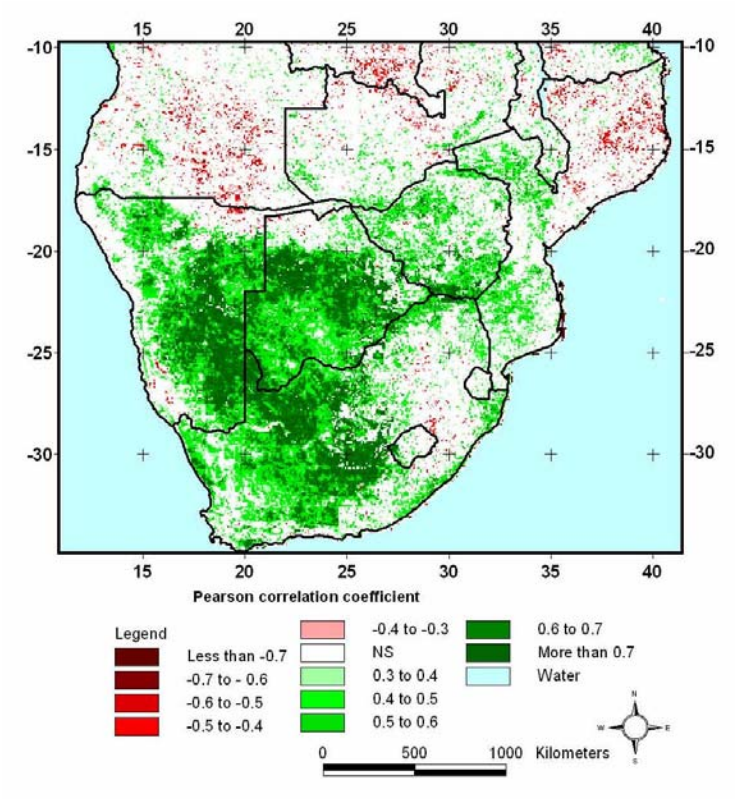

Fig. 5.4.15. Rainfall anomaly (0.5 degree) vs. NDVI anomaly (1982-2002).

As expected one can see a relatively good correlation between rainfall and NDVI for most of the South African region. Few areas of negative correlation are also present but they are located outside the dry region (mean NDVI < 0.1 and annual rainfall < 100 mm) in areas where rainfall is not necessarily the limiting factor for vegetation growth. It is interesting to note the strong agreement between the maps based on 2.5 degree gridded data and the maps based on 0.5 on degree gridded data as well the almost identical patterns observed between the use of integrated data and standardized data (Fig 8.12 and 8.14).

5.4.4. Residual analysis

The model residuals (i.e. the difference between observed and expected iNDVI) were computed for each pixel and subsequently inspected for any systematic trends that could invalidate the initial model specification.

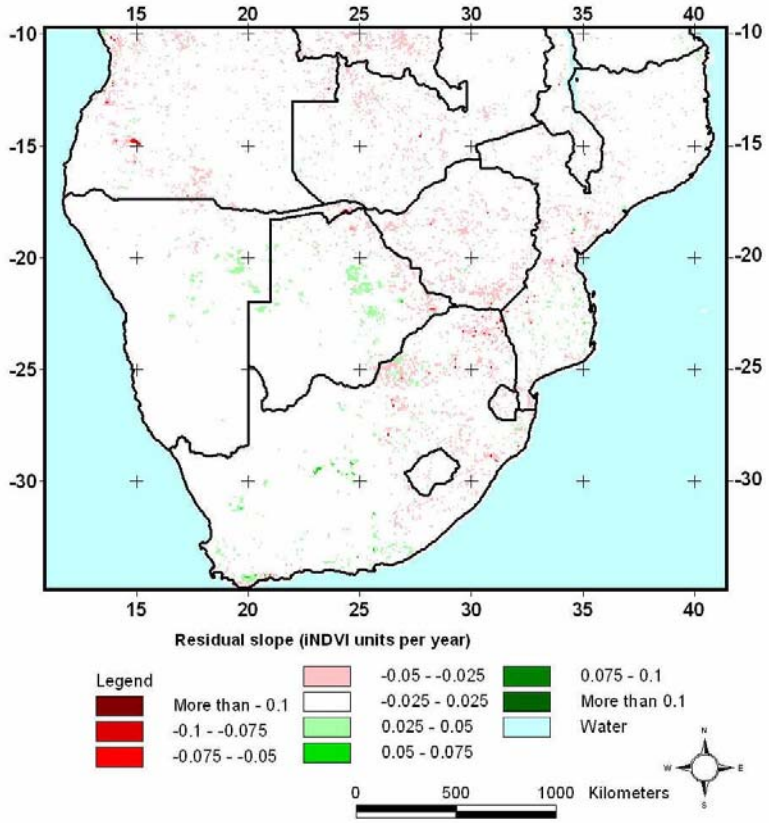

Fig. 5.4.16. Linear trends in residual slope of iNDVI when controlled for annual rainfall **(2.5 degree)** for the period 1982 to 2003. The trend is expressed in absolute values i.e. change in iNDVI units per year.

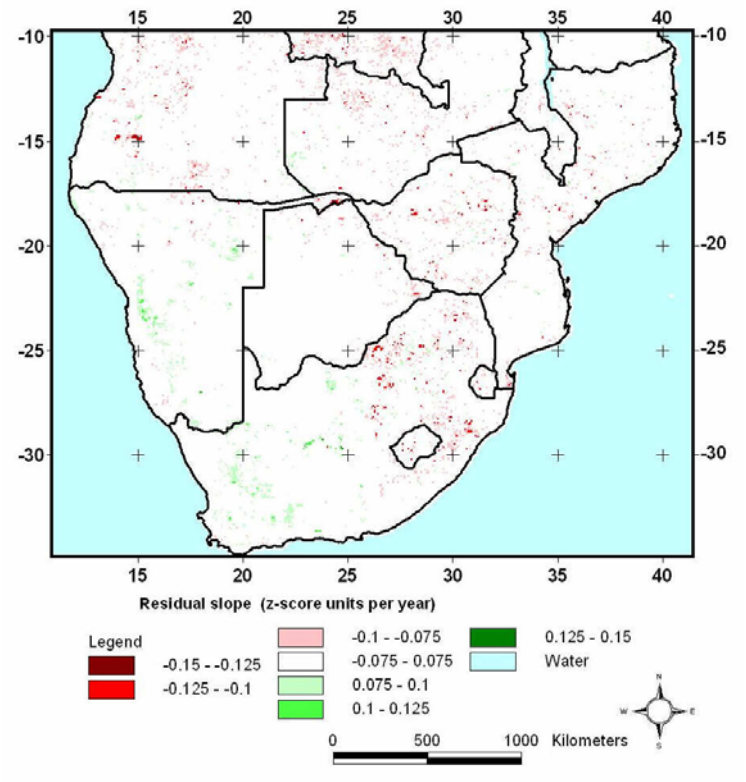

Fig. 5.4.17. Linear trends in residual slope of iNDVI z-scores when controlled for annual rainfall **(2.5 degree)** for the period 1982 to 2003. The trend is expressed in absolute values i.e. change in z-score units per year.

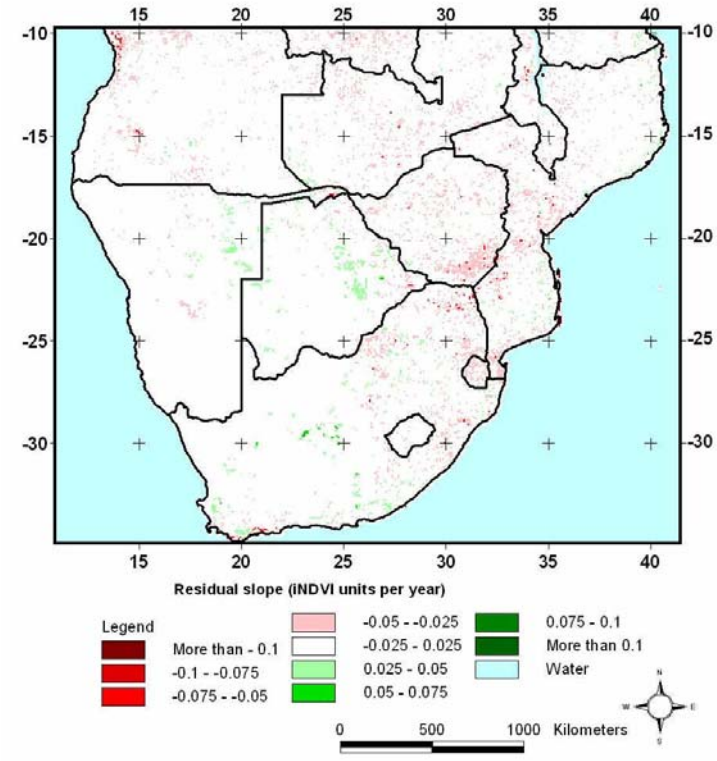

Fig. 5.4.18. Linear trends in residual slope of iNDVI when controlled for annual rainfall **(0.5 degree)** for the period 1982 to 2002. The trend is expressed in absolute values i.e. change in iNDVI units per year

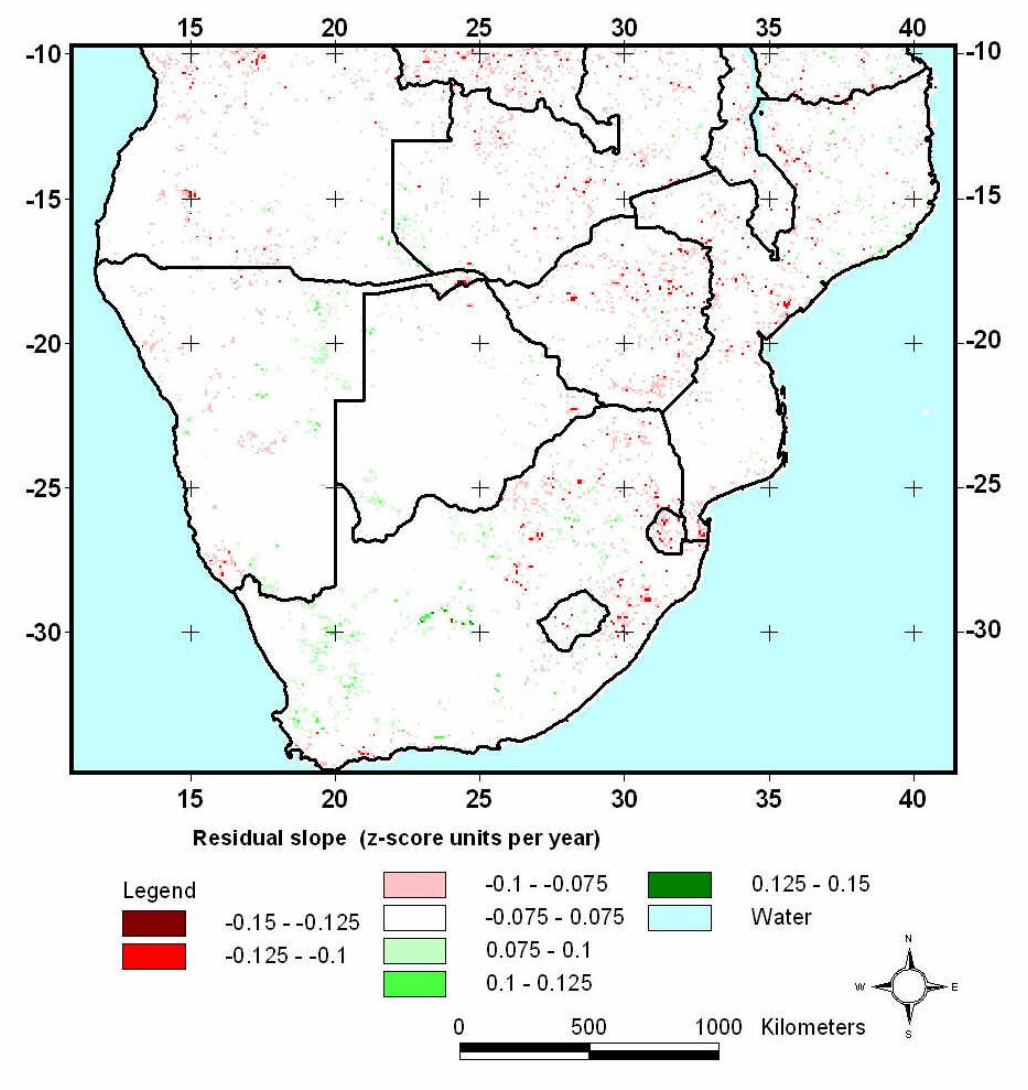

Fig. 5.4.19. Linear trends in residual slope of iNDVI z-scores when controlled for annual rainfall **(0.5 degree)** for the period 1982 to 2002. The trend is expressed in absolute values i.e. change in z-score units per year.

5.4.5. Hot Spot analysis

Example areas with significant residual trends (negative as well as positive) were identified and the trend in vegetation productivity relative to the long-term precipitation anomaly trends in the area were studied (Fig 5.4.20-5.4.26).

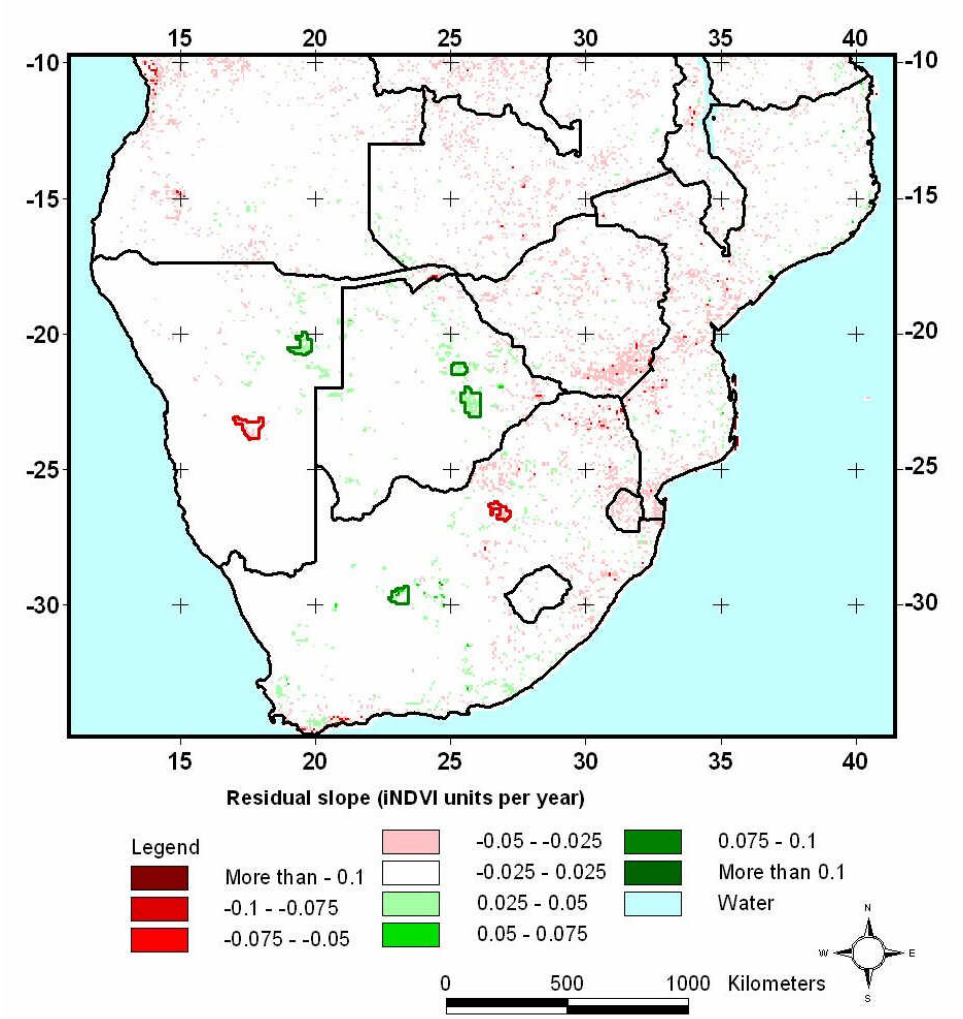

Fig. 5.4.20. South African negative (red vectors) and positive (green vectors) hot spots.

Fig 5.4.21. Malawi deforestation due to expansion of cropland and at the same time facing afforestation/agroforestry introduction, everything inside the size of an 8 km NOAA pixel (Photo: U. Helldén, 1990)

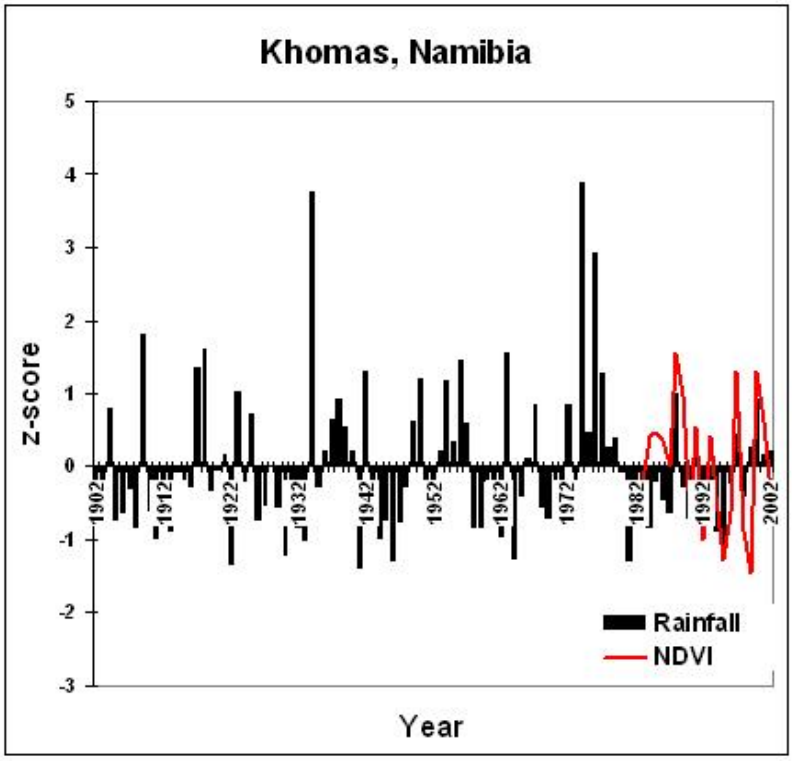

Fig. 5.4.22 Namibia negative (red) Hot Spot with rainfall and NDVI anomalies.

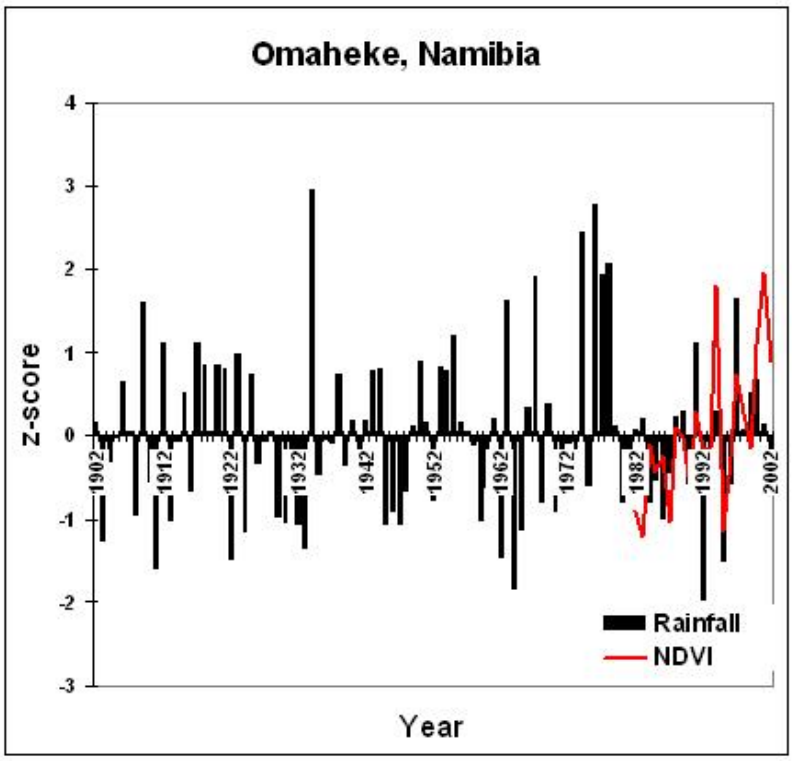

Fig. 5.4.23 Namibia positive (green) Hot Spot with rainfall and NDVI anomalies.

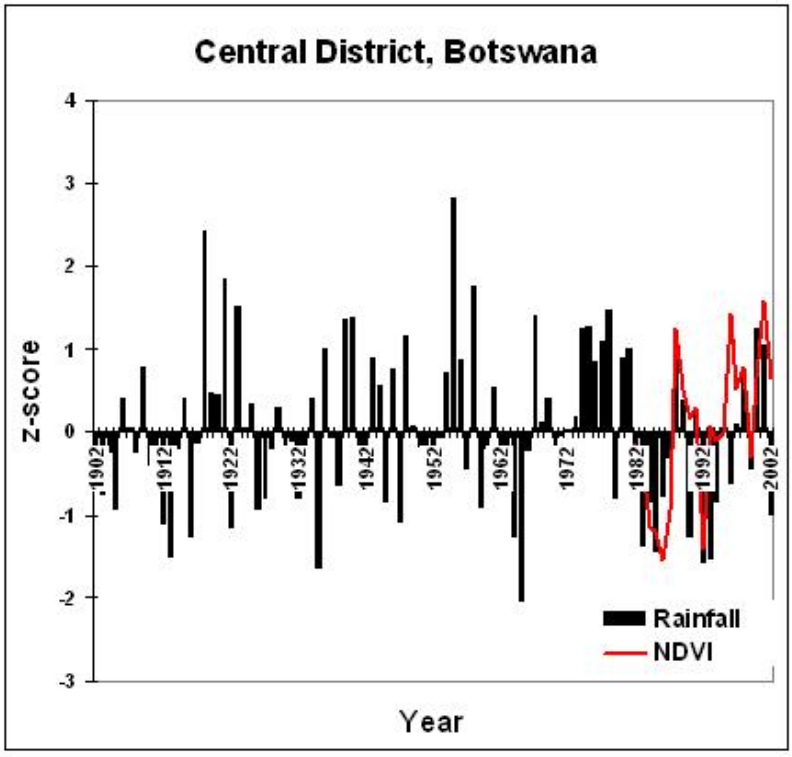

Fig. 5.4.24 North Botswana positive (green) Hot Spot with rainfall and NDVI anomalies.

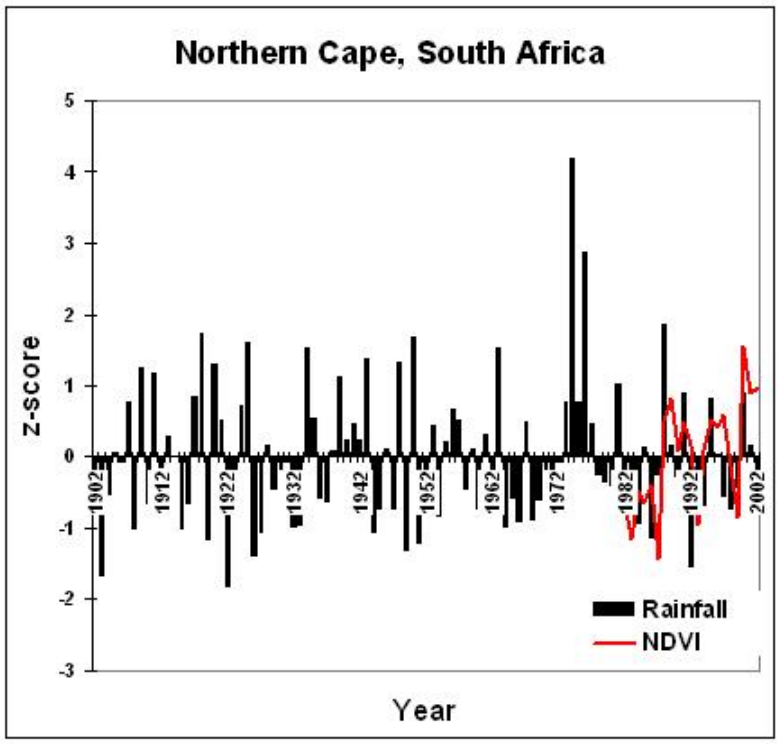

Fig. 5.4.25 South Africa positive (green) Hot Spot with rainfall and NDVI anomalies.

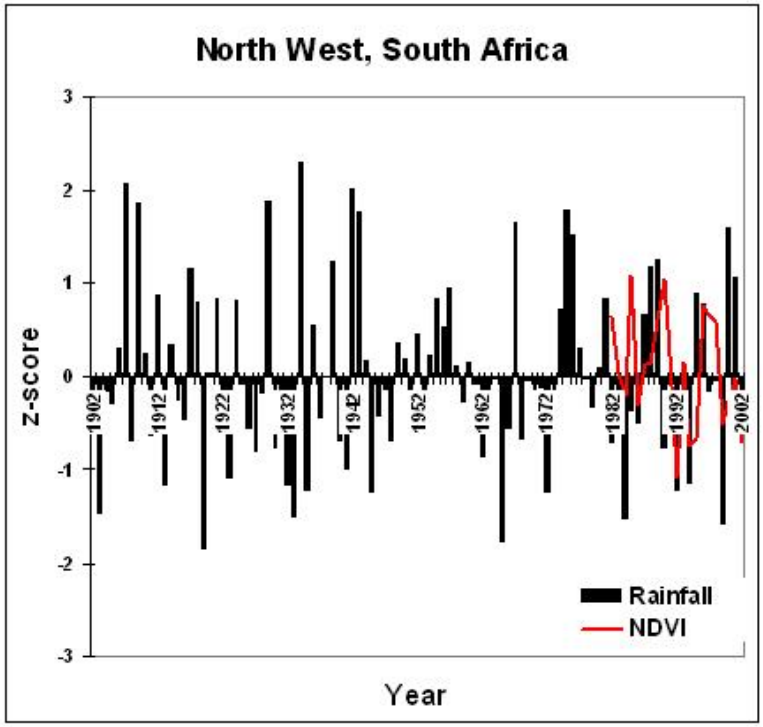

Fig. 5.4.26. South Africa negative (green) Hot Spot with rainfall and NDVI anomalies.

5.4.6. Desertification comments

- Signs of desertification, as reflected by significant downward trends in the vegetation productivity, after it was controlled for rainfall variability, are not very common. Population dense and humid areas including SE Zimbabwe and NE South Africa as well as Swaziland are sticking out indicating more severe vegetation degradation over the 1982-2003 period.

- However, both positive and negative trends are weak. When significant, they can often be explained by corresponding precipitation trends. It is difficult to pin point any regional trends (positive or negative) indicating any significant increase or decrease of vegetation cover conditions over larger areas during the 1982-2003 period, possibly with the exception for the areas mentioned above.

Fig. 5.4.27. Dune encroachment from the Namib Desert into Namibian rangeland. (Photo: U. Helldén, 1997).

5.5. EAST ASIA

5.5.1. East Asia overview

This study region extends from the western tip of Mongolia to the Eastern tip of China including all the major drylands of China (Fig. 5.5.1).

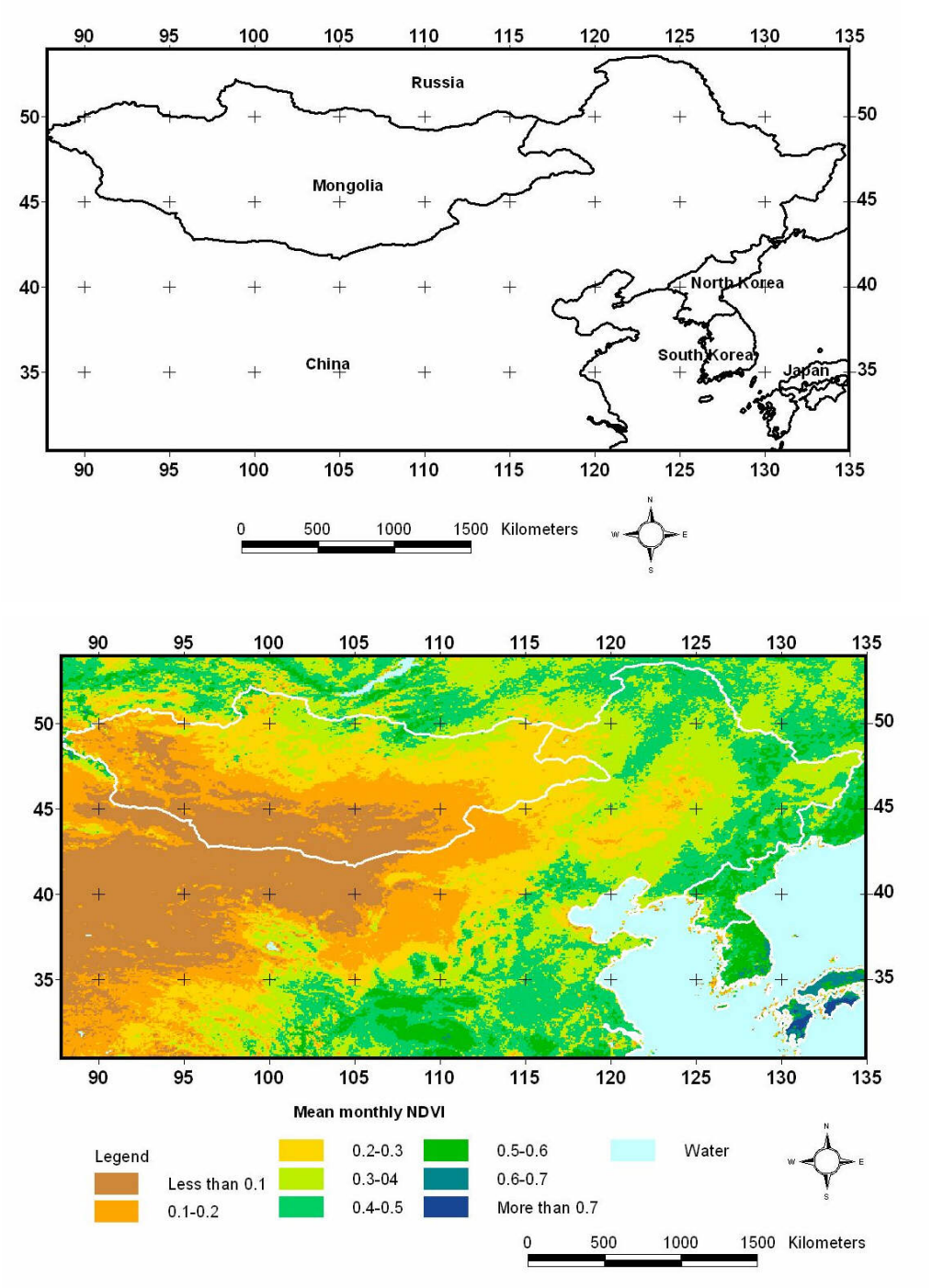

Figure 5.5.1. Country overview (top) and the mean monthly NDVI based on data from 1982 to 2003 (bottom).

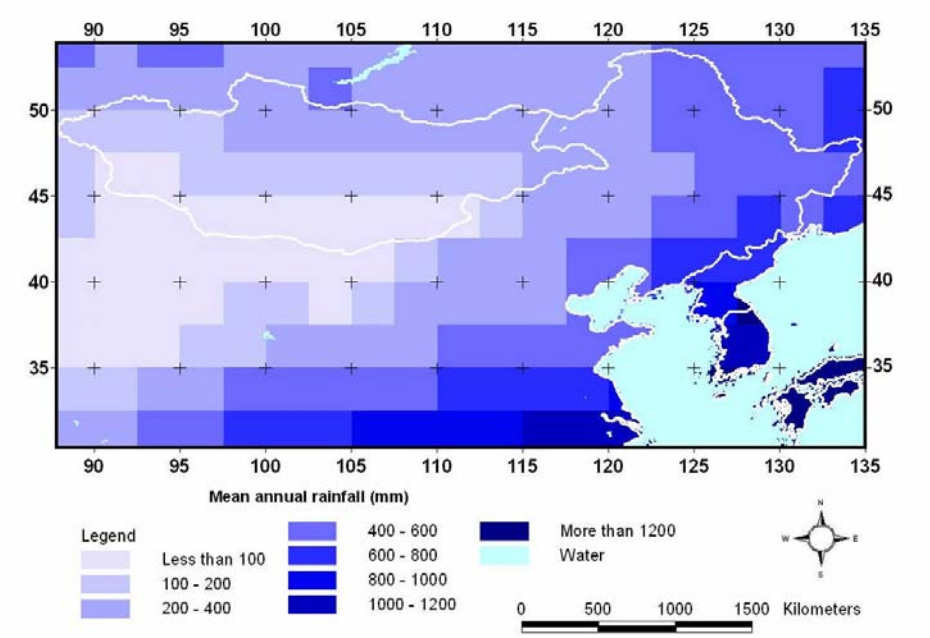

Figure 5.5.2. Mean annual rainfall based on 2.5 degree (~ 275 km) gridded rainfall data from 1982 to 2003.

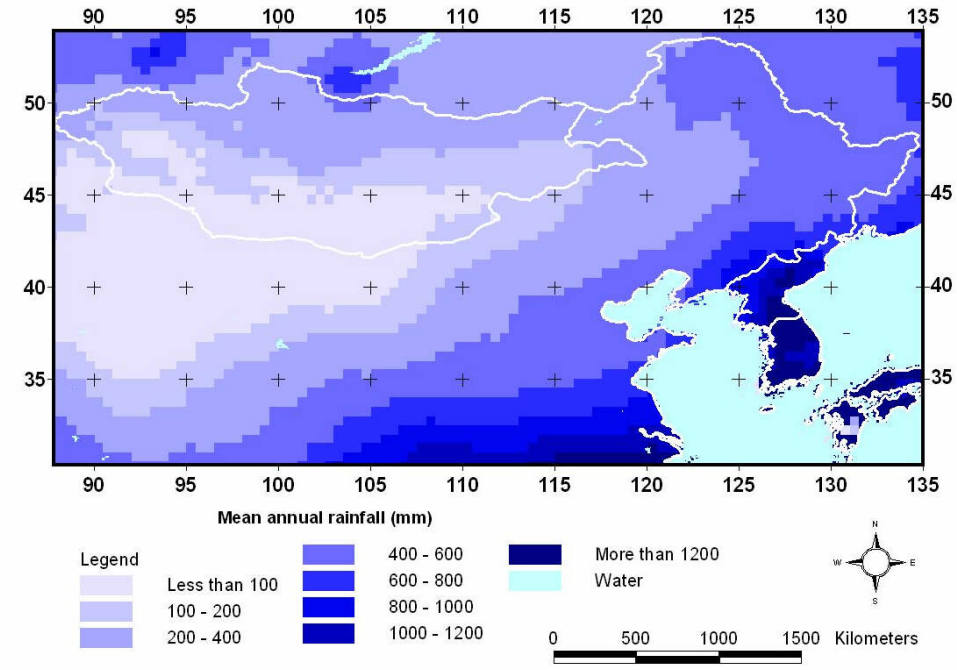

Fig. 5.5.3. Mean annual rainfall based on 0.5 degree (~55 km) gridded rainfall data from 1982 to 2002.

Inspection of time-series plots of both rainfall and NDVI revealed that the appropriate seasons for the drylands (i.e. the area delineated by a minimum of 0.1 and a maximum of 0.5 NDVI based on the long-term monthly average) of East Asia was “January to

December" and "February to January the following year" for rainfall and NDVI respectively (figure 5.5.4).

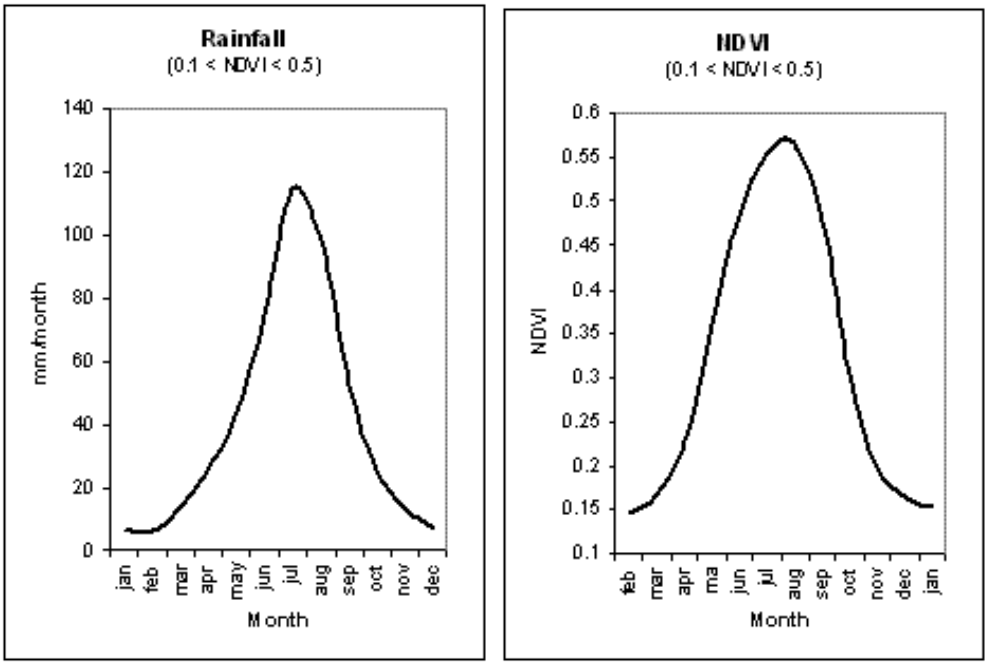

Figure 5.5.4. Monthly time-series plots of rainfall (left) and NDVI (right). The displayed values are mean values as calculated from the area defined by $0.1 \leq NDVI \leq 0.5$.

Consequently total annual rainfall was calculated by summarizing rainfall received within the months from January to December. Similar the annual vegetation productivity was estimated by integrating NDVI over the months from February until January the following year.

5.5.2. Vegetation trend analysis

The following figures summarize the results of the trend analysis approaches described under methods.

Figure 5.5.5-5.5.8 confirm the points raised in the method sections regarding the relative merits of the different characteristics (inclination, relative change or statistical significance) of the trend line. Especially it is clear that the statistical test is placing too much emphasis on areas with rather small slope inclinations. There is equally a tendency for the relative change to put emphasis on areas where the intercept value i.e. the starting point is low. In that case a relative low absolute slope value may actually come out as a quite significant relative change.

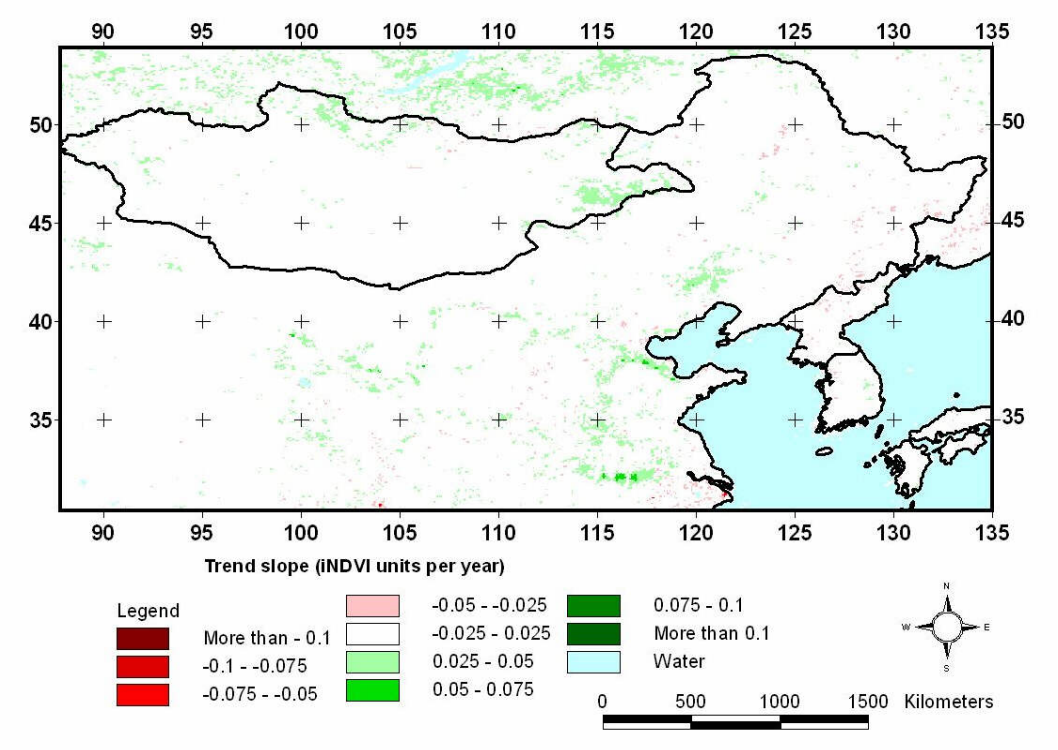

Figure 5.5.5. Linear trends in vegetation productivity for the period 1982 to 2002 based on annual integrated NDVI values. The trend is expressed in absolute values i.e. change in iNDVI units per year.

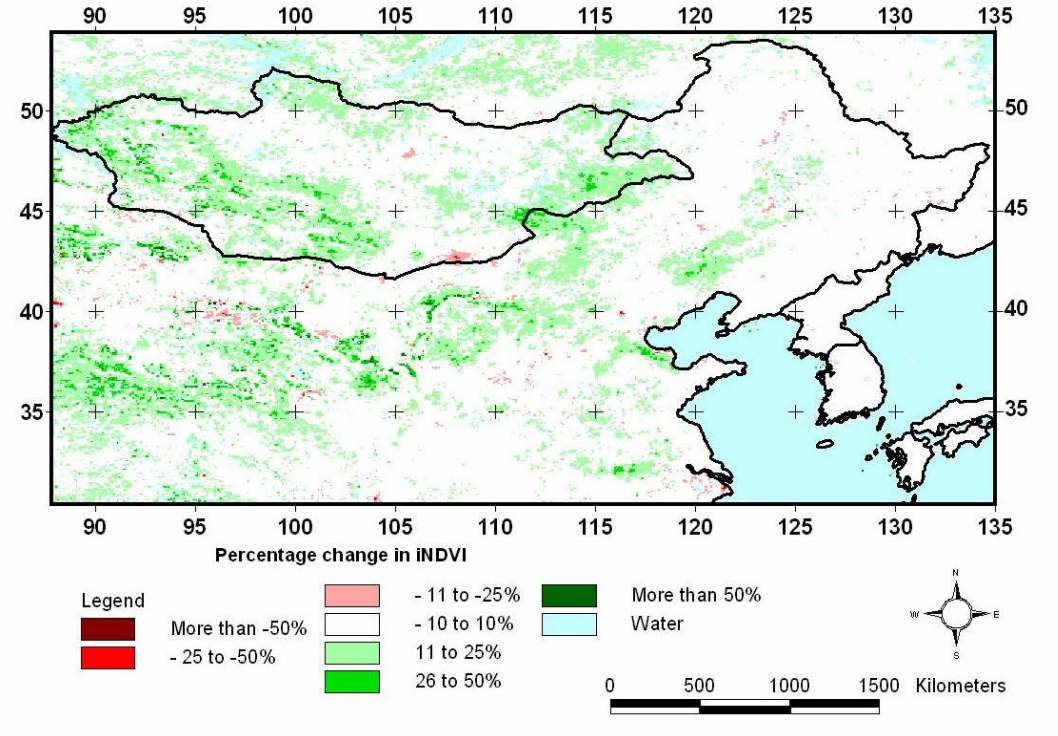

Fig 5.5.6. Linear trends in vegetation productivity for the period 1982 to 2002 based on annual integrated NDVI values. The trend is expressed as percentages i.e. the relative difference between the start and the end value of the linear trend

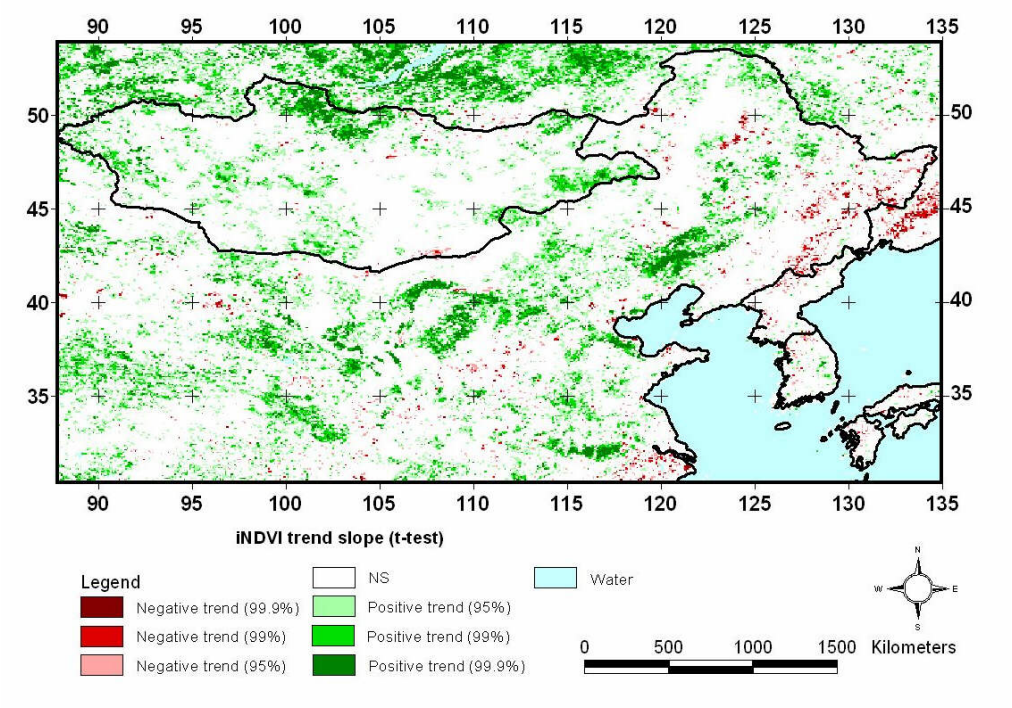

Fig. 5.5.7. Trend slope in NDVI based on linear least square regression (1982-2002). iNDVI trend slope (t-test).

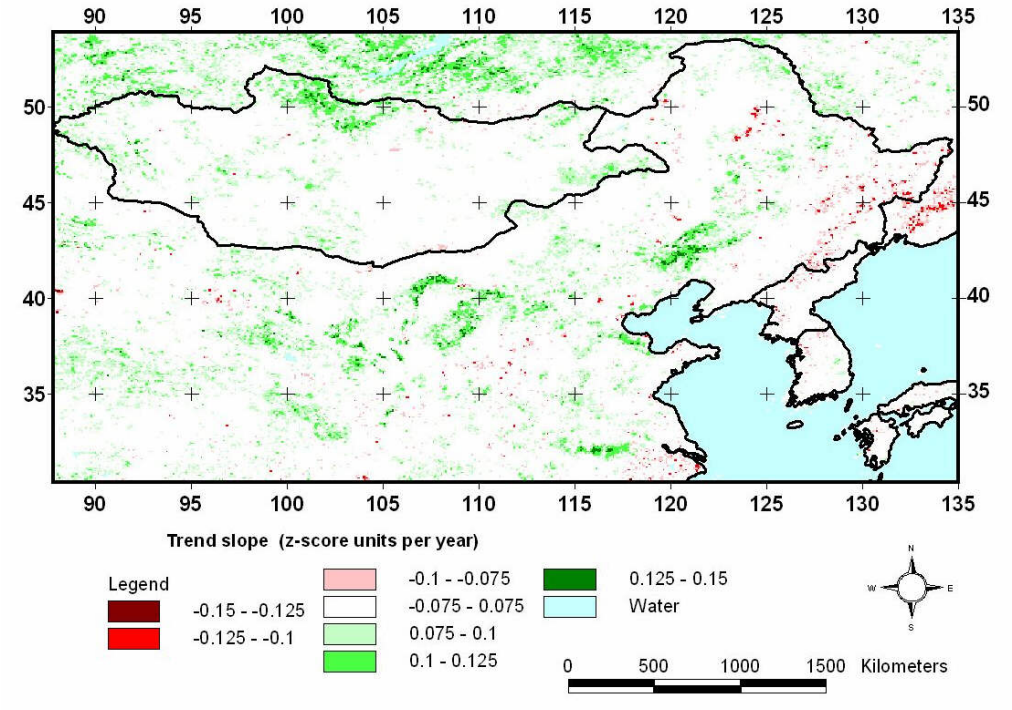

Figure 5.5.8. Standardized trend slope in NDVI based on linear least square regression and expressed as z-score units per year (1982-2002).

5.5.3. Vegetation versus rainfall analysis

Figure 5.5.9 (left) indicates the relationship between mean NDVI and mean annual rainfall. The strong positive relationship (r^2=0.7) confirms the fact that higher rainfalls normally yields higher vegetation productivity.

Yet, the relationship illustrated in Figure 5.5.9 (left) is biased due to the presence of spatial auto-correlation i.e. the phenomenon where locational (geographic position) similarity is matched by value similarity. Consequently Fig. 5.5.9 (left) demonstrates the geographic relationship between long-term means of total annual rainfall and monthly NDVI .In order to avoid this bias the anomaly analysis was introduced (figure 5.5.9 [right], figure 5.5.10, 5.5.11-5.5.15).

The results from the anomaly analysis illustrate a significant and valid relationship between rainfall variability and NDVI variability for large parts of the Chinese and Mongolian drylands. Despite the generalization level of these figures it remains clear that rainfall and NDVI are indeed closely associated. Figure 5.5.9 thereby supports the idea that NDVI trends should be controlled for rainfall variability before elucidating on the possible anthropogenic causes.

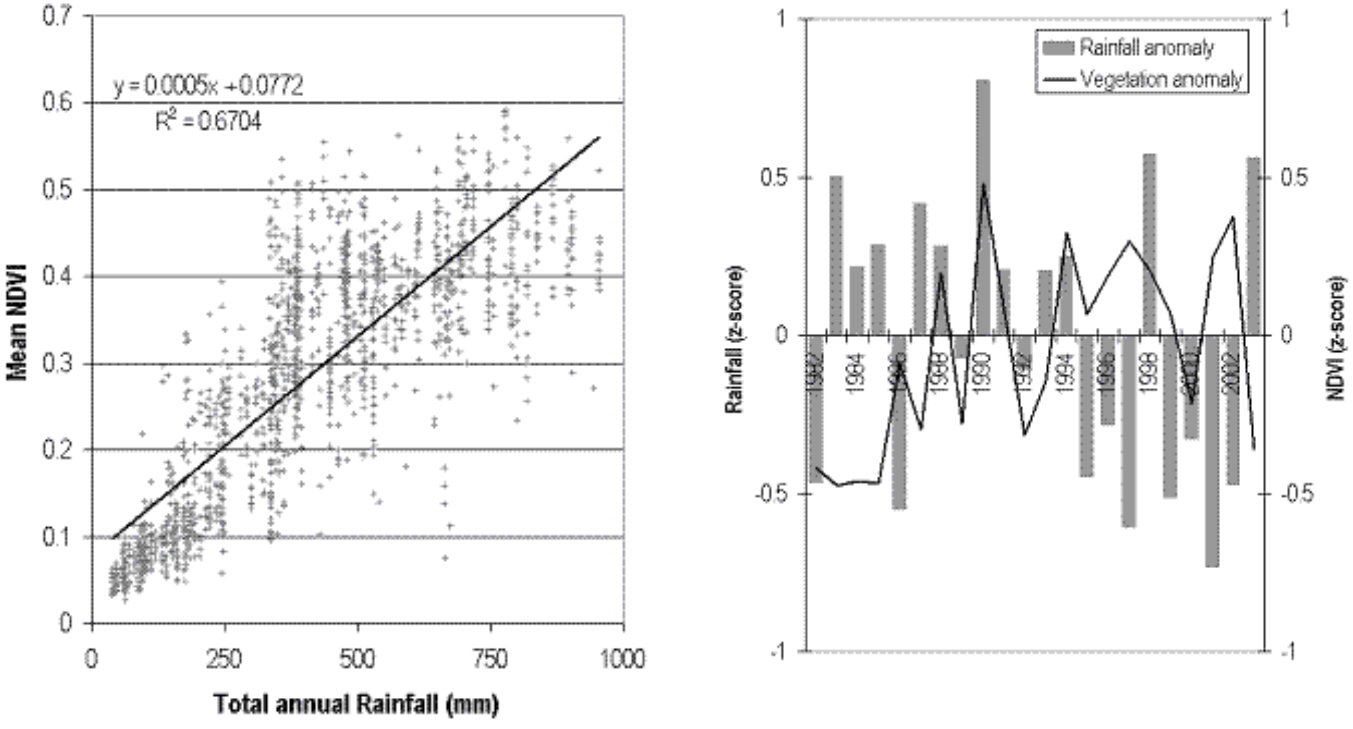

Fig. 5.5.9. (LEFT)Annual rainfall plotted against mean NDVI. The displayed values are mean values for the period 1982 to 2003. (RIGHT) Average z-scores of NDVI and rainfall for West Sahel. On display are mean z-scores as calculated from the area defined by 0.1 < NDVI < 0.5.

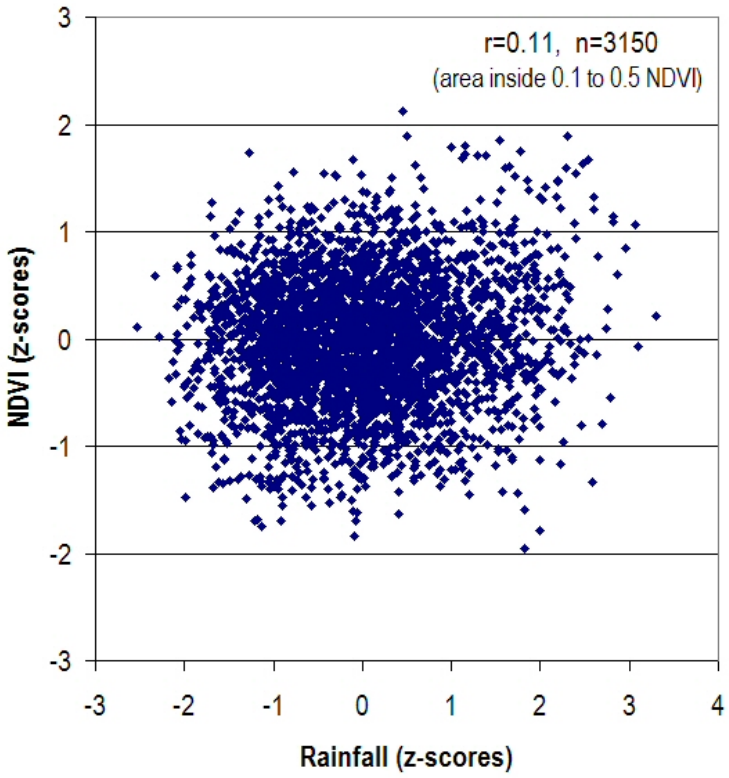

Fig. 5.5.10. Annual NDVI anomalies plotted against annual rainfall anomalies. Every pixel in the 2.5 degree rainfall data was selected and plotted against the average NDVI value for the corresponding NDVI 8 km pixels under each 2.5^0 cell. Only pixels inside the area defined by 0.1<NDVI<0.5 where NDVI denotes mean monthly NDVI for the 1982-2003 period. All data for the 1982-2003 period were merged into one data set.

It should be noted that it is only a very small fraction (~1 %) of the interannual NDVI anomaly variation that can be explained by corresponding interannual (seasonal) rainfall anomalies under the given circumstances (Fig 5.5.10.). It implies there are large areas (many pixels) where the strong NDVI-rainfall anomaly relationship is not valid. This is also illustrated in the figures below.

The following maps summarizes the results from the per pixel analysis of the temporal relationship between rainfall and NDVI.

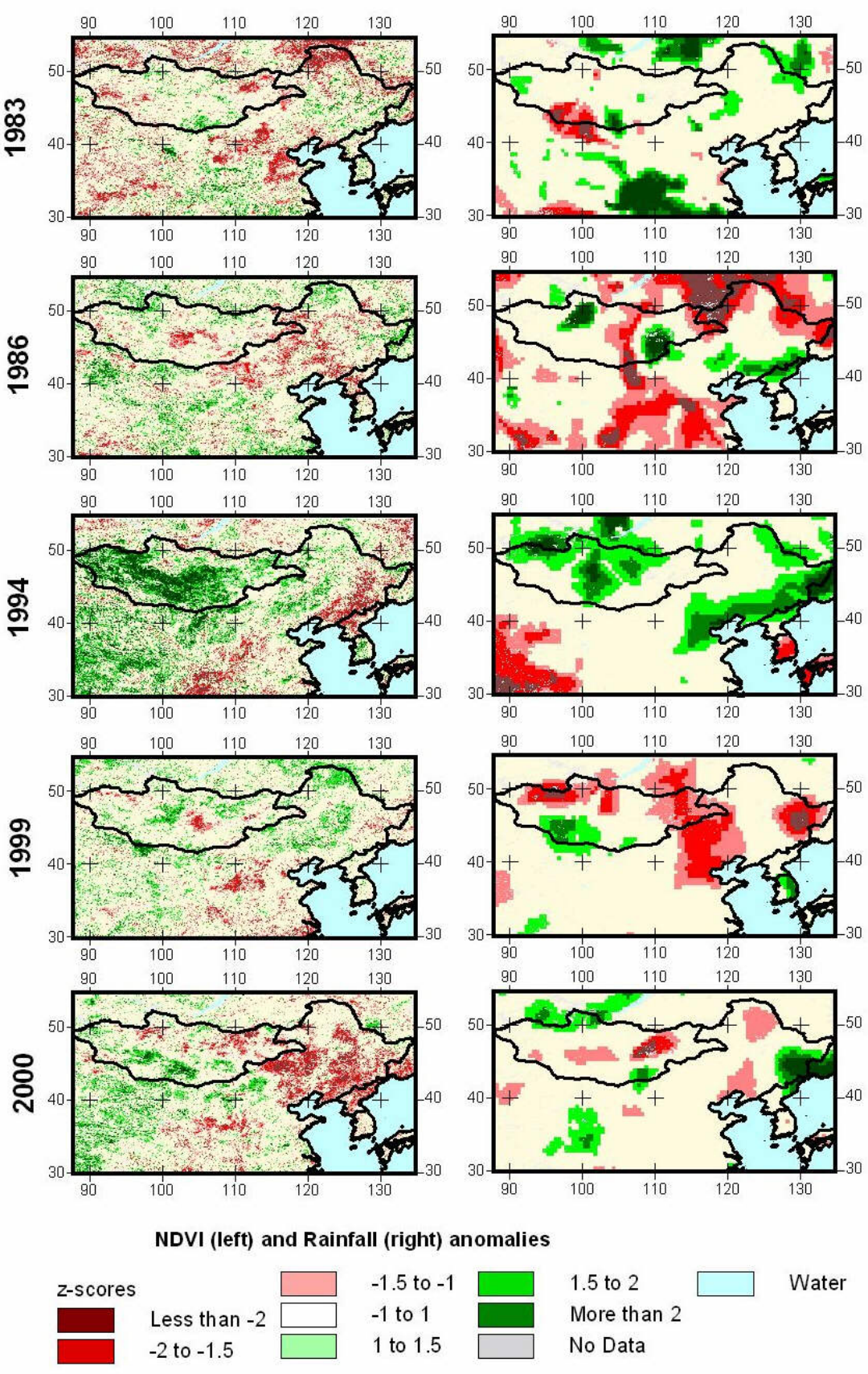

Figure 5.5.11. NDVI (8 km) and rainfall (0.5 degree grid) anomalies for 5 random "non-calendar" years during the 1982 to 2003 period.

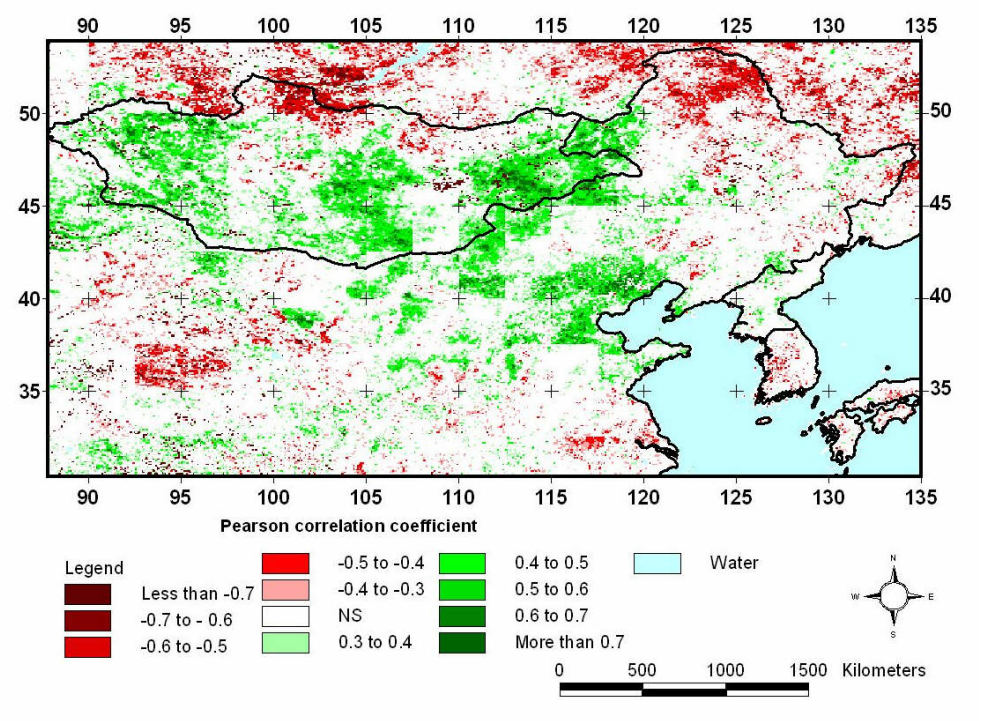

Fig. 5.5.12. Total annual rainfall (2.5 degree) vs. annual integrated NDVI (1982-2003)

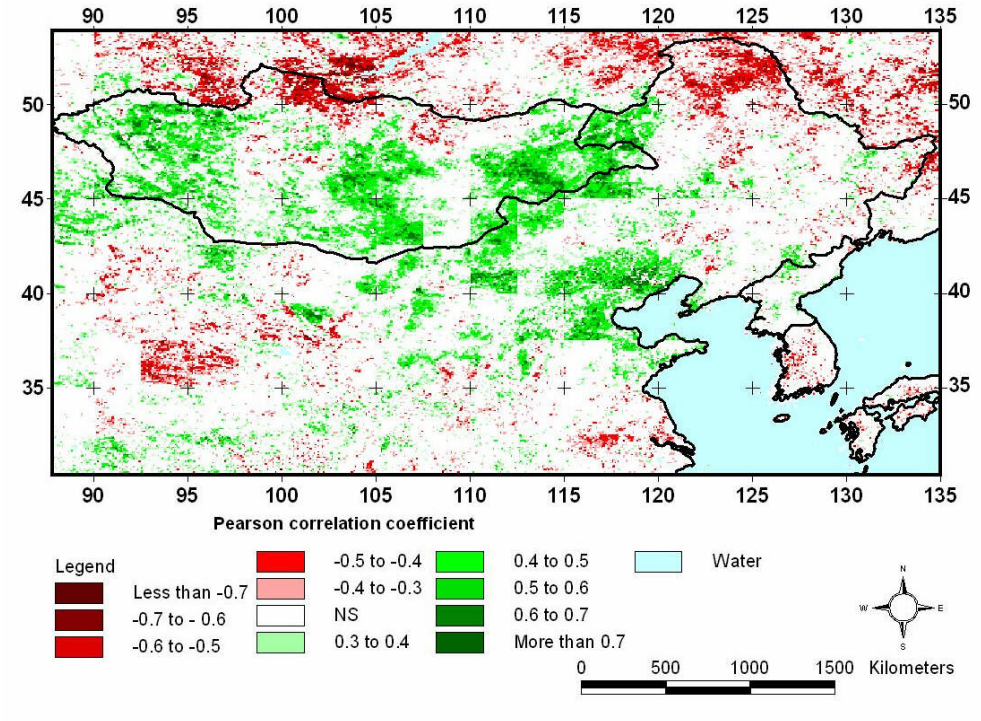

Fig. 5.5.13. Rainfall anomaly (2.5 degree) vs. NDVI anomaly (1982-2003).

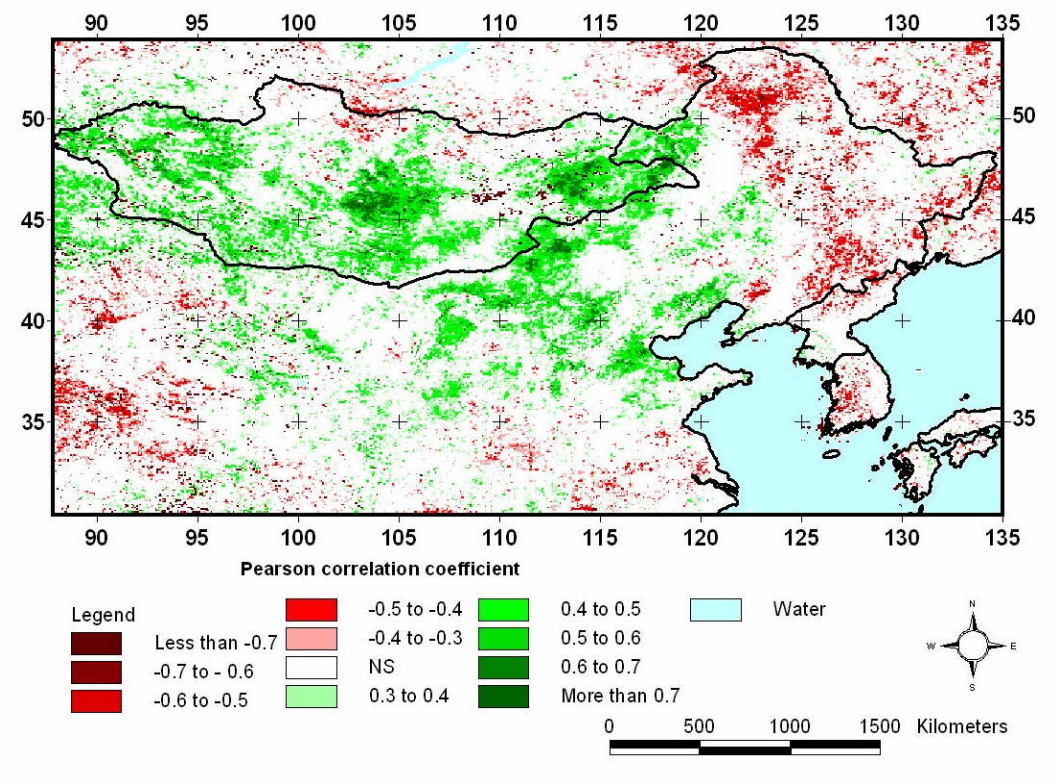

Fig. 5.5.14. Total annual rainfall (0.5 degree) vs. annual integrated NDVI (1982-2002**)**

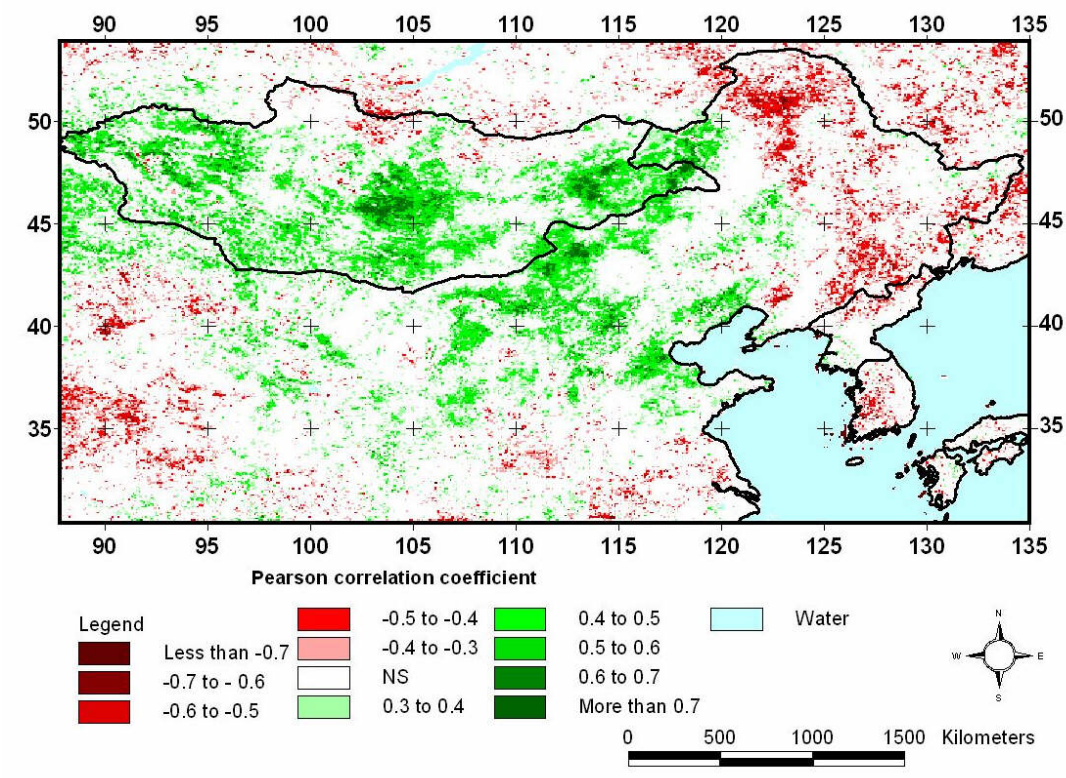

Fig. 5.5.15. Rainfall anomaly (0.5 degree) vs. NDVI anomaly (1982-2002).

As expected one can see a relatively good correlation between rainfall and NDVI for considerable areas of the East Asian dryland region. Areas of negative correlation are also present but they are mainly located outside the dry region (mean NDVI < 0.1 and annual rainfall < 100 mm) in areas where rainfall is not necessarily the limiting factor for vegetation growth. It is interesting to note the strong agreement between the maps based on 2.5 degree gridded data and the maps based on 0.5 on degree gridded data as well the almost identical patterns observed between the use of integrated data and standardized data (Fig 8.12 and 8.14).

5.5.4. Residual analysis

The model residuals (i.e. the difference between observed and expected iNDVI) were computed for each pixel and subsequently inspected for any systematic trends that could invalidate the initial model specification.

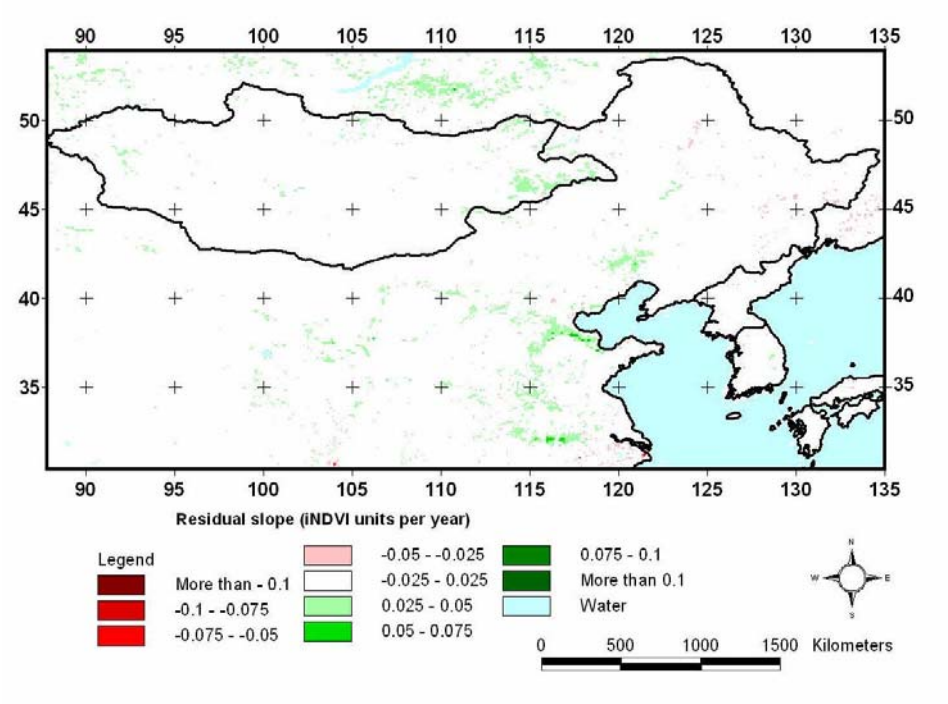

Fig. 5.5.16. Linear trends in residual slope of iNDVI when controlled for annual rainfall **(2.5 degree)** for the period 1982 to 2003. The trend is expressed in absolute values i.e. change in iNDVI units per year.

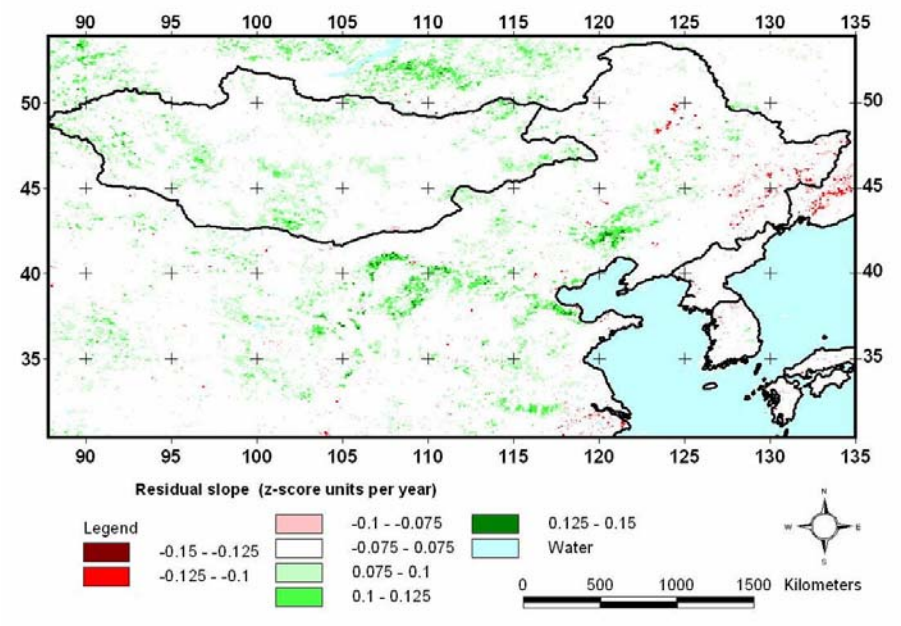

Fig. 5.5.17. Linear trends in residual slope of iNDVI z-scores when controlled for annual rainfall **(2.5 degree)** for the period 1982 to 2003. The trend is expressed in absolute values i.e. change in z-score units per year.

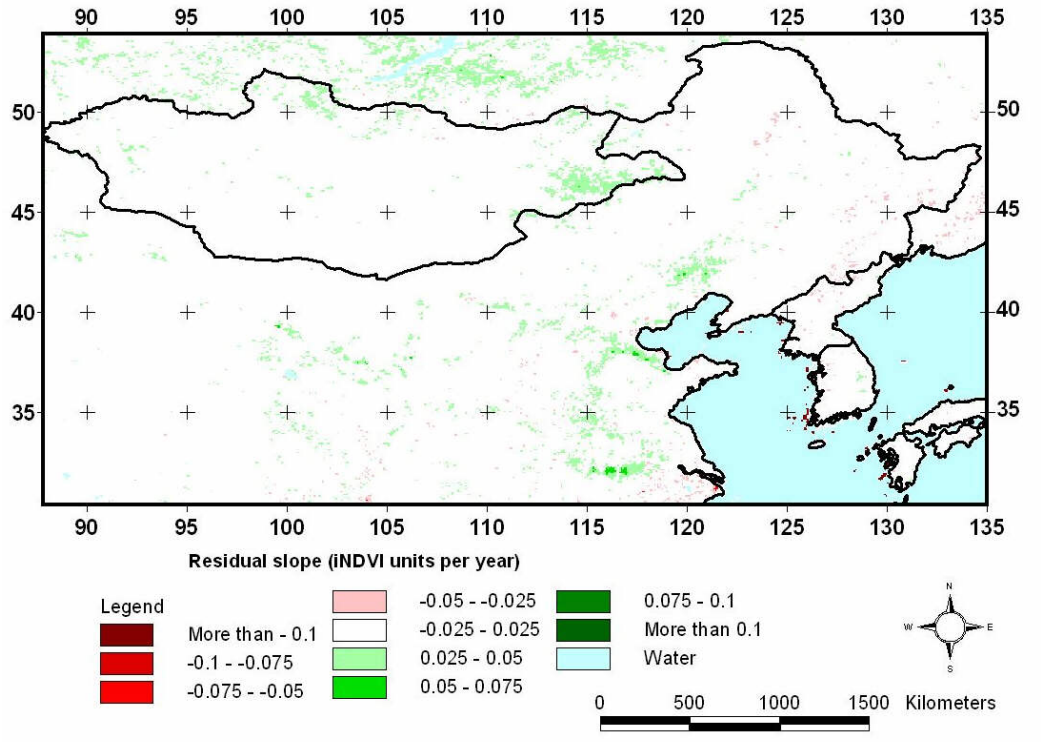

Fig. 5.5.18. Linear trends in residual slope of iNDVI when controlled for annual rainfall **(0.5 degree)** for the period 1982 to 2002. The trend is expressed in absolute values i.e. change in iNDVI units per year

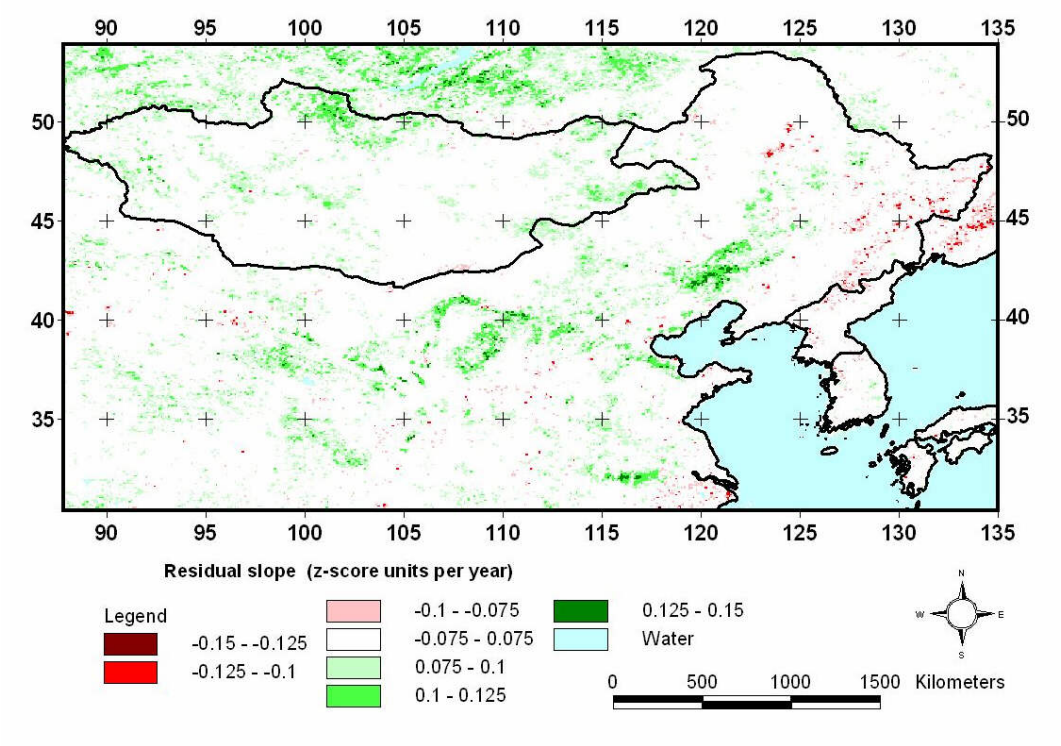

Fig. 5.5.19. Linear trends in residual slope of iNDVI z-scores when controlled for annual rainfall **(0.5 degree)** for the period 1982 to 2002. The trend is expressed in absolute values i.e. change in z-score units per year.

5.5.5. Hot Spot analysis

Example areas with significant residual trends (negative as well as positive) were identified and the trend in vegetation productivity relative to the long-term precipitation anomaly trends in the area were studied (Fig 5.5.20-5.5.24).

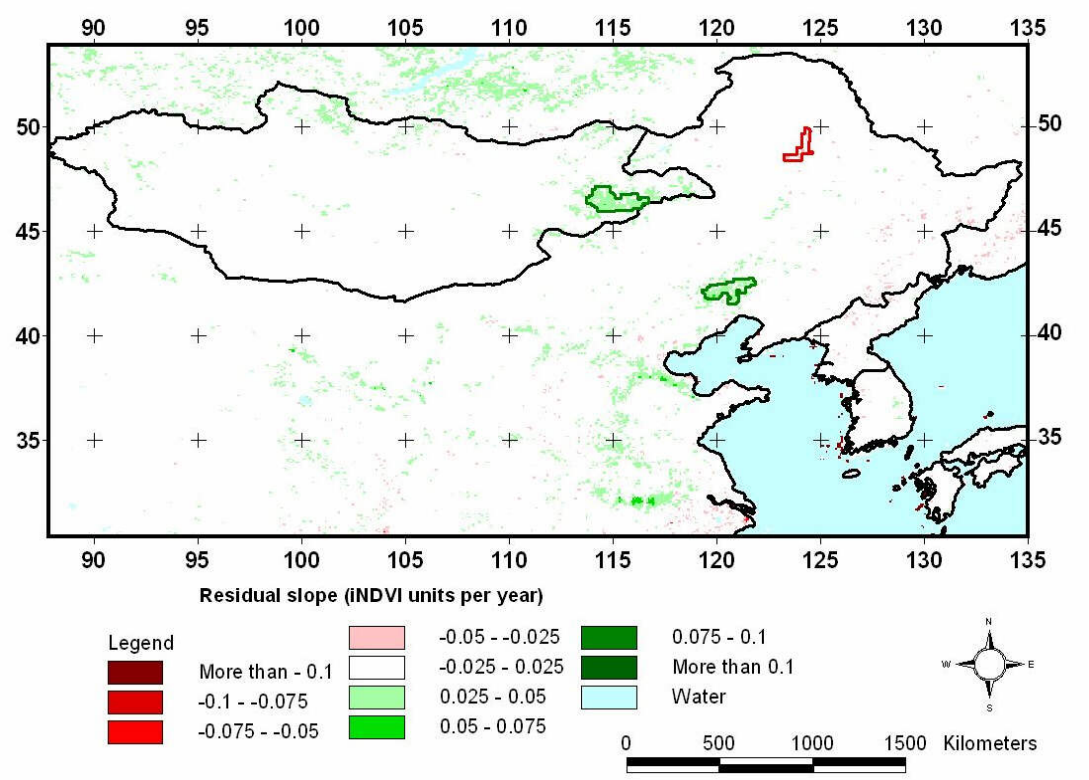

Fig. 5.5.20. East Asian negative (red vectors) and positive (green vectors) hot spots.

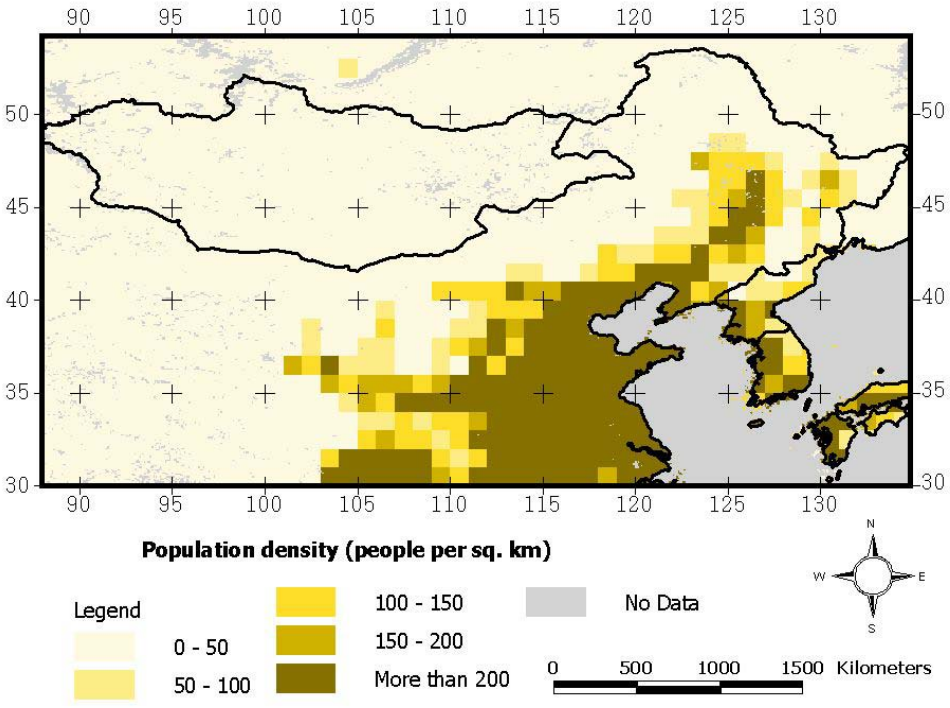

Fig. 5.5.21. East Asia population density for comparison. Data are from 2000 and produced by CIESIN (2005).

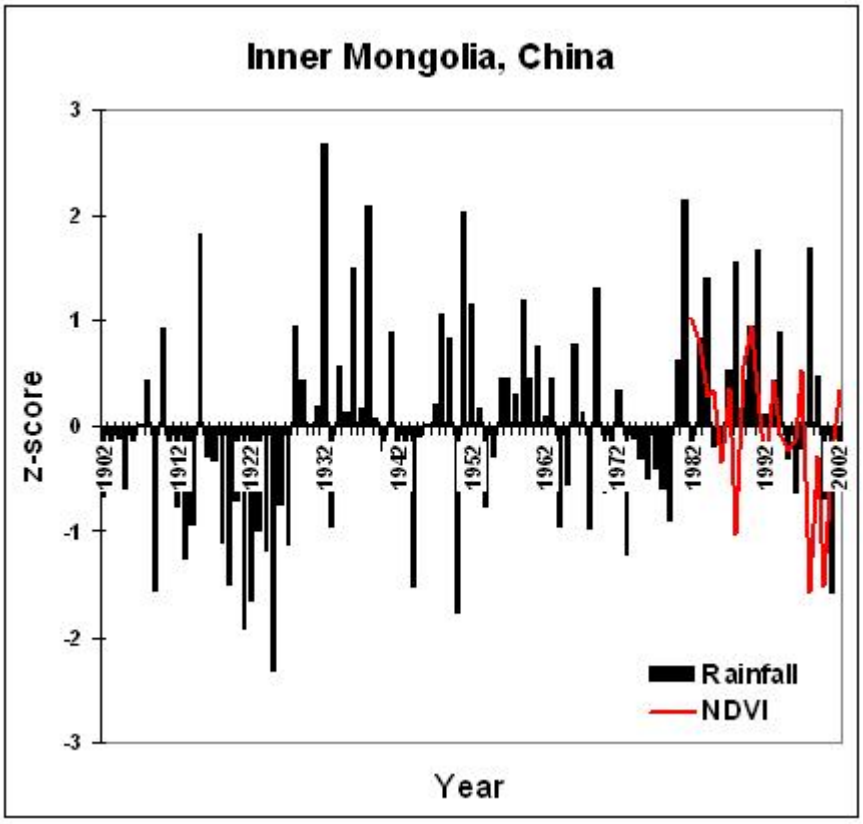

Fig. 5.5.22. Inner Mongolia negative (red) Hot Spot with rainfall and NDVI anomalies.

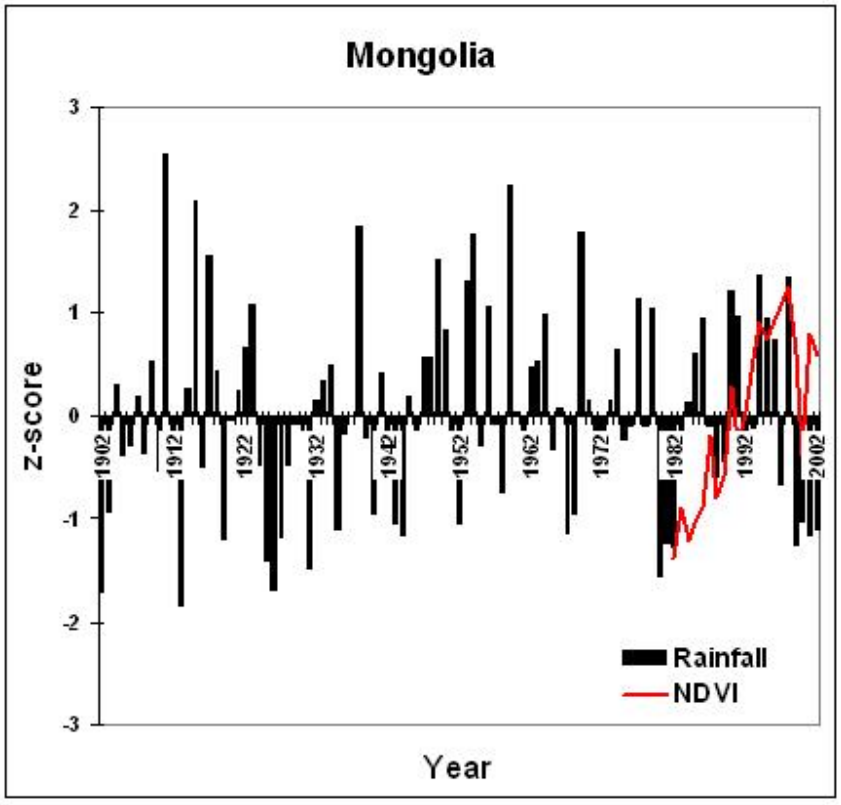

Fig. 5.5.23. Mongolia positive (green) Hot Spot with rainfall and NDVI anomalies.

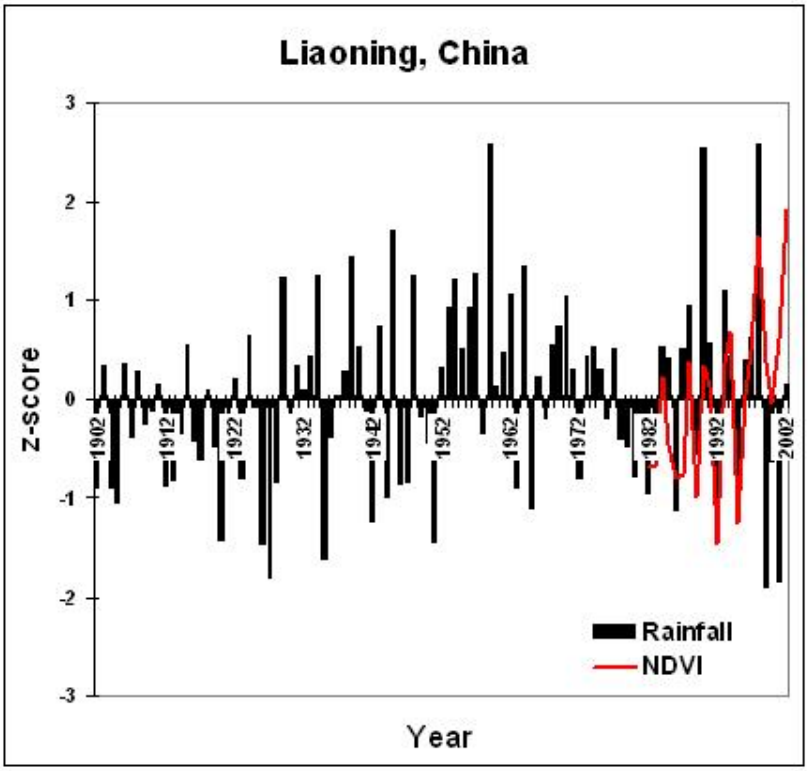

Fig. 5.5.24. Liaoning, Inner Mongolia, China positive (green) Hot Spot with rainfall and NDVI anomalies.

5.5.6. Desertification comments.

- Signs of desertification, as reflected by significant downward trends in the vegetation productivity, after it was controlled for rainfall variability, are hardly found anywhere inside the drylands. The residual trend analysis indicate a certain concentration of a few scattered negative trend areas mainly in NE China

- However, both positive and negative trends are weak. When significant, they can be explained by corresponding precipitation trends. The "greening up" trend seems to dominate the area together with areas of no significant change at all. It confirms the conclusions presented by recent studies on land degradation and desertification in China based on both high resolution Landsat TM 1978-1996 data and NOAA AVHRR pathfinder NDVI data (1982-1993) focusing on the MU Us Sandy Lands in Inner Mongolia, China (Runnström 2000, 2003a). Runnström concluded that the trend of GPP was generally positive over the period 1982-1999 for the Inner Mongolian grasslands (Runnström 2003b). The increased biomass production was explained by land management factors and governmental measures to halt desertification rather than by rainfall trends, although interannual biomass variations could be related to rainfall variations. The conclusions may contradict the results of a land use change study of the MU Us Sandy Lands based on manual interpretation of air photos from the 1958 and Landsat imagery from 1993 by Wu and Long (2001). They found that the shifting and semi fixed sandy lands had increased considerably between 1958 and 1993. However, we know that a lot of work has been invested in land management and anti-desertification measures in Mu Us Sandy lands and northern China since 1993 resulting in increased vegetation cover over large areas.

- A study on climate and human impacts on winter wheat production and land use 1955-2004 in the Loess Plateau Region, Shaanxi (neighbor province to the Runnström study region) was recently presented by Simelton (2007). It was concluded that wheat yields and vegetation production increased considerably over the period, not due to climate but mainly due to human land management related impact (Simelton et al. 2007, Ostwald et al. 2007). Increased crop yields but varying (positive as well as negative) development of vegetation cover was reported by Brogaard and Zhao (2002) in a case study on rural reforms and changes in land management from Keerquin Sandy Lands, Inner Mongolia. However, it was indicated by a NOAA AVHRR and precipitation based model that a large area in central Inner Mongolia showed a marked increase in biological production (GPP) for the period 1982-1999 while the western parts showed no change (Brogaard 2003).

Fig. 5.5.25. Grasslands in Inner Mongolia, China. (Photo: U. Helldén, Sep. 1993)

Fig. 5.5.26. Expanded agriculture into former grasslands, Horquin Sandy Lands, Inner Mongolia, China. (Photo: U. Helldén, May 1994).

5.6. SOUTH AMERICA

5.6.1. South America overview

This study region stretches from Peru in the north to Tierra del Fuego in the South and from Chile in west to Uruguay in east (Fig. 5.6.1).

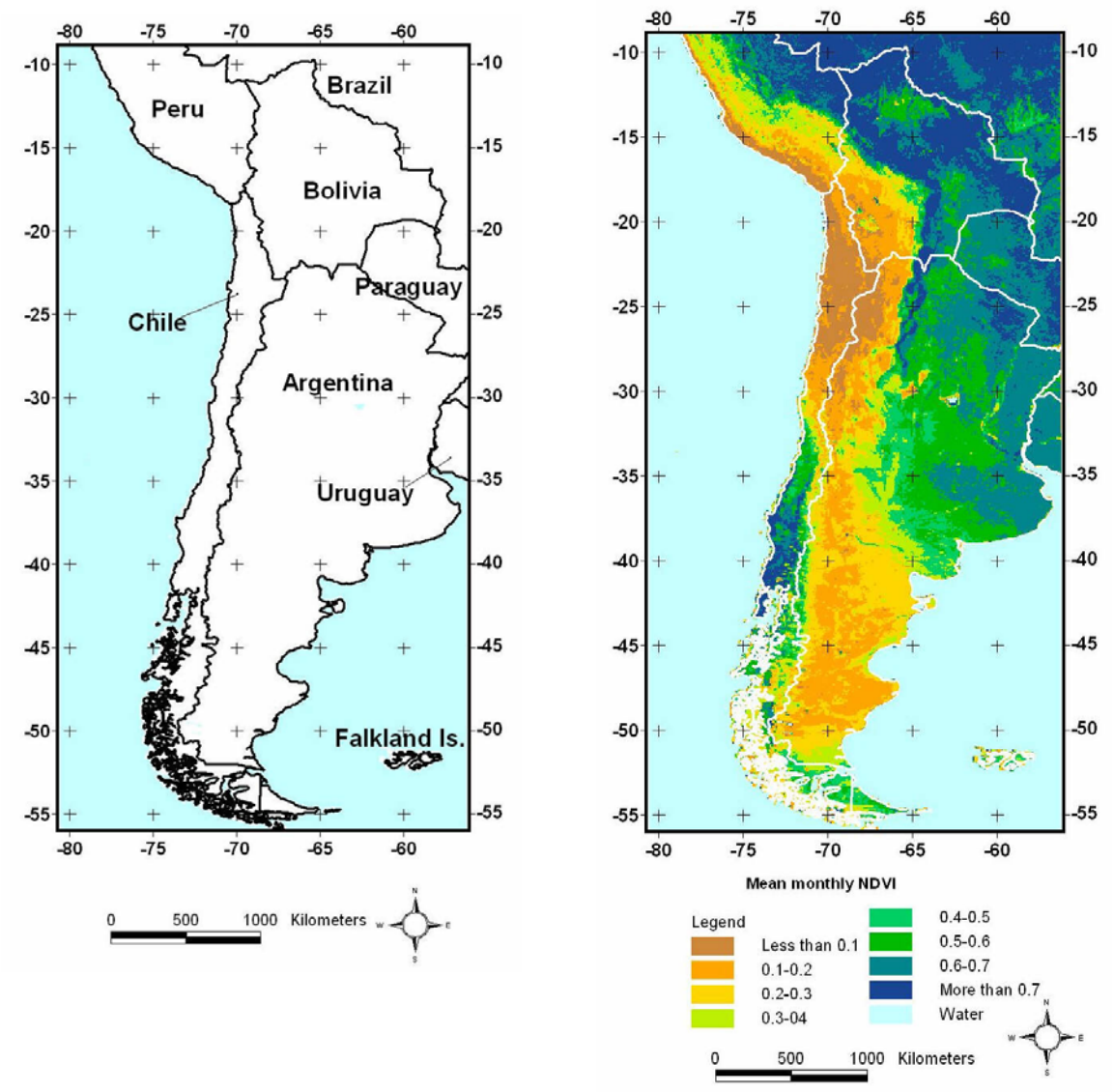

Figure 5.6.1. Country overview (left) and the mean monthly NDVI based on data from 1982 to 2003 (right).

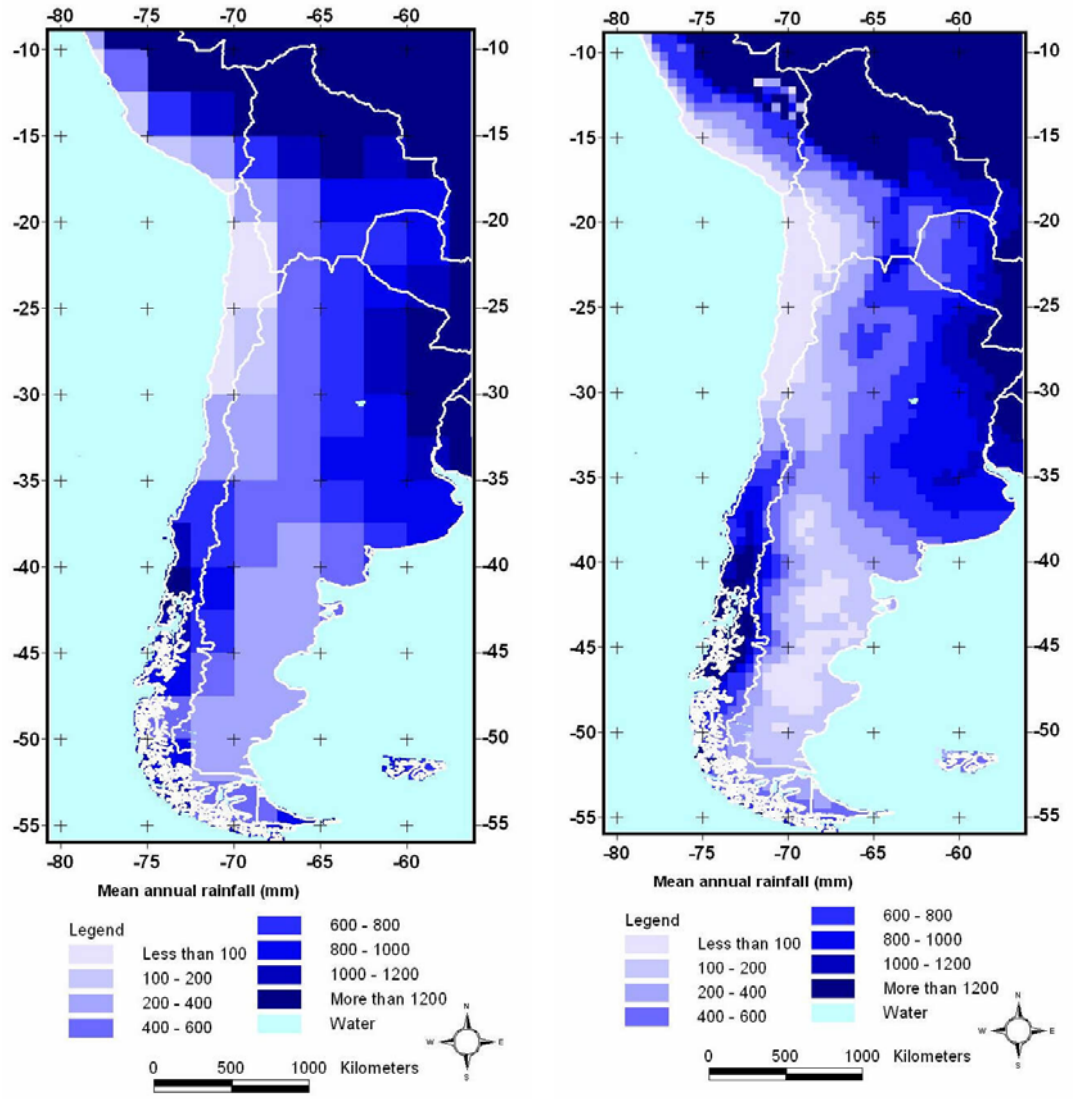

Figure 5.6.2.(Left) Mean annual rainfall based on 2.5 degree (~ 275 km) gridded rainfall data from 1982 to 2003.

Fig. 5.6.3. (Right) Mean annual rainfall based on 0.5 degree (~55 km) gridded rainfall data from 1982 to 2002.

Inspection of time-series plots of both rainfall and NDVI revealed that the appropriate seasons for the drylands (i.e. the area delineated by a minimum of 0.1 and a maximum of 0.5 NDVI based on the long-term monthly average) of the South American region was from “August to July” for both rainfall and NDVI (figure 5.6.4).

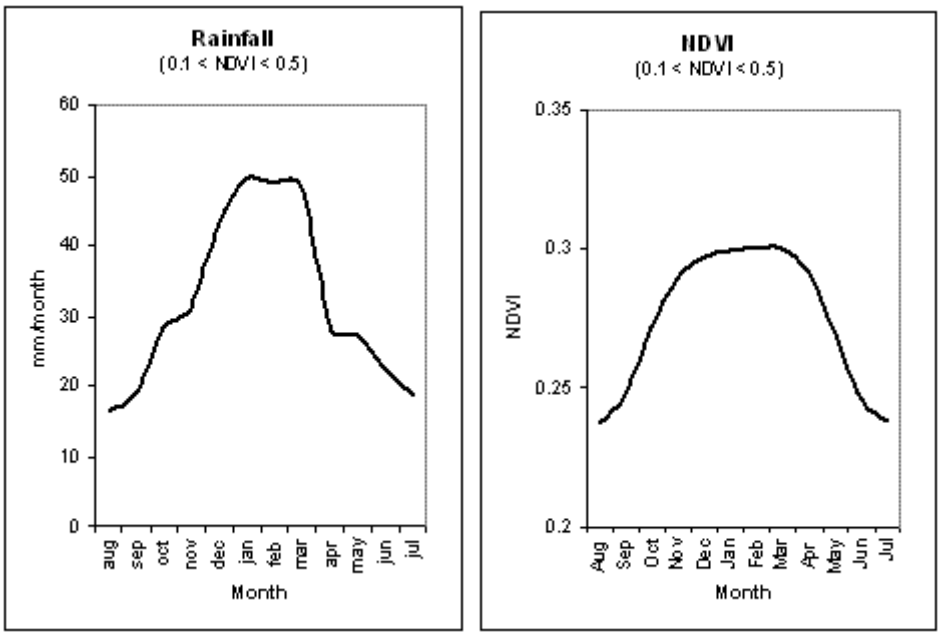

Figure 5.6.4. Monthly time-series plots of rainfall (left) and NDVI (right). The displayed values are mean values as calculated from the area defined by $0.1 \leq NDVI \leq 0.5$.

Consequently total annual rainfall as well as annual vegetation productivity was calculated by summarizing rainfall and NDVI over the months from August to July

5.6.2. Vegetation trend analysis

The following figures summarize the results of the trend analysis approaches described under methods.

Figure 5.6.5-5.6.8 confirm the points raised in the method sections regarding the relative merits of the different characteristics (inclination, relative change or statistical significance) of the trend line. Especially it is clear that the statistical test is placing too much emphasis on areas with rather small slope inclinations. There is equally a tendency for the relative change to put emphasis on areas where the intercept value i.e. the starting point is low. In that case a relative low absolute slope value may actually come out as a quite significant relative change.

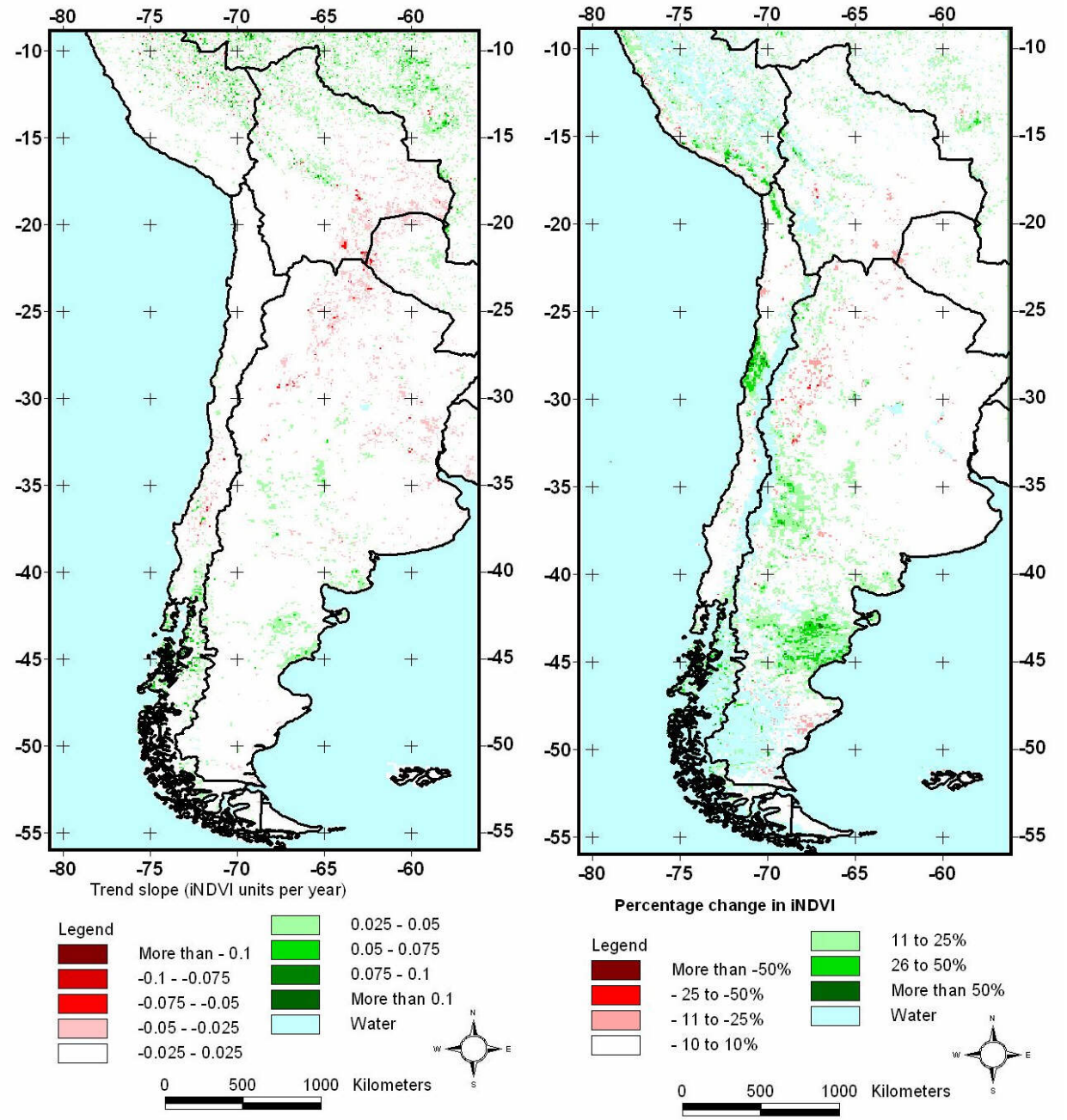

Figure 5.6.5. (Left) Linear trends in vegetation productivity for the period 1982 to 2002 based on annual integrated NDVI values. The trend is expressed in absolute values i.e. change in iNDVI units per year.

Fig 5.6.6. (Right) Linear trends in vegetation productivity for the period 1982 to 2002 based on annual integrated NDVI values. The trend is expressed as percentages i.e. the relative difference between the start and the end value of the linear trend

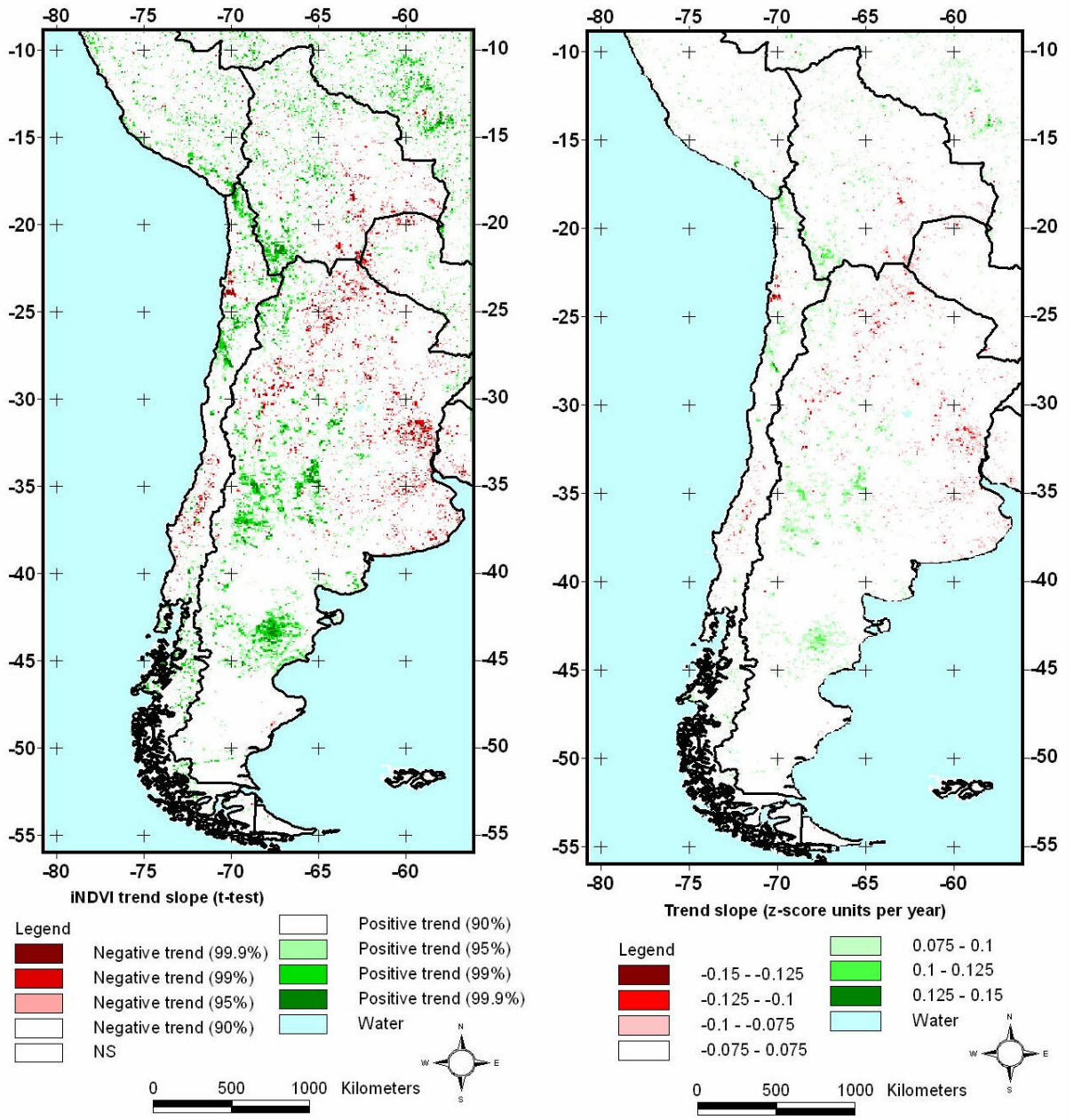

Fig. 5.6.7. (Left)Trend slope in NDVI based on linear least square regression (1982-2002). iNDVI trend slope (t-test).

Figure 5.6.8. (Right) Standardized trend slope in NDVI based on linear least square regression and expressed as z-score units per year (1982-2002).

5.6.3. Vegetation versus rainfall analysis

Figure 5.6.9 (left) indicates the relationship between mean NDVI and mean annual rainfall. The strong positive relationship (r^2=0.6) confirms the fact that higher rainfalls normally yields higher vegetation productivity.

Yet, the relationship illustrated in Figure 5.6.9 (left) is biased due to the presence of spatial auto-correlation i.e. the phenomenon where locational (geographic position) similarity is matched by value similarity. Consequently Fig. 5.6.9 (left) demonstrates the geographic relationship between long-term means of total annual rainfall and monthly NDVI .In order to avoid this bias the anomaly analysis was introduced (figure 5.6.9 [right], figure 5.6.10, 5.6.11-5.6.15).

The results from the anomaly analysis illustrate a significant and valid relationship between rainfall variability and NDVI variability for large parts of the South American drylands. Despite the generalization level of these figures it remains clear that rainfall and NDVI are indeed closely associated. Figure 5.6.9 thereby supports the idea that NDVI trends should be controlled for rainfall variability before elucidating on the possible anthropogenic causes.

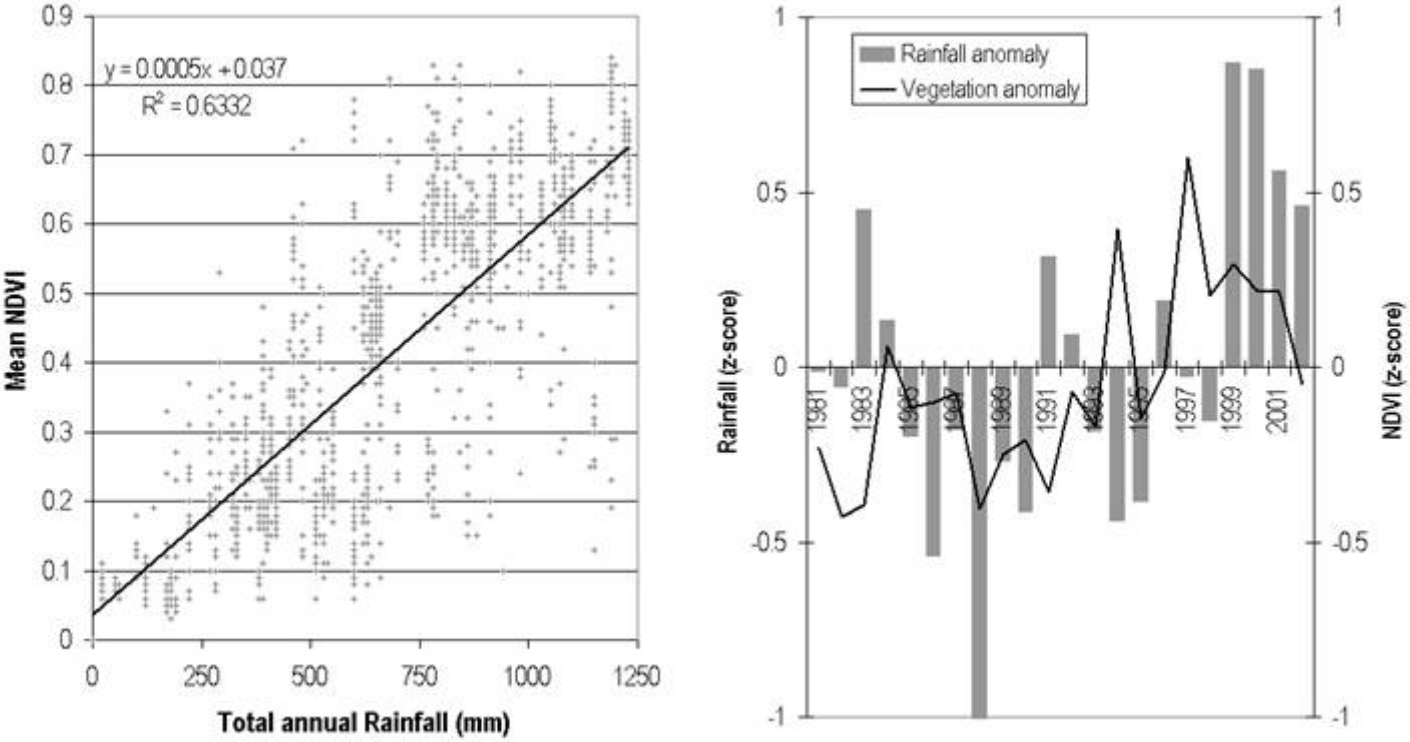

Fig. 5.6.9. (LEFT)Annual rainfall plotted against mean NDVI. The displayed values are mean values for the period 1982 to 2003. (RIGHT) Average z-scores of NDVI and rainfall. On display are mean z-scores as calculated from the area defined by 0.1 < NDVI < 0.5.

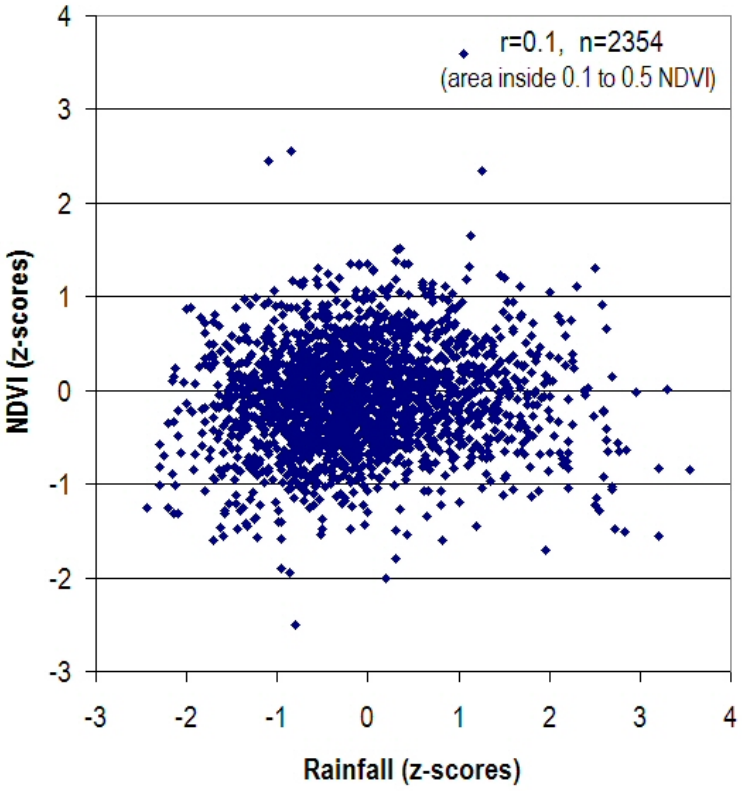

Fig. 5.6.10. Annual NDVI anomalies plotted against annual rainfall anomalies. Every pixel in the 2.5 degree rainfall data was selected and plotted against the average NDVI value for the corresponding NDVI 8 km pixels under each 2.5^0 cell. Only pixels inside the area defined by 0.1<NDVI<0.5 where NDVI denotes mean monthly NDVI for the 1982-2003 period. All data for the 1982-2003 period were merged into one data set.

It should be noted that it is only a very small fraction (~1 %) of the interannual NDVI anomaly variation that can be explained by corresponding interannual (seasonal) rainfall anomalies under the given circumstances (Fig 5.6.10). It implies there are large areas (many pixels) where the strong NDVI-rainfall anomaly relationship is not valid. This is also illustrated in the figures below.

The following maps summarizes the results from the per pixel analysis of the temporal relationship between rainfall and NDVI.

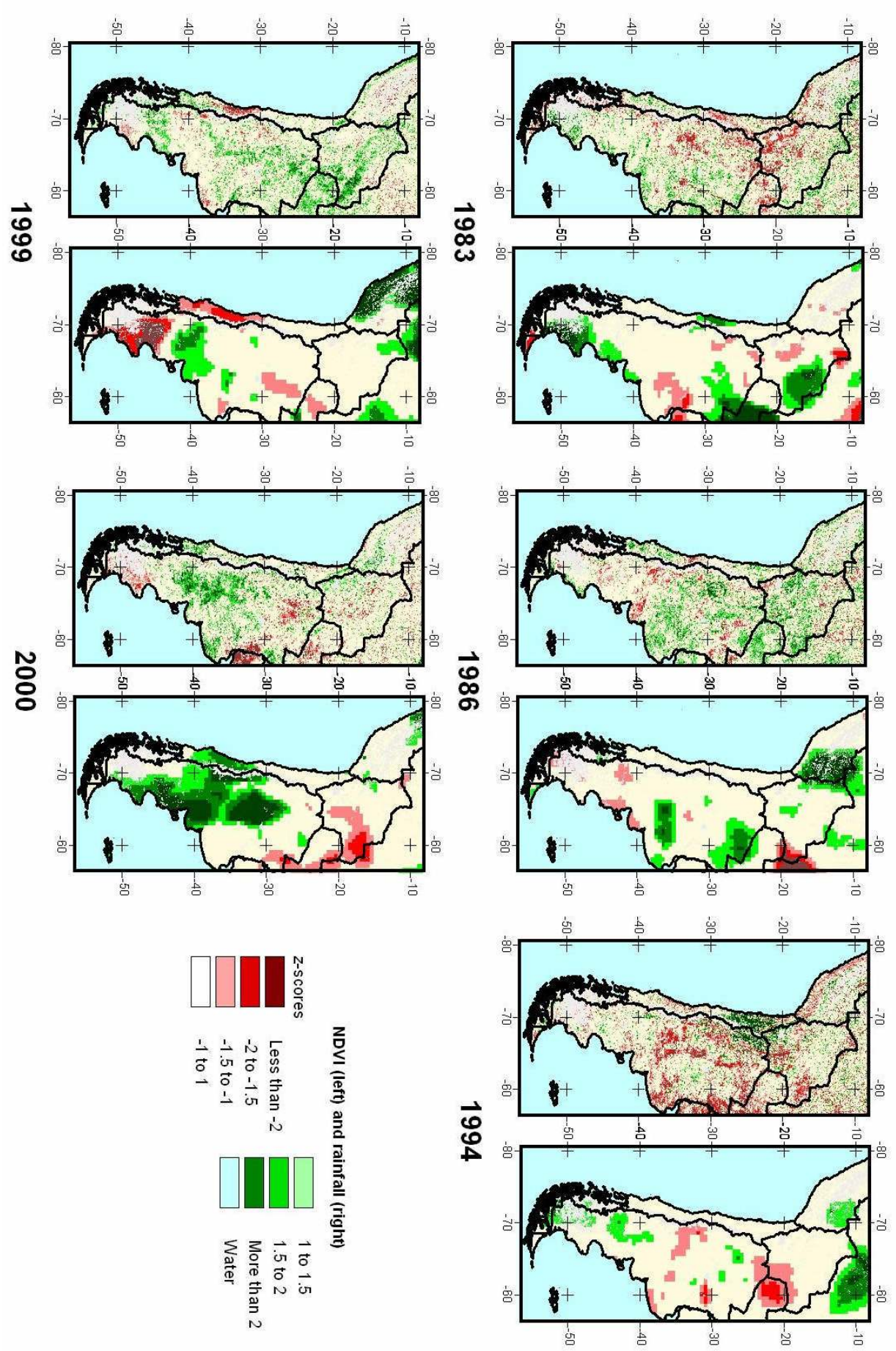

Figure 5.6.11. NDVI (8 km) and rainfall (0.5 degree grid) anomalies for 5 random "non-calendar" years during the 1982 to 2003 period.

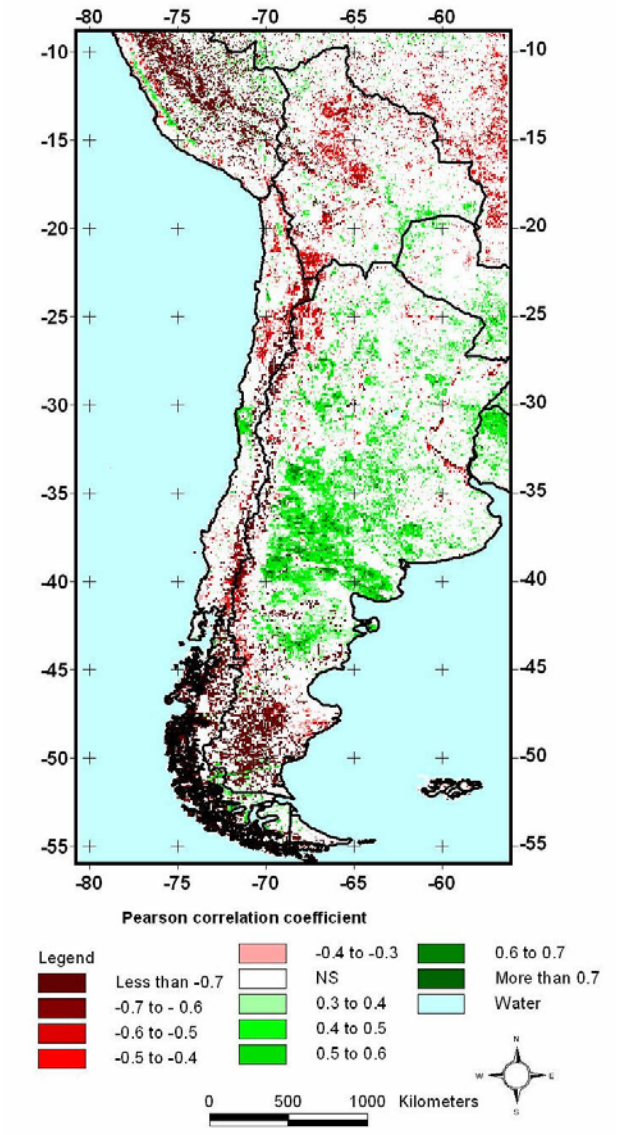

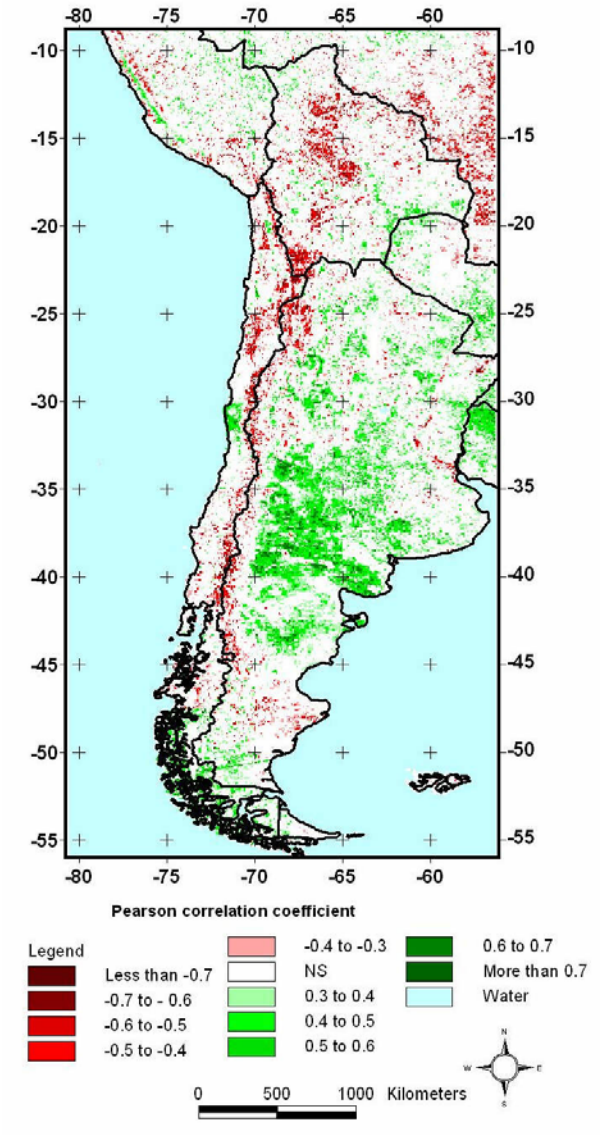

Fig. 5.6.12. (Left) Total annual rainfall (2.5 degree) vs. annual integrated NDVI (1982-2003)

Fig. 5.6.13. (Right) Rainfall anomaly (2.5 degree) vs. NDVI anomaly (1982-2003).

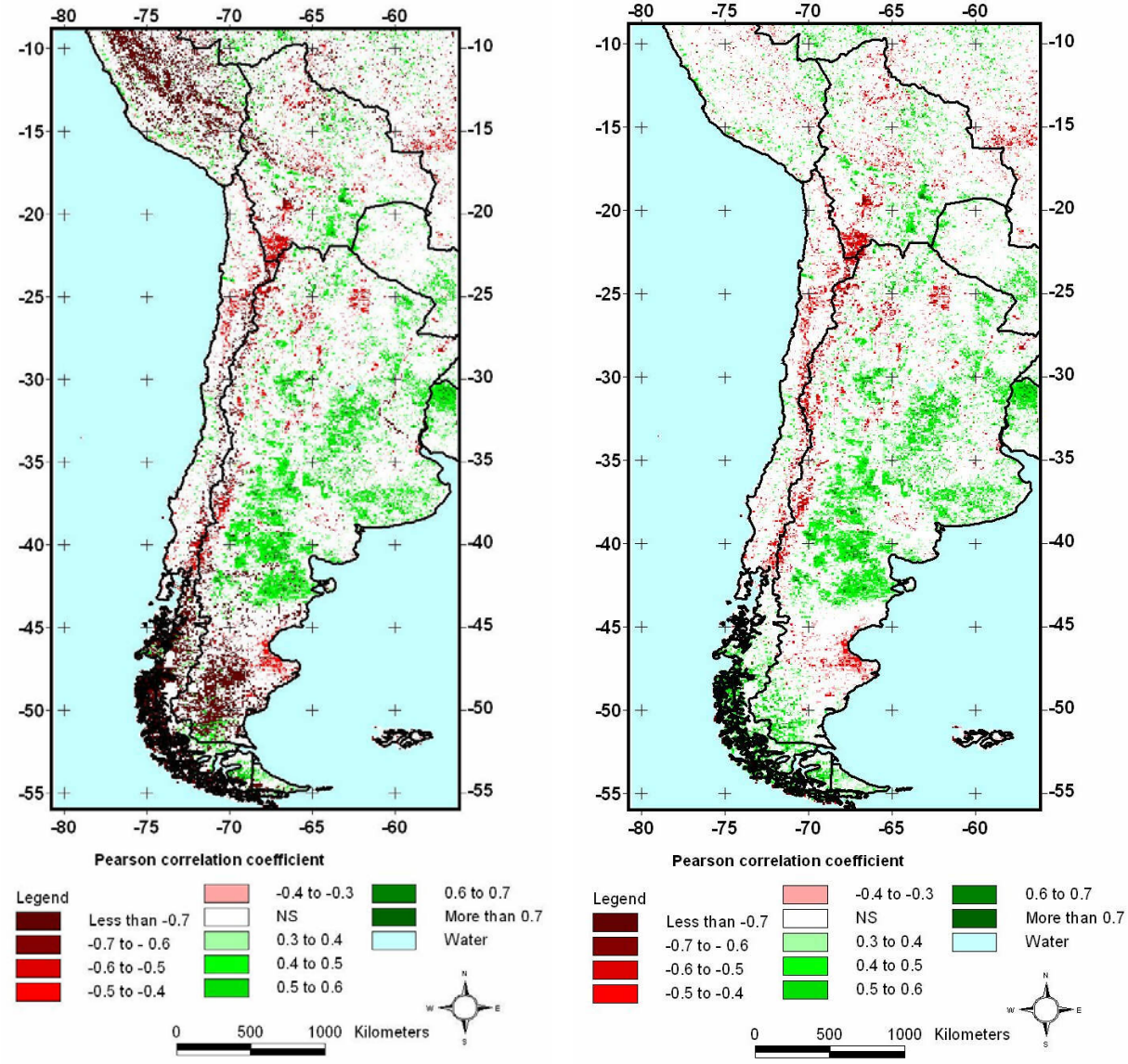

Fig. 5.6.14. (Left) Total annual rainfall (0.5 degree) vs. annual integrated NDVI (1982-2002**)**

Fig. 5.6.15. (Right) Rainfall anomaly (0.5 degree) vs. NDVI anomaly (1982-2002).

As expected one can see a relatively good correlation between rainfall and NDVI for large areas of the South America region. However, large areas of negative correlation are also present. They are often areas where rainfall is not necessarily the limiting factor for vegetation growth but rather temperature. Much of the negative correlation is located to the Andes Mountains, where this is suggested to be the case. It is interesting to note the strong agreement between the maps based on 2.5 degree gridded data and the maps based on 0.5 on degree gridded data as well the almost identical patterns observed between the use of integrated data and standardized data.

5.6.4. Residual analysis

The model residuals (i.e. the difference between observed and expected indri) were computed for each pixel and subsequently inspected for any systematic trends that could invalidate the initial model specification.

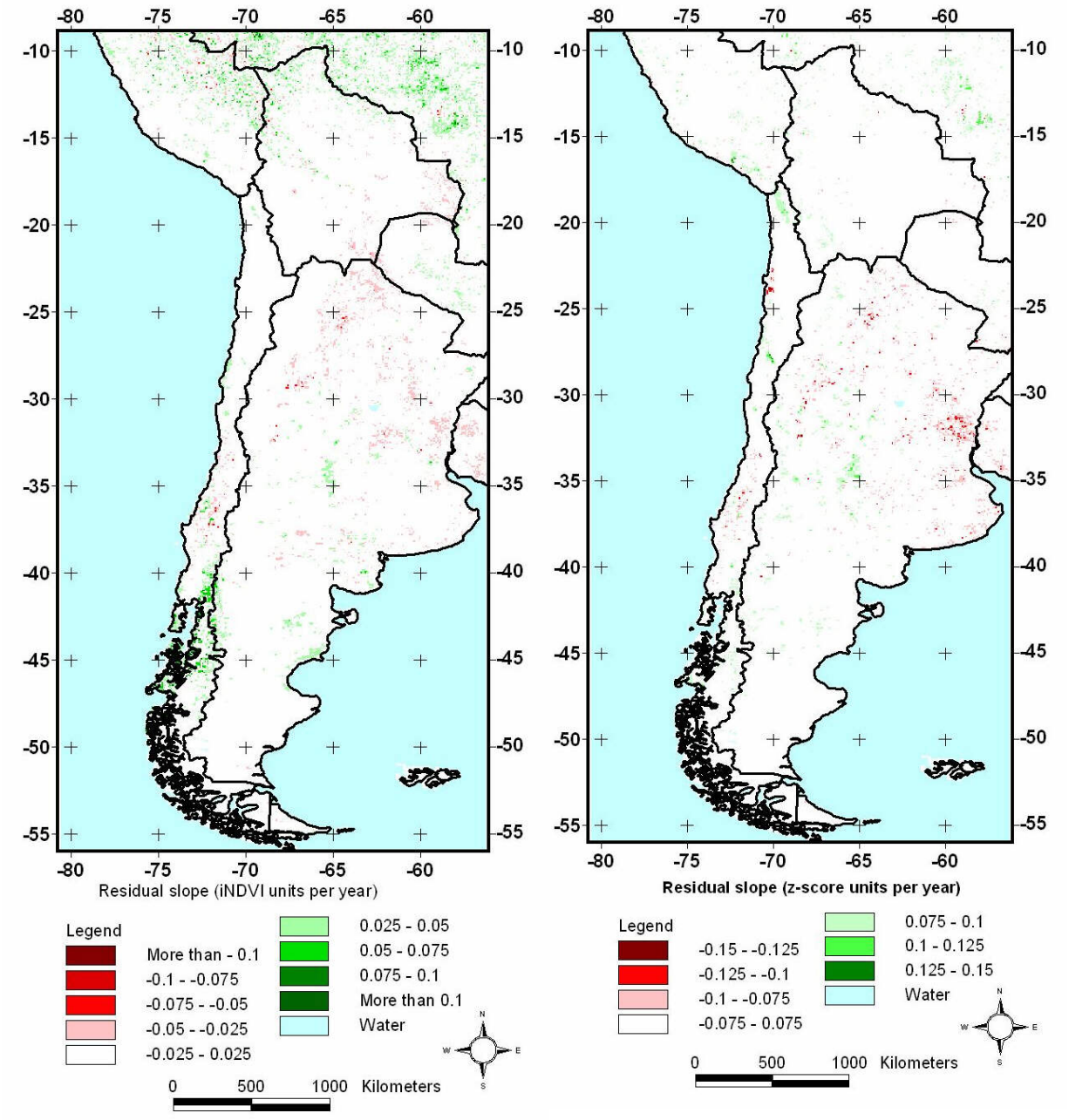

Fig. 5.6.16. (Left) Linear trends in residual slope of iNDVI when controlled for annual rainfall **(2.5 degree)** for the period 1982 to 2003. The trend is expressed in absolute values i.e. change in iNDVI units per year.

Fig. 5.6.17. (Right) Linear trends in residual slope of iNDVI z-scores when controlled for annual rainfall **(2.5 degree)** for the period 1982 to 2003. The trend is expressed in absolute values i.e. change in z-score units per year.

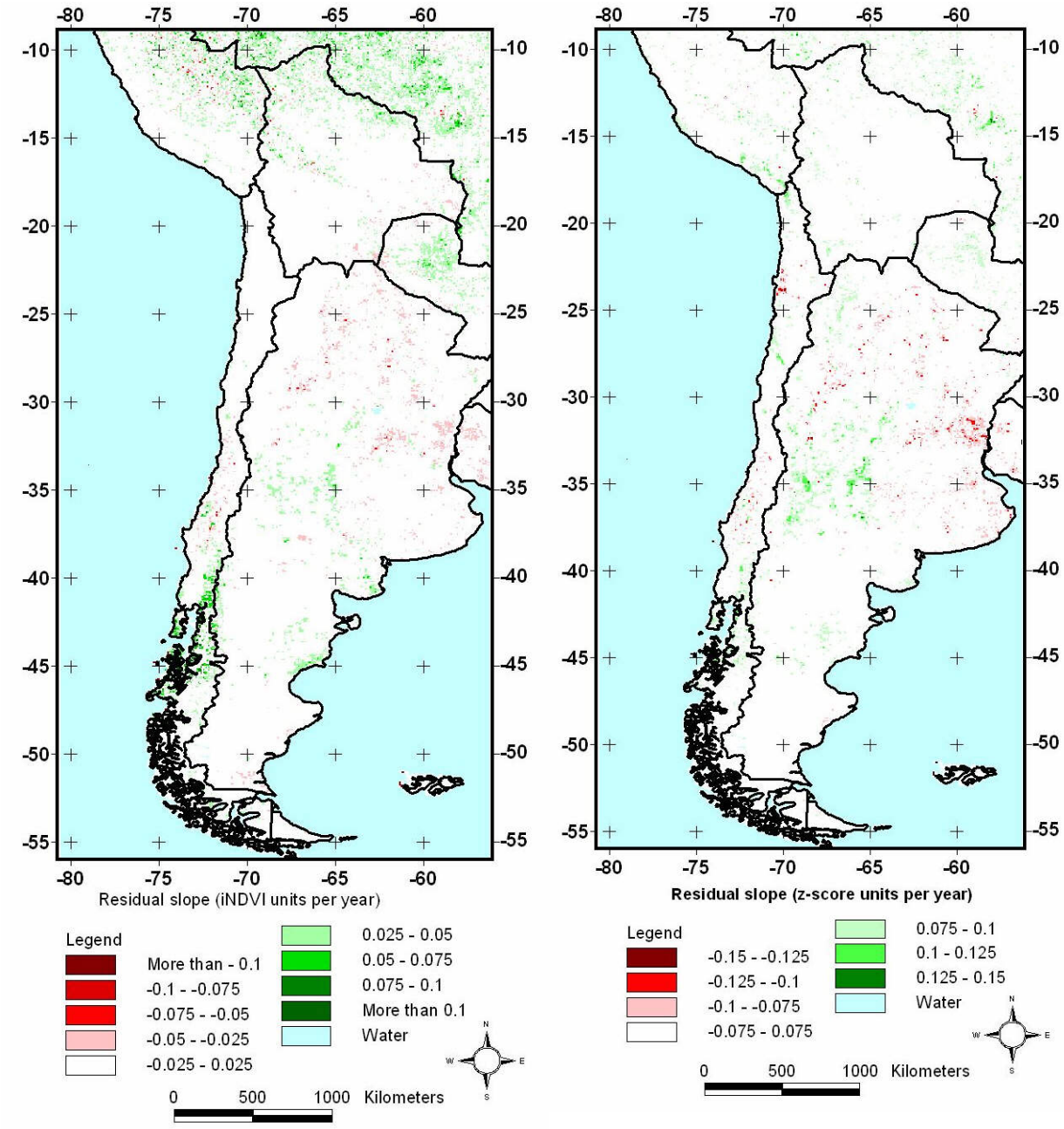

Fig. 5.6.18. (Left) Linear trends in residual slope of iNDVI when controlled for annual rainfall **(0.5 degree)** for the period 1982 to 2002. The trend is expressed in absolute values i.e. change in iNDVI units per year

Fig. 5.6.19. (Right) Linear trends in residual slope of iNDVI z-scores when controlled for annual rainfall **(0.5 degree)** for the period 1982 to 2002. The trend is expressed in absolute values i.e. change in z-score units per year.

5.6.5. Hot Spot analysis

Example areas with significant residual trends (negative as well as positive) were identified and the trend in vegetation productivity relative to the long-term precipitation anomaly trends in the area were studied (Fig 5.6.20-5.6.23).

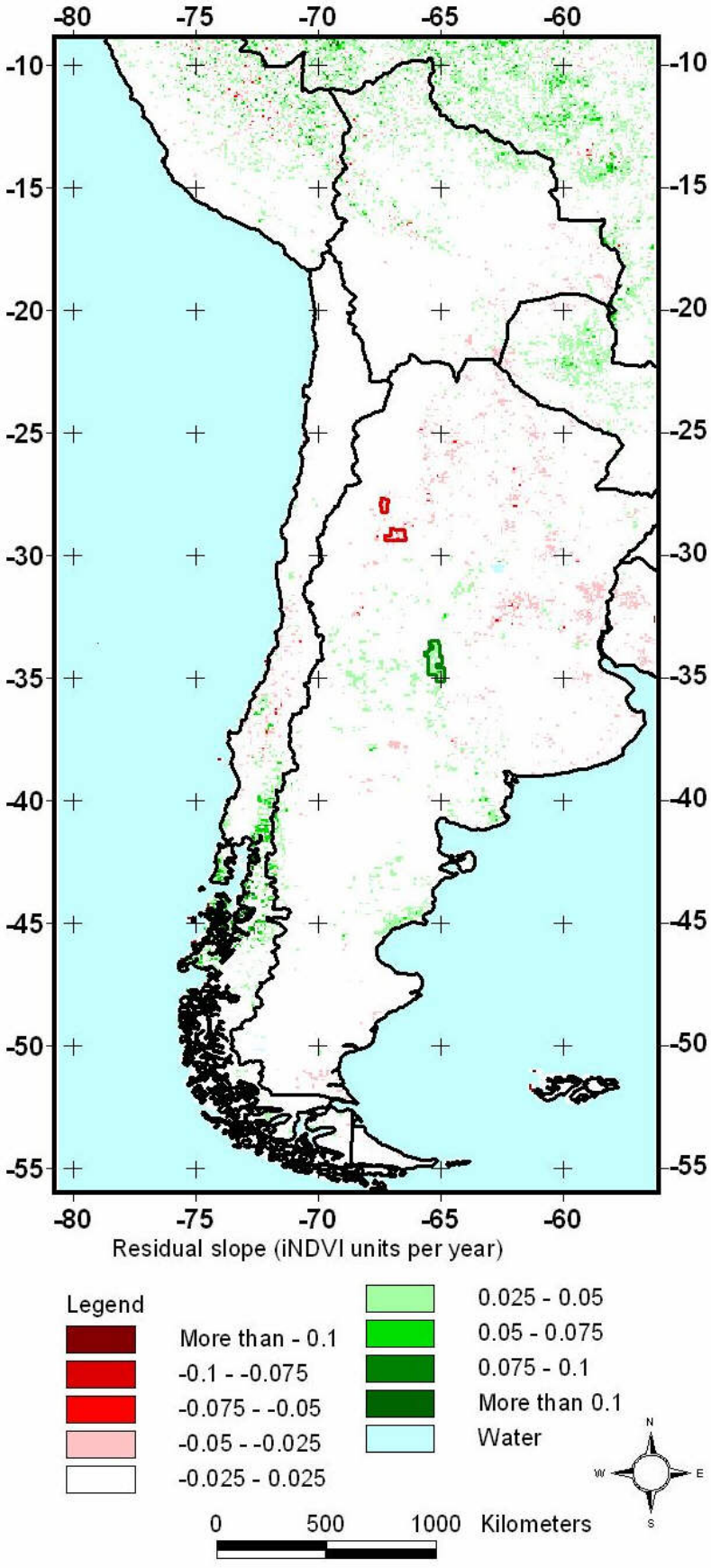

Fig. 5.6.20. East Asian negative (red vectors) and positive (green vectors) hot spots.

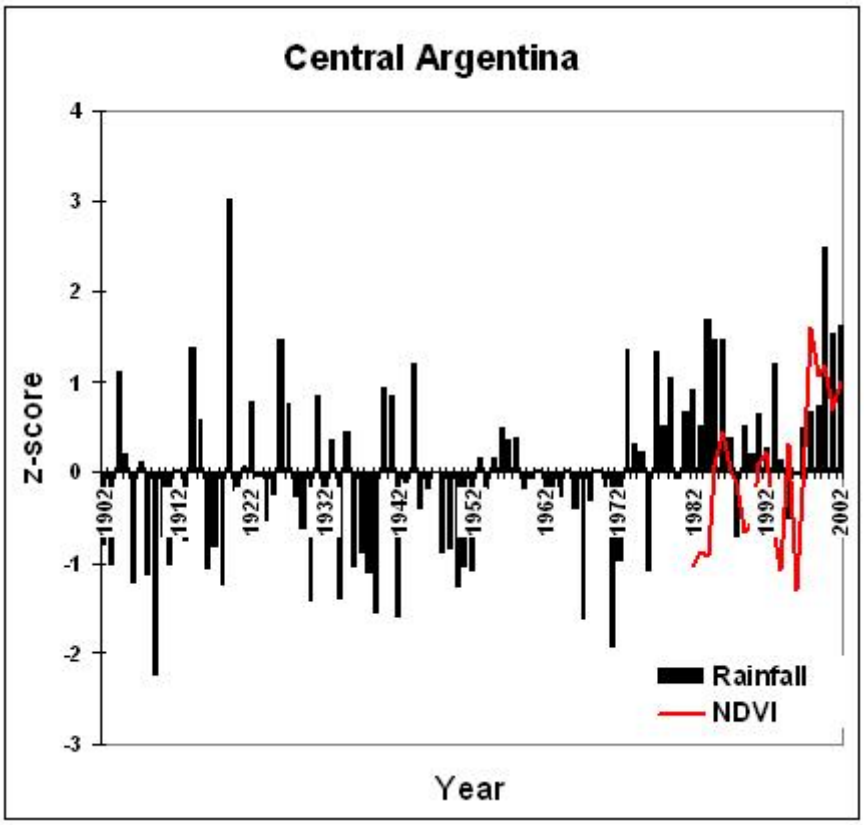

Fig. 5.6.20 Central Argentina positive (green) Hot Spot with rainfall and NDVI anomalies.

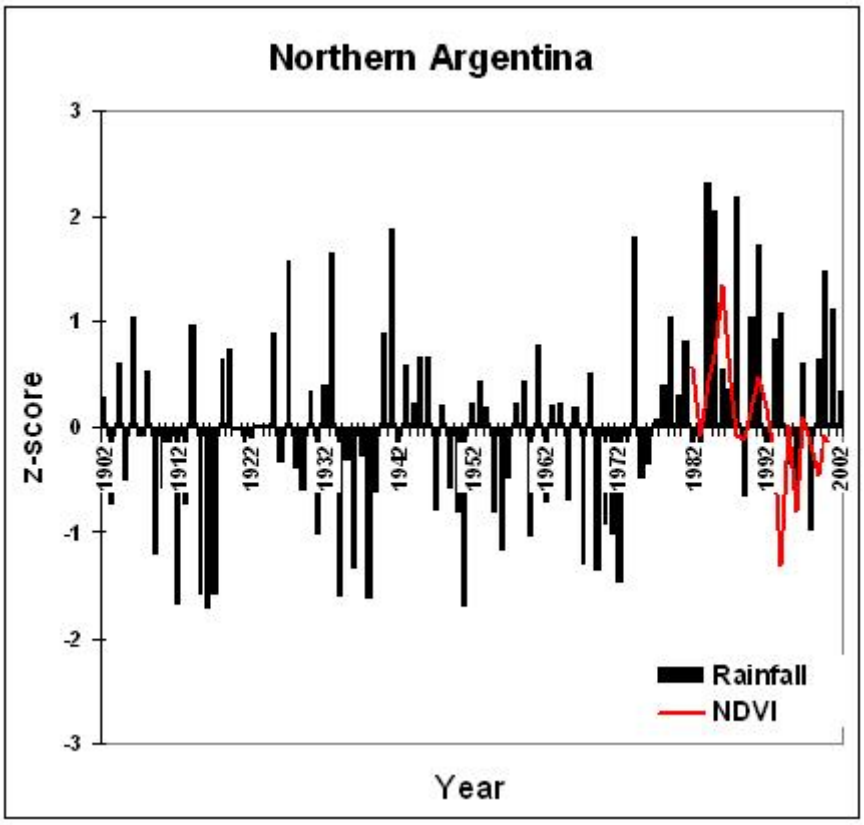

Fig. 5.6.21 Northern Argentina negative (red) Hot Spot with rainfall and NDVI anomalies.

5.6.6. Desertification comments

- Signs of desertification, as reflected by significant downward trends in the vegetation productivity, after it was controlled for rainfall variability, is hardly found anywhere inside the drylands. The residual trend analysis indicates a certain concentration of scattered negative trend areas mainly in NE Argentina.

- However, both positive and negative trends are weak. When significant, they can often be explained by corresponding precipitation trends. The “greening up” trend seems to slightly dominate the area together with areas of no significant change at all.

Fig. 5.6.22. Marginal dryland farms in Chile are being abandoned and often replaced by large commercial irrigated wine yard and avocado schemes. (Photo U.Helldén, 2006).

6. CONCLUSIONS

Trend analysis of time series of NOAA NDVI GIMMS data can be used to assess long-term changes in vegetation production. The variations in integrated NDVI trends can be understood in relation to a complex interaction of climatic and human drivers.

The methodological framework presented in this report can be used to investigate broad-scale environmental changes, and serve as a starting point for more detailed studies by pinpointing areas (regions & hot spots) of radical change and interest. In this respect, the method will complement studies on long-term change based on statistical records, indicators or in-depth local studies. More specifically, the proposed methodology will be an important tool for obtaining an overview of desertification—not only in terms of assessing the magnitude or importance of potential degradation, but also as a first global-regional-national-sub national indicator on where to apply more expensive in depth studies and where to intervene with support and mitigation programs . The methods can also be used to identify areas with positive trends in vegetation development, where detailed studies may provide information and knowledge about factors enabling vegetation growth.

However, it should be recognized that the data and methods applied in this study cannot be used to assess all important aspects of vegetation change as an indicator of desertification. Changes in vegetation quality e.g. positive or negative changes in species composition, diversity and palatability may not be possible to identify. A suggested trend of "greening- up" may e.g. include, or even be dominated by, a decreasing rangeland palatability and quality; i.e. increased degradation.

In reference to the research objective some of the key findings of this study include:

- A global NDVI and precipitation database has been compiled and a standard framework for handling and analyzing the data has been proposed (a temperature data base has been compiled as well but not yet integrated in the analysis).

- The database has been used to search for indications of desertification within six of the world's major dryland regions. A method has been developed that identify areas where observed trends and anomalies in NDVI (read - vegetation productivity) cannot be explained by rainfall variability alone.

- Although scattered pockets of apparent desertification (i.e. downwards trends in NDVI) can be found in all six regions the results indicate that all six regions have an accent towards land improvement (i.e. increasing trends of "greenness") and no region more so than the Sahel in Western Africa.

At this stage, it is too early to draw any firm conclusions on the basis of these results though it is worth mentioning that they do contest existing narratives about "marching deserts" or massive desertification as a global threat. Before proceeding with the recommendations for future work it is important to recall the limitations and scope of this work.

First of all it should be noted that desertification is the result of complex processes that act over many scales and are linked together in hierarchies. Phenomena occurring at any scale are affected by phenomena occurring at scales below and above. The important lesson is that the choice of scale, extent and resolution critically affect statistical associations and identified patterns: patterns and associations that appear at one level of resolution may be lost at lower or higher levels; patterns and associations that occur over one extent of a dimension may disappear if the extent is increased or decreased (Verburg and Chen 2000). Multi-scale and multi-resolution analysis, preferably backed up and combined by field studies, is a must in order to fully understand the link between these different scales and resolutions.

Secondly we need to underline that the strength of remote sensing lies in its synoptic coverage and its ability to map and monitor the state and change in land conditions, yet remote sensing do not necessarily answer what has caused this state and/or change. In other words remote sensing derivatives cannot tell us where desertification is taking place but rather it can be used to deliver a qualified guess i.e. point towards interesting patterns/trends in land conditions that may or may not be desertification. The final affirmation of where desertification is taking place and why it happens can only come from the integration of all the DeSurvey system components including the ultimate and very important local field studies.

Mapping and monitoring of land degradation over large areas is a huge task and it is realized that the results presented are merely touching upon the surface of this subject. Needless to say, a number of tasks have been identified that could help to bring this work forward:

- The per pixel based interannual anomaly analysis of NDVI versus annual precipitation suggests that we should try to limit the NDVI anomaly studies to $0.1<NDVI<0.4$ rather than using 0.5 as the upper mean monthly limit to better explain NDVI anomalies as a function of rainfall anomalies.

- An important next step will be to integrate the temperature dataset into the analysis: Preliminary tests indicate that using rainfall and temperature in a multi-variate model of NDVI trends add significantly to the explanatory power of the model. On the other hand, the contrary was found in a recent DeSurvey study on Spain based on 1 km NOAA AVHRR NDVI data by Udelhoven et al. (2007).

-Another important step may be to further integrate population data into the analysis for in depth analysis of the role of rural population dynamics and pressure as drivers of vegetation conditions indicated by NDVI.

- Methods exist by which the appropriate season for a time-series can be estimated (Jönsson and Eklundh 2002). Using such methods it will be possible to optimise the integration period on a per pixel basis rather than using an integration period based on a regional average as in the current analysis.

- In a similar way methods are available that can extract seasonal parameters from a data time-series (including maximum, minimum, amplitude and seasonal adjusted integrals). These parameters represent different aspects of the land surface than the annual integrals and should be tested in future work. Also the Coefficient of Variation (COV) is an important parameter to be used in future trend analysis.

7. REFERENCES

Abdi,H.,2007: Z-scores-In: N.J. Salkind (Ed): Encyclopedia of Measurement and Statistics.-Thousand Oaks, CA:Sage.

Brogaard,S., Zhao, X., 2002: Rural Reforms and Changes in Land Management and Attitudes: A Case Study from Inner Mongolia, China.- Ambio Vol. 31, No 3, pp. 219-225.

Brogaard, S., 2003: Recent changes in land use and productivity in agro-pastoral Inner Mongolia, China.- Ph. D. Thesis Department of Physical Geography and Ecosystem Analysis, Meddelanden från Lunds Universitets Geografiska Institutioner, Avh 151, ISBN: 91-973857-7-8.

CIESIN, 2005: The Center for International Earth Science Information Network; http://www.ciesin.org/data.html. and http://sedac.ciesin.columbia.edu/gpw/.

Diallo,O., Diouf,A., Hanan,N.P., Ndiaye,A., Prevost,Y., 1991: AVHRR Monitoring of Savanna Primary Production in Senegal, West Africa - 1987-1988.- International Journal of Remote Sensing 12: 1259-1279.

Dregne,H.E., Tucker,C.J., 1988: Desert Encroachment-Desertification Control Bulletin, UNEP, Nr 16, pp. 16-19.

Eklundh,L., 1996: AVHRR NDVI for monitoring and mapping of vegetation and driught in East African environments.-Ph.D. Thesis. Department of Physical Geography, Lund university. Meddelanden från Lunds Universitets Geografiska Institutioner, Avhandlingar 126, 187 pp. Lund university press, ISBN 91-7966-359-1.

Eklundh,L., 1998: Estimating relations between AVHRR NDVI and rainfall in East Afria at 10-day and monthly time scales.-Int. J. Remote Sensing 19:563-568.

Eklundh, L. and L. Olsson. 2003: Vegetation index trends for the African Sahel 1982-1999. - Geophysical Research Letters 30 (8).

Franklin, S.E. and M.A. Wulder. 2002: Remote sensing methods in medium spatial resolution satellite data land cover classification of large areas.- Progress in Physical Geography 26: 173-205.

Fuller, D.O., 1998: Trends in NDVI time series and their relation to rangeland and crop production in Senegal, 1987-1993.- International Journal of Remote Sensing 19: 2013-2018.

Grove, A.T., Rackham,O., 2003: The Nature of Mediterranean Europe. An Ecological History.- Yale University Press, ISBN 0-300-10055-8, 384 pp.

Hammond, R.,McCullagh., 1982: Quantitative techniques in Geography-Clarendon Pres, Oxford ISBN 0 19 874067 0, 364 pp.

Helldén,U.,1984: Drought Impact Monitoring- A remote sensing study of desertification in Kordofan, Sudan. - Lunds Universitets Naturgeografiska Institution, Rapporter och Notiser Nr 61, 61 pp. ISSN 0348-3339.

Helldén,U., 1991: Desertification-Time for An Assessment.-Ambio Vol 20, No 8: 372-383.

Helldén,U., Eklund, L., 1988: National drought impact monitoring-A NOAA NDVI and precipitation data study of Ethiopia- Lund Studies in Geography. Ser C. General, Mathematical and Regional Geography No 15, 55 pp. Chartwell-Bratt Ltd, ISBN 0-86238-201-7

Herrmann,S.M., Anyamba,A., Tucker,C.J., 2005: Recent trends in vegetation dynamics in the African Sahel and their relationship to climate. - Global Environmental Change-Human and Policy Dimensions 15, 394-404.

Hickler,T., Eklundh,L., Seaquist,J.W., Smith,B., Ardö,J., Olsson,L., Sykes,M., Sjöström,M., 2005: Precipitation controls Sahel greening trend- Geophysical Research Letters 32.

Hielkema, J.U., S.D. Prince, W.L. Astle. 1987: Monitoring of global vegetation dynamics for assessment of primary productivity using NOAA advanced very high resolution radiometer. - Advances in Space Research 7: 81-88.

Holben, B. N., 1986. Characteristics of maximum-value composite images from temporal AVHRR data. - International Journal of Remote Sensing 7: 1417 - 1434.

Jönsson, P. and Eklundh, L., 2002: Seasonality extraction by function fitting to time-series of satellite sensor data.- Ieee Transactions on Geoscience and Remote Sensing 40: 1824-1832.

Jönsson, P. and Eklundh, L., 2004: TIMESAT - a program for analyzing time-series of satellite sensor data. - Computers & Geosciences 30: 833-845.

Maselli,F. and Rembold, F., 2002: Integration of LAC and GAC NDVI data to improve vegetation monitoring in semi-arid environments. - International Journal of Remote Sensing 23: 2475-2488.

Mitchell,T.D., Jones, P.D., 2005: An improved method of constructing a data base of monthly climate observations and associated high resolution grids- Int. J. Climatol. 25, pp. 693-712.

Nemani,R.R.,Keeling, C.D.,Hashimoto,H., Jolly, W.M.,Piper, S.C.,Tucker, C.J., Myneni, R.B., Running,S.W.,2003: Climate-Driven Increases in Global Terrestrial Net Primary Production from 1982 to 1999.-Science, Vol 300, pp 1560-1563.

Nicholson,S.E., Tucker, C.J., 1998: Desertification, drought, and surface vegetation: An example from the West African Sahel.- Bull. Am. Met. Soc. 79, 815.

Ostwald,M., Simelton, E., Chen,D., Liu, A., 2007: Relation between vegetation changes, climate variables and land-use policy in Shaanxi Province, China.- Geografiska Annaler (in press) and in: Simelton,E., 2007: Climate and human ipacts on wheat production and land use in the Loess Plateau region, China.-Eart Sciences Centre Doctoral Thesis A115, ISSN 1400-3813.

Pinzon, J.,M.E. Brown, C.J. Tucker., 2004: Satellite time series correction of orbital drift artifacts using empirical mode decomposition.-In: Albert-Huang Transform: Introduction and Applications, eds N. Huang, pp. Chapter 10, Part II. Applications.

Pinzon, J., 2002: Using HHT to successfully uncouple seasonal and interannual components in remotely sensed data. SCI 2002.- Conf. Proc. Jul 14-18. Orlando, Florida.

Rasmussen, M.S., 1998a: Developing simple, operational, consistent NDVI-vegetation models by applying environmental and climatic information: Part I. Assessment of net primary production. - International Journal of Remote Sensing 19: 97-117.

Rasmussen, M.S., 1998b: Developing simple, operational, consistent NDVI-vegetation models by applying environmental and climatic information. Part II: Crop yield assessment. - International Journal of Remote Sensing 19: 119-139.

Reynolds, J.F. and Stafford Smith, D.M. (eds.), 2002. Global Desertification: Do Humans Cause Deserts? (Dahlem University Press, Berlin).

Ricotta, C., Avena, G., De Palma, A., 1999: Mapping and monitoring net primary productivity with AVHRR NDVI time series: statistical equivalence of cumulative vegetation indices. -ISPRS Journal of Photogrammetry & Remote Sensing 54: 325-331.

Rigina, O. and Rasmussen, M.S., 2003b: Using trend line and principal component analysis to study vegetation changes in Senegal 1986–1999 from AVHRR NDVI 8 km data. -Danish J. Geogr.103: 31–42.

Rouse, J.W., Haas,R.H., Schell,J.A., Deering,D.W., 1973: Monitoring vegetation ystems in the Great Plains with ERTS- Third Earth Resources Twechnology Satellite-1 Symp. Vol. 1, Section A, GSFC, NASA, 10-14 Dec., 1973, pp. 309-317.

Runnström, M.C., 2000: Is northern China winning the battle against desertification? - Ambio 29: 468-476.

Runnström, M.C., 2003a: Rangeland development of the Mu Us Sandy Land in semi-arid China: An analyis using Landsat and NOAA remote sensing data.-Land Degrad. Develop 14: 189-202.

Runnström,M.C., 2003b: Land degradation and mitigation in northern China evaluated from the biological production.- Ph.D. Thesis. Department of Physical Geography and Ecosystems Analysis, Lund University-Meddelanden från Lunds Universitets Geografiska institutioner, Avh 150. ISBN 91-973857-6-X.

Simelton,E., 2007: Climate and human impacts on wheat production and land use in the Loess Plateau region, China.-Earth Sciences Centre, Göteborg University, Doctoral Thesis A115, ISSN 1400-3813.

Simelton,E., Zhang,S., Song,Y., Holmer, B.,Chen,D., Ostwald, M., 2007: Climate and non-climate impacts on Wheat production, Shaanxi, NE China.- In: Simelton,E., 2007: Climate and human ipacts on wheat production and land use in the Loess Plateau region, China.-Eart Sciences Centre, Göteborg University, Doctoral Thesis A115, ISSN 1400-3813

Snedecor, G.W., Cochran,W.G., 1980: Statistical Methods-Seventh Edition.-The Iowa State University Press, ISBN 0-8138-1560-6, 507 pp.

Tappan,G.G.,Tyler,D.J., Wehde, M.E., 1992: Moniroting Rangeland Dynamics in Senegal with Advanced Very High Resolution Radiometer Data.- Geocarta International (1), pp. 87-98.

Thornes, J., Helldén, U.,2006: Desertification syndromes for the target & validation DeSurvey areas- DeSurvey Deliverable 1.3.3.1., 29 pp + figures (11 pp.).

Tucker, C.J., 1979: Red and photographic infrared linerar combinations for monitoring vegetation.- RemoteSensing of Environment 8(2): 127-150.

Tucker,C.J., Dregne, H.E., Newcombe, W.W., 1991: Expansion and Contraction of the Sahara Desert from 1980-1990. - Science, Vol 253, pp. 299-301.

Tucker, C.J., J.E. Pinzon.,M.E. Brown, D. Slayback, E.W. Pak, R. Mahoney, E. Vermote, N. El Saleous, 2005: An extended AVHRR 8-km NDVI Data Set Compatible with MODIS and SPOT Vegetation NDVI Data.- Int. J. Remote Sensing. Submitted.

Udelhoven, T., Stellmes, M., Del Barrio,G., Hill,J., 2007: Assessment of rainfall and NDVI anomalies in Spain (19819-1999) using distributed lag models and 1 km AVHRR data.- DeSurvey Deliverable 1.5.1.16, 16 pp.

UNCED 1992: Report of the United Nations Conference on Environment and Development, Chapter 12: Managing fragile ecosystems: Combating desertification and drought- (Rio de Janeiro, 3-14 June 1992), General A/CONF.151/26 (Vol. II), Chapter 12.

Utrier, 2007: NOAA Pathfinder to MEDOKADS, GIMMS intercomparison.-DeSyurvey Deliverable 1.5.1.6, 16 pp. Delivered by partner 2, University of Trier, Germany (J.Hill).

Verburg, P.H., Chen, Y., 2000: Multiscale characterization of land-use patterns in China.-
Ecosystems, 3: 369-385.

Weiss, E., S.E. Marsh, and E.S. Pfirman. 2001: Application of NOAA AVHRR NDVI time series to assess changes in Saudi Arabia's rangelands. -International Journal of Remote Sensing 22:1005-1027.

Wu,B., Ci, L.J., 2002:Landscape change and desertification development in the Mu Us Sandland, Northern China- Journal of Arid Environment 50: 429-444.